Investigation of Layered Calcium Phosphates and Related Materials for Biomaterial Applications

By
Matthew Robert Cave

A thesis submitted to
The University of Birmingham
for the degree of
DOCTOR OF PHILOSOPHY

School of Chemistry
University of Birmingham
November 2009

smith&nephew

UNIVERSITY OF BIRMINGHAM

University of Birmingham Research Archive

e-theses repository

Abstract

The purpose of this study was to identify and investigate novel layered materials with potential as biomaterials. This study has concentrated on layered calcium phosphate phases and their analogues due to their obvious biocompatibility and potential for resorption.

Materials were prepared using a range of synthetic techniques including ceramic methods, acid flux and hydrothermal synthesis. Some of the layered phases prepared were then modified using intercalation and exfoliation. Characterisation was performed mainly using powder X-ray diffraction with thermogravimetric and fourier transform infrared providing further means of analysis. When possible, single crystal X-ray diffraction was also utilised.

Investigations were performed on metal alkyl phosphates with strontium pentyl and phenyl phosphate phases being fully characterised by single crystal X-ray diffraction. To our knowledge, this represented a rare family of inorganic/organic hybrid materials whose structures have been characterised in any detail. These structures show inorganic metal phosphate layers separated by organic layers containing alkyl chains displaying an unexpected cooperative ordering.

The intercalation and exfoliation properties of monocalcium phosphate monohydrate [MCPM] were studied and a monoamine intercalated version of this MCPM was successfully prepared. These materials were investigated as a component of a calcium phosphate bone cement system, whereby, the inclusion of this amine intercalated MCPM species had a potentially useful retarding effect upon the setting of the cement.

Layered calcium pyrophosphates were investigated due to their similar lamellar structure and slower dissolution rates compared with MCPM. Two previously known layered calcium pyrophosphate phases were successfully synthesised, namely calcium pyrophosphate tetrahydrate ($Ca_2P_2O_7\cdot4H_2O$) and calcium disodium pyrophosphate tetrahydrate ($CaNa_2P_2O_7\cdot4H_2O$) and their intercalation, ion exchange and exfoliation reactions were studied to determine whether it was possible to exploit their layered structures. Results of this study indicated that these phases were highly stable, allowing limited modification. When modification was suggested it resulted in as yet unidentified new phases.

Acknowledgments

I would like to thank my supervisor Dr. Adrian Wright for all his help, support and encouragement throughout the past 4 years – without it; I wouldn't have had the opportunity to complete a PhD in Birmingham. This PhD has been a great experience and I have thoroughly enjoyed the challenges and rewards that this research has brought. I should also like to thank Smith & Nephew and the School of Chemistry for providing the funding to enable me to complete my PhD.

I would like to thank those who have been involved in my training and development, for providing analysis and interpretation of some of the results in this thesis. I am grateful to Dr Benson Kariuki for his work on the single crystal X-ray diffraction analysis of the strontium alkyl phosphate species. I am also thankful to Geology and Earth Sciences for their ICP-MS analysis of my metal alkyl phosphates and Paul Stanley for training on the use of the ESEM with EDX for general analysis of some of my samples.

A special mention should go to members of the fifth floor, past and present that have provided help, guidance and many an enjoyable moment throughout my time at Birmingham. I would especially like to thank former and current members of the *Wright Group*, Lauren, Shezad, Tom, Fiona, Colin, Yasmin and Katie.

"There are some things so serious you have to laugh at them."

"An expert is a man who has made all the mistakes which can be made in a very narrow field."

Niels Bohr

"If we knew what it was we were doing, it would not be called research."

Albert Einstein

"The most exciting phrase to hear in science, the one that heralds the most discoveries, is not "Eureka!" (I found it!) but "That's funny...""

Isaac Asimov

When William Gladstone met Michael Faraday, he asked him whether his work on electricity would be of any use.
"Yes, sir" remarked Faraday, "One day you will be able to tax it."

Table of Contents

List of Figures

List of Tables

List of Abbreviations

Bu-MCPM = Butylamine Intercalated MCPM

CHA = Carbonate Hydroxyapatite

CPC = Calcium Phosphate Cement

DMF = Dimethylformamide

DTA = Differential Thermal Analysis

EDX = Energy Dispersive Analysis of X-rays

ESEM = Environmental Scanning Electron Microscopy

FTIR = Fourier Transform Infrared

HTXRD = High Temperature X-ray Diffraction

HA = Hydroxyapatite

ICP-MS = Inductively Coupled Plasma with Mass Spectrometry

MCPM = Monocalcium Phosphate Monohydrate

PMMA = Polymethylmethacrylate

Pr-MCPM = Propylamine Intercalated MCPM

SCXRD = Single Crystal X-ray Diffraction

TBA-Br = Tetrabutylammonium Bromide

TBA-OH = Tetrabutylammonium Hydroxide

TCP = Tricalcium Phosphate

TGA = Thermogravimetric Analysis

TTF = Tetrathiafulvalene

XRD = X-ray Diffraction

ZrP = Zirconium Phosphate

Chapter 1:

Introduction

1.1 Phosphate Chemistry

Phosphate chemistry has a long established history but has received much renewed attention over the past 50 years due to the versatile nature of the possible compounds produced and their many applications. These include use as fertilizers,[1] biomaterials,[2] phosphate glasses[3] and ionic conductors.[4]

The term phosphate refers to oxygen containing species of phosphorus (V) which range from single units (orthophosphate, PO_4^{3-}) to ring and chain anions and infinite networks. A large number of phosphates have been found as natural minerals in rocks such as fluorapatite[3] ($Ca_5(PO_4)_3F$) and francolite[5] ($(Ca, Mg, Sr, Na)_{10}(PO_4, SO_4, CO_3)_6F_{2-3}$). Living organisms such as ammonites use these minerals to form the rings of their shells.

Phosphates can be classed into two main groups, namely orthophosphates and condensed phosphates. The orthophosphates are derived from salts of orthophosphoric acid (H_3PO_4) and thus contain PO_4^{3-} derivates within their structures. The phosphate unit is arranged in a tetrahedral geometry with a central phosphorus atom surrounded by four oxygen atoms, as shown on figure 1.1.

The orthophosphate anion is analogous to orthosilicate (SiO_4^{4-}) or sulfate anions (SO_4^{2-}) and as such, some commonality of structures and behaviour exists between these species.
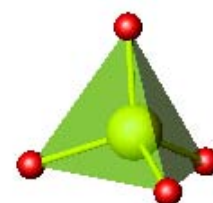
Figure 1.1: Representation of a PO_4^{3-} Orthophosphate Unit

Condensed phosphates can be considered as derived from these orthophosphate units but the orthophosphate units share oxygens to form one or more P – O – P bonds. This bond is often formed by the condensation reaction of two hydrogen orthophosphates (e.g. $[HPO_4]^{2-}$) to release water and form the P – O – P bond. More details regarding condensed phosphates can be found in Chapter 6 of this thesis.

1.2 Zirconium Phosphate

The structures of zirconium orthophosphate phases have been much studied and characterised. The alpha phase of zirconium phosphate (α-Zr(HPO$_4$)$_2$·H$_2$O) has a similar layered structure to the monocalcium phosphate monohydrate [MCPM] phase that will be presented in this thesis. It is therefore important to appreciate the behavioural similarities that may exist between these materials and therefore better understand the potential of similar calcium phosphate phases.
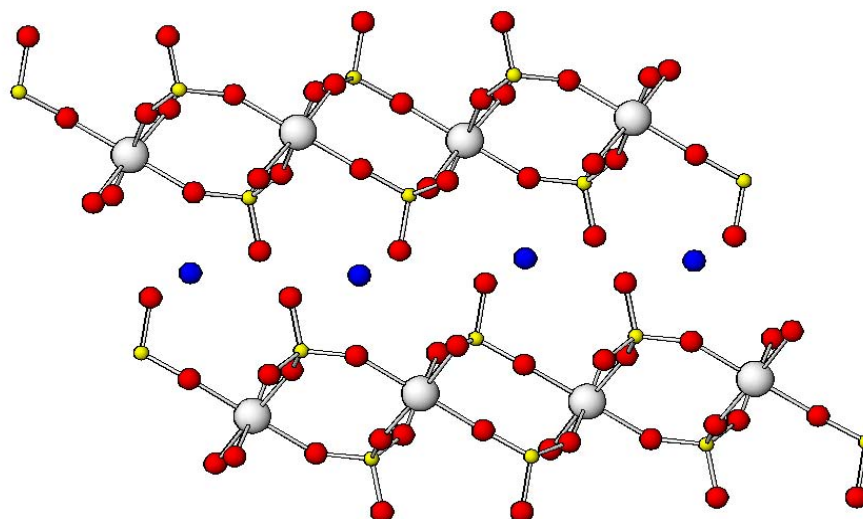
Figure 1.2: Structural Representation of α-Zr(HPO$_4$)$_2$·H$_2$O.
White = Zirconium, Yellow = Phosphorus, Red = Oxygen, Water Molecules are Represented as Blue Spheres and Protons Omitted for Clarity.

Several forms of zirconium phosphate exist, the two most important and widely studied forms being the α- and γ-zirconium orthophosphates. The crystal structure of Zr(HPO$_4$)$_2$.H$_2$O (α-ZrP)[6] shown in figure 1.2[7] displays a layered structure consisting of corner shared phosphate tetrahedra and ZrO$_6$ octahedra with the zirconium atoms separated from each other by a distance of 8.1 Å. Each phosphate unit contains one P-OH group that is directed into the interlayer region. The individual layers are held together by a network of hydrogen bonds formed between these hydroxyl groups.

1.2.1 Intercalation in Zirconium Phosphate

The layered nature of α-zirconium phosphate and the accessible voids within the structure provides possible sites for the intercalation of molecules/ions or pillaring of the layers to occur.

Successful intercalation of organic species into zirconium phosphate have been reported, most notably by the groups of *Clearfield* and *Alberti*.[6,8] The intercalation of monoamines into the layered structure has been achieved due to the highly acidic nature of the host materials, allowing an acid base reaction to drive the intercalation of the basic amines. *Benes*[9,10] *et al.* also successfully introduced amino alcohols into α-ZrP and thus further expanded the portfolio of molecules that could be inserted into this structure.

Some novel intercalation compounds have been formed in these structures which allow a variety of applications. These include intercalated ethylene oxide derivatives of γ-ZrP which provide a 'high' temperature (~200°C) intercalated phase possibly for use in catalysis.[11]

It has been found that zirconium phosphate allows proton conduction, due to the acidic nature of the zirconium phosphate layers transferring the protons. Therefore intercalation of diamines and heterocyclic bases (diazoles) into the structure were attempted to improve the proton conductivity of the zirconium host.[12,13]

Zirconium structures which display increased electron conductivity have been prepared via the intercalation reaction of tetrathiafulvalene (TTF) into copper pre-exchanged γ-ZrP ($Zr(PO_4)(H_2PO_4)\cdot2H_2O$).[14] This zirconium phosphate phase was used to allow a spatial confinement of the organic molecules in such a way to enable these TTF molecules to form a π-donor stack. This produced a hybrid organic electron conductor structure.

Biomolecules such as haemoglobin[15] and other proteins[16] have also been intercalated within the interlayer region of zirconium phosphate. Proteins and enzymes are useful for catalytic activities and have been researched previously, but they have been found to be particularly sensitive to pH and temperature. The use of a layered zirconium phosphate support for the enzyme or protein has overcome some of these limitations. An advantage of these bound proteins is the ease of separation and recycling which reduces the cost of the processing. However, the effects of binding the protein onto the support material can alter the protein shape and structure, which can affect the catalytic activity.[15]

Zirconium phosphate has been tested for the uptake of small pharmaceuticals (drug molecules not proteins or enzymes) for the purpose of drug delivery in the body. This uptake relies upon intercalation to adsorb the drugs due to the layered nature of zirconium phosphate. This can then provide an environment to help stabilise the drug and also enable some control on the release rate of the drug.[17] It was found that zirconium phosphate had a limited potential in this application as it has a low rate of resorption in vivo. Therefore there is potential for alternative materials that can intercalate drug molecules and possess better resorption rates; one such being layered calcium phosphates.

Modification of the zirconium phosphate phases can also be achieved by the pillaring of the zirconium phosphate layers, similar to that observed in clay minerals (see section 1.4). This pillaring mechanism is found to be necessary to enable larger ions to be inserted into the interlayer region of the zirconium host phase. By this process, metal oxides such as chromium and aluminium have been inserted between the phosphate layers.

One example involved the intercalation of an acetate ion into the zirconium phosphate [ZrP] layers with subsequent polymerisation to form a pillared phase. A second example involved intercalating the host ZrP with butylamine and then inserting a larger species in a

step-wise opening of the ZrP layers. It was at this stage that the metal oxide was added and the sample calcined to remove the organic species.[18] An alternative method was also reported by *Dines et al.*[19] using diphosphates or diphosphonates as the pillaring species.

1.2.2 Intercalation Reactions in Layered Metal Phosphates

Successful intercalation reactions in layered metal phosphates have been obtained using zirconium (as mentioned above) and titanium phosphates. Intercalation reactions have been reported with α-titanium phosphate (α-Ti(HPO$_4$)$_2$·H$_2$O), which was successful with linear α,ω-diamines from 2 to 9 carbons in length and appeared to form a monolayer between the phosphate sheets in an angled form at ~ 71° (to the phosphate layer).[20] Quaternary ammonium salts (such as alkyltrimethylammonium ions) have also been intercalated into this titanium phosphate phase.[21] Linear monoamines (R-NH$_2$) have been intercalated into the alpha[22] phase of titanium phosphate and cyclic monoamines such as aniline, benzylamine and pyridine have also been intercalated into the gamma form of titanium phosphate (Ti(H$_2$PO$_4$)(PO$_4$)·2H$_2$O).[23] In these cases, a standard acid-base exchange reaction occurs between the intercalating amine species and the protons on the hydrogen phosphate unit.

Intercalation of a range of organic species into aluminium phosphate phases has also been studied for possible use in catalysis and thermally stable pillared materials. A range of neat monoamines[24] have been used in an attempt to intercalate the aluminium phosphate phase [(C$_2$H$_5$)$_2$NH$_2$]$_4$[Al$_8$P$_{10}$O$_{40}$H$_2$]·(H$_2$O)$_{2.5}$. Another layered phase of aluminium phosphate, [Al$_3$P$_4$O$_{16}$][CH$_3$(CH$_2$)$_3$NH$_3$]$_3$ was shown to intercalate monoamines when these species were present in an alcohol/water solution.[25]

From these reports, it is clear that intercalation reactions can be achieved in layered phosphate materials. The intercalation reactions described above relate to the insertion of amine species which appears relatively straightforward for the hydroxyl functionality

exhibited by many structures. Therefore these molecules would appear sensible candidates in intercalation reactions undertaken with any layered calcium phosphates phases that are isolated.

1.3 Calcium Phosphate Materials

Calcium phosphate materials are of particular interest due to their similarity to natural hard tissue within the body (e.g. teeth and bone) and thus they possess inherently high biocompatibility. These materials have a potential in clinical applications for use in medical devices and cements. However, their properties have yet to be optimised for use within the body. The development of new calcium phosphate materials is therefore an important route to the production of new biomaterials with improved properties.

There are many different phases of calcium phosphate which are classified into groups by their calcium to phosphorus ratio. The lower the calcium/phosphorus molar ratio, the more acidic and water soluble the calcium phosphate will be. Monocalcium phosphate monohydrate (MCPM) [$Ca(H_2PO_4)_2 \cdot H_2O$] (or calcium dihydrogen orthophosphate monohydrate) has by far the highest water solubility and is also the most acidic in solution. Due to the high acidity, this phase is not normally found in the body, instead, a more stable form of calcium phosphate is found such as carbonate hydroxyapatite (See section 1.5.4).

Calcium phosphates have been used for many purposes in the past. A major commercial application has been the use of calcium phosphates in fertilizers to increase the phosphate content of soils. Indeed, the properties of certain calcium phosphate phases are suitable for many commercial applications. For instance, β-TCP ($Ca_3(PO_4)_2$) has been used as a gentle polishing agent in toothpaste, as well as an anti-clumping agent for dry powdered food products[3]. This material has also received much interest as a component in brushite forming bone cements. This is due to its alkaline pH as it will react with other acidic phases of calcium phosphate to form a fast setting cement (See Chapter 5 for more details).

The next section describes the known examples of layered calcium phosphate phases. These relatively rare examples provide a basis for much of the research into the isolation and manipulation of layered calcium phosphates in this thesis.

1.3.1 Layered Calcium Phosphate Phases

1.3.1.1 Monocalcium Phosphate Monohydrate

Monocalcium phosphate monohydrate ($Ca(H_2PO_4)_2 \cdot H_2O$)[26,27] [MCPM] has a layered structure as can be seen in the structural representation[7] shown in figure 1.3.1.1. However, it is susceptible to dissolution in water, especially in physiological conditions, which limits its direct use as a biomaterial. On dissolution, it forms an acidic solution and will re-precipitate as brushite ($CaHPO_4 \cdot 2H_2O$) when the water is removed from this solution. It can, however, be used as a precursor for the formation of other calcium phosphate phases such as brushite. In this reaction, MCPM is mixed with β-tricalcium phosphate ($Ca_3(PO_4)_2$) [TCP] in water to form a setting calcium phosphate cement based on brushite.[28]
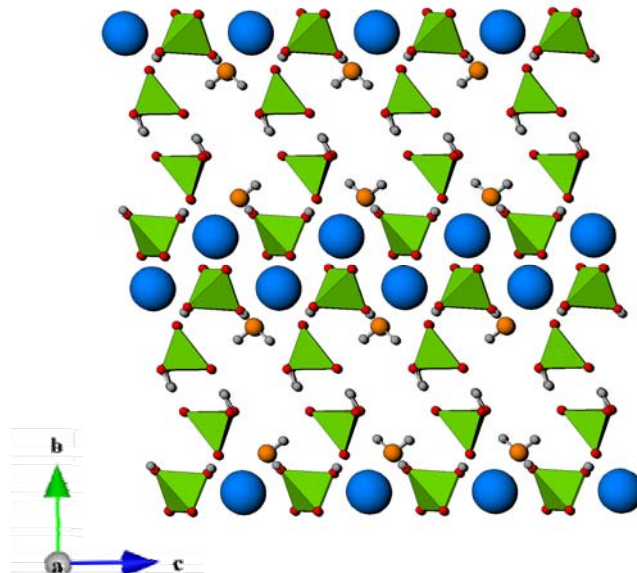
Figure 1.3.1.1: Structural Representation of MCPM ($Ca(H_2PO_4)_2 \cdot H_2O$).
Blue = Calcium, Green = Phosphate ions, Orange = Oxygen of Water Molecules, Grey= Hydrogen.

1.3.1.2 Calcium Pyrophosphate Tetrahydrate

Pyrophosphates constitute the largest family of condensed phosphates. These can be generally classified into the formula $[P_nO_{(3n+1)}]^{(n+2)-}$ with one P-O-P bond present in the ion which constitutes the condensed phosphate.[29] These pyrophosphate phases can be synthesised by various methods, either by condensation reactions from the monophosphate (PO_4^{3-}) unit, or by ion exchange methods from another pyrophosphate phase. The chemistry of the pyrophosphates has received considerably less attention than simple phosphates. However, a number of potentially interesting layered pyrophosphate phases have been identified containing calcium, including calcium pyrophosphate tetrahydrate. Studies on this phase and related materials have been investigated in this thesis (See Chapter 6).

Pyrophosphate has been found naturally in the body and as such can be classified as a biocompatible material. Materials containing pyrophosphate have proved to be enigmatic in their behaviour in the body as calcium pyrophosphate dihydrate has been found to be present in certain forms of arthritis and crystal deposition diseases in the bone joints.[30,31] This suggests reasonable insolubility in vivo. However, pyrophosphates are present in the body as essential stores of phosphate, with enzymes, such as alkaline phosphatase, known to hydrolyse phospho-ester bonds[32] (i.e. P-O-P). This allows the release of orthophosphate units (PO_4^{3-}) for use in the body as energy stores or DNA production. Therefore it is conceivable that biomaterials based on pyrophosphate phases can utilise these phosphatase enzymes[33-35] allowing them to elicit an advantageous biological response, in order to enhance resorption and release phosphate or calcium to the surrounding tissues.

Calcium pyrophosphate tetrahydrate $(Ca_2P_2O_7 \cdot 4H_2O)$[36] is an important example of a pyrophosphate phase. It is a layered material which possesses a very distinct interlayer region containing water molecules. This structure suggests potential for intercalation reactions due to

the presence of exchangeable water molecules. Some of the water molecules are directly coordinated to the calcium ions. A structural representation[7] of this phase is shown in figure 1.3.1.2.
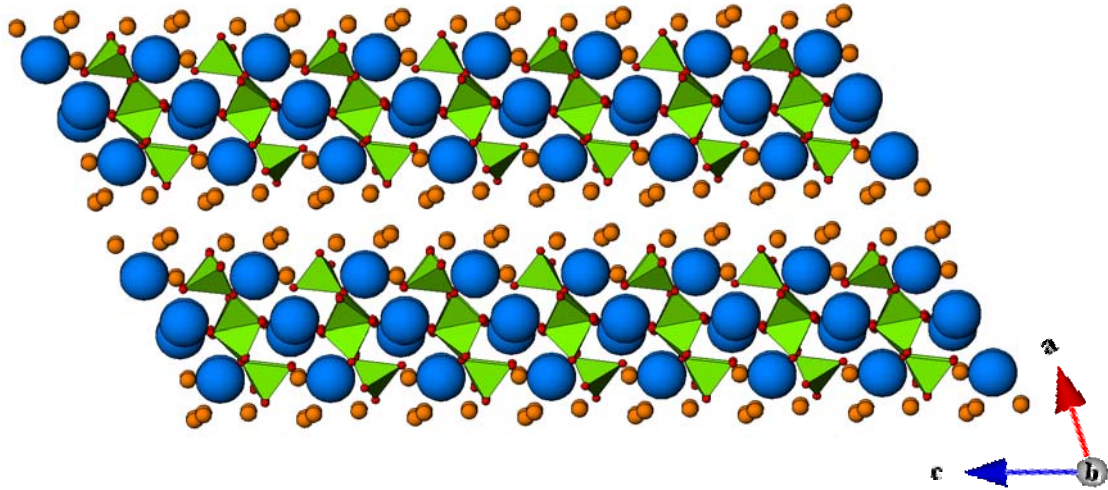
Figure 1.3.1.2: Structural Representation of Calcium Pyrophosphate Tetrahydrate ($Ca_2P_2O_7 \cdot 4H_2O$).
Blue = Calcium, Green = Phosphate, Orange = Water.

1.3.1.3 Brushite

This material is a layered phase with the general formula $CaHPO_4 \cdot 2H_2O$[3] which possesses water molecules in the interlayer region. These water molecules may be exchangeable with other species to allow intercalation reactions to alter the properties of the material. This phase has primarily been researched for the application of calcium phosphate bone cements and more details about this phase can be found in Chapter 5 of this thesis.

This material is slowly soluble in vivo and therefore finds application as a resorbable cement. However, it has low compressive strength in its pure form which limits its use for load-bearing applications.[37] Although development has improved the strength of these types of cements, more research is required. A structural representation[7] for this brushite phase is shown in figure 1.3.1.3.
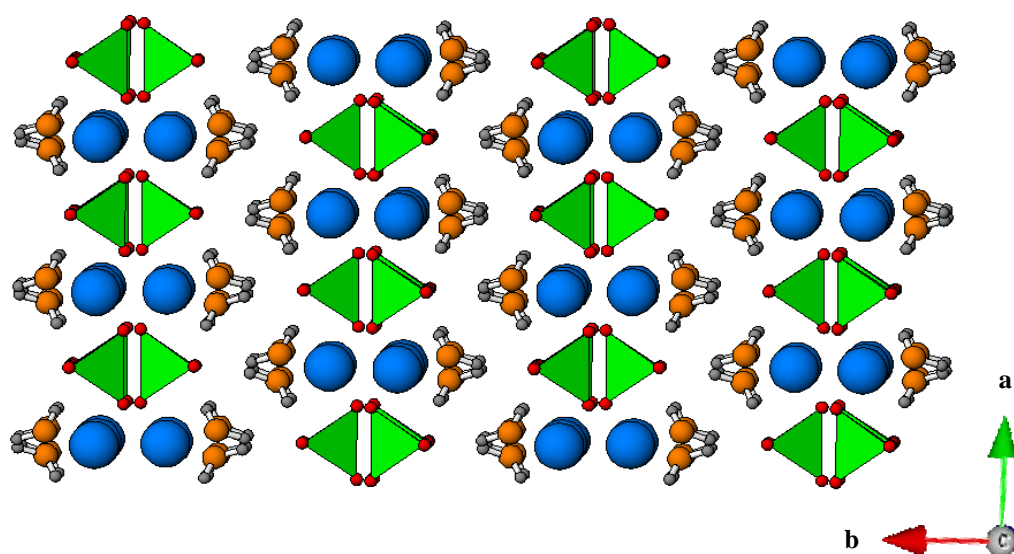
Figure 1.3.1.3: Structural Representation of Brushite (CaHPO$_4$·2H$_2$O).
Blue = Calcium, Green = Phosphate, Orange = Water.

The phases mentioned in this section will be described in more detail in the main experimental results sections of this thesis.

1.4 Nanocomposites and Hybrid Materials

There are a number of definitions to describe a nanocomposite material. The distribution of nano-dimensional inorganic fragments (e.g. exfoliated clays) in polymers is often referred to as a nanocomposite. However, a more general definition of *"materials containing dissimilar components mixed at the nanometre scale"* will be used.[38]

Nanocomposites are usually advantageous due to the improvement in the properties of the material by the combination of the components. Nanocomposites have also been produced to give large surface areas per unit volume due to the nanometre scale mixing of the components. As a larger surface area is usually important for most chemical interactions, the improvement in the properties of a material can be quite noticeable.

There are two main types of nanocomposites. The first type is the intercalated nanocomposite, where the organic species are inserted between the layers of the inorganic host. Examples of these include montmorillonite clays modified with amine,[39,40] terephthalate,[41] and organoammonium species.[42] The second type is the exfoliated nanocomposite, where the individual layers are well dispersed into an organic matrix.

As mentioned previously, a large proportion of the nanocomposites research has been focussed on polymer hosts with an exfoliated clay derived component. The clay minerals utilised are usually layered aluminosilicates consisting of stacks of negatively charged sheets, (See section 1.4.1) and the thickness of these inorganic sheets is of the nano-dimensional scale. Examples of these include montmorillonite $[(Na,Ca)_{0.3}(Al,Mg)_2Si_4O_{10}(OH)_2 \cdot n(H_2O)]$ clays modified with polymethylmethacrylate[43] and epoxy.[44] Montmorillonite is one particular example of clay that has been used for this purpose due to its high stiffness, in addition to possessing a lamellar structure with potential for chemical modification.

A problem with the use of clay based materials for composite formation is the natural hydrophilic state of the clay layers. This hydrophilic nature impedes homogeneous mixing due to aggregation of the clay layers within the organic matrix, which tend to be more hydrophobic in nature. Homogeneous mixing is essential for a successful composite, hence chemical modification is usually required to alter the hydrophilic nature of the clay layers and thus reduce the possible aggregation. Some aggregation of the layers is often unavoidable, however, a lack of complete separation of the clay layers (exfoliation) and addition of chemical modifiers can also affect the strength and ductility of the composites produced.

There are other examples of nanocomposites based upon 'clay-like' layered materials which are not classified as clays but possess some similar properties. These nanocomposite materials are prepared from inorganic host structures which have weak interlayer bonding which enable other species to be inserted into this region. A typical example of this type of host structure would be layered zirconium phosphate.[45] This host phase has been intercalated with amino acids,[46] tetrabutylammonium hydroxide[47] and epoxy[45] to form the nanocomposite material.

There are also many examples where a porous 3-dimensional network structure rather than a layered material have been used as the inorganic component of the composite. For these to be classified as nanocomposites, 'nanosized' crystals of the inorganic component were blended with the polymeric materials. Examples include hydroxyapatite [HA] $(Ca_{10}(PO_4)_6(OH)_2)$ with liposomes[48] as well as (nanosized) HA with alumina[49] and polymers such as polyethylene[50] and acrylic acid[51] which forms a three component composite. Further examples include α-hydroxy acids with tetracalcium phosphate $(Ca_4(PO_4)_2O)$ which form an injectable calcium phosphate composite cement[52] and tricalcium phosphate [TCP] with collagen or polylactic acid.[50]

The nature of the inorganic component can affect the properties of the composite formed. This is especially true when comparing the phases with 3-dimensional or layered structures. The use of 3-dimensional structures in nanocomposite formation will have been prepared by control of the morphology of the crystals to keep them in approximately nanoscale dimensions. Layered materials on the other hand are prepared as layered structures and then separated to form nano-dimensional fragments. Therefore structural control is important to form the correct phase before preparing the composite. In this case, the inorganic component will be plate-like and therefore most likely to be nano-dimensional in the thickness of the plate only with the other dimensions of the plate being larger.

This difference in morphology versus structure could affect the properties of the nanocomposites that are formed and therefore the choice of components will be dependent upon the requirements of the composite.

1.4.1 General Structure of Clay Minerals

Many of the nanocomposites that have been researched in the past have used layered clay materials as the inorganic host component of the composite. Clay minerals are based upon naturally occurring aluminosilicate materials similar to zeolites. They are often found as components of soil or sediment. The smectite clays consist of a layered structure, with 2-dimensional sheets of corner sharing silicate $[SiO_4]$ tetrahedra. These tetrahedral sheets are bonded to octahedral sheets formed from small cations such as aluminium or magnesium.[53] The tetrahedra are linked through three corners to form a flat sheet and the octahedra edge link to sit between two pointed silicate tetrahedra, point to point, to form the layered structure. Depending upon the composition of these sheets, a neutral or negative charged layered clay mineral will be produced. There are many different clay materials that possess some level of ion substitution and hence have a charge to the layers. Usually a negative charge is

predominant in the layers, being situated upon the oxygen atoms of the layer surface and as such, charge balancing by interlayer cations (such as Na^+ or Ca^{2+})[54] can occur.

The layered nature and exchangeable cation behaviour allows the clays to have very useful intercalation and ion exchange properties. The intercalation properties of clays and clay-like materials will be detailed in section 1.4.2, however, as a brief overview, water and organic molecules such as ethylene glycol ($HOCH_2CH_2OH$) have been introduced into the interlayer region of the clay materials causing the clay to expand. This behaviour has mainly been observed in clay minerals with few examples of other materials displaying this property. It has been suggested[55] that the reason for this is due to a lower lattice charge which allows the interlayer region to expand considerably.

If a larger, more rigid organic molecule were to be intercalated between the layers of the clay, a so called pillaring reaction can occur. This causes the clay layers to be propped apart. This forms a much larger interlayer gap for further molecule insertion, especially at higher temperatures (> 100°C) whereby swelling agents (such as water) might have evaporated. Specific pillaring agents include tetraalkyl ammonium ions, Al_{13} Keggin[18] ions $[Al_{13}O_4(OH)_{28}]^{3+}$ and silica.[54] These species (excluding the organo-ammonium species) can be heated to high temperature (> 200°C) whereby they will be calcined to form metal oxide clusters which pillar the layers and therefore keep them separated.[18]

1.4.2 Inorganic-Organic Hybrid Materials

The synthesis of these hybrid composite materials is based upon the reaction of both organic and inorganic moieties in order to obtain new composite materials. These hybrids can be classified into two types depending upon the nature of the interaction between the organic and inorganic components. Class I hybrids possess a weak physical interaction between the components such as hydrogen bonding or van der waals forces which hold the structure in

place or physically trap an organic species inside an inorganic matrix. If a layered inorganic host material is used with intercalation of organic moieties between the layers, a class I hybrid material would be formed.

Class II hybrids possess a strong chemical bond between the components and are therefore held together more strongly than those of the class I type. Class II hybrids can be produced by many procedures, however, two well known methods involve the use of sol-gel processing or by the use of organic surface modification of an inorganic host. The organic surface modification method can be used to reduce the hydrophilic nature of an inorganic surface. This allows hydrophobic species such as polymers to mix more favourably with the inorganic host surface with less agglomeration of the host material.[56]

A number of inorganic host materials have been researched to form inorganic/organic hybrids but for the purpose of this research, only calcium phosphate phases will be investigated. The main calcium phosphate phase that has been researched previously, for the formation of inorganic/organic hybrid phases, has been the apatite forms of calcium phosphate. The main benefits of these phases are their low solubility and their ability to form 'nanoscale' particle sizes, therefore increasing their surface area for adsorption of organic species. One particular example where hydroxyapatite $(Ca_{10}(PO_4)_6(OH)_2)$ [HA] has been produced as an inorganic-organic hybrid is in the form of HA-alginate micro-spheres that contain a void in the centre. This void allows the incorporation of another species (such as a drug) and therefore can provide a delivery vehicle for a particular species to the appropriate site in the body. The example mentioned here used these composites for the delivery of enzymes to a specific target.[57]

The anti-cancer agent, cisplatin, has also been tested with hydroxyapatite. In this case, the drug was loaded into hydroxyapatite particles to form a material which might possess

controlled drug release characteristics when the drug was chemically bound to the HA particles. The release of cisplatin ($Cl_2Pt(NH_3)_2$) was controlled by the presence of chloride ions. This allowed desorption of the cisplatin species from the chemical binding present on the HA particle surface. Due to the structure of apatitic calcium phosphates, the adsorption of neutral as well as positive and negatively charged molecules is possible. Therefore, this method of delivery has potential for use with many pharmaceutical agents. However, the controlled release of these drugs from the apatite material is currently still under investigation as there is some variation of the desorption rate, depending upon the crystallinity of the material. There is potential for replacement of some of the chloro sites in the drug with phosphate which would affect the efficacy of the entire drug once released.[58]

The materials mentioned above are derived from the control of the morphology of the components to produce nanosized crystals. However, equally as important is the control of the structure of the phases thereby allowing the formation of nano-dimensional fragments.

1.4.3 Exfoliation of Clay-Like Materials

Layered materials can commonly undergo two types of reaction when organic species are present. The first type is intercalation whereby the guest molecule is incorporated into the interlayer region of the host. The second type is exfoliation which occurs again by allowing a guest molecule to enter the interlayer region. However, this species destabilises the interlayer bonding either reducing the attractive nature between the layers or even making them repulsive. Thus the layers can be separated either by a choice of solvent, agitation or sometimes, the presence of the guest molecule is sufficient.

The reason for exfoliating layered materials is because of the different properties that the fragments can introduce due to their size and shape when used as a component of a composite material. Information can also be obtained on the interactions between the layers in

the bulk host by studying the individual layer interactions. Some examples of exfoliation in layered materials are shown below, with the choice of exfoliating species that were used to prepare these phases.

There are a few examples of exfoliation using layered phosphates which is of principal interest in the research presented in this thesis. The formation of exfoliated zirconium phosphate gels and colloidal suspensions have been prepared by *Casciola and Alberti et al.* In this case, a 0.1M aqueous solution of propylamine is used to exfoliate the layered α-zirconium phosphate.[59,60] This method of exfoliation using dilute propylamine was successful for the α-ZrP form. However, the γ-ZrP phase showed limited success with this exfoliating species,[61] although more success was attained using ethyl- and methylamine. The most successful method for exfoliating the γ-ZrP crystals was in the use of a 1:1 acetone/water solution at > 60°C.[62] The exfoliation of the zirconium phosphate species has also be achieved using the standard exfoliating species used with clay materials, namely, tetrabutylammonium ions.[59]

Titanium oxide nanosheets have been prepared by the reaction of the host titanium acid oxide ($H_{1.07}Ti_{1.73}O_4 \cdot H_2O$) with tetrabutylammonium hydroxide [TBAOH][63] which exfoliated this layered structure. Therefore the TBA species has been used successfully on a range of phosphate materials. This species should therefore be attempted on the layered calcium phosphates produced in this thesis.

However, exfoliation of a layered vanadium phosphate phase ($VOPO_4 \cdot 2H_2O$) was achieved by using small chained (3-4) alcohol species.[64] The most efficient exfoliating species in this case was either butan-1-ol or butan-2-ol which was refluxed at 30 – 70°C for 1 hour.[65] This produced a homogenous solution which on removal of the alcohol would give a solid exfoliated material.

Another class of layered materials that have been exfoliated are the layered double hydroxides [LDH]. These may be considered as 'reversed' clays as their layers possess positive charges with charge balancing anions between their layers. These phases were produced using a dodecylsulfate ($C_{12}H_{25}SO_4$) pre-intercalated zinc aluminate ($Zn_3Al(OH)_6$) LDH material refluxed in xylene. A linear low density polyethylene polymer was then refluxed with this material also in xylene to produce an exfoliated nanocomposite.[66] This form of in situ exfoliation/polymer nanocomposite formation has been used to produce some of the clay nanocomposite phases described. For example, montmorillonite/polymer nanocomposites have been formed by this process. These composites are produced using a montmorillonite solution which was first modified with hexadecyltrimethyl ammonium bromide to increase the clay layer separation. The addition of solvated dimethylsiloxane or polyvinylchloride[67] to this modified montmorillonite was used to form the polymerised exfoliated clay composite materials.

It was found that a range of exfoliating species and methods have been attempted to separate layered compounds. The materials themselves will also dictate which methods can be attempted and whether specific species will be successful. Therefore a range of exfoliation methods will be attempted depending upon the structure of the host phase.

In summary, tetrabutylammonium species and acetone/water solutions will initially be used on the layered phosphate phases in this thesis. If protons are present in the interlayer region of the layered phosphates phase, amine or alcoholic solutions will also be attempted depending upon the stability of the host material.

1.5 Biomaterials

The area of biomaterials research essentially involves the study of materials and their interactions in biological environments. This field of research is a diverse multidisciplinary topic, especially due to the nature of producing a valid biomaterial which can involve many wide ranging techniques and clinical tests to check the compatibility of the product for its intended use. There are many biomaterials but these can be classified into four main types, namely *metals, polymers, ceramics* and *natural materials.* Biomaterials can be composed of one or more of these types; however, combining more than one of these classes has enabled materials to be produced with enhanced performance compared to the individual components. This has given rise, for example, to the formation of composite materials, such as layered inorganic species dispersed in polymers.

1.5.1 Metals

At present, most applications of load-bearing implants in the body are made from metals. One particular metal that has been used in the past has been titanium[68] because it has favourable mechanical properties. It is relatively light and has good biocompatibility.[69]

Metals have been used previously in knee, hip and tooth replacements due to their strength and load bearing properties. However, the use of this material creates problems because of the great difference in mechanical properties between the metal and the surrounding bone and also the slow dissolution of the implant in physiological solution can release harmful and sometimes toxic ions. Metallic implants are usually classified as 'inert' materials and as such will remain in the body until they are physically removed by surgery and will not regenerate natural bone. Ceramic coatings have been applied to the surface of the metal implants in order to improve the biocompatibility and cell adhesion to the implant.[70]

The main coating that has been applied in the past has been hydroxyapatite due to the good cell adhesion and biocompatibility that is afforded by this coating.

1.5.2 Polymers

These materials are by far the most prolific in the biomaterials field. There are a few naturally occurring polymers such as collagen,[71,72] rubber and cellulose. There are however a range of synthetic polymers that have been used in this field such as polymethylmethacrylate (PMMA), polyacrylic acid[73] and polyvinyl chloride.

These polymers have been used on their own for biomaterial applications but their properties have been greatly improved by their incorporation into composites. The addition of a stronger, less flexible material, such as calcium phosphate, has been mixed with these materials to form a new phase that has better strength whilst still maintaining some flexibility. Further enhancement of these composites is still required to improve their properties but the results are showing great potential.

1.5.3 Ceramics

Ceramic materials used in replacement surgery can be classified into two main groups; *bioinert and bioactive.* Bioinert ceramics have virtually no effect upon living tissue present near the device. A typical example of this material would be alumina. *Bioactive* ceramics on the other hand are capable of bonding with living tissue. Typical examples of this type of a ceramic would be some phases of calcium phosphate, and some ceramic glasses. A further advantage to these bioactive ceramics is the possibility to substitute damaged hard tissue and thus form a surface allowing the attachment of living tissue. The use of hydroxyapatite and tricalcium phosphate ceramics, in particular, have shown ingress of new bone that has physically bonded to this material. This is not evident on the surface of metal implants. This is

a further advantage to the use of calcium phosphates, as this material has been used as a coating for the surface of a metal implant to aid fixation of the implant into the replacement site.

Unfortunately there are also a range of disadvantages to the use of ceramic materials for loads bearing applications. The main problem is their rigidity and the potential for fractures to occur in these materials because although these materials are very hard, they are also very brittle. This property does not prevent these materials from being used as hard tissue substitutes but only in applications in non load-bearing implants such as orthopaedic surgery, bone defect filling and middle ear surgery.[2]

1.5.4 Natural Materials

Natural materials are an important category of biomaterials due to the low toxicity, good biocompatibility and cell recognition with the ability to be degraded easily by enzymes when used in the body. There are however some disadvantages with these materials as they are usually very complex and thus difficulties arise in understanding the full composition of the material. This makes these structures extremely difficult to synthesise thus relying on naturally produced materials. The process of degradation is also a cause of concern as this can sometimes occur very rapidly in the body and as such some of the properties of the host material can be lost due to too rapid resorption of the material by the body. This rapid degradation however is not solely limited to natural materials.

Calcium phosphates can be generally classified as bioactive ceramic materials which means that they can bond with living tissues.[2] The main advantage for the use of calcium phosphate is the ability of these materials to be resorbed by the body,[74] which in turn can then use the ions as a scaffold. This will aid the regeneration of the natural calcium phosphate present in the hard tissues within the human body.

The main calcium phosphate containing hard tissues in the body are in the bones and teeth. Calcium phosphate forms the main inorganic component of these structures in the form of carbonate hydroxyapatite. There are two types of substitution that can occur in the hydroxyapatite structure to form the carbonate hydroxyapatite structure, namely A-type (OH$^-$ substituted by CO_3^{2-}) and B-type (CO_3^{2-} for PO_4^{3-}) substitution. A general formula for carbonate hydroxyapatite with both A-type and B-type substitutions can be represented as $[Ca_{10-x-y}M_y(PO_4)_{6-x-y}(CO_3)_{x+y}(OH)_{2-x-2z}(CO_3)_z]$[75] with M = monovalent cation for charge balancing.

In the human bone, this material equates for about 65%[2,3] of the bone mass, with the remaining 35% composed of organic matter and water. The main organic part is composed of collagen, which is arranged in fibres to produce a scaffold where the calcium phosphate crystals can deposit (Figure 1.5.4.1).[76]
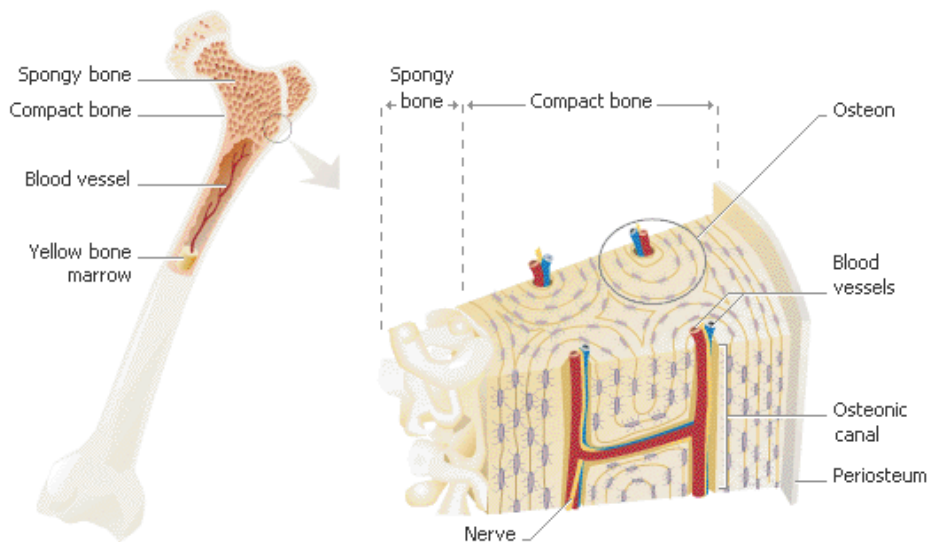
Figure 1.5.4.1: Cross Section of Human Bone (Reproduced from Reference 76)

Bone represents one of the best known natural nanocomposite materials found in the body. This material provides support for the entire body, as well as being a store for minerals. Natural bone is composed of a mixture of plate-like carbonate hydroxyapatite (CHA)

nano-crystals with a collagen rich fibrous organic matrix.[50] The CHA crystals deposit along the long axis of the collagen fibre in a continuous manner without aggregation of the CHA mineral phase.[77] This lack of aggregation is difficult to achieve in many of the synthetic composites produced to mimic bone. These synthetic composites have been composed of mixed organic and inorganic materials (mainly apatite based calcium phosphate phases). The combination of CHA and collagen fibres, with many other organic species in small quantities[78] as well as some water, gives bone the rigidity, flexibility and tensile strength required to fulfil its function as a supporting structure.

There are however, situations where bone defects occur, due to illness, damage or surgery. There is therefore a need for potential replacement materials which can mimic bone and can also be resorbed by the body.

A synthetic form of hydroxyapatite and collagen has been prepared for the purpose of mimicking bone.[79,80] However, some of the additional strength of bone, compared to the synthetic types, occurs due to the orientation of certain components within the composite. The exact mechanism of bone formation in the body is not fully understood, which makes mimicking bone by synthetic methods more difficult. One problem with the composites produced in the laboratory is the orientation and processing of the materials used to produce the final form. Aggregation of the hydroxyapatite and the fact that more than one form of collagen fibre was produced by synthetic methods limits the strength of the composite synthesised.[72] Aggregation of the filler components, due to hydrophobic effects, has proved a problem with nanocomposite formation and therefore modification of the materials using grafting polymers or surface modification of the filler has been necessary. This was in order to reduce the extent of the aggregation. A great deal of research is continuing in this area as these materials show great potential if they can be optimised for use in the body.

Typically the choice of composite is usually designed to improve certain properties of the material depending upon the mixing ratio of the components or the formation temperature. A typical example would be the use of alumina with hydroxyapatite. Usually hydroxyapatite possesses low mechanical strength and thus is quite brittle. The use of a small amount of alumina helps to strengthen the hydroxyapatite without dramatically affecting the resorption rate of the hydroxyapatite. However, alumina will not be resorbed by the body and therefore presents new difficulties due to the presence of this material in the healed implant site.

Human teeth exhibit similar characteristics to bone except for an additional surface coating of enamel. This enamel has a much larger inorganic content than bone of up to 90%,[2] with much larger crystals of carbonate apatite present compared with bone. A cross section of a human tooth can be seen in figure 1.5.4.2.[81] The main disadvantage to enamel over bone is the lack of any living cells present and thus the inability to regenerate or repair this material when damaged, resulting in the problems of tooth decay in adults and children.
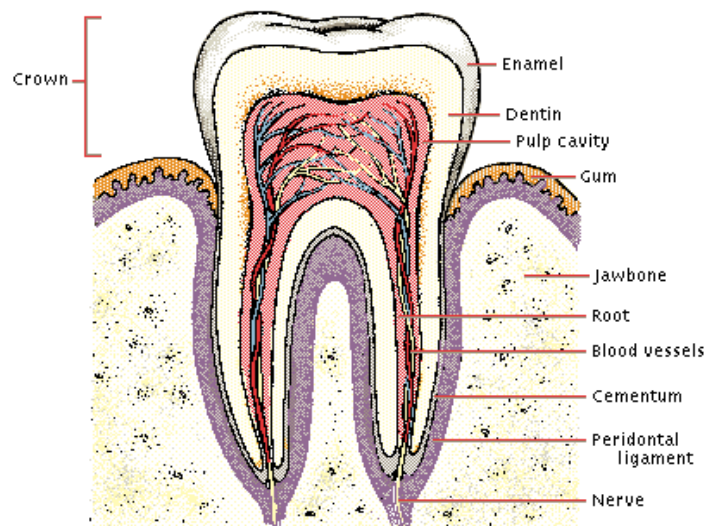
Figure 1.5.4.2: Cross Section of a Human Tooth (Reproduced from Reference 81)

1.5.5 Hard Tissue Replacement

Although many attempts to produce replacement materials have shown promise, these have had limited success due to the diverse range of properties required to allow these materials to integrate fully in the body. These include biocompatibility, mechanical stress and strain as well as stability in physiological fluids. Thus research in this area is important to optimise current replacement materials in order to mimic the natural structures in the body.

There are many different varieties of hard tissue replacement biomaterials, too numerous to be mentioned in detail here. However, the main focus of the research in this thesis is directed towards calcium phosphate materials, which, although currently unsuitable for load bearing applications, offer much potential as hard tissue replacements.

1.6 Aims of this Research

Due to the diverse nature of the biomaterials field, the aim of this research has focussed upon utilising some of the developed research on layered materials as hosts and components in composites, in a search for potential biocompatible calcium phosphates with suitable features. Once viable phases were identified, the structures and properties of these materials would be explored for potential applications as composite components, drug delivery materials or bone cement components.

The synthesis and potential modification of these layered calcium phosphate materials formed the basis of the experiments conducted. These investigations mainly concentrated on the intercalation and exfoliation properties of layered calcium phosphate materials and their analogues due to their biocompatible and potentially resorbable nature. More details on the individual aims of each material investigated are given below.

The research has been split into four distinct experimental chapters dictated by the different materials that have been investigated in this thesis. The first chapter investigated the properties of the metal alkyl phosphate inorganic/organic hybrid materials, which due to their hydrophobic nature, could show potential in nanocomposite formation. The second chapter concentrated upon the intercalation and exfoliation properties of the layered calcium phosphate phase monocalcium phosphate monohydrate [MCPM]. The goal of these experiments was to investigate the possible encapsulation of drug molecules in a resorbable material. The third chapter explored the potential of utilising an amine modified MCPM phase as a component of a brushite bone cement. The final experimental chapter examined layered calcium pyrophosphate phases which, due to the structures of the materials investigated, showed potential to intercalate or exfoliate and therefore could be beneficial for drug delivery vehicle or nanocomposite formation.

1.7 References

1. MacIntire, W.; Hardin, L.; Oldham, F., *Ind. Eng. Chem.,* **28**, 711, (1936).
2. Vallet-Regi, M.; Gonzalez-Calbet, J., *Prog. Solid State Chem.,* **32**, 1, (2004).
3. Dorozhkin, S., *J. Mater. Sci.,* **42**, 1061, (2007).
4. Leclaire, A.; Caignaert, V.; Raveau, B., *Solid State Sci.,* **7**, 109, (2005).
5. Benmore, R.; Coleman, M.; McArthur, J., *Nature,* **302**, 516, (1983).
6. Clearfield, A.; Smith, D., *Inorg. Chem.* **8**, 431, (1969).
7. *ATOMS*, Shape Software: 2005.
8. Alberti, G.; Marmotti, F.; Cavaglio, S.; Severi, D., *Langmuir,* **16**, 4165, (2000).
9. Benes, L.; Melanova, K.; Zima, V.; Patrono, P.; Galli, P., *Eur. J. Inorg. Chem.,* **2003**, 1577, (2003).
10. Benes, L.; Zima, V.; Melanova, K.; Steinhart, M.; Kriechbaum, M.; Amenitsch, H.; Bernstorff, S., *J. Phys. Chem. Solids,* **65**, 615, (2004).
11. Yamanka, S., *Inorg. Chem.,* **15**, 2811, (1976).
12. Casciola, M.; Costantino, U.; Calvei, A., *Solid State Ionics,* **61**, 245, (1993).
13. Casciola, M.; Chieli, S.; Costantino, U., *Solid State Ionics,* **46**, 53, (1991).
14. Backov, R.; Bonnet, B.; Jones, D.; Roziere, J., *Chem. Mater.,* **9**, 1812, (1997).
15. Bhambhani, A.; Kumar, C., *Chem. Mater.,* **18**, 740, (2006).
16. Kumar, C.; Bhambhani, A.; Hnatiuk, N., *Handbook of Layered Materials*. Marcel Dekker: New York, 2004.
17. Kijima, T.; Ueno, S.; Goto, M., *J. Chem. Soc: Dalton Trans.,* **1982**, 2499, (1982).
18. OliveraPastor, P.; MairelesTorres, P.; RodriguezCastellon, E.; JimenezLopez, A.; Cassagneau, T.; Joner, D.; Roziere, J., *Chem. Mater.,* **8**, 1758, (1996).
19. Dines, M.; Digiacomo, P.; Callahan, K.; Griffith, P.; Lane, R.; Cooksey, R., *ACS Symp. Ser. No. 192*. Washington D.C., 1982.
20. Espina, A.; Menendez, F.; Jaimez, E.; Khainakov, S.; Trobajo, C.; Garcia, J.; Rodriguez, J., *Mater. Res. Bull.,* **33**, 763, (1998).
21. Danjo, M.; Baba, Y.; Tsuhako, M.; Yamaguchi, S.; Hayama, M.; Nariai, H.; Motooka, I., *Bull. Chem. Soc. Japan,* **68**, 1607, (1995).
22. Menendez, A.; Barcena, M.; Jaimez, E.; Garcia, J.; Rodriguez, J., *Chem. Mater.,* **5**, 1078, (1993).
23. Espina, A.; Jaimez, E.; Khainakov, S.; Trobajo, C.; Garcia, J.; Rodriguez, J., *J. Mater. Res.,* **13**, 3304, (1998).
24. Peng, L.; Yu, J.; Li, J.; Li, Y.; Xu, R., *Chem. Mater.,* **17**, 2101, (2005).
25. Huang, Q.; Wang, W.; Yue, Y.; Hua, W.; Gao, Z., *Micro. Meso. Mater.,* **67**, 189, (2004).
26. Dickens, B.; Bowen, J., *Acta. Cryst.,* **27B**, 2247, (1971).
27. Maclennan, G.; Beevers, C., *Acta Cryst.,* **9**, 187, (1956).
28. Mirchi, A.; Lemaitre, J.; Terao, N., *Biomaterials,* **10**, 475, (1989).
29. Averbuch-Pouchot, M.; Durif, A., *Topics in Phosphate Chemistry*. World Scientific Publishing: 1996.
30. Beutler, A.; Rothfuss, S.; Clayburne, G.; Sieck, M.; Schumacher, H., *Arthritis and Rheumatism,* **36**, 704, (1993).
31. Ishikawa, K.; Masuda, I.; Ohira, T.; Yokoyama, M., *J. Bone Joint Surg.,* **71A**, 875, (1989).
32. Grover, L.; Gbureck, U.; Wright, A.; Tremayne, M.; Barralet, J., *Biomaterials,* **27**, 2178, (2006).
33. Shinozaki, T.; Xu, Y.; Cruz, T.; Pritzker, K., *J. Rheum.,* **22**, 117, (1995).

34. Xu, Y.; Cruz, T.; Pritzker, K., *J. Rheum.,* **18**, 1606, (1991).
35. Yoza, N.; Onoue, S.; Kuwahara, Y., *Chemistry Letters*, 491, (1997).
36. Christoffersen, M.; Balic-Zunic, T.; Pehrson, S.; Christoffersen, J., *J Cryst. Growth,* **212**, 500, (2000).
37. Bohner, M.; Gbureck, U.; Barralet, J., *Biomaterials,* **26**, 6423, (2005).
38. Ajayan, P.; Schadler, L.; Braun, P., *Nanocomposite Science and Technology*. Wiley VCH: 2003.
39. Yoon, K.; Sung, H.; Hwang, Y.; Noh, S.; Lee, D., *Applied Clay Science,* **38**, 1, (2007).
40. Greenwell, C.; Harvey, M.; Boulet, P.; Bowden, A.; Coveney, P.; Whiting, A., *Macromolecules,* **38**, 6189, (2005).
41. Kim, S.; Kim, S., *J. Applied Poly. Sci.,* **103**, 1262, (2007).
42. Pospisil, M.; Capkova, P.; Merinska, D.; Malac, Z.; Simonik, J., *J. Colloid Interf. Sci.,* **236**, 127, (2001).
43. Zheng, J.; Wang, J.; Gao, S.; Yao, K., *J. Mater. Sci.,* **40**, 4687, (2005).
44. Seo, K.; Kim, D., *Polymer Eng. Sci.,* **46**, 1318, (2006).
45. Sue, J.; Gam, K., *Chem. Mater.,* **16**, 242, (2004).
46. Ding, Y.; Jones, D.; Maireles-Torres, P.; Roziere, J., *Chem. Mater.,* **7**, 562, (1995).
47. Kim, H.; Keller, S.; Mallouk, T., *Chem. Mater.,* **9**, 1414, (1997).
48. Chu, M.; Liu, G., *Nanotechnology,* **16**, 1208, (2005).
49. Viswanath, B.; Ravishankar, N., *Scripta Materialia,* **55**, 863, (2006).
50. Murugan, R.; Ramakrishna, S., *Composites Sci. and Tech.,* **65**, 2385, (2005).
51. Furuichi, K.; Oaki, Y.; Ichimiya, H.; Komotori, J.; Imai, H., *Sci. Tech. Adv. Materials,* **7**, 219, (2006).
52. Barralet, J.; Tremayne, M.; Lilley, K.; Gbureck, U., *Chem. Mater.,* **17**, 1313, (2005).
53. Mott, C., *Catalysis Today,* **2**, 199, (1988).
54. Smart, L.; Moore, E., *Solid State Chemistry*. CRC Press: 2005.
55. Dyer, A.; Leigh, D., *J. Inorg. Nucl. Chem.,* **34**, 369, (1972).
56. Mutin, H.; Guerrero, G.; Vioux, A., *Comp. Rend. Chemie,* **6**, 1153, (2003).
57. Ribeiro, C.; Barrias, C.; Barbosa, M., *Biomaterials,* **25**, 4363, (2004).
58. Barroug, A.; Kuhn, L.; Gerstenfeld, L.; Glimcher, M., *J. Orth. Res.,* **22**, 703, (2004).
59. Casciola, M.; Alberti, G.; Donnadio, A.; Pica, M.; Marmotti, F.; Bottino, A.; Piaggio, P., *J. Mater. Chem.,* **15**, 4262, (2005).
60. Alberti, G.; Casciola, M.; Costantino, U., *J. Colloid Interf. Sci.,* **107**, 256, (1985).
61. Alberti, G.; Cavalaglio, S.; Dionigi, C.; Marmotti, F., *Langmuir,* **16**, 7663, (2000).
62. Alberti, G.; Giontella, E.; MurciaMascaros, S., *Inorg. Chem.,* **36**, 2844, (1997).
63. Tanaka, T.; Fukuda, K.; Ebina, Y.; Takada, K.; Sasaki, T., *Advanced Materials,* **16**, 872, (2004).
64. Nakato, T.; Furumi, Y.; Terao, N.; Okuhara, T., *J. Mater. Chem.,* **10**, 737, (2000).
65. Yamamoto, N.; Hiyoshi, N.; Okuhara, T., *Chem. Mater.,* **14**, 3882, (2002).
66. Chen, W.; Feng, L.; Qu, B., *Chem. Mater.,* **16**, 368, (2004).
67. Ma, J.; Xu, J.; Ren, J.; Yu, Z.; Mai, Y., *Polymer,* **44**, 4619, (2003).
68. Geesink, R.; de Groot, K.; Klein, C., *J. Bone Joint Surg.,* **70B**, 17, (1988).
69. Tisdel, C.; Goldberg, V.; Parr, J.; Bensusan, J.; Staikoff, L.; Stevenson, S., *J. Bone Joint Surg.,* **76**, 159, (1994).
70. Lopez-Heredia, M.; Sohier, J.; Gaillard, C.; Quillard, S.; Dorget, M.; Layrolle, P., *Biomaterials,* **29**, 2608, (2008).
71. Wan, Y.; Hong, L.; Jia, S.; Huang, Y.; Zhu, Y.; Wang, Y.; Jiang, H., *Composites Sci. and Tech.,* **66**, 1825, (2006).

72. Roveri, N.; Falini, G.; Tampieri, A.; Landi, E.; Sandri, M.; Sidoti, M., *Mater. Sci. Eng.,* **23C**, 441, (2003).

73. Liou, S.; Chen, S.; Liu, D., *J. Biomed. Mater. Res.,* **73B**, 117, (2005).

74. Okuda, T.; Ioku, K.; Yonezawa, I.; Minagi, H.; Kawachi, G.; Gonda, Y.; Murayama, H.; Shibata, Y.; Minami, S.; Kamihira, S.; Kurosawa, H.; Ikeda, T., *Biomaterials,* **28**, 2612, (2007).

75. Lee, Y.; Hahm, Y.; Matsuya, S.; Nakagawa, M.; Ishikawa, K., *J. Mater. Sci.,* **42**, 7843, (2007).

76. http://encarta.msn.com/, Cross Section of a Bone. (2007).

77. Currey, J., *Handbook of Composites*. Elsevier Science Publishers B. V. 1983: 1983; p 501.

78. Suchanek, W.; Yoshimura, M., *J. Mater. Res.,* **13**, 94, (1998).

79. Tenhuisen, K.; Martin, R.; Klimkiewicz, M.; Brown, P., *J. Biomed. Mater. Res.,* **29**, 803, (1995).

80. Tampieri, A.; Celotti, G.; Landi, E.; Sandri, M.; Falini, G.; Roveri, N., *J. Biomed. Mater. Res.,* **67A**, 618, (2003).

81. http://encarta.msn.com/, Cross Section of a Tooth. (2007).

Chapter 2:

Experimental

2.1 Introduction

The main experimental techniques used in this research are centred upon the synthesis and modification of layered materials and their subsequent characterisation. The synthesis and modification of the phases produced will be discussed in more detail in the appropriate section in each chapter of this thesis. However, a general overview of the synthesis methods are described in sections 2.2.1 – 2.2.5.

Characterisation of the materials was performed primarily using powder X-ray diffraction as well as single crystal X-ray diffraction where appropriate (Sections 2.3.1 and 2.3.2 respectively). Thermogravimetric analysis (section 2.3.3) was used to study the stoichiometry of the phases produced from their decomposition pathways. Fourier transform infrared (section 2.3.4) analysis [FTIR] was used to determine some of the bonds present in the material and to compare stretching and bending frequencies between different samples. Environmental Scanning Electron Microscopy [ESEM] with Energy Dispersive Analysis of X-rays [EDX] was used on some of the materials produced (section 2.3.5) to analyse the morphologies of the crystals and give an approximate metal ion to phosphorus ratio. A more accurate metal ion to phosphorus ratio was determined using inductively coupled plasma with mass spectrometry (ICP-MS) described in section 2.3.6.

The samples produced for the calcium phosphate bone cements in Chapter 5 used further different analytical techniques than those described above. Additional compressive strength and setting time measurements were also performed on the cement samples that were prepared. Details of these procedures can be found in sections 2.3.7.1 and 2.3.7.2.

2.2 Synthesis Methods

2.2.1 Ceramic Method

This method involved the intimate grinding of a range of solid reagents in an agate pestle and mortar in order to reduce the particle size and enable mixing of reactant materials. High temperatures are usually required to enable diffusion of ions across reactant particle interfaces and therefore the resultant mixtures were heated in a crucible or alumina boat either in an oven or furnace to the required temperature for the reaction conditions.

2.2.2 Acid Flux Method

This method was used to produce the calcium acid pyrophosphate phase. The flux method involves an excess of orthophosphoric acid (the flux) with the required cation(s). On heating, condensation of the orthophosphoric acid occurred which eliminated water and formed the P-O-P cross links that produced the pyrophosphate ($P_2O_7^{4-}$) units. These pyrophosphate ions react with the cations present and crystallise out of the flux.

In this work, this involved intimately mixing 6.00g of orthophosphoric acid (85% by weight in water) with 1.29g calcium hydroxide (anhydrous) giving a 3:1 molar ratio to form a thick paste that was then heated in a crucible to 150°C for 12 hours to form the desired product.[2] Other ratios were used with some success, but this ratio produced the greatest quantity (per gram of reagent) of the desired phase. The sample was then filtered under suction and washed copiously with water to remove any excess acid or calcium hydroxide and left to dry in air, at room temperature.

2.2.3 Hydrothermal Synthesis

Hydrothermal synthesis methods were performed to, either, improve crystallinity in the metal alkyl phosphates produced or to provide more forceful conditions to enable

intercalation in the calcium pyrophosphate phases. Specific reaction conditions can be found in the synthesis sections in Chapters 3 and 6 respectively.

Experiments were performed in Parr hydrothermal bombs with 23 ml sized Teflon liners, which had a maximum operating temperature of 220°C. These liners were filled with 10 cm^3 of intercalating solution (approximately 50% filled) and then the solid phosphate material was added and the container screwed tightly closed.

2.2.4 Intercalation

It is well known that layered materials possess the capability to accommodate organic molecules and ions between their layers to form intercalation compounds.

A number of layered calcium phosphate materials were tested for their intercalation properties and a brief overview of the intercalation procedure has been described in this section. A more detailed explanation of the individual experiments attempted with any deviations from the procedure given here has been noted in the relevant experimental sections in Chapters 3 – 6.

A small quantity (0.3g) of the layered calcium phosphate was added to a sample bottle and an excess quantity of the intercalating species solution was added to this vial.

The intercalation experiments were initially attempted using monoamines from propylamine to octylamine. These were left either standing in the amine solution or were continually stirred for a 24 hour period in the sample vials.

After this time period, the sample was filtered under vacuum in a Buchner flask and washed with a suitable solvent. This washing was necessary to remove any intercalants from the surface of the material. When MCPM was present, ethanol had to be used as the solvent since MCPM was sensitive to water. Any water present caused the material to change phase

to brushite ($CaHPO_4(H_2O)_2$). Ethanol was capable of dissolving the amine before it could react with air to leave a solid deposit on the calcium phosphate surface. After washing, the sample was put into a sample vial and stored in a desiccator. This solid amine would be observed on the X-ray diffraction patterns produced and therefore had to be prevented from forming so the real intercalation peaks could be observed clearly.

To determine whether intercalation was successful, a small sample of the calcium phosphate was ground and a powder X-ray diffraction pattern collected (See characterisation techniques below). If this initial intercalation was successful, more complex intercalants such as diamines, triamines, alcohols, carboxylic acids and small drug molecules in solvent solutions were also attempted. The procedure for the addition of these molecules has been explained in more detail in later chapters of this thesis.

2.2.5 Exfoliation

The primary exfoliating agent was a tetrabutylammonium species (($C_4H_9)_4N^+$) [TBA] with counter-ion either of bromide or hydroxide (TBA-Br or TBA-OH respectively). Often this was performed on pre-intercalated samples given their greater potential for exfoliation. The choice of counter ion in exfoliating agents depended upon the pH which was required for the reaction. Bromide ions were less alkaline (~ pH 8) and thus could be used with most layered materials. The hydroxide species was quite alkaline (~ pH 10) and thus could react unfavourably with acidic phosphates such as MCPM. Both of these TBA species were solid at room temperature and thus were mixed with either water or ethanol (shown to be an inert solvent) depending upon the stability of the host phosphate material in water. Two concentrations of these solutions were made namely 0.25M and 0.5M.

The same 0.3g mass of the intercalated calcium phosphate samples was mixed with the TBA-Br ethanol solutions. Initially 0.25M solutions were used for the reactions. The

resulting suspension was then left to stand for a few days with X-ray diffraction analysis performed daily.

As TBA-Br is a crystalline solid material, this had to be completely removed from the calcium phosphate before an X-ray pattern could be collected otherwise this TBA pattern would be observed preferentially (due to strong reflections). This was completely removed by washing the material with copious amounts of water or organic solvent (ethanol) depending upon water stability considerations. The calcium phosphate materials generally had quite small particle sizes and had been observed sometimes to pass through filter paper. Thus an alternative filtering procedure was adopted when necessary.

This was accomplished by centrifuging the calcium phosphate material in solution, extracting the solvent by pipette and then rewashing with a further aliquot of solvent. A further centrifuging process was then necessary, in order to separate the small particulate solid material from the solution and to remove any traces of extraneous exfoliant species from the solid surface. At this stage the solvent and calcium phosphate could be separated and the solid material was dried in air before being analysed by powder X-ray diffraction.

2.3 Characterisation Techniques

2.3.1 X-ray Diffraction

2.3.1.1 X-ray Generation

X-rays are generated by the bombardment of a water cooled metal target (usually copper) with a beam of electrons that are produced by the heating of a filament, usually made from tungsten and then accelerating the electrons using a high voltage. The target emits a continuous spectrum of X-ray radiation (white radiation) with specific sharp and intense peaks which are dependent upon the metal used as the target. The energy of the electron beam that bombards the target is of a higher energy than required to remove an electron from one of the core orbitals of the metal. This 'hole' is then filled by an electron from a higher orbital which loses energy by the emission of X-ray photons of radiation. A copper target tube source was used throughout the X-ray diffraction analysis in this thesis. Copper is a relatively heavy metal and contains many orbitals. As such, there are a few different decay routes for the high energy electrons and thus the X-ray spectrum contains a few intense maxima due to these various transitions (most intense termed K_α and K_β peaks). To perform an X-ray diffraction experiment, a single wavelength of X-rays is preferred and thus a nickel metal thin foil is used to filter out the K_β radiation (Due to the higher energy of the K_β radiation causing excitation of the nickel atoms whereas the K_α radiation does not) and also a shaped germanium single crystal monochromator was used to give the required single wavelength ($K_{\alpha 1}$) of X-ray radiation.[1,3]

2.3.1.2 Diffraction of X-rays

Crystalline solids consist of atoms, ions or molecules which arrange in a regular pattern with approximately 1Å spacing between the crystal planes of the solid. For diffraction

to be effective, the wavelength of the incident radiation needs to be in the same order of magnitude as the spacing of the diffraction grating (crystalline solid). As such, a crystal can act as a 3-dimensional diffraction grating to X-ray radiation.
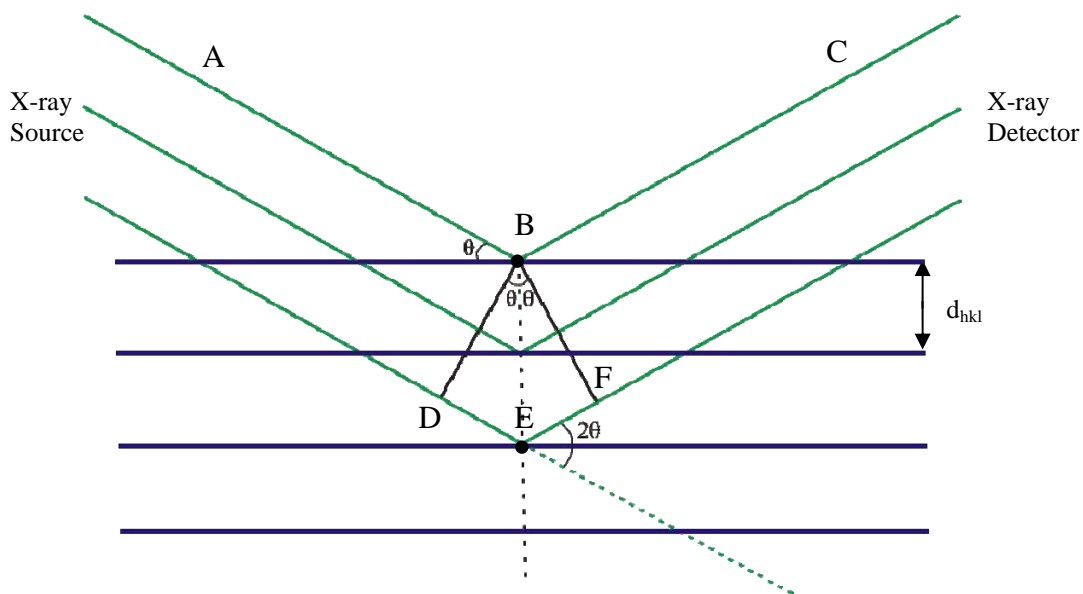
Figure 2.3.1.2.1: Schematic Representation of the Scattering of X-rays by Crystalline Solids

Figure 2.3.1.2.1 shows the required conditions for the diffraction of X-rays by a crystalline solid.[1] The horizontal lines represent the planes of the crystal with an interplanar spacing of d_{hkl}. A parallel beam of monochromatic X-rays is produced at position A and is incident on the crystal planes at an angle θ. The X-ray beam is scattered by the atom present at B and reflected back along C. When the beam intercepts the atom, some of the energy of this beam will be lost to excitation, thus a loss in intensity of the reflected X-ray wave will occur. A number of X-rays will need to interfere with each other constructively for a noticeable beam intensity to be detected from the reflected rays off the sample. Therefore, for constructive interference to occur, the path lengths of the reflected beams must differ by an integral number of wavelengths. This path length difference can be represented on figure

2.3.1.2.1 by the distance between DE+EF. As the path length needs to be an integer number of wavelengths (λ) then an equation can be written for this such that: -

$$n\lambda = 2d\sin\theta$$

This equation is known as the Bragg equation and is fundamental to the method of X-ray diffraction, as it relates the spacing of the planes, *d*, to the Bragg angle, *θ*, at which the reflections from those planes are observed.

2.3.1.3 Powder X-ray Diffraction

Polycrystalline materials are composed of many different, randomly ordered crystals. An X-ray beam hitting this sample would be diffracted in multiple directions. The best way to represent the scattering of X-rays is to treat each crystal as a series of planes of atoms. The separation between the planes is known as the d-spacing and equidistant planes make up the crystal structure. If the planes are separated by a distance similar to the wavelength of the X-ray beam then interference between the X-ray waves scattered from the electron centres of the atoms in planes can occur. If there is an ordered lattice within the crystal structure then the scattering will create interference maxima and minima. Thus as the crystallites can lie in all directions, the diffraction of the X-ray beam will produce 'cones' of reflected X-rays when the beams interfere constructively. If a detector is scanned through these 'cones' a signal will be produced and thus X-ray diffraction patterns are produced using intensity as a function of the detector angle, 2θ. (See figure 2.3.1.3.1).[1] Thus structural information was gained by studying the diffraction patterns obtained.
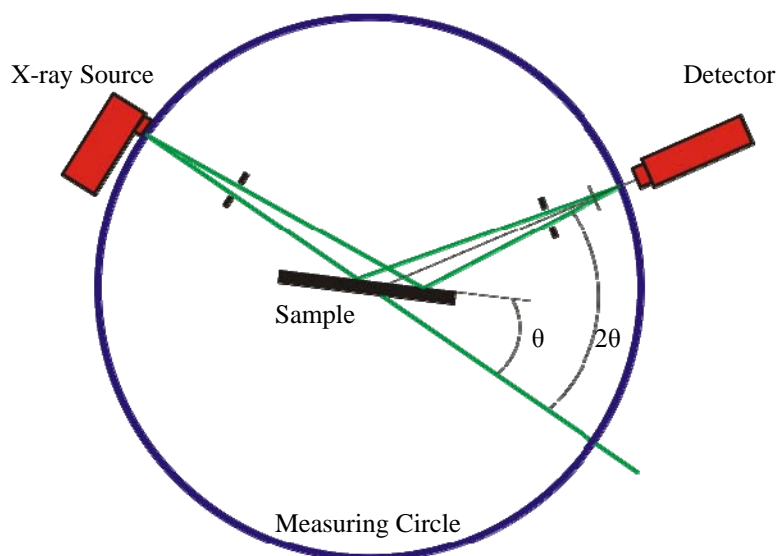
Figure 2.3.1.3.1: Schematic Representation of the Arrangement of a Powder X-ray Diffractometer (Reflection Mode)

This technique is especially useful because crystalline solids have characteristic diffraction patterns upon which a definite identification is generally possible. This analysis of powders and not single crystals is beneficial in this thesis as a vast majority of the samples synthesised were not suitable for single crystal X-ray diffraction.

Crystallite size influences the diffraction peak broadness in powder X-ray diffraction. To produce a sharp peak, to either side of the most intense part of the peak, the X-ray waves should interfere destructively and thus cancel each other to reduce the intensity surrounding the peak maximum to produce a sharp peak. However, as the size of the crystallites decreases, fewer crystal planes exist to diffract the X-ray beam sufficiently so that many waves can interfere destructively and thus a larger angle range will produce sufficient intensity to be detected and thus a much broader peak is observed.

2.3.1.4 Absorption Factor

A reduction in the intensity of the diffracted X-rays can be caused by some absorption from the sample. This reduction can be accounted for by the use of an absorption factor, A. When a diffractometer is used in reflection mode, there are fewer problems with absorption due to the X-rays being reflected off the sample towards the detector. However, if transmission mode is used, the X-rays must travel straight through the sample and this is where the vast majority of the absorption occurs. This is especially true if the sample contains heavy elements, such as lead, where the interactions with many electrons will increase the chance of absorption. Corrections can be made to samples relatively easily to reduce the effects of this phenomenon.

2.3.1.5 Powder X-ray Diffraction Instrumentation

The vast majority of the samples analysed at room temperature, in this thesis, were performed on a Siemens D5000 diffractometer. This instrument was set up in transmission mode with the sample being rotated at 15 rpm. The copper X-ray source used is both filtered and monochromated to use only the $K_{\alpha 1}$ X-ray radiation. The diffractometer scans through 2θ angles from 3 - 50°. The detector used was a position sensitive detector (PSD). All diffraction patterns collected were displayed as X-ray intensity versus 2θ.

Any data collected at higher than room temperature was performed using a Siemens D5005 diffractometer which has an *in situ* Anton Parr heating stage. The D5005 uses a nickel filtered copper X-ray source but is not monochromated and therefore both $K_{\alpha 1}$ & $K_{\alpha 2}$ X-ray radiation is produced. This means that further steps in the analysis need to be performed to remove the effects of the $K_{\alpha 2}$ X-ray radiation from the diffraction patterns. This instrument collects data in reflection mode through an angle θ-θ from 5 - 60° using a static alumina sample holder inside the heating stage.

2.3.1.6 Characterisation of Powder X-ray Diffraction Patterns

In order to characterise the diffraction pattern obtained, the phases were identified using the EVA X-ray evaluation software from Bruker-AXS[4] with an X-ray pattern database from the JCPDS (Joint Committee on Powder Diffraction Standards).[5] Computer programs CRYSFIRE[6], DSPACE[7] and CELL[8] were used on the observed diffraction peaks to obtain refined unit cell parameters.

CRYSFIRE is a MS-DOS based program developed by *R. Shirley*[6] which uses a variety of indexing programs to calculate possible unit cell sizes and parameters, based upon input diffraction peak positions. Once a sensible unit cell was determined from this program or using prior knowledge, DSPACE could then be used to assign *hkl* values based upon the space group and unit cell parameters. CELL[8] could then be used to refine the unit cell parameters using a least squares refinement method. This program automatically generated an estimate of the reliability of the results which was termed the R-Factor.

$$R = \sum_{i=1}^{nref} \varpi_i \left(\sin^2 \theta_{obs} - \sin^2 \theta_{calc} \right)^2$$

Where: - nref = number of reflections
ω_i = appropriate weighting

2.3.2 Single Crystal X-ray Diffraction

2.3.2.1 Single Crystal X-ray Diffraction Method

From a single crystal, it is possible to determine atomic positions, space group and unit cell from the position and intensity of the reflections. This technique is usually quick and quite versatile and as such is one of the most useful techniques available. It is possible to measure the position and intensity of all the *hkl* reflections without the problem of peak overlap and from the information gained, the whole structure could be determined.

Unfortunately single crystals are not easy to grow and it is not always the case that they are representative of the bulk material and thus this technique could not be used on all samples.

The interaction between an X-ray beam and a crystal is dependent upon the number of electrons within the crystal. Therefore the more electrons present in each atom that forms the crystal, the greater the scattering. This degree of scattering is termed the scattering factor (f_0) and its size is determined by the atomic number, the Bragg angle (θ) and the X-ray wavelength (λ).

In an atom, the electrons are distributed about the nucleus in a finite way and as the diffraction angle increases, the X-rays scattered from the electron interactions at one part of the atom are scattered increasingly out of phase to those from a different cross section of the same atom. Thus the X-rays interfere destructively and reduce the intensity and therefore, a decrease in the peak intensity is observed as the diffraction angle increases.

As a crystal is composed of multiple layers of atoms, the X-rays that interact with the crystal planes will be scattered in the direction of the *hkl* reflections from the unit cell which is determined by a mathematic formula called the *structure factor (F_{hkl})*. This factor is dependent upon the both the position of each atom and its scattering factor. Therefore if the structure factors are known, the electron density distribution can be calculated which will give the atomic positions within the unit cell.

Relating to structure factors, the intensity of the *hkl* reflection is proportional to the square of the structure factor. One problem with this method of data collection relates to the fact that the atomic positions need to be known to find the structure factors. Unfortunately, to find the atomic positions, the amplitude and phase of the resulting X-rays need to be known. However, in the calculation of the structure factor using the intensity of the reflected rays, a

square root is employed which means that the modulus of the structure factor is actually collected and thus the phase of the reflected X-rays is lost.

There are however methods that can be employed to create a set of trial phases for the structure factors and thus enable the crystal structures to be solved. There are two main methods to accomplish this phase analysis. The first is called the *Patterson* method which requires there to be at least one heavy atom in the unit cell as a reference and uses *Fourier transforms* of the intensity (rather than structure factors). This method calculates the interatomic distances weighted by the product of the number of electrons in the atoms concerned and therefore atomic positions can be deduced. The second method, the *Direct* method is used where structures have similar atomic weight species and thus their scattering factors are close. This method uses mathematical probabilities and statistical correlations to estimate the magnitude of the phase from the Fourier transform of the scattering density. From these values, the electron densities within the unit cell can be determined and refined and from these, the atomic positions can be calculated.

2.3.2.2 Single Crystal X-ray Diffractometer Setup

Single crystal X-ray data are collected by measuring the diffraction angle, 2θ and the intensity for each hkl reflection. A four circle diffractometer can be used whereby the crystal used can rotate about all 3 axes (χ,ω,φ) with the detector rotating around the fourth circle, 2θ, which is concentric with ω. A flat-plate detector or area detector is used so that many reflections can be recorded simultaneously thus reducing the sample analysis time significantly. A schematic representation can be seen in figure 2.3.2.2.1.

Indexing the diffraction data, taking into account systematic absences, will enable the Bravais lattice and translational symmetry elements of the crystal to be determined and thus reduce the number of possible spacegroups which the crystal could possess.
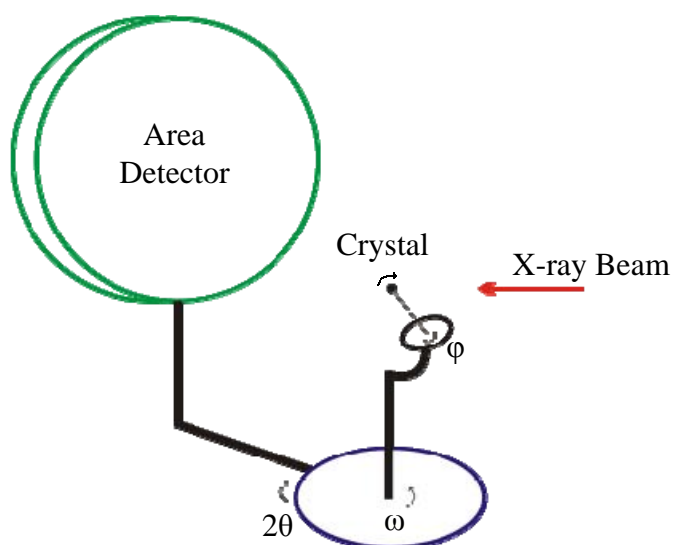
Figure 2.3.2.2.1: Schematic Representation of the Arrangement of a Single Crystal X-ray Diffractometer.

2.3.2.3 Single Crystal X-ray Diffraction Refinement

When the atoms in the structure have been located, further factors for the thermal motion of the atoms need to be taken into account. This depends on the temperature of the atom as well as the mass and bond strengths. This refinement procedure allows the electron density of each atom to form a sphere around the nucleus. This is usually referred as the *Isotropic Temperature Factor.* In addition, the electron density also has to be formed in an elliptical fashion around the nucleus and this parameter is defined as the *Anisotropic Displacement Parameter.*

A residual index (or R factor) can be calculated by comparing data with a simulated function to measure the difference between the calculated and observed structure factors (F_{obs} and F_{calc} respectively). This value is used as a guide to the correctness and precision of the refinement of the structure and is summed over all the data.

It is defined as: -

$$R = \frac{\sum |(|F_{obs}| - |F_{calc}|)}{\sum |F_{obs}|}$$

These R factors are used as only a guide to the quality of the data as it could be possible, but usually rare, to have a low R factor and the structure to be incorrect.

In summary, a single crystal X-ray diffraction method is capable of producing an accurate representation of the structure after appropriate refinement. However, for some materials it is not straightforward to produce pure large crystals to enable this technique to be utilised. In these situations, powder X-ray diffraction can provide some measure of phase analysis, particularly if similarities with patterns held on the database can be found (fingerprinting). However, this may not lead to complete structural detail. Thus other techniques are often needed to provide more information.

All single crystal diffraction experiments and calculations were performed by Dr. Benson Kariuki at the University of Cardiff. All single crystal data was collected on a Bruker Smart 6000 diffractometer at 23°C equipped with CCD detector and a copper tube source, with the crystal mounted on a glass fibre using epoxy resin. A structure solution and refinement was performed using SHELXL.[9] Thermal factors for all atoms were refined anisotropically.

2.3.3 Thermogravimetric Analysis (TGA) with Differential Thermal Analysis (DTA)

This method involves performing a precise measurement of the weight change of a small (< 50mg) sample of the material of interest as it is heated in a small alumina vessel, through a temperature range at a controlled rate. Often, linked with this analysis is differential thermal analysis (DTA). When a phase change occurs in a sample, either an absorption or release of thermal energy will occur. A second 'inert' material in another sample boat is used as a reference to the material that is being analysed. In most cases, finely ground alumina is used as the reference material as it will not undergo any mass of phase changes during

experiments. When both vessels are heated at the same controlled rate in the TG furnace, the difference in temperature between the reference and the sample is recorded. The balance itself uses a finely balanced cantilever which will move slightly up or down when the sample loses or gains mass. Measurement of these changes is converted into a mass loss that is recorded on the instrument.

When using the TGA, a ramp time of 5°C/min was generally used from room temperature up to 1000°C. However, the actual heating rates used and temperatures were sample dependent and were dealt with in the individual sections of this thesis. In the case of MCPM samples (Chapter 4), isotherms were also employed so that crystallisation water was removed at certain stages so that further mass losses not associated with this crystal water could be seen more clearly.

Thermogravimetric analysis was performed on a Stanton Redcroft STA-780 thermogravimetric analyser. This instrument was used to measure the mass changes of a sample as a function of increase in temperature with all thermal events monitored *in situ*. This instrument uses a pen-plotting system to record data and interpretation was based upon analysing the charts produced. This relatively old system was used due to its better tolerance to the release of carbon from the samples analysed. Where no carbon components were present, a Rheometric Scientific STA 1500 instrument was used due to the increased sensitivity and resolution. All experiments were conducted in air.

2.3.4 Fourier Transform Infrared Analysis (FTIR)

2.3.4.1 Fourier Transform Infrared Theory

This technique arises from the characteristic bond vibrations that occur in all materials when they are at a temperature above absolute zero. The use of an infrared laser enables vibrational excitation of the bonds and relaxations of these vibrations back down to the

ground state will emit characteristic infrared radiation at specific wavelengths that are detected and plotted. The data produced are then Fourier transformed to produce the classic infrared spectrum. This spectrum can be displayed either in absorbance or transmission modes in which case either peaks or troughs will be observed respectively. The FTIR spectrum shown in figure 2.3.4.1.1 is displayed in transmission mode which will be used for all FTIR spectra shown in this thesis.
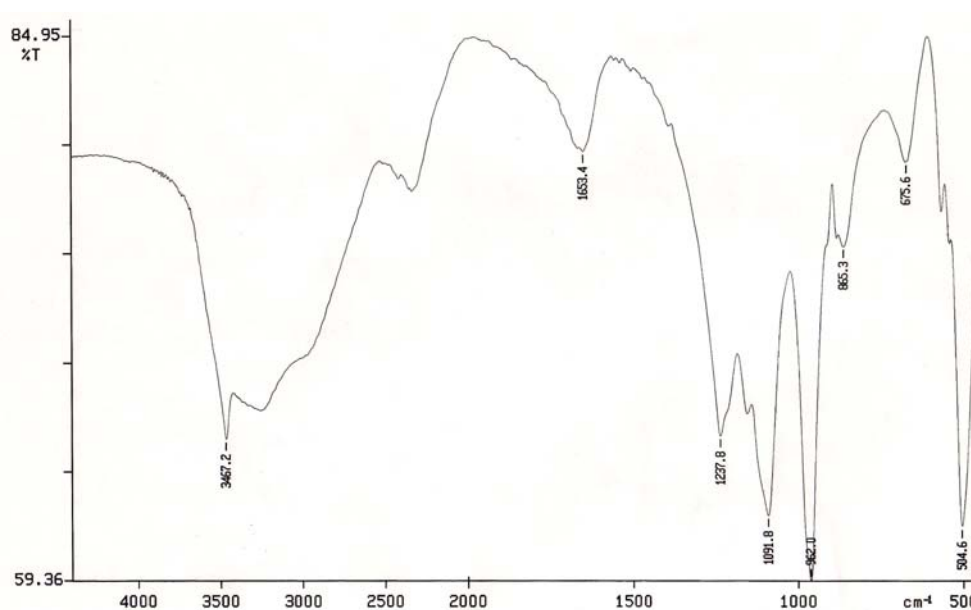
Figure 2.3.4.1.1: Infrared Spectrum of MCPM

The scale used on the infrared spectra is usually recorded in wavenumbers (cm^{-1}), which is derived from the number of wavelengths per cm. This nomenclature is not officially an SI unit; however, convention dictates how the spectrum is displayed.

In order for a material to be infrared active, there must be a change in dipole during the vibrational excitation. Thus most homonuclear diatomic molecules (H_2 etc.) possess no permanent dipole. However, most of the molecular species presented in this thesis were

heteronuclear molecules and thus were likely to possess a dipole moment due to the differences in electronegativity between the constituent atoms.

Fourier transform infrared (FTIR) was used to measure the absorption of infrared radiation at specific wavelengths of the compounds produced in this thesis. The main purpose of this type of analysis was for the identification of specific functional groups in the samples tested.

The principle behind this type of analysis is the use of infrared energy to promote bond vibrations within a material. There are two types of excitation that are possible. These are stretching and bending modes, of which stretching modes are usually of higher energy (See figure 2.3.4.1.2).

Stretching Vibration

Bending Vibration
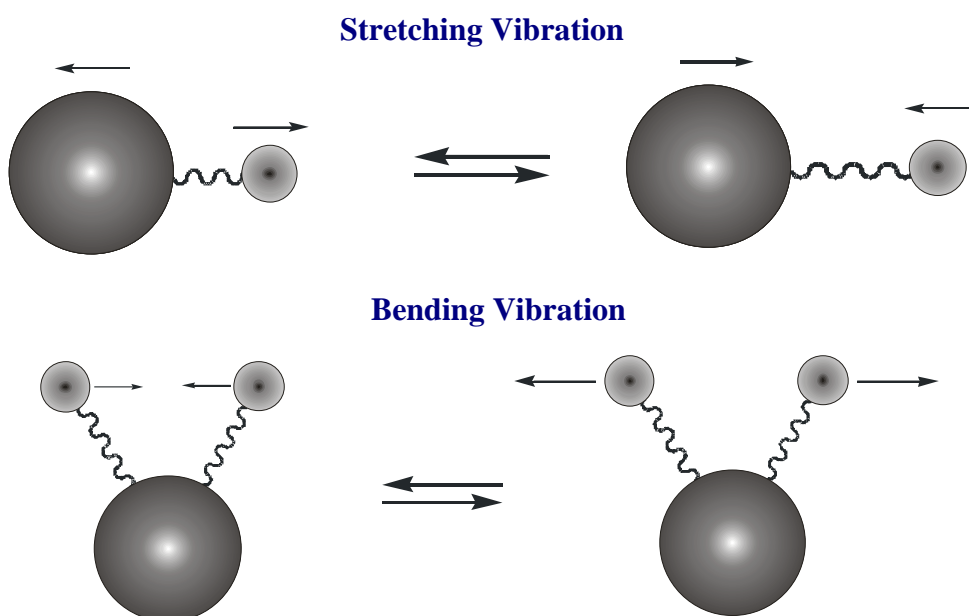
Figure 2.3.4.1.2: 'Ball and Spring' Schematic Diagram Depicting the Two Types of Vibrations Within Molecules. (adapted from[1])

The vibration diagram in figure 2.3.4.1.2 above shows vibration on one or two bonds only, however, these particular vibrations cannot be considered in isolation as sometimes it is

possible that vibrations within a complex molecule will interact and thus cause shifts in the specific wavelength from the isolated vibrational frequency. In addition, the use of liquid films can have increased complexity due to the presence of hydrogen bonding from some of the solvents that could have been used.

There are three generalisations that can be applied to gauge the frequency range of a specific bond vibration within a complex molecule.

1) Bond stretching requires more energy than bond bending and thus stretching frequencies are generally higher due to the shorter wavelength radiation (inversely proportional to frequency).

2) The smaller the mass of the bond, the greater the energy required to excite the bond. Thus O-H and C-H bonds stretch at higher frequency than C-O and P-O.

3) Double and triple bonded species require higher energy for vibrational excitation than single bonds. Thus P=O stretches at a higher frequency than P-O or C-O.

The exact number of vibrational modes can be calculated based upon the number of atoms, *n,* present in the molecule. The number of vibrational modes for non linear molecules is determined by the formula *(3n – 6)*.[10] Thus ammonia (NH_3) possesses 6 modes; however, some of the modes possess the same energy and are thus classed as degenerate. Furthermore, the nature of infrared spectroscopy relies upon a fluctuating dipole, therefore symmetric stretches are generally not observed on IR spectra (see figure 2.3.4.1.3). Weak absorptions could be observed if molecular deformations occurred during the symmetric stretch.

Stretching Modes

Symmetric   Antisymmetric

Bending Modes

Scissoring   Rocking   Twisting   Wagging
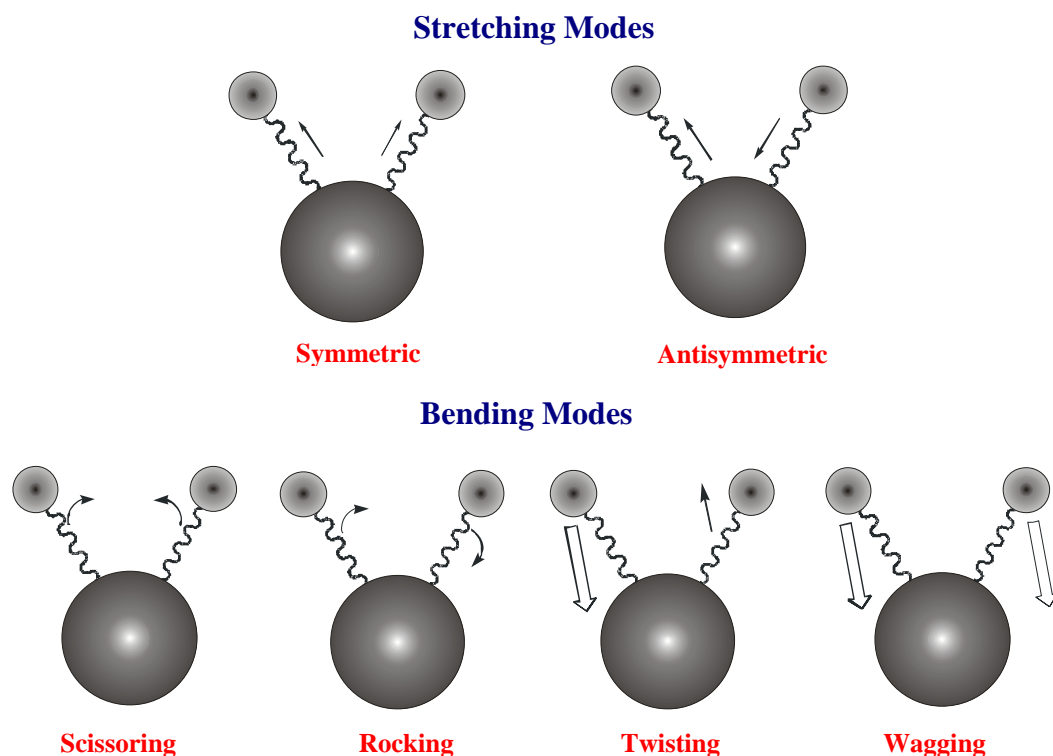
Figure 2.3.4.1.3: Vibrational Modes of a Triatomic Molecule (adapted from[1])

2.3.4.2 Fourier Transform Infrared Instrument

This type of instrument uses a radiation source which is an electrically heated filament, either of a Nernst type (Mixed Zr, Th and Ce oxides) or a Globar (silicon carbide) type to generate the infrared radiation.

The infrared beam produced from the source initially passes through a beam-splitter to separate the beam into two parts, the first passes through to a moving mirror that enables the wavelength of the beam to be altered and then reflects back to the beam splitter where it will be further reflected through the sample and then to a detector (See figure 2.3.4.2.1).[11] The second part of the initial beam will pass through a stationary mirror before reflecting back through the beam-splitter. When both parts of the beam interact at the beam-splitter, interference occurs. This beam will be reflected from the beam-splitter through the sample to the detector. Thus the modulation of the mirror is important to produce a series of

wavelengths that are coherent (integer wavelengths difference between the two beams) then a signal will be obtained, whose absorption intensity can be measured and Fourier transformed to produce an absorption curve on the spectrum.

The moving mirror is tracked across a pre-determined distance to enable the full range of wavelengths (and thus wavenumber ranges) to be observed, Fourier transformed and reconstructed to form the infrared spectrum.
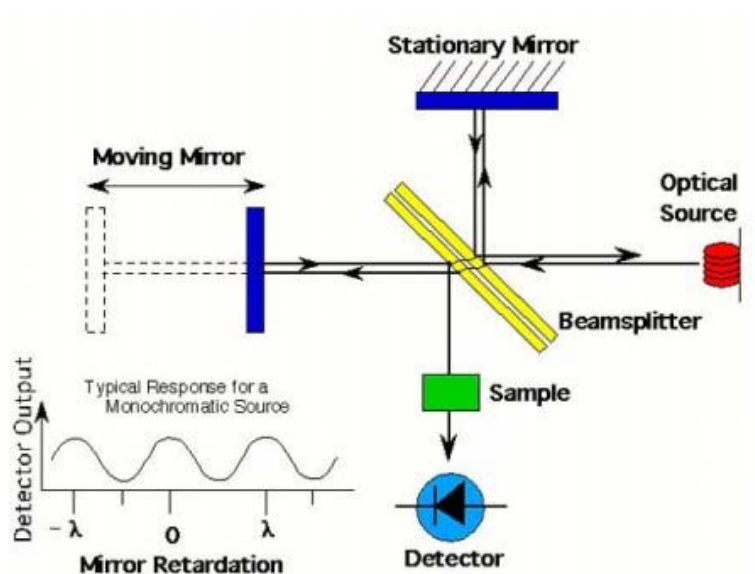
Figure 2.3.4.2.1: Schematic representation of a FTIR Spectrometer

As the energy of the infrared radiation is varied across a range, at certain frequencies, bonds will absorb the energy and resonate. These are characteristic of the bond type and therefore a drop in transmitted intensity will be recorded by the detector and displayed on the infrared spectrum produced.

Samples were prepared by one of two methods. If a liquid sample was used, a drop of the neat solution was placed on a solid polished sodium chloride disc and a second disc placed on top to form a liquid film between the discs. If however, a solid material was to be analysed, then this was mixed with excess solid potassium bromide (spectroscopy grade) and then a

small quantity (10 mg, half microspatula size) of the sample added and ground together with ~ 4 microspatula amounts of KBr. This material was then pressed into a pellet. The action of the increased pressure turned the white KBr into a transparent glassy disc, provided the sample and KBr were reasonably dry.

2.3.5 Scanning Electron Microscopy

To investigate the appearance of samples produced, scanning electron microscopy (SEM) was employed. This microscope uses electrons rather than light to image the materials under investigation. The electron beam is produced by heating a tungsten filament and focussed using magnetic fields and the beam accelerated using a large potential difference (many kV) with the sample and machine kept under high vacuum. By scanning with an electron beam, an image is formed from the electrons reflected off the surface and secondary electrons ejected from the sample hitting a detector. This technique is widely used in the characterisation of solids to determine the structure, morphology and crystal size as well as to study any defects present. SEM can produce a much greater degree of magnification than standard optical microscopes, partly due to the short wavelength of the electrons and therefore, quite small particles can be analysed.

2.3.5.1 Scanning Electron Microscopy Instrument

For the majority of the samples, a Philips XL30 ESEM-FEG microscope was used due to the fact that this could set up for 'wet mode' which enables a damp atmosphere to be maintained under a partial vacuum. This reduces the drying effects upon the samples thus maintaining some of the crystallisation water that might be present in the sample during the analysis using this technique. This mode is not available on many SEM microscopes and as such this machine is termed an *Environmental Scanning Electron Microscope* (ESEM).

2.3.5.2 Energy Dispersive Analysis of X-rays (EDAX)

When an electron beam is incident on a surface, the emission of characteristic X-rays from that surface occurs. Thus the use of an electron microscope will also generate these characteristic X-rays. These can be detected and will give qualitative analysis of the elements (above atomic number 11) present in a sample.

2.3.6 Inductively Coupled Plasma Analysis Linked to Mass Spectrometry (ICP-MS)

This type of analysis uses high temperature plasma to enable samples to be analysed. Plasma is a gaseous phase which is composed of a high concentration of ions and electrons to make the gas electrically conductive. The plasma itself is generated using argon gas that is then ionised ($Ar \rightarrow Ar^+ + e^-$) by pulsing a radio frequency through the water cooled coil that surrounds the quartz torch (see figure 2.3.6.1). This generates an intense magnetic field which enables acceleration of the ions within the gaseous plasma. The plasma, by virtue of its formation, is neutrally charged due to the equal composition of both positive ions and negative electrons.

The inductively coupled plasma (ICP) is sustained in a torch that consists of three concentric quartz tubes. The end of this torch is placed inside an induction coil supplied with a radio-frequency electric current. A flow of argon gas passes through the two outermost tubes of the torch and an electrical spark is applied for a short time to introduce free electrons into the gas stream. These electrons interact with the radio-frequency magnetic field of the induction coil and are accelerated first in one direction, then the other, as the field changes at high frequency. The accelerated electrons collide with argon atoms, and ionise them, thus releasing further electrons. The released electrons are in turn accelerated by the rapidly changing magnetic field. The process continues until the rate of release of new electrons in

collisions is balanced by the rate of recombination of electrons with argon ions. This produces the vast majority of the plasma which contains argon atoms with a rather small fraction of free electrons and argon ions. The temperature of the plasma is high with the ability to reach up to 10000 K, although 7000K is the standard operating temperature.

The plasma is retained in the quartz torch by a flow of gas between the two outermost tubes to keep the plasma away from the walls of the torch. A second flow of argon is usually introduced between the central tube and the intermediate tube to keep the plasma away from the end of the central tube. A third flow of gas is introduced into the central tube of the torch. This gas flow passes through the centre of the plasma, where it forms a channel that is cooler than the surrounding plasma and is aimed at allowing introduction of the sample to be analysed (see later).

Samples to be analysed are introduced into this central channel by passing the liquid sample into a nebuliser. This device creates a very fine aerosol from the liquid introduced which was then swept into the plasma using the argon carrier gas through the central channel.

As a droplet of nebulised sample enters the central channel of the torch, it evaporates and any solids that were dissolved in the liquid vaporise and then break down into atoms due to the very high temperature. At the high temperatures in the plasma and due to the number of collisions with the free electrons, a significant proportion of the atoms from the introduced sample are ionised, each atom losing its most loosely-bound electron to form a singly charged ion. Due to the high ionisation energy of argon, it is more favourable for argon ions to remove an electron from the plasma and revert back to argon atoms rather than to remain charged and allow further ionisation of the introduced sample ions in the plasma. Thus singly charged ions are produced from the sample that was introduced into the plasma.
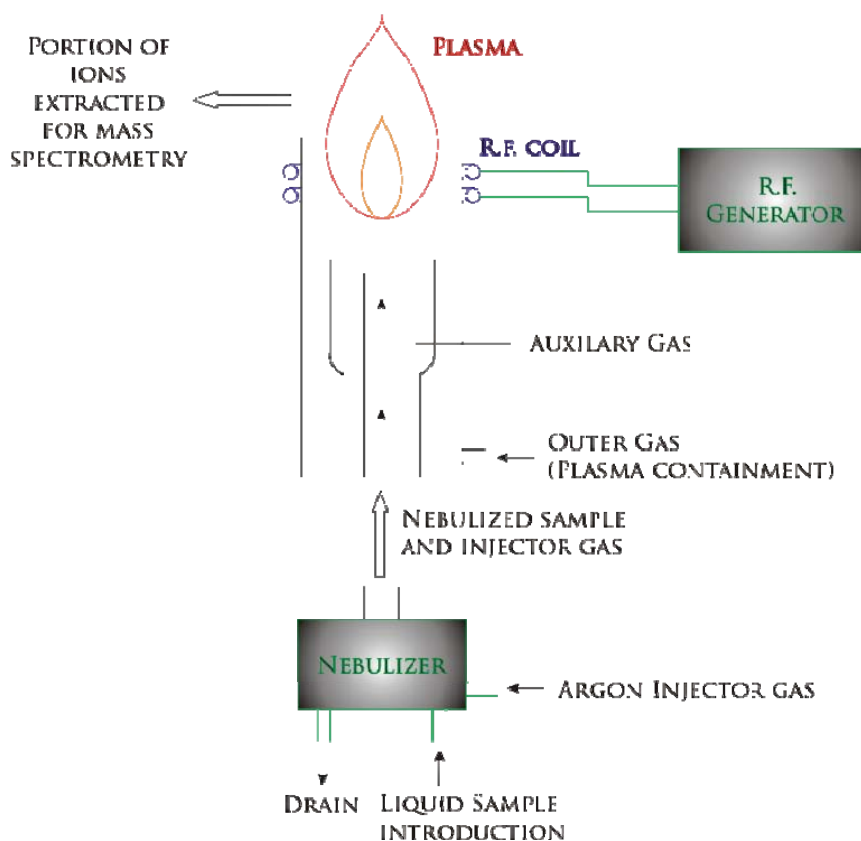
Figure 2.3.6.1: Schematic Representation of an Inductively Coupled Plasma Torch Linked with a Mass Spectrometer

ICP-MS Sample Preparation

ICP-MS samples were prepared by dilution in weak nitric acid (2% by mass) to provide a solid-free solution that could then be introduced into the ICP instrument. In general, 100 mg of sample was added to 100 cm^3 of the 2% nitric acid standard in a volumetric flask.

2.3.6.1 Elemental Analysis of Inductively Coupled Plasma Using Mass Spectrometry

A portion of the ions from the plasma torch are extracted due to the creation of a partial vacuum which is required to enable the mass spectrometer to function. These ions are then focused through a series of cones which are under a much lower pressure. This reduces the number of ions entering the spectrometer and produces a more homogenous beam. Extraneous particles and photons can be removed by guiding only the ions along a different

path to these other species. The ions that enter the mass spectrometer are separated on the basis of their mass-to-charge ratio using a quadrupole and a detector receives an ion signal proportional to the concentration. The concentration of a sample can be determined through calibration with elemental standards.

2.3.7 Bone Cement Characterisation Techniques

Two additional techniques were used on the calcium phosphate bone cements that were produced in Chapter 5 of this thesis. The two techniques were used to measure additional properties of the calcium phosphate cements. Ultimate compressive strength measures the strength of the set materials, whereas the Gilmore Needles measure the setting times for the cements.

2.3.7.1 Ultimate Compressive Strength Measurement

Measurements were made to obtain the compressive strength of the brushite cement samples produced in this thesis. The samples were prepared using a PTFE mould which kept the diameter and length of each sample constant at 6mm diameter with a length of 15 mm. Each cylinder was carefully measured in advance and only whole cylinders with no obvious defects were used.

A Dartec HC-10 hydraulic press with a separate compressor using a 2 kN flat plate load cell was used for all measurements. A maximum compression of 1 kN was enabled so that no damage to the instrument could occur and was sufficient to allow all samples to break before this limit was reached. The sample cylinders were placed between the load plates and a single cycle compression was enabled and the data capture was set to record the maximum load before the cylinder breaks.
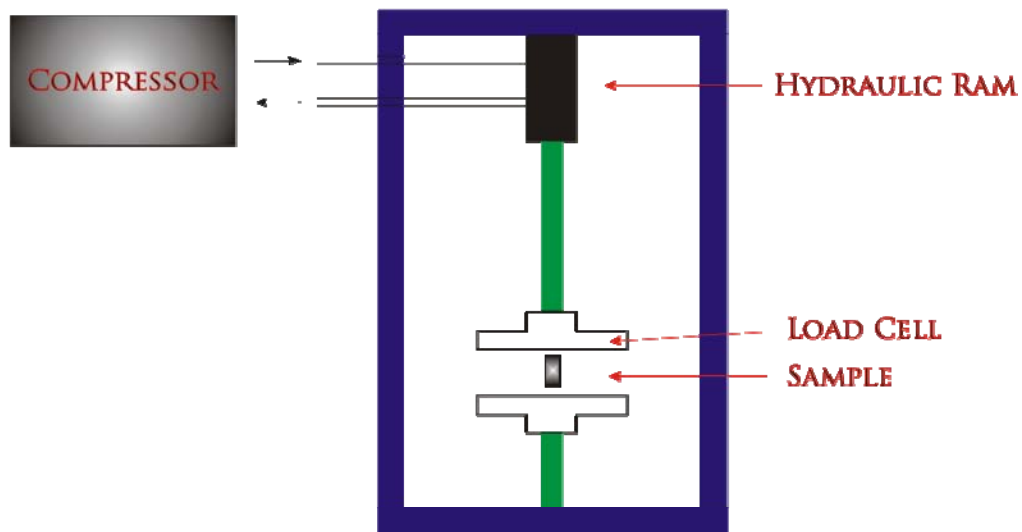
Figure 2.3.7.1.1: Simplified Schematic Representation of the Hydraulic Press for the Compressive Strength Measurements

2.3.7.2 Gilmore Needles Measurement

This method involved the use of a needle which was applied to the surface of the setting cement. The point at which no indentation was seen on the surface of the cement was deemed to be the setting time. The setting time for the cement is composed of two values, the initial and final setting times. To find the initial setting time, a needle of 2.13mm in diameter and 113.4g in weight was placed on the surface of the material every 30 seconds and balanced for 10 seconds on the surface. Once no impression was left, the initial setting time is known. The final setting time was determined using another needle with a smaller diameter of 1.05mm and a mass of 454g. Once again it is measured at 30 second intervals after the initial setting time has been determined and once again, when no impression was observed, the final setting time has been reached.

A cement cylinder was used for this test with a diameter of 8 mm and length of 15mm. The larger diameter was chosen to give a greater surface area for the needle tests. This

ensured that a new position could be chosen for successive indentation tests. This would

prevent increased compaction of the cement which could potentially give invalid results.

2.4 References

1. Smart, L.; Moore, E., *Solid State Chemistry*. CRC Press: 2005.
2. Webb, L. Synthesis and Characterisation of Calcium Phosphate Biomaterials. University of Birmingham, (2007).
3. Weller, M., *Inorganic Materials Chemistry*. Oxford University Press: 1994.
4. *EVA X-ray Evaluation*, Bruker-AXS.
5. *Joint Committee on Powder Diffraction Standards (JCPDS)*, 1999.
6. *CRYSFIRE*, Shirley, R., Guildford, Surrey: 2002.
7. *DSPACE*, Greaves, C., University of Birmingham: 1982.
8. *CELL*, Pye, M., Inorganic Chemistry Laboratory, Oxford.
9. *SHELXL*, Sheldrick, G., University of Gottingen.
10. Harwood, L.; Claridge, T., *Introduction to Organic Spectroscopy*. Oxford University Press.
11. NIST; What is a Fourier Transform Spectrometer. "http://physics.nist.gov/Divisions/Div842/Gp1/fts_intro.html ", (2002).

Chapter 3:

Formation and Characterisation of Calcium Alkyl Phosphates and their Analogues

3.1 Introduction

Calcium phosphate materials are of particular interest due to their similarity to natural hard tissue within the body (e.g. teeth and bone) and thus they possess inherently high biocompatibility. The use of these biomaterials in medical devices and cements is increasing rapidly but their properties are yet to be optimised for use within the body. The isolation of new calcium phosphate materials is therefore an important route to the development of new biomaterials with improved properties. A key advantage of using calcium phosphates is that they are easily resorbed by the body. This provides a ready supply of ions as raw materials to regenerate the natural calcium phosphate structures present in the human body.[1]

There has also been significant recent interest directed towards layered phosphates, which have the ability to intercalate organic species within their layers and thus form inorganic/organic hybrid materials.[2-4] Such hybrid materials offer the opportunity to tailor their properties through appropriate control of the organic and inorganic components.[5] Although most host structures that have been studied are based on silicate clays, phosphates have also been shown to successfully form hybrid structures. One example is a family of structures based on zirconium phosphates, whose structures have been shown to intercalate organic species between their layers and thus form inorganic/organic hybrid phases.[6-9] Although zirconium phosphates are relatively biocompatible they do not resorb particularly effectively. The research therefore seeks to discover similar structures to those of the clays and zirconium phosphates, but composed of calcium phosphate.

Past interest in calcium phosphate materials has been centred on their use as a fertilizer and more recently as a potential biomaterial.[10-12] However, to date, little research appears to have been undertaken on exploring layered calcium phosphates, in particular, as hosts for hybrid materials. Calcium phosphates can be generally classified as bioactive

ceramic materials because they can bond with living tissues. Therefore, calcium phosphate materials which also contain various organic species would offer significant potential for novel biomaterial behaviour.[13-15]

As mentioned previously, reports on the preparation of hybrid materials containing phosphate have been relatively limited, with the most well studied being the zirconium phosphates.[7,8,16,17] However, one interesting group of phosphate materials that do not rely on the intercalation of host materials, have recently been reported. These materials are synthesised from alkyl phosphates where the organic moiety is covalently bound to the phosphate unit. Examples of metal alkyl phosphates include those with calcium ($ROPO_3Ca \cdot 1.7H_2O$ (R=alkyl group))[18,19], titanium ($(ROPO_3)_2Ti \cdot 0.44H_2O$)[20] and aluminium ions ($ROPO_3Al(OH) \cdot 1.2H_2O$)[21]. Although no crystal structures for these materials have been reported, powder diffraction data presented suggests these materials possess a layered structure.

The alkyl phosphate intermediates mentioned above are related to the class of species known as phosphate esters. These phases are formed using a similar procedure to the production of organic esters, using reactions between acids and alcohols. One particular use for the ester formation reaction is in sol-gel chemistry for the formation of phosphate glasses[22] and other products.

Organic esters are prone to hydrolysis and as such will be broken down to the acid and alcohol components. The same would be true of the phosphate esters, but due to the higher electronegativity of phosphorus, hydrolysis is much slower and thus the alkyl phosphates produced will be more stable in aqueous solutions, even when acidified. The hydrolysis reaction is proposed to occur via an S_N2 nucleophilic attack of water on the P – O – R bond[22] and thus when a water molecule binds to the phosphorus, a slight δ+ charge will be generated

with a δ- oxygen on the water. With phosphorus, this δ+ charge is likely to be smaller compared to carbon and therefore the hydrolysis, although still possible, is likely to be less favoured and therefore slower.

Reports in the literature[18,20,21] suggest that the formation of these hybrid alkyl phosphate phases into layered structures appears to occur with alkyl chain lengths greater than 5 carbon atoms long (pentyl) using the method first reported by *Nelson and Toy*.[23] These reports mainly concentrated on producing structures with 5 – 10 carbon atom alkyl chains lengths but contain no information on whether the shorter chain versions of these materials have been investigated or whether modified chains were possible. Furthermore, these metal alkyl phosphate phases have been reported for divalent, trivalent and tetravalent cations with no mention of any monovalent cations, thus there is much potential scope for further investigation of biocompatible phases.

Alternatives to *Nelson and Toy's*[23] route to producing alkyl phosphates have also been suggested,[24,25] however, to date, most produce mixed intermediates of mono- and dialkyl phosphates. This causes additional problems in the separation of these intermediates, as well as requiring greater sample sizes to produce the same yield of material.

Alkyl phosphate intermediates have also been used to modify existing materials to increase their hydrophobic character as the presence of alkyl chains, particularly bound to a surface, would increase the hydrophobic nature of the material. This is important when considering composite formation where a homogenous distribution of components is required. Mixtures of hydrophobic and hydrophilic components can lead to problems with agglomeration. A more homogenous distribution of components is possible with the treatment of inorganic surfaces with a hydrophobic "coating". This is commonly used in nanocomposite materials composed of polymers and nano-dimensional inorganic fillers.[13,14] Similarly, if a

layered material is modified with alkyl phosphate, there is increased potential for the material to exfoliate when placed in an organic solvent, due to the solvation of the alkyl chains that will disrupt the interlayer bonding. This methodology has also been attempted with calcium carbonate to reduce the particle size for use as fillers for applications in plastics and rubber to increase their stiffness. In this example, octadecyl dihydrogen phosphate has been used to coat the material and provide a more hydrophobic surface.[26] Examples of the use of alkyl phosphates in surface modification of materials include the formation of self-assembled monolayers[27] from alkyl silanes on silicon oxides[28] to aluminium phosphates to modify catalytic processes.[29]

Thus, the main aim of this section of the thesis was to investigate the formation and characterisation of biocompatible hybrid metal phosphates with monovalent and divalent cations.[7,8,17] In addition, an investigation into the use of alkyl phosphate intermediates in the modification of pre-made calcium phosphates was undertaken to assess their effectiveness in nanocomposite formation.

3.2 Experimental

3.2.1 Preparation of Straight Chained Metal Alkyl Phosphates

The synthesis of the metal alkyl phosphates was achieved by a two step reaction adapted from *Tanaka et al.*[18,19] and *Nelson et al.*[23] A liquid alkyl phosphate was prepared from 0.056 moles of pyrophosphoric acid and the appropriate mass of alcohol (see table 3.2.1.1). These reagents were mixed in a 1:1.1 alcohol to pyrophosphoric acid ratio. To the resultant solution was added 10 cm^3 of hexane to increase the general volume and the mixture was stirred at room temperature for 48 – 72 hours. The solution was kept dry by the use of a calcium chloride guard tube. After this time, the organic alkyl phosphate phase was separated by washing with 3×20 cm^3 water portions and a 10 cm^3 portion of hexane.

Table 3.2.1.1: Mass of Alcohol to Use in Preparation

Alcohol to Use	Mass (g)
Pentanol	4.928
Hexanol	5.730
Octanol	7.280
Decanol	8.848

The alkyl phosphate, in 10 cm^3 of hexane, was then added to 6.1×10^{-3} moles of metal hydroxide or nitrate in 300 cm^3 of de-ionised water (see table 3.2.1.2) and the resultant colloidal suspension was aged at 100°C for 18 – 24 hours in order to produce the metal alkyl phosphate. Longer heating periods were trialled up to a maximum of seven days. The solution was then filtered under vacuum with further water washing which removed any un-reacted metal hydroxide or nitrate. The residue was a white platy solid. This procedure was performed with calcium, magnesium and strontium salts to produce the metal alkyl phosphates. The reaction scheme for the above procedure is shown in figure 3.2.1.1.

Table 3.2.1.2: Mass of Metal Hydroxide to Use in Preparation

Metal Hydroxide	Mass (g)
Strontium Hydroxide Octahydrate	1.626
Magnesium Hydroxide	0.355
Calcium Hydroxide	0.45
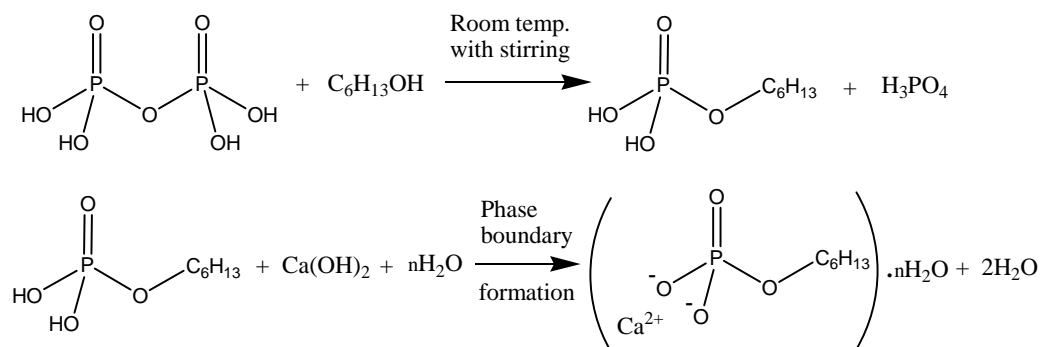
Figure 3.2.1.1: Reaction Scheme for Calcium Alkyl Phosphate Formation.

3.2.2 Calcium Alkyl Phosphates - Larger Crystal Formation

In an attempt to produce larger crystals for structural analysis, a more concentrated reaction solution was used in the formation of calcium alkyl phosphates. Here, 0.45g of calcium hydroxide was weighed and added to 100 cm^3 of water. To this solution was added either 1.11g of hexyl phosphate or 1.28g of octyl phosphate as used in the standard reaction scheme.

Equally, dilute reaction solutions were also employed to determine whether this effect would aid the production of larger crystals. This method used 0.15g of calcium hydroxide in 300 cm^3 of water, with 0.370g of hexyl phosphate or 0.427g of octyl phosphate in 10 cm^3 of hexane, added to this solution. The standard procedure was applied to this material to form the required calcium alkyl phosphate.

3.2.3 Preparation of Monovalent Alkyl Phosphates

The same experimental procedure in section 3.2.1 was used to prepare the monovalent metal alkyl phosphates. One minor difference involved the use of twice as much monovalent metal hydroxide in order to keep the correct stoichiometry for the product. The list of species used is shown in table 3.2.3.1.

Table 3.2.3.1: Table Showing the Relevant Masses and Ions Used to Prepare Monovalent Alkyl Phosphates

Cations Used	Mass or Volume Used	Alkyl Phosphate Used
Sodium	0.2432g NaOH	1.11g Hexyl phosphate
Ammonium	3 cm^3 NH$_4$OH	1.11g Hexyl phosphate
Ammonium and sodium	1.5 cm^3 NH$_4$OH and 0.1216g NaOH	1.11g Hexyl phosphate
Ammonia solution 35%	0.3 cm^3 ammonia solution in water	1.11g Hexyl phosphate
Ammonium and calcium	1.5 cm^3 NH$_4$OH and 0.225g Ca(OH)$_2$	1.11g Hexyl phosphate
Sodium and calcium	0.225g Ca(OH)$_2$ and 0.1216g NaOH	1.11g Hexyl phosphate

The final two samples included divalent calcium to test whether a mixed phase product could be formed.

3.2.4 Preparation of Branched Alkyl Phosphates

The same experimental procedure in section 3.2.1 was used to produce branched phases. To 5.5g of pyrophosphoric acid was added 3.646g of 2-ethyl-1-hexanol (Fluka Chemicals), 5.216g of 2-butyl-1-octanol (Fluka) or 2.864g of 3-hexanol (Aldrich) with continuous stirring for 3 days. After the designated stirring period, the alkyl phosphate intermediates were separated using the hexane/water method described in section 3.2.1. This was followed by reaction with a calcium solution again, as described for the straight chained alkyl phosphates. The usual mass of calcium hydroxide was added in 300 cm^3 of de-ionised

water and heated to 100 °C for 19 – 24 hours to produce the calcium analogue. The appropriate stoichiometry for the reaction required 1.281g of 2-ethyl-1-hexyl phosphate, 1.629g of 2-butyl-1-octyl phosphate or 1.110g of hexyl-3-phosphate. Strontium analogues of these materials were prepared using 1.626g of strontium hydroxide octahydrate in water with the above masses of intermediate alkyl phosphate.

3.2.5 Cyclohexyl and Aryl Phosphate Preparation

As an alternative to the straight chained alkyl phosphates targeted above, two cyclic compounds were attempted. The first phase involved a cyclohexyl phosphate form. This was accomplished by using the methodology described in section 3.2.1. In this case, 2.8g of cyclohexanol was mixed with 5.5g of pyrophosphoric acid with an additional 5 ml of hexane added to increase the volume. This sample was left to stir at room temperature for 3 days, where a pale orange-brown coloured liquid was formed. This was washed and separated in the usual manner.

The second compound prepared involved a phenyl phosphate, which was prepared by reacting disodium phenyl phosphate ($Na_2C_6H_5PO_4$) with a 25:1 ratio of calcium ions. The source of calcium was a 90% calcium chloride (9.744g): 10% calcium hydroxide (0.728g) mix in water and a water solution containing 1.14g of disodium phenyl phosphate was added. All chemicals were purchased from Aldrich chemical company.

This phenyl phosphate reaction was further repeated using ethanol as the solvent in order to determine whether solvent influenced the formation of the reaction product. 0.25g of sodium phenyl phosphate was dissolved in 10 cm^3 of ethanol to form a colourless solution. To this was added another colourless solution of 0.1968g calcium chloride in 10 cm^3 of ethanol. The ethanol solvent contained a small amount of water to enable solvation of the sodium phenyl phosphate and calcium chloride.

The strontium analogue of this phenyl phosphate was also formed using the same ratio of 25:1 with strontium chloride (0.1554g) and the same mass of the sodium phenyl phase (0.25g). All chemicals in this section were sourced from Aldrich or Fluka chemical companies.

3.2.6 Formation of Alkyl Diphosphate Esters Using Diols

Attempts at forming alkyl diphosphate esters were undertaken using the standard reaction (See section 3.2.1) of pyrophosphoric acid with alkanediol in a respective ratio of 2:1. Three diols were chosen for this reaction namely ethylene glycol (1.736g), butan-1,4-diol (2.52g) and hexan-1,6-diol (3.304g), all purchased from Aldrich chemical company. In each case, the diols were placed in 100 cm^3 round bottomed flasks to which 11g of pyrophosphoric acid (Fluka Chemicals) was added whilst the alcohol was stirred. A small quantity of hexane was also added to increase volume and the flask was kept dry using a calcium chloride guard tube.

The standard separation procedure was performed (as in section 3.2.1) to produce the intermediate alkyl phosphate. The metal ions were added using the aqueous metal hydroxide route with heating to 100°C for 24 to 72 hours.

3.2.7 Modified Chain Alkyl Phosphates

The modified alkyl phosphates were prepared by following the standard phosphate ester methodology for the straight chained alkyl phosphate production (section 3.2.1). Attempts were made to prepare two phases, 2-aminoethyl phosphate and a 2-phenylethyl phosphate.

The calcium 2-aminoethyl phosphate phase was prepared by the addition of 0.45g calcium hydroxide in 300ml water to a stoichiometric amount (0.8578g) of 2-aminoethyl

dihydrogenphosphate (Aldrich). Two days were allowed for the formation and crystallisation of the white precipitate.

The calcium 2-phenylethyl phosphate was prepared in a 2 step reaction as mentioned for the straight chained phases in section 3.2.1. The 2-phenylethyl phosphate intermediate was prepared from 6.832g of 2-phenylethanol with 11g of pyrophosphoric acid. It was left for 4 days where it was then separated with water and hexane portions. A portion of this intermediate was then added to a solution of calcium hydroxide and the solution and precipitate was then heated to 100°C for 24 to 72 hours.

3.2.8 Mixed Alkyl Chain Length Calcium Alkyl Phosphates

A series of octyl and hexyl phosphates were mixed together in different ratios to determine whether components of mixed chain lengths could be synthesised. Only calcium phases were targeted. For these materials, ratios of 25/75 (0.320g/0.830g), 50/50 (0.640g/0.550g) and 75/25 (0.960g/0.278g) were used with octyl/hexyl phosphates. One sample containing 75/25 pentyl/decyl phosphate (0.256g/1.09g) was also prepared. To these mixed ratios of alkyl phosphate was added 10 cm^3 of hexane for improved mixing. All these were added to the usual aqueous 300 cm^3 solution of calcium hydroxide (0.450g) and the suspension was heated to 100°C for 18 hours.

3.2.9 Modification of Calcium Phosphates Using Alkyl Phosphate Intermediates

In all cases, 0.2M octyl phosphate solution was used with 1g of MCPM. Three different solvents were used in this preparation and refluxes were conducted for 5 hours. The solvents used in this case were hexane, hexane/water 1:1, acetone/water 1:1 and ethanol/water 1:1, the total volume of all solutions was 25 ml. Further reflux experiments were attempted

with 1g samples of brushite (CaHPO$_4$·2H$_2$O), calcium pyrophosphate tetrahydrate and hydroxyapatite with 0.2M octyl phosphate in hexane in order to compare the phases produced.

A milder version of this modification was also attempted with MCPM and calcium pyrophosphate tetrahydrate (CaP$_2$O$_7$·4H$_2$O) at room temperature for a longer time period. To these samples was added 0.2M octyl phosphate in either ethanol or hexane and samples were left to stand at room temperature for up to a day.

To examine the influence of concentration, more dilute versions of the pentyl, hexyl or octyl phosphate in acetone solvent (0.1M) were also tested on 0.3g of MCPM, brushite, calcium pyrophosphate and hydroxyapatite respectively. In each case, the calcium phosphate material was left to stand in solution for a day.

3.2.10 Exfoliation of Calcium Alkyl Phosphates

Potential exfoliation of calcium octyl phosphate involving the loss of organic material with the retention of the metal phosphate layers was investigated using the method described by *Tanaka et. al.*[19] This method involved heating the material in an oven in a fumehood to various temperatures ranging from 200 – 300°C. It was determined from the colour of the material produced and X-ray diffraction patterns that 260°C was the optimal temperature. A higher temperature produced more coking in the material (much darker brown) whereas any temperature lower than 260°C did not produce the amorphous pattern reported by *Tanaka et. al.*[19] and thought to evidence exfoliation.

To determine whether the material had in fact exfoliated or completely decomposed, a re-intercalation step was performed. This initially involved using 0.1M solutions of tetradecyl trimethylammonium bromide (0.841g in 25 cm^3 of water), hexadecyl trimethylammonium bromide (0.911g in 25 cm^3 of water) or octadecyl trimethylammonium bromide (0.981g in 25 cm^3 of water)[19] which were added to 0.3g of calcium octyl phosphate that had been

pre-heated to 260°C. The sample was stirred for 5 hours and then left in solution overnight at 50°C in order to maintain the liquid state.

A set of much smaller monoamine species was also used to establish whether the material had retained its inorganic layers. These smaller species were more likely to cause a restacking of these layers, due to their small size and their ability to hydrogen bond with the hydroxyl groups likely to be present on the calcium phosphate layers. Therefore neat propylamine, butylamine, heptylamine and octylamine were added to 0.15g of 260°C heat-treated calcium alkyl phosphates and left, with occasional stirring, for up to 11 days to react. A more forceful set of conditions was also applied to determine whether it was possible to restack the layers of this material. This involved refluxing 0.3g of 260°C heat treated alkyl phosphate material in butylamine, heptylamine or octylamine for 5 – 24 hours.

A different method of attempting to exfoliate the calcium alkyl phosphates involved the use of 20cm^3 of hexane, acetone/water (50/50) or THF to disrupt the interactions between the organic chains and cause a separation of the layers. A range of calcium and strontium alkyl phosphates were investigated for their response to exposure to these solvents. Calcium and strontium pentyl, hexyl, octyl and decyl phosphates were chosen and either left for a total of 8 days in solution before filtering or sonicated for 15 minutes. Analysis using powder X-ray diffraction was undertaken to establish whether any structural changes had occurred.

3.2.11 Characterisation of the Prepared Alkyl Phosphates

The composition and structure of all the alkyl phosphate materials were investigated by powder X-ray diffraction using a Siemens D5000 diffractometer (transmission mode with Cu Kα$_1$ radiation). Thermogravimetric (TG) and differential thermal analysis (DTA) were performed on a Stanton Redcroft STA-780 thermogravimetric analyser at a heating rate of 3°C/min under air. FT-IR was used to determine whether the alkyl phosphate intermediate

species had formed. These measurements were performed on a Perkin-Elmer Paragon 1600 FT-IR spectrometer in transmission mode by liquid film on NaCl solid discs.

Where appropriate, single crystal X-ray diffraction was performed in order to probe the structure of these materials. This method however required a sufficiently large single crystal which was generally quite difficult to prepare using the described methodology.

3.3 Results and Discussion

3.3.1 Calcium Alkyl Phosphate Formation

The powder X-ray diffraction patterns for calcium alkyl phosphates with carbon chain lengths from 5 to 10 atoms in length are shown in figure 3.3.1.1. The diffraction patterns possessed three significant peaks below $2\theta = 15°$ which shift to lower diffraction angle on increasing the numbers of carbon atoms in the alkyl chain. The diffraction data also indicated a small impurity of metal carbonate (accounting for ~ 2% of the sample). This had formed from dissolved CO_2 in the de-ionised water used to produce the hybrid material. This impurity was most evident in the calcium analogue and steps were taken to minimise its presence, but it was difficult to completely eliminate the adsorption of carbon dioxide.
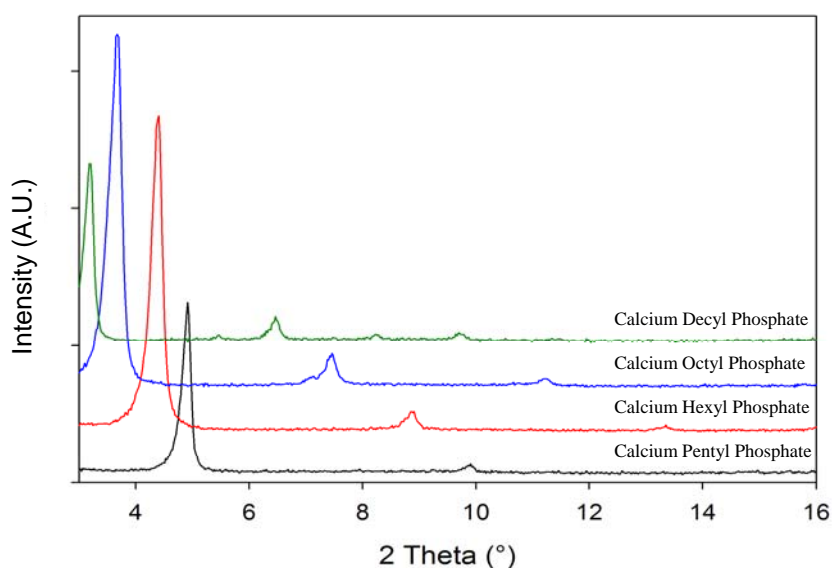
Figure 3.3.1.1: X-ray Diffraction Patterns of Calcium Alkyl Phosphates.
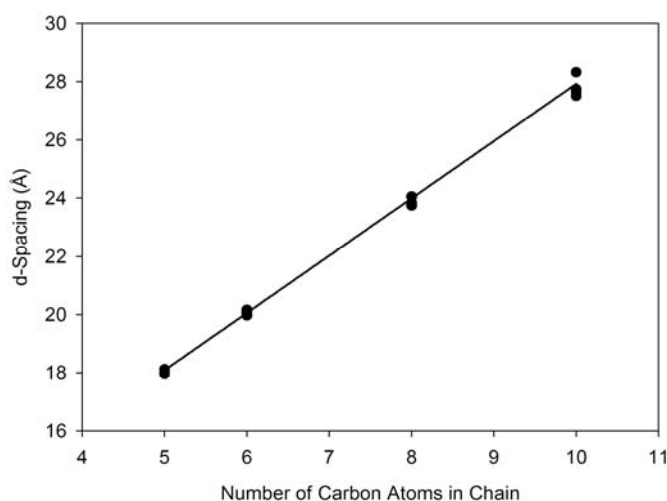
Figure 3.3.1.2: Graph of d-Spacing of the Principal Diffraction Peak against the Increase in the Carbon Number in the Alkyl Chain for a Series of Calcium Alkyl Phosphates.

From the d-spacings of the first main diffraction peak, which is related to interlayer spacing, a graph of d-spacing against number of carbon atoms was constructed. A variation in the d-spacing for the same carbon chain length alkyl phosphate was observed. This can be explained if there was a difference in the water content of the calcium alkyl phosphate or a variation in the chain stacking when the phase was formed. The gradient of this graph (Figure 3.3.1.2) gave the average increase in interlayer separation for every carbon atom added to the alkyl chain. This value was calculated at 1.96 Å for the calcium alkyl phosphates. The expected increase in spacing for a monolayer of alkyl chains in between the calcium phosphate layers per additional carbon atom would be 1.26Å[4] and thus for a true perpendicular bilayer this would be expected to be 2.52 Å. The experimental value calculated must therefore represent a bilayer formation. This could be accomplished in one of two ways. Firstly, we might envisage the alkyl chains being oriented at a ~51° angle to the calcium phosphate layers to form an angled end-to-end bilayer. Alternatively, the alkyl chains could be orientated at a greater angle to the layers, by inter-digitating with each other to form an interlocking bilayer arrangement. From the powder X-ray diffraction alone, it was not

possible to differentiate which of these arrangements was actually present but it was clear from figures 3.3.1.1 and 3.3.1.2 that all these calcium phases adopted a similar structure.

The relatively simple powder X-ray diffraction patterns produced by these materials clearly contained insufficient information to provide an opportunity to obtain a full structure determination. Therefore efforts were undertaken to form single crystals of the alkyl phosphate materials to allow single crystal X-ray diffraction to be performed. Obviously, by obtaining a detailed description of the structure, the understanding of the material and how its inorganic/organic hybrid properties might be exploited would be more likely. Attempts to achieve a sufficiently large single crystal involved modifying the synthetic method by varying the concentration of both the alkyl phosphate intermediate and the calcium salt. A minor increase in crystallite size was observed with the more concentrated solutions; however it was still too small an increase in size to enable single crystal X-ray diffraction to be performed. Therefore other ions were tested to determine whether these might have produced an analogous structure and larger crystals. The ions chosen were strontium and magnesium due to the biocompatibility of these metal alkyl phosphates when present in the body.

3.3.2 Divalent Metal Alkyl Phosphate Formation

Strontium Alkyl Phosphate Formation

Strontium alkyl phosphates were prepared for carbon chains from 5 to 10 carbons. The strontium alkyl phosphate phase ($Sr(ROPO_3)\cdot H_2O$) displayed similar structural features to the calcium alkyl phosphates previously reported,[18,30] with a linear relationship between layer separation increases and alkyl chain length and almost identical powder X-ray diffraction patterns. (See figures 3.3.2.1 & 3.3.2.2). A variation in the d-spacing for the same carbon chain length alkyl phosphate was observed. This can be explained if there was a difference in the water content of the strontium alkyl phosphate (possibly due to a longer heating process)

or a small variation in the chain stacking when the phase was formed. More variation is evident in the strontium analogue compared with the calcium phase. However, the strontium analogues showed a greater degree of crystallinity and as such were of more interest in the determination of the structure of these materials. Comparison of the diffraction patterns produced for the calcium materials and strontium analogues (Figures 3.3.1.1 & 3.3.2.1) showed a good correlation between the peak positions and were thus likely to possess similar structures.
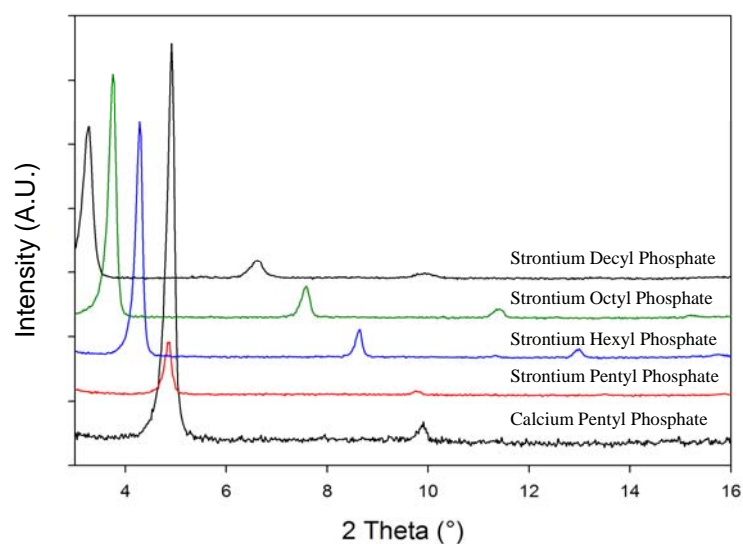
Figure 3.3.2.1: X-ray Diffraction Pattern of Strontium Alkyl Phosphates with Calcium Pentyl Phosphate Included for Comparison.

From the studies on the strontium alkyl phosphate phases, a sufficiently large strontium pentyl phosphate crystal was grown to allow single crystal X-ray diffraction [SCXRD] analysis to be performed and the resulting structure is shown in figures 3.3.2.3a[31] & 3.3.2.3b. To our knowledge this is the first time that the structure of a metal alkyl phosphate has been determined and is therefore a rare example of the structure of a hybrid material.
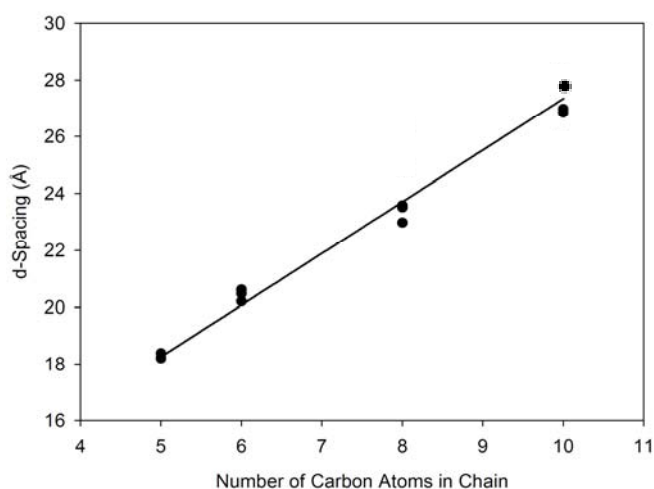
Figure 3.3.2.2: Graph of d-Spacing of the Principal Diffraction Peak against the Increase in the Carbon Number in the Alkyl Chain for a Series of Strontium Alkyl Phosphates.

This structure contains strontium phosphate layers, probably ionically bonded and hydrophilic, separated by pentyl chains pointing into the interlayer region. These hydrocarbon chains appeared to interact with chains from the adjacent layer by van der waals forces. It was the hydrophobic nature of the carbon chains that dominated the overall nature of the material and this could suggest that the crystals were terminated by the alkyl rich surfaces, given the apparent weak van der waals interactions that exist between these organic layers. Thermogravimetric analysis (see section 3.3.4) of this material showed that one mole of water was present in the sample per mole of strontium phosphate. The single crystal data (figure 3.3.2.3a), was unable to show the exact position of the water molecules in the structure due to some disorder of the water molecules in the crystal.
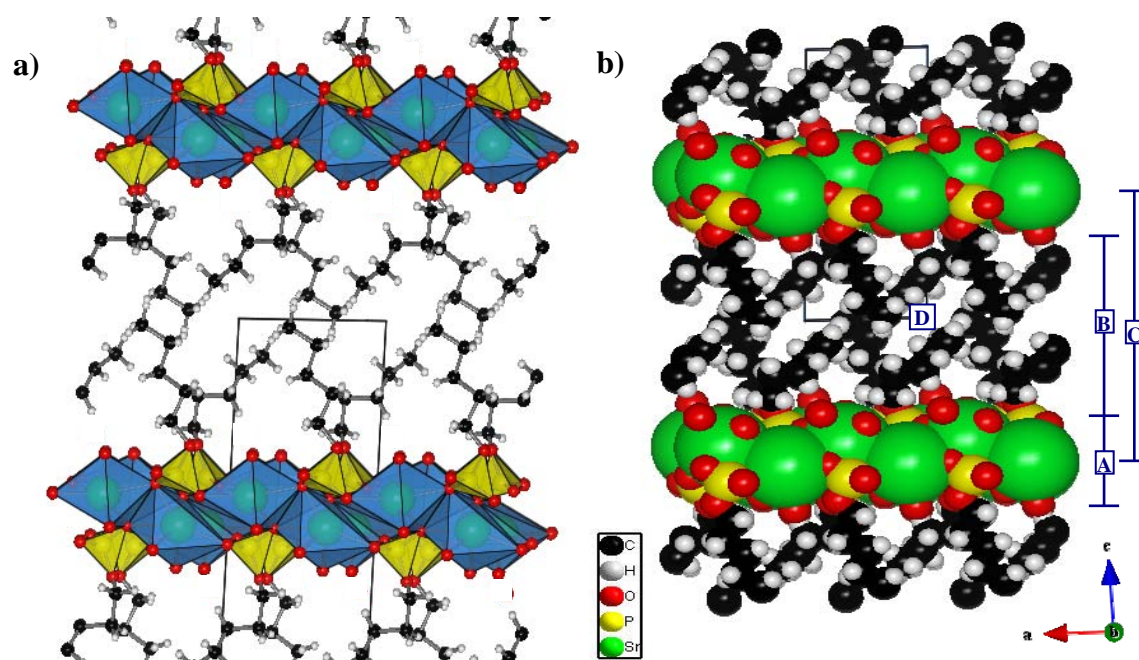
Figures 3.3.2.3a & b: Structural Representation and Space Filling Model of Strontium Pentyl Phosphate from SCXRD.

Table 3.3.2.1: Data from the Single Crystal X-ray Diffraction Analysis for Strontium Pentyl Phosphate

Structure	$C_5H_{11}O_4PSr$, (H_2O)
Crystal type	Triclinic
Space group	P-1
Structure factor	F = 280.75
Temperature of scan	T = 293(2) K
Wavelength	λ = 1.54178 Å
Unit cell dimensions	a = 6.915(3) Å
	b = 8.594(4) Å
	c = 18.165(7) Å
	α = 85.88(2)°
	β = 87.60(2)°
	γ = 86.01(2)°
Unit cell volume	V = 1073.4(8) Å^3
ρ(calc)	1.737 Mg/m^3
Absorption coefficient	8.389 mm^{-1}
Crystal size	0.08 x 0.02 x 0.01 mm^3
Reflections collected	7023
Independent reflections	2657
R(int)	0.198
Parameters	151
Final R1	0.1335
wR2	0.3159 for I>2σ(I)
and R1	0.2701
wR2	0.3947

Simulation of the powder X-ray diffraction pattern from the single crystal data using ATOMS software[31] (see figure 3.3.2.4), was consistent with our previously observed patterns. This indicated that we have found a viable structure for strontium pentyl phosphate and therefore the analogous calcium system. Also the layered nature of the structure was consistent with what we expected, given the trends observed in the X-ray diffraction patterns with varying chains lengths.
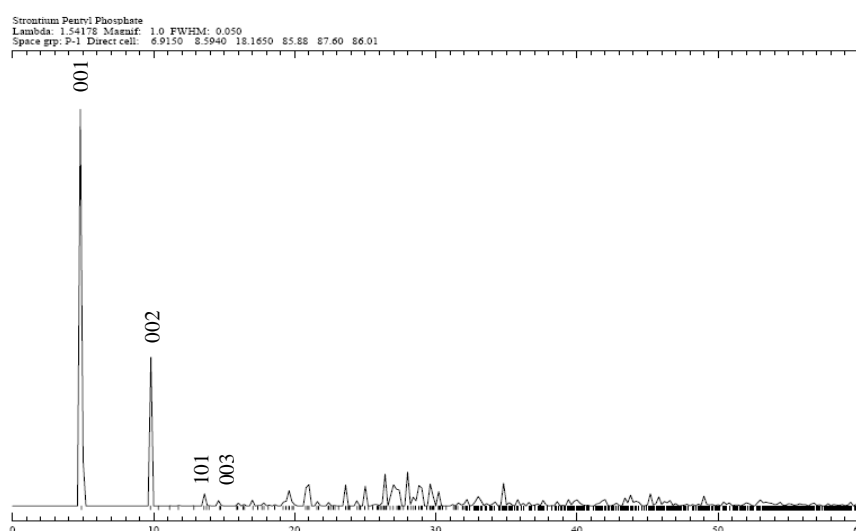
Figure 3.3.2.4: Simulated Diffraction Pattern of Strontium Pentyl Phosphate Based upon SCXRD Data Using ATOMS Software

From the strontium pentyl phosphate phase shown in figure 3.3.2.3a, an actual metal phosphate layer thickness was calculated. This gave a layer thickness of 8.10 Å (Labelled A on figure 3.3.2.3b). The structure contained inorganic layers that were a single strontium phosphate thick and therefore suggested that these layers were likely to lack robustness when separated. This could cause problems when attempting the complete exfoliation of the material but does not preclude partial exfoliation where the resulting separated layers are several units thick.

Figure 3.3.2.5a & b: Structural Representation of the Chain Arrangement in Strontium Pentyl Phosphate Based Upon SCXRD Data.
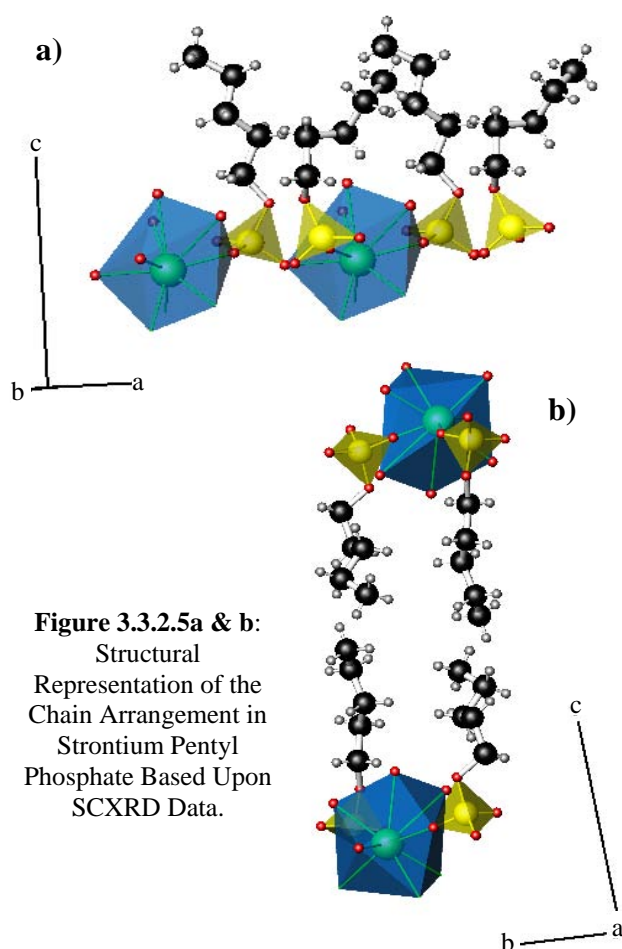
The representation shown in figure 3.3.2.5b depicts the chain arrangement in the strontium pentyl phosphate structure viewed along the *a-axis* from the single crystal X-ray analysis. This shows that there are two chain arrangements within this structure. One chain aligns perpendicular to the strontium phosphate layer (although the chain is tilted in the third dimension) and the other arranges in a spiral manner. Therefore, the structure possesses one chain that terminates further from the strontium phosphate layer to which it is attached, and one chain that terminates much closer (see figure 3.3.2.5a). The layers then pack so that the inverse of each chain is located above and below each other. This enables a smaller interlayer spacing to be accommodated, even though the chains fit end-to-end. To our knowledge, no other similar hybrid phases containing alkyl chains have had their structures determined. This structure shows that simple models based on angled bilayers or interdigitated structures are not adequate as the chain arrangements appear more complex.

The representation shown in figure 3.3.2.3b depicts the space-filling model for the strontium pentyl phosphate structure. It can be clearly seen that there were apparent voids (Labelled D on figure 3.3.2.3b) in the structure in the alkyl chain region which could permit for variations in chain packing and may allow space for further modification of the alkyl

chains, whilst retaining the layered structure. The labels B and C on this figure relate to the interlayer region and spacing respectively. The interlayer spacing was calculated at 18.2Å (Labelled C) from the representation in figure 3.3.2.3a. From the 001 *hkl* X-ray diffraction peak in figure 3.3.2.4, using DSpace[32] to account for the triclinic unit cell, a value of the d-spacing was calculated at 18.1Å. These two values of the d-spacing from the powder X-ray diffraction data and the single crystal X-ray diffraction structural representation are reasonably consistent. This is further evidence that the single crystal data are representative of the bulk structure of this material.

Analysis of the strontium pentyl phosphate showed that the strontium ions in the structure have a coordination number of 9. A coordination number of between 8 and 12 is typical for an ion of this size. Examples of strontium containing phases which possess a coordination number within this range include barium $(Sr_{2-x}Ba_xCuO_{3+\delta})$[33] or bismuth and calcium $(Bi_2Sr_2CaCu_2O_{8+\delta})$[34,35] doped strontium copper oxide superconducting materials.

The same coordination number range is less common for calcium phases since this is a smaller cation and therefore it is more difficult to coordinate 9 ions or molecules around this cation. However, calcium polyphosphate $(\gamma\text{-}Ca(PO_3)_2)$ displays a similar coordination number.[36] Since similar coordination numbers are observed in both calcium and strontium phases, it is possible that the calcium alkyl phosphate structure is analogous with the strontium structure, as observed with the powder X-ray diffraction patterns.

As the metal alkyl phosphate phase was synthesised using an alkyl phosphate intermediate with aqueous ion solution, it was feasible that the alkyl chains in the phosphate solution were potentially directing the crystallisation of the structure. Therefore, a similar coordination number would have been observed with both the strontium and calcium analogues of this phase.

Magnesium Alkyl Phosphate Formation

Investigation into the magnesium alkyl phosphates revealed a similar appearance to their powder diffraction patterns suggesting a layered structure (figure 3.3.2.1). However, the linear increase in interlayer separation observed in the calcium and strontium alkyl phosphates was not apparent. The first significant diffraction peak for the pentyl and hexyl phosphate phases had identical 2θ diffraction angles and thus identical d-spacings, as seen in figure 3.3.2.6. This suggested that there was a change in structure to accommodate the change in alkyl chain length, whilst retaining the same apparent interlayer separation. This might have involved either a change in angle of the bilayer or a change from an angled bilayer to an interlocking bilayer or both.
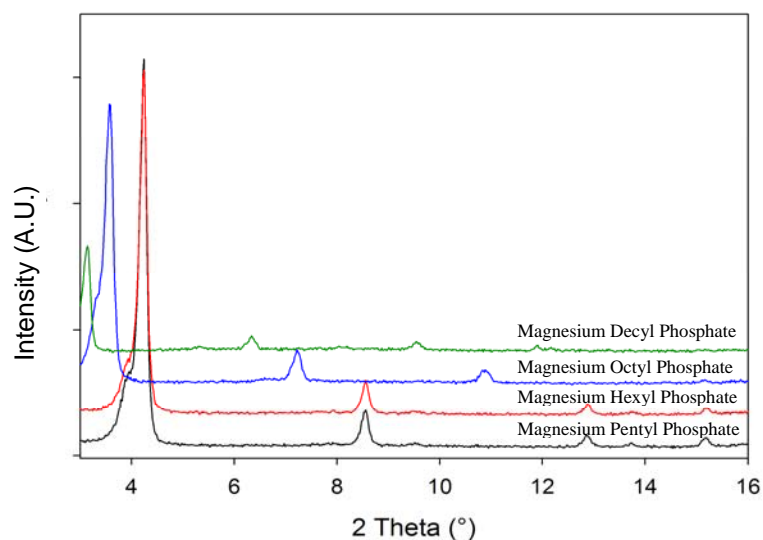
Figure 3.3.2.6: X-ray Diffraction Patterns of Magnesium Alkyl Phosphates.

As mentioned earlier, the structure contained voids which could accommodate the extra carbon atom without increasing interlayer spacing. There was also the appearance of a shoulder to these most intense peaks which was not observed in either of the other metal phosphates synthesised. This suggested that the sample contains two separate phases with different carbon layer stacking arrangements, or this may occur within the same phase in an

ordered manner. Powder X-ray diffraction was unable to differentiate between these possibilities.

In the patterns produced for the magnesium phases, there was always some excess magnesium hydroxide present as an impurity. The samples were thoroughly washed with water, but this failed to remove this supposedly soluble impurity. A repetition of the sample preparation, but with a larger excess of alkyl phosphate intermediate, still showed the presence of a similar level of this impurity.

3.3.3 Monovalent Alkyl Phosphate Formation

The formation of two monovalent cation forms of the metal alkyl phosphate phase was attempted using the method in section 3.2.1. The two chosen cations were sodium and ammonium ions due to their biocompatibility and relative size. From the stoichiometry of the calcium alkyl phosphate, it was clear that one 2+ cation was present per phosphate and therefore if monovalent cations were being tested, then two ions would be required per phosphate.

Unfortunately, when ammonium hydroxide or sodium hydroxide was tested with hexyl phosphate, no reaction was observed and no white suspension formed at the bilayer boundary. The same lack of reaction was also observed when a 50/50 mixed ammonium/sodium hydroxide solution was prepared.

When a mixed aqueous calcium/sodium or calcium/ammonium hydroxide solution was used with the hexyl phosphate intermediate the white colloidal suspension was observed. However, the only product observed when a powder X-ray diffraction analysis was performed on the solid was calcium hexyl phosphate with no additional peaks due to any sodium phase. This result suggested that only the divalent cations reacted with the alkyl phosphate using the current experimental procedure.

3.3.4 TGA Analysis of Metal Alkyl Phosphates

From analysis of the TG-DTA curves of calcium hexyl phosphate in air, the stoichiometry of the material was ascertained through the mass losses observed. These mass losses indicated that for every mole of calcium phosphate, there was a loss of an equivalent of one mole of the alkyl chain and approximately one mole of water removed from this phase, confirming the structure as $Ca((C_nH_{2n+1})OPO_3) \cdot H_2O$. The thermal stability of the calcium alkyl phosphates was investigated up to 1000°C. After the loss of the alkyl groups, an amorphous material was observed. Upon further heating, a crystalline calcium pyrophosphate $(Ca_2P_2O_7)$ phase was observed at 700°C. A suggested decomposition pathway is given in figure 3.3.4.1.

$$2Ca((C_nH_{2n+1})OPO_3) \cdot xH_2O \xrightarrow[\text{- }H_2O]{100°C} 2Ca((C_nH_{2n+1})OPO_3) \xrightarrow[\text{- }C_nH_{2n}]{210°C} 2Ca(HOPO_3) \xrightarrow[\text{- }H_2O]{700°C} Ca_2P_2O_7$$
$$\text{Amorphous}$$
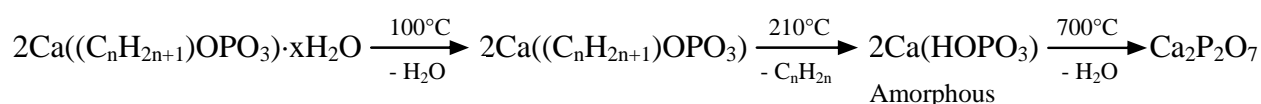
Figure 3.3.4.1: Proposed Reaction Scheme for the Decomposition of Calcium Alkyl Phosphates.

Similar TGA procedures were also performed on the strontium alkyl phosphate analogues with a loss of an equivalent of one mole of the alkyl chain and approximately one mole of water. This concurred with the calcium phase and confirmed that the strontium and calcium phases were analogous. This analysis confirmed that the stoichiometry of the strontium phase was $Sr((C_nH_{2n+1}OPO_3) \cdot H_2O$.

The magnesium phase was also analysed using TGA and a loss of about 0.9 equivalents of the alkyl chain was observed with about one mole of water per magnesium ion in the structure. A similar stoichiometry for this phase could be expected compared to the strontium and calcium forms. The fact that fewer hydrocarbons were present in the material could have been due to the hydrolysis of some of the P-O-R bonds in the alkyl phosphate

intermediate during the magnesium alkyl phosphate synthesis step. This would produce some magnesium phosphate in the product rather than magnesium alkyl phosphate. Therefore, the alkyl chain content would be reduced as observed from the TG analysis.

3.3.5 FTIR Analysis of Metal Alkyl Phosphates

Figure 3.3.5.1 shows the infrared spectrum of calcium hexyl phosphate at room temperature and after treating at 260°C in air using a KBr solid disc method. The calcium hexyl phosphate material produced at 100°C (figure 3.3.5.1A) showed absorption bands at 3488, 2957, 2931, and 2860 cm^{-1}. The first band at 3488 cm^{-1} could be assigned to the vibration mode of OH groups of H_2O present either in the material itself or adsorbed on the surface. The next 3 bands at 2957, 2931, and 2860 cm^{-1} were due to the stretching frequencies of CH groups present on the alkyl chains. A small band at approximately 2300 cm^{-1} (not labelled specifically on figure) would be due to the C=O bond stretch from CO_2 introduced during the disc preparation. Further bands were observed at 1654, 1467, 1085 and 1024 cm^{-1}. The band at 1654 cm^{-1} was due to the bending mode of water present in the sample as crystallisation water. The 1467 cm^{-1} bending mode was due to carbonate anions which were present as a calcium carbonate impurity and introduced CO_2 in the FTIR sample preparation. The 1085 and 1024 cm^{-1} bands could be assigned to the P-O-C stretching modes of the alkyl phosphate groups. Any bands present below 900 cm^{-1} were assigned to the fingerprint region and will not be discussed here.

The 260°C pre-heated sample showed a much less complicated spectrum, due to the removal of the alkyl chains (Spectrum B fig 3.3.5.1). This spectrum displays absorption bands at 3386, 1652, 1455, 1112 and 924 cm^{-1}. The band formed at 3386 cm^{-1} was due to OH groups now present on the phosphate anion following the removal of the alkyl chain. This alteration could be further observed by the lack of the

Figure 3.3.5.1: Infrared Spectrum of Calcium Hexyl Phosphate Treated at Various Temperatures in Air: Spectrum A, Untreated; B, 260°C Heat Treated.

characteristic CH stretching frequencies just below or around 3000 cm^{-1}. The bands at 1652 and 1455 cm^{-1} were observed in both samples and were due to the bending mode of OH and carbonate respectively. The 1112 and 924 cm^{-1} bands correspond to the vibrations of phosphate (PO_4^{3-}) units present in the material. The change in frequency of these two stretches, with respect to the alkyl phosphate sample that was not heat treated, was further proof that this procedure had removed the alkyl chain from the structure.

3.3.6 Environmental SEM and EDX Analysis of Metal Alkyl Phosphates

ESEM images were collected for both the calcium and strontium materials. The typical image of calcium decyl phosphate shown in figure 3.3.6.1, is consistent with the lamellar structure determined in the X-ray diffraction analyses. From ICP-MS data an accurate strontium/phosphorus ratio was calculated for the strontium pentyl and hexyl
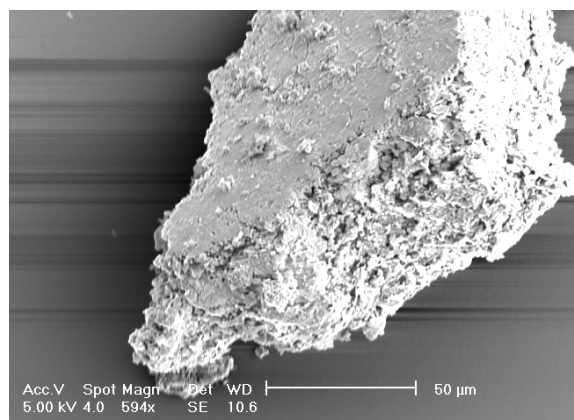
Figure 3.3.6.1: SEM Image of Calcium Decyl Phosphate.

phosphate samples. This ratio was calculated from the experimental data as 1.15 ± 0.02, which represents a close approximation to the 1:1 ratio that was expected.

3.3.7 Branched Metal Alkyl Phosphates

The initial attempts to form branched alkyl phosphate intermediates produced liquid organic phases with 2-ethyl-1-hexyl phosphate, 2-butyl-1-octyl phosphate and 3-hexyl phosphate (figure 3.3.7.1). These three intermediates were produced using the standard phosphate ester reaction from section 3.2.1. There was little increase in temperature when water was added to the mixtures for separation. This indicated that much less pyrophosphoric acid was present. This showed that a successful reaction had occurred.

When the calcium hydroxide solution was added to the pre-formed alkyl phosphates, an off-white solid was formed with 2-ethyl-1-hexyl phosphate and 2-butyl-1-octyl phosphate. No product was formed with the 3-hexyl phosphate and thus examination of the infrared spectrum of the intermediate 3-hexyl phosphate showed that there was no characteristic P-O-C stretch around 1030 cm^{-1}. X-ray diffraction of the two successful materials showed a similar pattern to those observed for the straight chained alkyl phosphates. However, analysis

of the diffraction pattern for the calcium 2-butyl-1-octyl phosphate phase showed two closely spaced low angle diffraction peaks, which suggested two stacking modes.
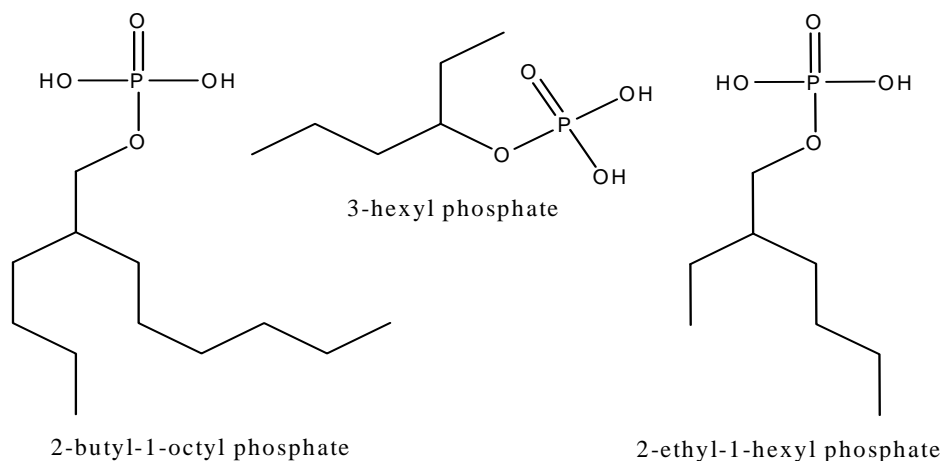
Figure 3.3.7.1: Representation of Branched Alkyl Phosphate Intermediates

Calcium 2-ethyl-1-hexyl phosphate possessed a similar diffraction pattern (figure 3.3.7.2) to the calcium hexyl phosphate, with a small (~0.1° 2θ) shift to a higher diffraction angle. It has not been possible to index this structure as no unit cell was known and there were few reflections available to obtain a reliable cell. These samples had been prepared numerous times and the same pattern was obtained with the same small shift compared to the equivalent straight chained hexyl phosphate.

This small difference could have been a result of a zero point error in the data or, following a different arrangement of the layers, due to the additional ethyl side chain causing an altered stacking arrangement of the chains compared to the single chained hexyl species. It was somewhat surprising that a larger shift in angle was not observed due to the extra steric effects caused by the ethyl side chain on the main hexyl chain. From the single crystal data for the strontium pentyl phosphate phase, figures 3.3.2.3A & B, there were distinct voids in the chain packing arrangements. It may have been possible for the side chain from the branched

alkyl phosphates to be accommodated in these regions. It was equally possible that a rearrangement of both chains occurred so that little effect of the side chain was observed in the interlayer spacing as the alkyl chains could have extended perpendicular to the interlayer region. Without single crystal X-ray diffraction and therefore a known unit cell, a more detailed explanation could not be given.
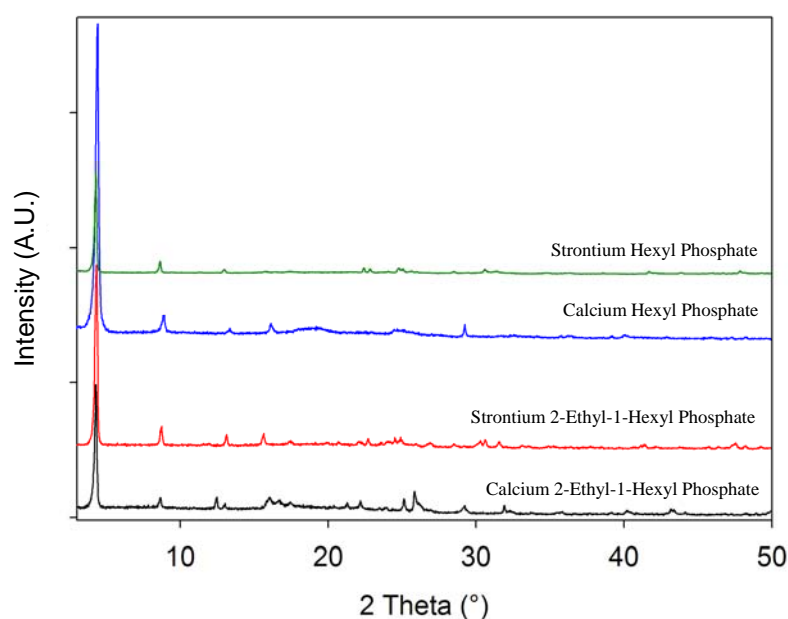
Figure 3.3.7.2: X-ray Diffraction Pattern of Branched Calcium and Strontium 2-Ethyl-1-Hexyl Phosphates Compared to the Calcium and Strontium Hexyl Phosphates.

A similar effect was observed with the strontium analogue of this phase and comparison of the strontium and calcium 2-ethyl-1-hexyl phosphates showed that identical X-ray patterns were observed for the first two peaks. Some minor differences were observed above 16° 2θ diffraction angle, probably due to differences between the strontium and calcium phosphate layers.
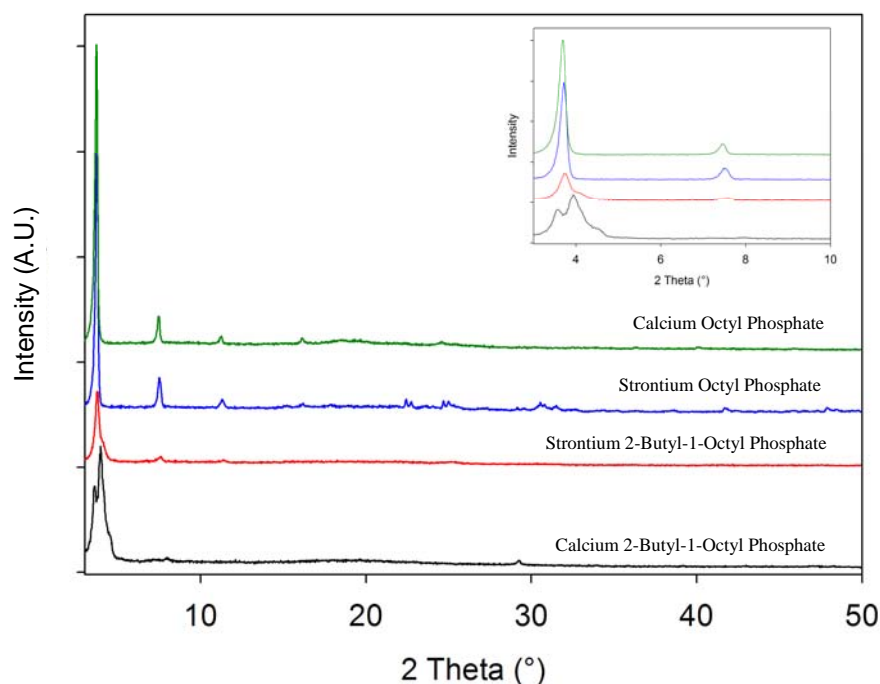
Figure 3.3.7.3: X-ray Diffraction Pattern of Branched Calcium and Strontium 2-Butyl-1-Octyl Phosphates Compared to the Calcium and Strontium Octyl Phosphates.

Figure 3.3.7.3 depicts the calcium and strontium 2-butyl-1-octyl phosphate X-ray diffraction pattern with a comparison to the straight chained octyl phosphate phases. From this diagram it is evident that the strontium 2-butyl-1-octyl phase possessed a similar interlayer spacing to those of the straight chained forms. The calcium 2-butyl-1-octyl phase however appeared as a double first peak, suggesting two different interlayer spacings, probably derived from two different chain stacking arrangements.

3.3.8 Cyclohexyl and Aryl Phosphates

It was not possible to form the cyclohexyl phosphate intermediate using the procedure mentioned in the experimental section. During the separation procedure, very little organic phase product was isolated which suggested that the intermediate was not formed in the reaction, possibly due to a more favourable side-product or possibly a hydrolysis reaction was

occurring to cleave the phosphate ester that was formed. Attempts to modify the procedure using acid catalysis had little effect on the production of the required phase.
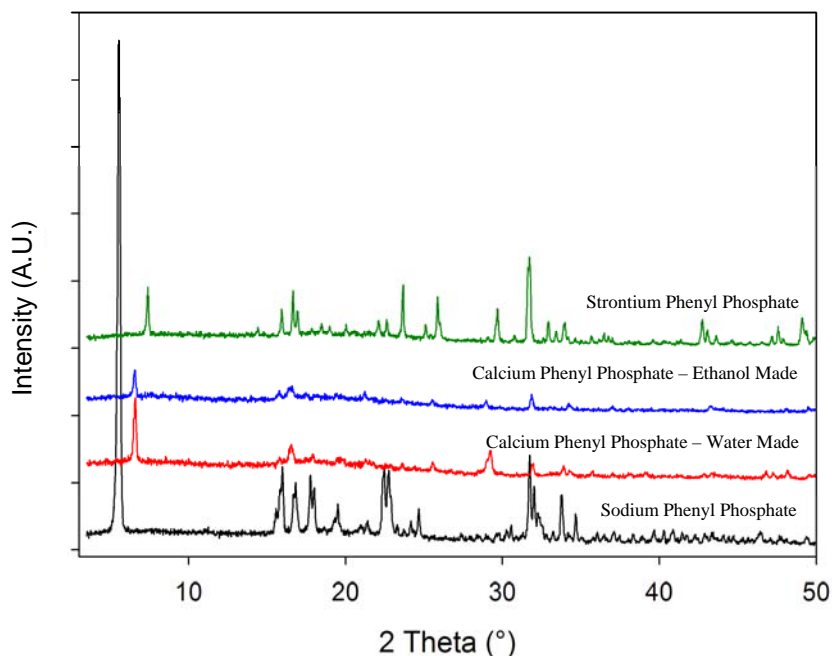
Figure 3.3.8.1: X-ray Diffraction Pattern of Calcium and Sodium Phenyl Phosphates.

From analysis of the X-ray diffraction pattern for the calcium phenyl phosphate phase, it was apparent that there was a change in the principal diffraction peak to higher 2θ from the initial sodium phase (figure 3.3.8.1). A repetition of this experiment also in water and with an alternative solvent was attempted to determine whether solvent would affect the crystallinity of the structure formed.

Light microscope studies on this calcium phenyl phosphate phase prepared in water showed an off-white powder, which contained a few small crystallites. This observation prompted the change of solvent for this reaction as sodium phenyl phosphate was also soluble in ethanol and acetone. A small volume of water was added to aid dissolution. Microscope analysis showed that many small shiny plate-like white crystals were prepared when ethanol

was used as a solvent in the reaction to form this phase. The large yield of crystals suggested that ethanol was a good solvent for crystal formation.

Analysis of the X-ray patterns showed that the same phase had been formed in both water and ethanol solvents. The fact that both of the calcium phases had an identical pattern, with a smaller interplanar spacing compared to the sodium phase, suggested that there must have been a reaction with the calcium source used. However, the decrease in layer spacing of the calcium phase compared to the sodium reagent was difficult to explain without knowing the structures of both species.
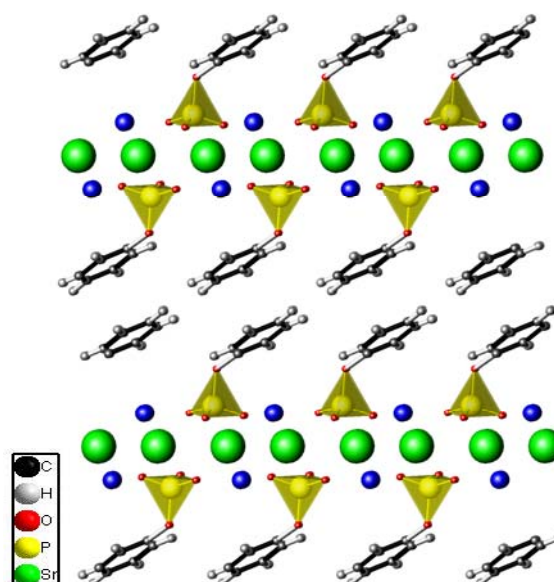
Figure 3.3.8.2: Structural Representation of Strontium Phenyl Phosphate.
(Blue Spheres Represent Water)

As observed with the straight chained metal alkyl phosphates, the use of a strontium ion enhanced the size of the crystallites produced in the strontium phenyl phosphate samples. Single crystal data (table 3.3.8.1) was obtained for this particular phase and the structural representation for this layered material is displayed in figure 3.3.8.2.[31] From the representation in figure 3.3.8.2, it could be observed that the phenyl rings were orientated parallel so that they could π-stack and stabilise the structure with ~ 3.5Å distance between each of the rings.

Simulation of the powder X-ray diffraction pattern from the single crystal data using ATOMS software[31] (see figure 3.3.8.3), was consistent with our previously observed patterns

and indicated that a viable structure had been ascertained for strontium phenyl phosphate and therefore the analogous calcium system.
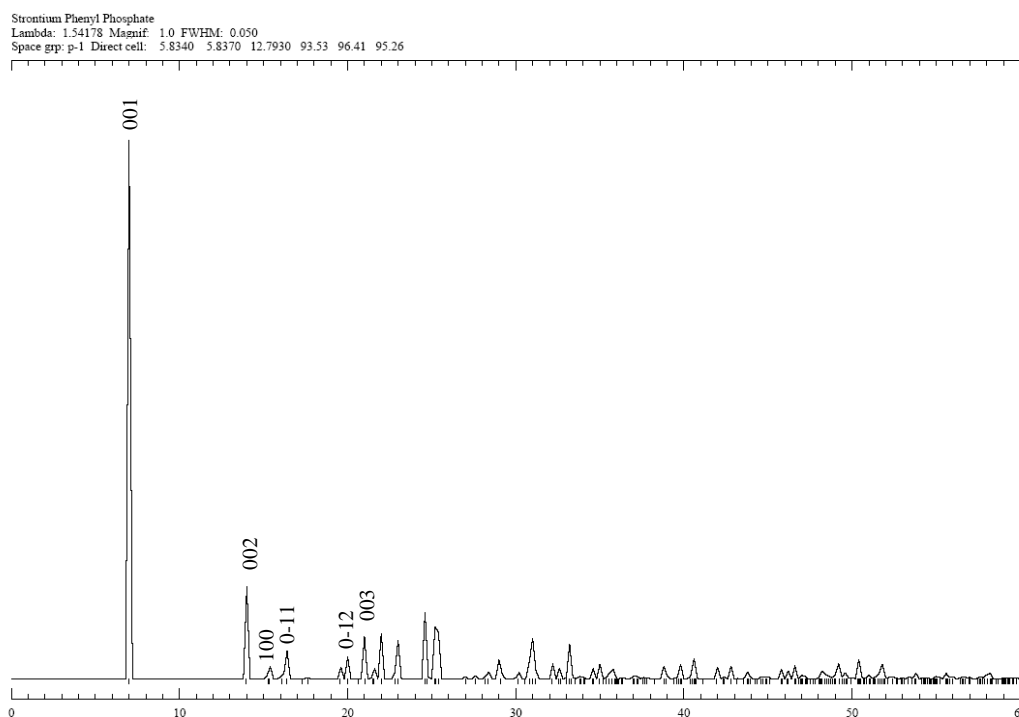
Figure 3.3.8.3: Simulated Diffraction Pattern of Strontium Phenyl Phosphate Based upon SCXRD Data Using ATOMS Software

From the π-stacking arrangement shown in figure 3.3.8.2, it might be possible for certain drug molecules to be accommodated in the interlayer region if these possessed a benzene ring that could also π-stack.

Table 3.3.8.1: Data from the Single Crystal X-ray Diffraction Analysis for Strontium Phenyl Phosphate

Structure	$C_6H_5O_4PSr$, (H_2O)
Crystal type	Triclinic
Space group	P-1
Structure factor	F = 268.0
Temperature of scan	T =150.0(2) K
Wavelength	λ = 1.54178 Å
Unit cell dimensions	a = 5.834(2) Å
	b = 5.837(2) Å
	c =12.793(5) Å
	α = 93.532(1)°
	β = 96.412(2)°
	γ = 95.260(3)°
Unit cell volume	V = 430.0(3) Å^3
ρ(calc)	2.130 Mg/m^3
Absorption coefficient	6.440 mm^{-1}
Crystal size	0.10 x 0.08 x 0.01 mm^3
Reflections collected	1870
Independent reflections	1296
R(int)	0.0898
Parameters	137
Final R1	0.1449
wR2	0.3157 for I>2σ(I)
and R1	0.1850
wR2	0.3435

3.3.9 Formation of Alkyl Diphosphate Esters Using Diols

Attempts were undertaken to produce intermediate alkyl diphosphates with a phosphate unit at each end of the alkyl chain. Therefore, on the addition of the metal salt, a pillared metal alkyl phosphate might have been formed with a more rigid, porous structure.

Unfortunately, it was not possible to synthesise the alkyl phosphate intermediate. This was confirmed by the lack of characteristic P-O-C stretches in the FTIR data. There was also a considerable exothermic reaction observed when water was added to the thick syrupy solution during the separation procedure. These facts suggested that the appropriate intermediate had not formed. The addition of an aqueous metal salt to the intermediate solution was still attempted but no colloidal suspension or white solid was formed during this step.

3.3.10 Modified Chain Alkyl Phosphates

Attempts to isolate a calcium 2-phenylethyl phosphate material proved unsuccessful due to problems forming the intermediate alkyl phosphate phase. It was possible that the presence of water in the reaction caused the hydrolysis of some of the P-O-C bonds formed in the intermediate, this being facilitated by the phenyl component. This resulted in a low yield of the organic intermediate when the sample was separated from solution.

This organic intermediate was analysed using FTIR which showed a shifted P-O-C stretch at $1017 \, cm^{-1}$. There was also a large OH stretch at $3417 \, cm^{-1}$ due to some excess alcohol remaining in the organic phase. From this analysis, there was also evidence of the presence of carbonyl stretches which had not been observed before. This suggested that some decomposition of the phenylethanol derivative to phenylethanoic acid had occurred.

2-aminoethyl phosphate

2-phenylethyl phosphate

Figure 3.3.10.1: Chemical Structures of Attempted Alkyl Phosphate Intermediates.

Similarly, calcium 2-aminoethyl phosphate was difficult to produce in reasonable yields. The X-ray diffraction pattern produced showed a low intensity pattern with 4 main peaks, none of which match the only solid reagent added which was calcium hydroxide. This would suggest that some form of reaction was occurring in solution.

However, the diffraction patterns matched the metal carbonate form of the reagent added therefore usually calcite ($CaCO_3$) or strontianite ($SrCO_3$) was formed when strontium hydroxide was used. This indicated that any dissolved carbon dioxide in the water was reacting with the metal hydroxide to form a metal carbonate side product.

The lack of formation of the calcium 2-aminoethyl phosphate could have been due to the presence of the amino functional group on the alkyl side chain of the alkyl phosphate intermediate. This group would have increased the pH of the alkyl phosphate solution. This could have prevented the aqueous hydroxide ions from reacting with the acidic protons on the phosphate unit of the 2-aminoethyl phosphate at the aqueous/organic layer interface. Therefore the calcium 2-aminoethyl phosphate phase would not have been produced.

3.3.11 Mixed Alkyl Chain Length Calcium Alkyl Phosphates

The possibility of forming calcium alkyl phosphates containing mixed alkyl chains was investigated. Two different alkyl phosphates with six and eight carbon chain lengths were mixed in varying proportions and reacted with calcium ions to form calcium alkyl phosphates.

X-ray diffraction data was collected on the products and shown in figure 3.3.11.1 with a summary of the d-spacing of the peaks for each sample also displayed in table 3.3.11.1. Diffraction data for the pure hexyl and octyl phosphate phases were included, for comparison, as the products could simply have formed two phases consisting of the pure calcium hexyl and octyl phosphates. The results appeared to show that the products were not simply the pure end members. The highest octyl phosphate ratio possessed a small peak that had a larger d-spacing than the pure calcium octyl phosphate phase and one larger peak with a smaller spacing. This suggested that for the higher ratio octyl to hexyl phosphate, there was the potential for two stacking arrangements.
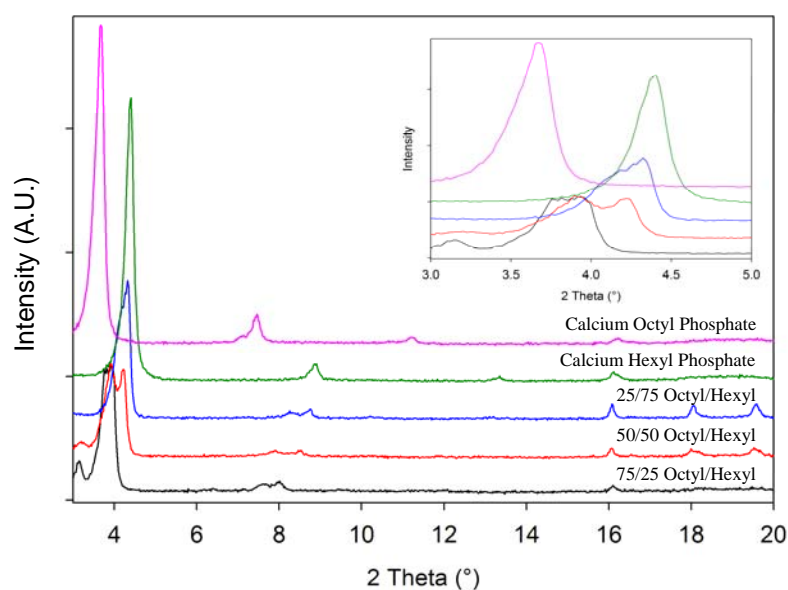
Figure 3.3.11.1: X-ray Diffraction Pattern of the Mixed Alkyl Chain Length Calcium Alkyl Phosphates.

When equal mixtures of hexyl and octyl phosphate were used, two equal height peaks were observed. Both of the peaks for this sample occurred at a d-spacing that was an intermediate value between the pure hexyl and octyl phosphates. This indicated that two potential stacking arrangements were present with the incorporation of both chains into the structure.

Table 3.3.11.1: d-Spacing Values for the Principal Diffraction Peaks of the Products Formed Using Various Ratios of the Alkyl Chains Lengths

Mixed Chain Ratio Octyl/Hexyl	d-Spacing (Å)
25/75	21.1(2) and 20.4(1)
50/50	22.6(7) and 21.2(3)
75/25	27.9(5) and 23.4(9)
0/100	20.0(4)
100/0	24.0(4)

The lowest octyl phosphate ratio possessed only one peak which had a larger d-spacing than the pure calcium hexyl phosphate phase but a broad shoulder could be

observed to the lower 2θ diffraction angle, consistent with a higher d-spaced phase. Thus it could be concluded that there was again two potential stacking arrangements with this sample.

3.3.12 Modification of Calcium Phosphates Using Alkyl Phosphate Intermediates

As mentioned in section 3.3.2, the use of alkyl phosphates has been shown to impose a hydrophobic nature to the naturally hydrophilic calcium phosphate.[15] A change to hydrophobic behaviour is especially useful should the calcium phosphate be dispersed in a hydrophobic polymeric material. Agglomeration often occurs due to the hydrophilic species attracting other hydrophilic species when surrounded in a hydrophobic environment. This non-homogenous mixing of the polymer and inorganic filler can cause defects in the composite material and these defects can reduce the strength of a composite and therefore compromise the properties of the composite.

The main aim of the experiments undertaken here was to alter the properties of layered calcium phosphates and determine the nature of any structural changes. The unmodified surface structure of calcium phosphates contained many surface P-OH groups which enable adsorption sites for H_2O and other aqueous molecules therefore making calcium phosphates hydrophilic.[15]

Four commonly used bioceramic calcium phosphates were examined. These were MCPM ($Ca(H_2PO_4)_2 \cdot H_2O$), brushite ($CaHPO_4 \cdot 2H_2O$), calcium pyrophosphate tetrahydrate ($Ca_2P_2O_7 \cdot 4H_2O$) and hydroxyapatite ($Ca_{10}(PO_4)_6(OH)_2$). The first three of these are layered materials with potential for alkyl phosphate reactions on their surfaces or between their layers. In contrast, hydroxyapatite can only react at its exterior surface.

In studying the reactions of these calcium phosphate phases it should be possible to determine whether any structural changes to the calcium phosphate hosts were due to surface reactions (internal/external) or complete conversions to form new materials. The three layered

phases were chosen due to their different layer thicknesses, thus if the alkyl phosphates were reacting within the layers, contrasts in the position of the low angle peak should evidence this.

As described in the experimental section 3.2.9, two methods of alkyl phosphate modification were tested. The first method involved refluxing the alkyl phosphate and calcium phosphate in boiling solvent; a harsh technique that has potential to cause some decomposition of the calcium phosphate samples. Therefore, a second method was also employed which involved room temperature experiments with calcium phosphate phases added to the alkyl phosphate solutions. Clearly this is a much 'softer' technique and less likely to decompose the calcium phosphate phases.

Reflux Experiments

In all cases white crystalline products were present when the calcium phosphate samples were filtered and washed to remove any excess alkyl phosphate. When the X-ray diffraction patterns were analysed, the appearance of a low angle peak was observed at the same position ($2\theta = 3.1°$). This was independent of the starting calcium phosphate phase.

When the X-ray diffraction pattern of the MCPM sample modified with octyl phosphate was compared to the starting MCPM material, a new low angle peak was evident, with some of the MCPM remaining. Comparison of the modified MCPM phase with the octyl phosphate modified brushite phase (figure 3.3.12.1) showed similar peak positions on the diffraction patterns. The brushite phase possessed additional peaks at 20, 27° and 31° 2θ due to some host structure remaining intact. However, the same additional low angle octyl phosphate peak at ~ 3° 2θ was present in both samples. Further calcium phosphate samples (calcium pyrophosphate tetrahydrate and hydroxyapatite) were then tested using these reflux conditions.
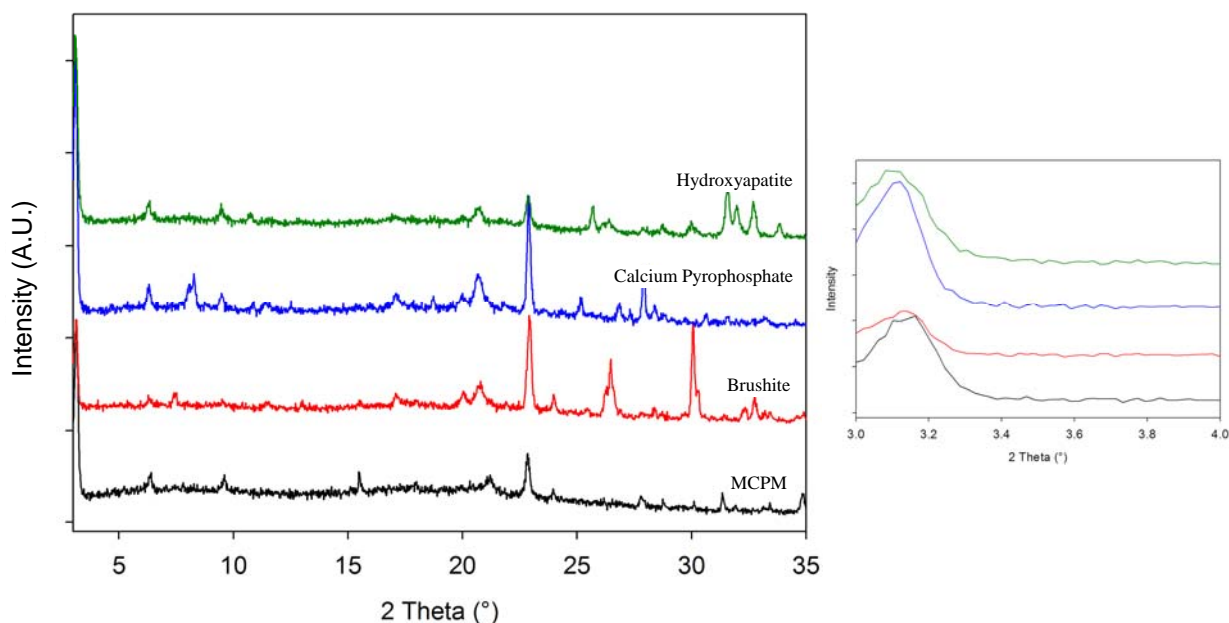
Figure 3.3.12.1: X-ray Diffraction Pattern of 0.2M Octyl Phosphate Modified Calcium Phosphates by Reflux for 5 Hours.

It is clear from a comparison of the MCPM, brushite, calcium pyrophosphate tetrahydrate and hydroxyapatite samples (figure 3.3.12.1) refluxed in octyl phosphate solution that the same phase had been produced with all four samples. An identical low angle peak between 3.1 – 3.13° 2θ diffraction angle was observed in all 4 calcium phosphate materials. If a reaction occurred within the layers of these phases then, given their different structures, a much greater difference between these low angle peaks would have been expected. This leaves two explanations. In one, the alkyl phosphates are forming an external surface coating, similar in all phases. Or, that the calcium phosphates are dissolving and new separate calcium alkyl phosphate phases are being formed. It should be noted that the host structure diffraction peaks have reduced intensity. This is consistent with the host being decomposed and a new layered alkyl phosphate phase being crystallised from solution. However, the alkyl phosphate peak present in this modified phase (3° 2θ) occurred at a lower angle to the peak position of calcium octyl phosphate formed using the method employed in section 3.2.1 (3.8° 2θ). The

reduction in intensity of the original calcium phosphate could also be a consequence of a thick surface coating of the alkyl phosphate phase limiting diffraction from the host.

Room Temperature Experiments

To determine whether a less harsh room temperature reaction rather than reflux methods would give different products, a set of experiments in a solution of octyl phosphate were undertaken, with X-ray diffraction results shown in figures 3.3.12.2 and 3.3.12.3. From comparison of the diffraction patterns for calcium pyrophosphate (figure 3.3.12.2) in the refluxed and room temperature samples, the three patterns matched quite closely. There was only a minor difference around 29 - 30° 2θ which could have been due to a small amount of starting material still remaining.

Comparison of the diffraction pattern for the MCPM samples (3.3.12.3) showed that the majority phase produced was identical between the refluxed samples and the room temperature samples.
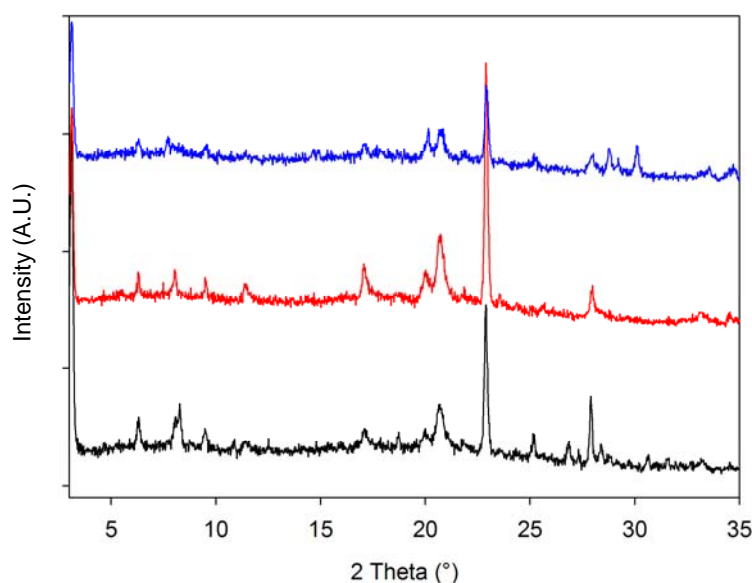
Figure 3.3.12.2: Comparison of the X-ray Diffraction Pattern of 0.2M Octyl Phosphate Modified Calcium Pyrophosphate Tetrahydrate.
(Black = Refluxed 5 hours; Red = Room Temperature in Hexane 4 Days; Blue = Room Temperature in Ethanol 4 Days)
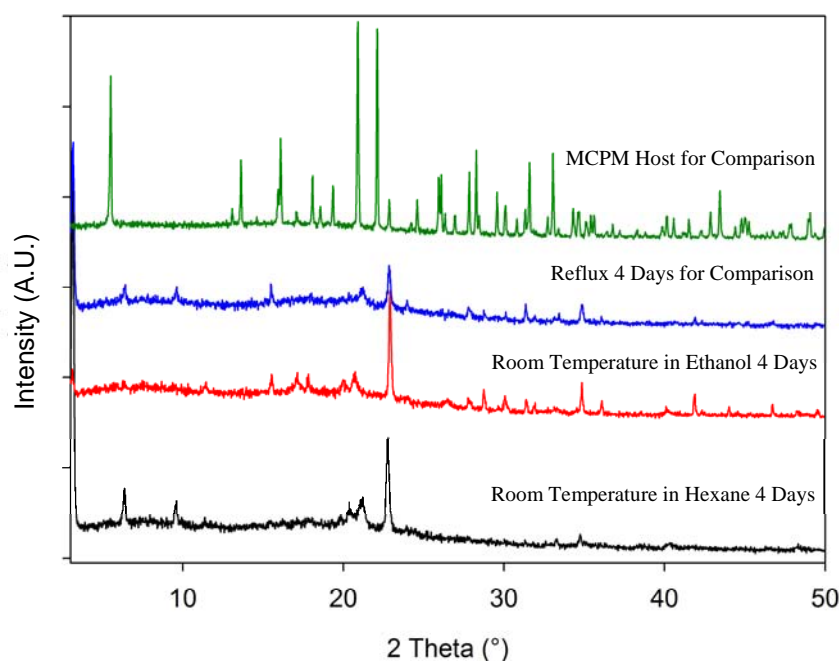
Figure 3.3.12.3: Comparison of the X-ray Diffraction Pattern of 0.2M Octyl Phosphate Modified MCPM.

A more dilute version of the alkyl phosphate solution was also used on the four calcium phosphate phases and the same low angle product phases were present, as observed in the more concentrated or refluxed samples. One difference between the results for these dilute solutions was a less intense low angle peak was observed but it was present in the same position. This suggests that the same reaction is occurring in all reactions, but in the dilute conditions, the reaction had not progressed as far when the samples were removed from solution. The fact that a weaker solution had produced the same phase indicated that significant dissolution of the calcium phosphate is not required to form the alkyl phosphate material. We might expect some surface dissolution from the acidity of the alkyl phosphate solution. When the intermediate alkyl phosphate was formed, it possessed two protons on the phosphate head group. These would normally react with the alkaline calcium hydroxide reagent to form the calcium alkyl phosphate phase as shown in section 3.3.1. Therefore the acidic alkyl phosphate intermediate solution should leach some of the calcium from the host

to allow the new calcium alkyl phosphate phase to form. The diffraction study is unable to confirm whether this modification is as a surface coating or as a separate phase.

Microscopy

When the materials were observed using optical and electron microscopy, a noticeable change in the appearance of the crystals compared to the host materials was seen for the MCPM, brushite and pyrophosphate tetrahydrate samples. With the modified MCPM and brushite phases, thin white fibres were observed in the samples whereas the original materials possessed shiny platy crystals similar to those observed in figure 3.3.12.4. The appearance of the modified pyrophosphate material was very similar to the modified MCPM sample, showing longer thin white fibrous crystals (figure 3.3.12.6) rather than the platy morphology of the host material (figure 3.3.12.4). The hydroxyapatite material appeared similar to the original host structure (figure 3.3.12.5) with partially round particles still present, although there were some fibres also present on the outer surface of the sample. This indicated that there was some degradation on the outer surface of the phase (figure 3.3.12.7) due to the interaction with the acidic alkyl phosphate solution.

From the microscopy images, it was clear that similar changes had occurred to all the calcium phosphate materials. Although the MCPM and brushite images are not shown, the morphology of these samples was identical to these images and therefore has not been displayed here.
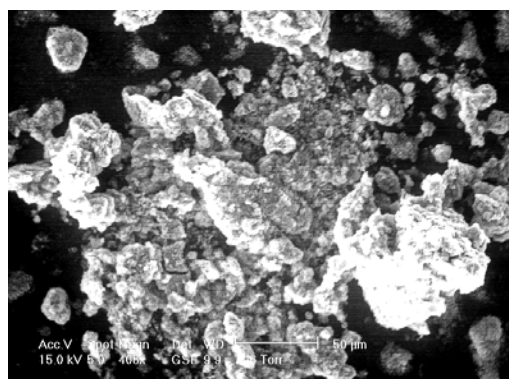
Figure 3.3.12.4: ESEM Image of Unmodified Calcium Pyrophosphate Showing Platy Morphology.
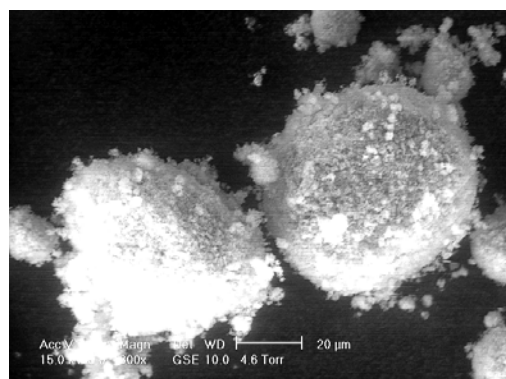
Figure 3.3.12.5: ESEM Image of Unmodified Hydroxyapatite Showing Spherical Morphology.

Figure 3.3.12.6: ESEM Image of Alkyl Phosphate Modified Calcium Pyrophosphate Showing Fibrous Morphology.
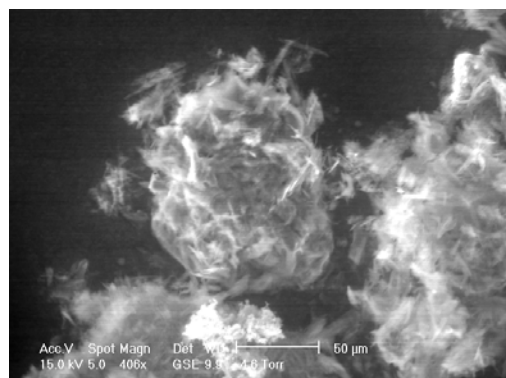
Figure 3.3.12.7: ESEM Image of Alkyl Phosphate Modified Hydroxyapatite Showing Some Fibrous But Still Rounded Morphology.

In summary, the microscope images suggested that distinct changes to the MCPM, brushite and calcium pyrophosphate tetrahydrate particles had occurred. This could be consistent with new materials being formed from the host structure by dissolution and re-precipitation of the calcium phosphate. The hydroxyapatite phase however still possessed a similar morphology after the treatment which suggested a surface coating of a calcium alkyl phosphate phase had occurred on the surface of the particles.

3.3.13 Exfoliation of Calcium Alkyl Phosphates

From the initial experiments conducted by *Tanaka et. al,*[19] the presence of a potentially exfoliated calcium alkyl phosphate was suggested. This was evidenced by the appearance of an amorphous X-ray diffraction pattern, before a further reaction with an ammonium species that produced another crystalline pattern. It might therefore be inferred that the sample had exfoliated and therefore lost long range ordering, hence the amorphous pattern. A restacking was then believed to have occurred with the addition of a quaternary ammonium species to the amorphous material, forming a crystalline phase again. The only way this could have occurred at this low temperature was if the sample's inorganic layer had remained intact. Further examination of this phase was therefore warranted as no discussion of exfoliation was given in this paper[19] or in further papers by these authors.[13,15,29]

When the metal alkyl phosphate was heated in air to 260°C, the alkyl chains would have been removed. This reaction would also have formed hydroxyl groups at the sites where the alkyl chains were lost (see equation 1). These groups were important to allow for further reactions.

$$M(C_nH_{2n+1})OPO_3 \text{ (s)} \rightarrow M(HOPO_3) \text{ (s)} + C_nH_{2n} \text{ (g)} \qquad \text{(Equation 1)}$$
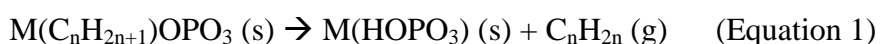
Powder X-ray diffraction analysis (Figure 3.3.13.1) of the alkyl phosphate sample heated to 260°C confirmed that an amorphous pattern was produced. The presence of small peaks above 25° 2θ in this pattern were due to a calcium carbonate impurity created during the formation of the crystalline calcium alkyl phosphate phase. As we might have expected an amorphous pattern to have been produced if the material had exfoliated, the quaternary ammonium species was added to this phase to instigate restacking of the layers and left for 5 hours as specified by *Tanaka*.[19] There was however, no change in the diffraction patterns of

the material after the alkylammonium treatment. A longer time period was also attempted and once again, no change was observed. If however, a less thorough wash was performed, a low angle peak consistent with the solid alkylammonium species was observed. However, the position of this peak was still at a higher 2θ diffraction angle than the data reported by *Tanaka*[19] and therefore this alkyl ammonium impurity could not account for their results.
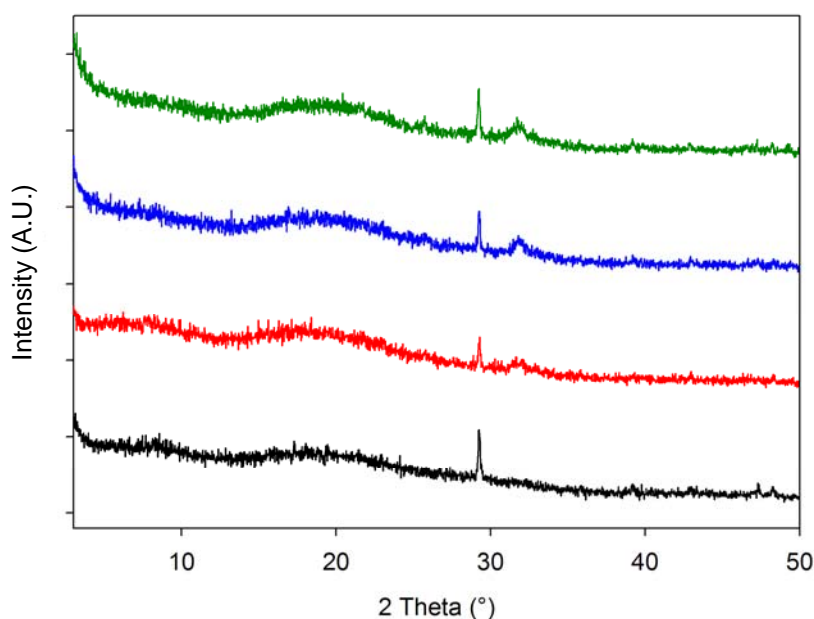
Figure 3.3.13.1: X-ray Diffraction Pattern of Calcium Octyl Phosphate Heated to 260°C then with aqueous solutions of Long Chained Alkyl Ammonium Species.
(Black = Heat Treated Calcium Octyl Phosphate; Red = Tetradecyltrimethylammonium Bromide 0.2M Solution with Heat Treated Calcium Octyl Phosphate 1 Day; Blue = Hexadecyltrimethylammonium Bromide 0.2M Solution with Heat Treated Calcium Octyl Phosphate 1 Day; Green = Octadecyltrimethylammonium Bromide 0.2M Solution with Heat Treated Calcium Octyl Phosphate 1 Day).

Given the lack of success with the quaternary ammonium species, much smaller amine species were used to determine whether this could facilitate restacking of the structure. Unfortunately, all monoamine species tried either at room temperature for 11 days or a 6 hour reflux did not cause any changes to the amorphous phase formed by the heat treated calcium alkyl phosphate samples. It was therefore likely that the heat treatment had caused a structural collapse rather than exfoliation. This would indicate that the crystalline peaks observed by

Tanaka et. al.[19] may have resulted from the formation of a new phase independent of the parent alkyl phosphate.

An alternative approach to exfoliation was therefore adopted which involved the use of different solvents with the un-treated calcium alkyl phosphates. The solvent (acetone in water 50/50%) was chosen for its ability to solvate the alkyl chains thus enabling the layers to separate from each other and potentially exfoliate. Sonication was used with the solvated material to aid the separation of the layers by the induced vibration. Unfortunately, this method was unsuccessful in enabling the layers to separate as the X-ray diffraction pattern remained unchanged following the treatment. A longer sonication time was also performed but again no effect was observed on the diffraction patterns of the material, apart from a reduction in particle size. Somewhat surprisingly, it appeared that the van der waals forces between the alkyl chains were sufficiently strong to preclude the use of a solvent and sonication to disrupt them. This suggested that the interactions between these chains must be integral to the stability of the entire structure.

The choice of solvent that was attempted with this sonication method was acetone in water. This solvent had been used by *Tanaka et al.*[13] for the modification of pre-formed calcium phosphates with alkyl phosphate and therefore this solvent proved influential with structure modification as shown in section 3.3.13. The acetone was believed to solvate the alkyl chains and as such might have enabled the individual layers within the structure to separate from each other and therefore exfoliate. This was the initial aim for the use of this solvent mix with the metal alkyl phosphates. However, no exfoliation appeared to have occurred, but some effect was noticed with samples that possessed two low angle peaks (first peak appeared as a doublet) on the powder X-ray diffraction patterns. The solvent caused a rearrangement of part the structure so that only one d-spacing was observed. This effect was

observed in some of the strontium pentyl (Figure 3.3.13.2) and hexyl phosphates. It would therefore seem feasible to suggest that the acetone/water solvent allowed the alkyl chains to rearrange in the samples to the most favourable position, if there was the potential for two possible orientations, as observed when a double peak was seen in some of the X-ray diffraction patterns.
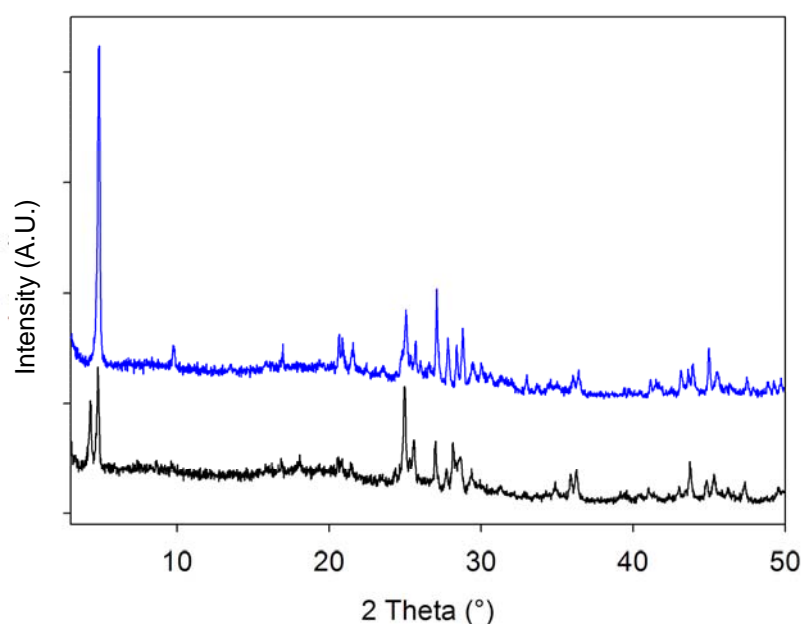
Figure 3.3.13.2: X-ray Diffraction Pattern of the Mixed Alkyl Chain Length Calcium Alkyl Phosphates. (Black = Strontium Pentyl Phosphate Formed in the Usual Way Possessing Doublet First Peak; Blue = Same Phase After Standing for 1 Day in Acetone/Water.

3.3.14 Summary of Phases Attempted and Prepared

This summary table below shows the phases that were prepared but excludes the results of the modification of existing calcium phosphate phases and the attempted exfoliation of the calcium alkyl phosphate phases.

Phase Attempted	Intermediate Alkyl Phosphate Prepared	Diffraction Evidence of Hybrid Product Formation
Calcium pentyl phosphate	Yes	Yes
Calcium hexyl phosphate	Yes	Yes
Calcium octyl phosphate	Yes	Yes
Calcium decyl phosphate	Yes	Yes
Strontium pentyl phosphate	Yes	Yes
Strontium hexyl phosphate	Yes	Yes
Strontium octyl phosphate	Yes	Yes
Strontium decyl phosphate	Yes	Yes
Magnesium pentyl phosphate	Yes	Yes
Magnesium hexyl phosphate	Yes	Yes
Magnesium octyl phosphate	Yes	Yes
Magnesium decyl phosphate	Yes	Yes
Sodium hexyl phosphate	Yes	No
Ammonium hexyl phosphate	Yes	No
Mixed sodium/ammonium hexyl phosphate	Yes	No
Calcium 2-ethyl-1-hexyl phosphate	Yes	Yes
Calcium 2-butyl-1-octyl phosphate	Yes	Yes
Calcium 3-hexyl phosphate	Yes	No
Strontium 2-ethyl-1-hexyl phosphate	Yes	Yes
Strontium 2-butyl-1-octyl phosphate	Yes	Yes
Strontium 3-hexyl phosphate	Yes	No
Calcium cyclohexyl phosphate	No	No
Calcium phenyl phosphate	N/A	Yes
Strontium phenyl phosphate	N/A	Yes
Calcium ethyl diphosphate	No	No
Calcium butyl diphosphate	No	No
Calcium hexyl diphosphate	No	No
Calcium 2-amino-ethyl phosphate	N/A	No
Calcium 2-phenyl-ethyl phosphate	No	No
Mixed Ca/Sr hexyl phosphate	25/75	Yes
Mixed Ca/Sr hexyl phosphate	50/50	Yes
Mixed Ca/Sr hexyl phosphate	75/25	Yes
Mixed Calcium hexyl/octyl phosphate	25/75	Yes
Mixed Calcium hexyl/octyl phosphate	50/50	Yes
Mixed Calcium hexyl/octyl phosphate	75/25	Yes

3.4 Conclusions

Metal alkyl phosphates have been prepared from chain lengths pentyl to decyl phosphate. For the first time, the structure of the strontium pentyl phosphate and strontium phenyl phosphate materials has been elucidated using single crystal X-ray diffraction. These phases appeared to be analogous to the calcium phases when both of the powder X-ray diffraction patterns were analysed. These hybrid materials possessed a layered structure with hydrophobic bilayers of alkyl chains between the hydrophilic metal phosphate layers. The structural detail has shown the unusual alkyl chain arrangements between the metal phosphate layers. These materials have been shown to be stable up to 210 °C. Above this temperature, the alkyl chains decomposed.

Metal alkyl phosphate materials with branched alkyl chains were successfully prepared. However, when additional functional groups were present on the alcohol reagent, such as an amino group, using the phosphate ester route to prepare the intermediate alkyl phosphate did not produce the required phase. Therefore either further protection of this additional functional group would be required before attempting to prepare the phosphate ester or an alternative preparation method would be necessary to form these materials.

Attempts to modify calcium phosphate phases with alkyl phosphates produced phases with identical low angle X-ray diffraction peaks between 3.1 – 3.13° 2θ diffraction angle. If a reaction occurred within the layers of these calcium phosphate phases then, given their different structures, a much greater difference between these low angle peaks would have been expected. This leaves two explanations: either the alkyl phosphates are forming an external surface coating, similar in all phases, or a new separate calcium alkyl phosphate phase is formed. X-ray diffraction studies are unable to confirm whether a surface coating or new phase is formed therefore other techniques were used. Scanning electron microscopy

analysis of the samples suggested that distinct changes to the MCPM, brushite and calcium pyrophosphate tetrahydrate particles had occurred. This could be consistent with new materials being formed from the host structure by dissolution and re-precipitation of the calcium phosphate. The hydroxyapatite phase however still possessed a similar morphology after the treatment which suggested a surface coating of a calcium alkyl phosphate phase had formed on the particles.

All the metal alkyl phosphates produced in this study were insoluble in aqueous solutions. This hydrophobic nature was due to the presence of the alkyl chains in the structure. These materials therefore represented a rare family of metal phosphates, with a hybrid combination of hydrophobic alkyl chains and hydrophilic metal phosphate regions. There is much interest in the development of such materials, particularly given their similarity to lipid bilayers present in cell membranes.

3.5 References

1. Vallet-Regi, M.; Gonzalez-Calbet, J., *Prog. Solid State Chem., * **32**, 1, (2004).
2. Alberti, G.; Cavalaglio, R.; Dionigi, C.; Marmottini, F., *Langmuir,* **16**, 7663, (2000).
3. Lima, C.; Airoldi, C., *Solid State Sci.,* **6**, 1245, (2004).
4. Kaschak, D.; Johnson, S.; Hooks, D.; Kim, H.; Ward, M.; Mallouk, T., *J Am. Chem. Soc.,* **120**, 10887, (1998).
5. Sun, L.; Boo, W.; Browning, R.; Sue, H.; Clearfield, A., *Chem. Mater.,* **17**, 5606, (2005).
6. Alberti, G.; Costantino, U., *J. Molec. Catal.,* **27**, 235, (1984).
7. Alberti, G.; Marmotti, F.; Cavaglio, S.; Severi, D., *Langmuir,* **16**, 4165, (2000).
8. Benes, L.; Melanova, K.; Zima, V.; Patrono, P.; Galli, P., *Eur. J. Inorg. Chem.,* **2003**, 1577, (2003).
9. Bhambhani, A.; Kumar, C., *Chem. Mater.,* **18**, 740, (2006).
10. MacIntire, W.; Hardin, L.; Oldham, F., *Ind. Eng. Chem.,* **28**, 711, (1936).
11. Brown, E.; Lehr, J.; Smith, J.; Frazier, W., *J. Agric. and Food Chem.,* **11**, 214, (1963).
12. Hill, W.; Faust, G.; Reynolds, D., *Am. J. Sci.,* **242**, 457, (1944).
13. Tanaka, H.; Yasukawa, A.; Kandori, K.; Ishikawa, T., *Langmuir,* **13**, 821, (1997).
14. Ishikawa, T.; Tanaka, H.; Yasukawa, A.; Kandori, K., *J. Mater. Chem.,* **5**, 1963, (1995).
15. Tanaka, H.; Yasukawa, A.; Kandori, K.; Ishikawa, T., *Colloids and Surfaces,* **125A**, 53, (1997).
16. Clearfield, A.; Smith, D., *Inorg. Chem.,* **8**, 431, (1969).
17. Benes, L.; Zima, V.; Melanova, K.; Steinhart, M.; Kriechbaum, M.; Amenitsch, H.; Bernstorff, S., *J. Phys. Chem. Solids,* **65**, 615, (2004).
18. Tanaka, H.; Watanabe, T.; Chikazawa, M.; Kandori, K.; Ishikawa, T., *Colloids and Surfaces,* **139A**, 341, (1998).
19. Tanaka, H.; Oomori, K.; Hino, R., *J. Colloid Interf. Sci.,* **273**, 685, (2004).
20. Tanaka, H.; Masuda, K.; Hino, R., *J. Colloid Interf. Sci.,* **254**, 331, (2002).
21. Tanaka, H.; Chikazawa, M., *J. Mater. Chem.,* **9**, 2923, (1999).
22. Livage, J.; Barboux, P.; Vandenborre, M.; Schmutz, C.; Taulelle, F., *J. Non-Cryst Solids,* **147-8**, 18, (1992).
23. Nelson, A.; Toy, A., *Inorg. Chem.,* **2**, 775, (1963).
24. Ali, A.; Mustarelli, P.; Quartarone, E.; Magistris, A., *J. Mater. Res.,* **14**, 327, (1999).
25. Lee, B.; Samuels, W.; Wang, L.; Exarhos, G., *J. Mater. Res.,* **11**, 134, (1996).
26. Sheng, Y.; Zhou, B.; Zhao, J.; Tao, N.; Yu, K.; Tian, Y.; Wang, Z., *J. Colloid Interf. Sci.,* **272**, 326, (2004).
27. Spori, D.; Venkataraman, N.; Tosatti, S.; Durmaz, F.; Spencer, N.; Zurcher, S., *Langmuir,* **23**, 8053, (2007).
28. Sagiv, J., *J. Am. Chem. Soc.,* **102**, 92, (1980).
29. Tanaka, H.; Chikazawa, M., *Mater. Res. Bull.,* **35**, 75, (2000).
30. Cave, M.; Farrar, D.; Wright, A., *Key Engineering Materials,* **361-363**, 383, (2008).
31. *ATOMS*, Shape Software: 2005.
32. *DSPACE*, Greaves, C., University of Birmingham: 1982.
33. Gao, W.; Liu, Q.; Yang, L.; Yu, Y.; Li, F.; Jin, C., *Phys. Rev.,* **80B**, Article:094523, (2009).
34. Lee, J.; Fujita, K.; McElroy, K.; Slezak, J.; Wang, M.; Ajura, Y.; Bando, H.; Ishikado, M.; Masui, T.; Zhu, J.; Balatsky, A.; Eisaki, H.; Uchida, S.; Davis, J., *Nature,* **442**, 546, (2006).
35. Andersen, B.; Hirschfeld, P.; Slezak, J., *Phys. Rev.,* **76B**, Article:020507, (2007).

36. Jackson, L.; Kariuki, B.; Smith, M.; Barralet, J.; Wright, A., *Chem. Mater.,* **17**, 4642, (2005).

Chapter 4:

Intercalation and Exfoliation Studies in Monocalcium Phosphate Monohydrate

4.1 Introduction

Phosphate chemistry has received much attention over the past 50 years due to the versatile nature of the compounds produced. Past applications have included fertilizers,[1-3] biomaterials,[4] phosphate glasses[5] and magnetic materials.[6]

Calcium phosphates have been researched more recently, due to their similarity to natural hard tissue in the body such as bone and teeth. It is the biocompatibility and resorption properties of these materials that have interested researchers and the potential to produce synthetic mimics of these hard tissues has increased the need for research in this field. Calcium phosphates can be generally classified as bioactive ceramic materials. This means that they are generally quite hard materials and will provide a surface that living tissue can actually bond to without adverse effects upon these tissues.[4]

The advantage of calcium phosphates is the ability of these materials to be resorbed by the body, which in turn can then use the constituent components of these materials as a scaffold to regenerate the natural calcium phosphate forms present in the human body.

The main calcium phosphate containing hard tissues in the body are in the bones and teeth. Calcium phosphate predominantly forms the inorganic component of these structures in the form of carbonate hydroxyapatite[7,8]. However, attempts to mimic this phase in the body to date have produced materials which are too hard (therefore brittle) and with much lower resorption rates than the natural bone mineral form. In addition, carbonate apatite will readily undergo conversion to different forms of apatite such as fluor- and hydroxyl- apatite where the carbonate groups have been replaced by fluoride or hydroxyl. These groups will further affect the properties and synthesis of the apatite structures.

Calcium phosphates have been used in applications such as drug delivery systems and composites materials, where the organic species or drug is either mixed with or inserted into the calcium phosphate host.

The apatite phases of calcium phosphate have been investigated for their potential as drug delivery systems. Due to the structure of apatitic calcium phosphates, the adsorption of neutral as well as positive and negatively charged molecules is possible. Therefore, this method of delivery has potential for many pharmaceutical agents. One particular example where hydroxyapatite $(Ca_{10}(PO_4)_6(OH)_2)$ [HA] has been produced was in the form of HA-alginate micro-spheres that contain a void in the centre. This void allows the incorporation of another species (such as a drug) and therefore can provide a delivery vehicle for a specific agent to the appropriate site in the body. The example mentioned here used these spheres for the delivery of enzymes to a specific target.[9]

The anti-cancer agent, cisplatin, has also been tested with hydroxyapatite. In this case, the drug was loaded into hydroxyapatite particles and chemically bound to the particles. The release of cisplatin $(Cl_2Pt(NH_3)_2)$ was controlled by the presence of chloride ions in the solution around the implantation site, which allowed desorption of the cisplatin species from the HA particle surface. However, the controlled release of these drugs from the apatite material is currently still under investigation as there is some variation of the desorption rates, depending upon the crystallinity of the material.[10]

Examples of calcium phosphate composites are based upon both the layered and apatite phases of this material. Examples of these composites include α-hydroxy acids with tetracalcium phosphate $(Ca_4(PO_4)_2O)$ which forms an injectable calcium phosphate composite cement[11] and tricalcium phosphate $(Ca_3(PO_4)_2)$ with collagen or polylactic acid[12]. There are also examples where a porous network structure rather than a layered material has been used

as the inorganic component of the composite such as hydroxyapatite [HA] ($Ca_{10}(PO_4)_6(OH)_2$) with liposomes[13], (nanosized) HA with alumina[14] and polymers such as polyethylene[12] and acrylic acid[15] to form a three component composite.

Another class of material other than the apatite structures that is of interest to researchers is layered materials. A difference between the layered material compared to the apatites is their 'two dimensional' repeating nature rather than a three dimensional structure. The layered materials also offer the opportunity for intercalation reactions where species can be inserted into the interlayer region of the layered phase. This cannot be achieved with the apatite species.

Early attempts to intercalate organic species into layered inorganic host materials were performed by *Clearfield*[16], *Alberti*[17] *and Benes*[18,19] in layered zirconium phosphates. This was achieved due to the highly acidic nature of these zirconium phosphate materials and thus acid-base reactions allowed the intercalation of alkaline species into these phases.

Certain forms of calcium phosphate exhibit a similar acidic nature and possess a greater solubility compared to zirconium phosphate. Monocalcium phosphate monohydrate ($Ca(H_2PO_4)_2 \cdot H_2O$) (MCPM, figure 4.1.1) exhibits the same acidic nature and as such, should present similar intercalation behaviour to the zirconium phosphate family.

The unit cell and crystal morphology for this material was initially obtained by *Lehr, Smith and Brown*[20] in 1952 and a full characterisation was conducted by *Maclennan and Beevers*[21] in 1956. This material was initially used as a fertiliser material, due to the high water solubility and acidity, enabling good dissolution in the soil where greater acidity and phosphate sources were required.

It is well known that layered materials possess the capability to accommodate organic molecules and ions between their layers to form intercalation compounds. Layered calcium

phosphates can therefore also be classified as potential intercalation hosts. Research has concentrated upon the structures of the calcium phosphate materials, however, little research has been conducted on the intercalation properties of this family of materials, until recently[17,22].
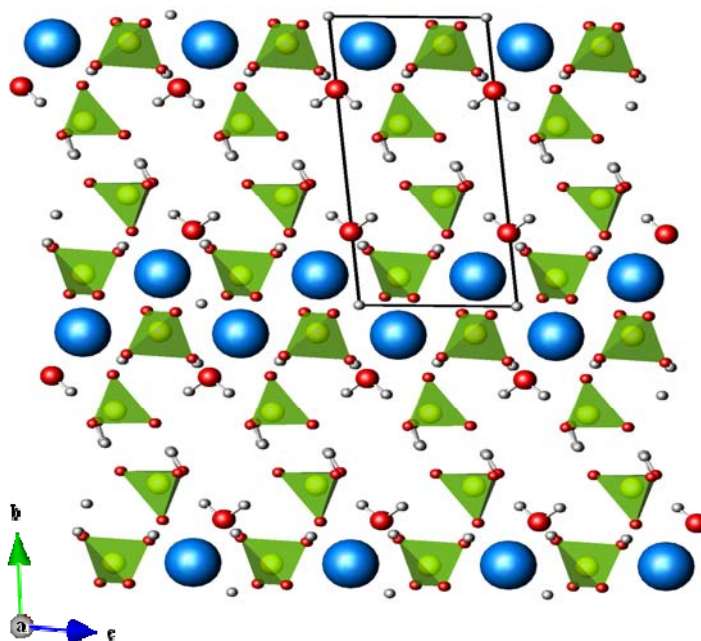
Figure 4.1.1: Structural Representation of MCPM (Blue Spheres=Calcium; Green Polyhedra=Phosphate; Red Spheres=Oxygen and White Spheres=Hydrogen)

The main aim of this section of this thesis was to attempt to use layered calcium phosphate materials and intercalate organic species between their layers to form an inorganic-organic hybrid material. This would potentially form resorbable calcium phosphate hybrid structures (See Chapter 1 of this thesis) for possible application in a biomaterial theme. These materials have potential as a drug delivery system where the proposed drug can be incorporated in the calcium phosphate and this material can be inserted into the body either as part of a solid implant or as a component of a calcium phosphate based bone cement (see Chapter 5).

Our research has concentrated on the layered monocalcium phosphate monohydrate (MCPM) phase of calcium phosphate. This material has a layered structure with strongly bonded $Ca-H_2PO_4$ layers that are held together by weaker hydrogen bonded layers (see structure diagram,[23] figure 4.1.1). This weak interlayer binding, together with accessible hydroxyl groups for strong hydrogen bonding, has potential to allow the intercalation of molecules and ions into the interlayer region of the material. This hydrogen bonding should provide a strong driving force for the potential intercalation of species that possess or can accept protons such as amines, acids and alcohols. This research will build upon some preliminary work conducted in the *Wright* group by *Lauren Webb,*[24] who initially intercalated a few simple amines into the MCPM host. An expanded selection of molecules were therefore chosen and examined with this host phase.

4.2 Experimental

4.2.1 Simple Molecule Intercalation Reactions in MCPM

The starting calcium phosphate material is available commercially from Fluka chemicals in the form calcium bis(dihydrogenphosphate)monohydrate ($Ca(H_2PO_4)_2 \cdot H_2O$) [MCPM]. A small quantity (0.3g) of this was added to a sample bottle ($\sim$ 10.5 cm^3 volume) and an excess quantity of the pure amine (Fluka or Aldrich Chemicals) was added to this vial.

Intercalation was performed using propylamine to octylamine reagents, diethylamine to dibutylamine and triethylamine to tributylamine. The addition of α,ω-diamines from 1,3-diaminopropane to 1,6-diaminohexane was also attempted. The solutions of amine and MCPM were left for a 24 hour period to react. After this time period, the sample was filtered in a Buchner filter and washed with neat amine. The long chained amines were also washed with ethanol after filtering in order to remove any surface amine. After washing, the sample was stored in a vial in a desiccator to avoid water uptake and phase conversion.

A further series of experiments were conducted with alcohols and carboxylic acids to determine whether these will intercalate into MCPM. Chemicals were purchased from Fluka or Aldrich Chemicals and the alcohols tested were ethanol to pentan-1-ol with a branched alcohol, propan-2-ol, also used (same suppliers). The standard mass of 0.3g of MCPM was used in all experiments. Ethanoic and propanoic acids were also attempted, due to the much greater acidity of these species.

If any of the materials showed partial intercalation, a longer time period in solution was attempted to allow for full intercalation to occur. This partial intercalation was evident by the use of powder X-ray diffraction where both the host phase and intercalated phase principal diffraction peaks were observed. Longer time periods were found to show a greater intensity for the intercalated phase with eventual full conversion to this phase, thereby proving that

only a partial intercalation had occurred previously. This observation will be discussed in more detail in section 4.3.

4.2.2 Complex Molecule Intercalation Reactions in MCPM

In this section, the complex molecules referred to are biomolecules that would be found in the body such as amino acids. In the body these molecules represent simple building units, but they represent quite complex intercalation species due the presence of both carboxylic and amine functional groups.

The first intercalation experiments that were attempted with the amino acids involved the use of 0.5g MCPM with saturated aqueous solutions of the amino acids alanine, arginine, cysteine, glycine and lysine (see figure 4.3.5.1 for structures) using 3g of solid amine in all five samples. MCPM was kept in the solution initially overnight and then for a prolonged period of 7 days. A final set of aqueous experiments was performed using dilute (0.25M) aqueous solutions of the amino acids with 0.3g MCPM for up to 7 days.

Alternative methods were sought using organic solvents due to the effect of water upon the MCPM structure. The first solvent used was pure methanol with sonification to reduce the amino acid particle size and therefore aid dissolution. The five amino acids (0.3g each) were added to 5 cm^3 of methanol and sonification performed for 30 minutes. The second organic solvent method used ethanol as the solvent, with a single drop of water to dissolve the 0.3g of amino acids first, before excess ethanol (10 cm^3) was added. In both organic solvent experimental sets, 0.3g of MCPM was added to the prepared amino acid solutions.

A final experimental set involved the use of solid state conditions with the five amino acid solids. In this case, 0.3g of amino acid and 0.3g MCPM were intimately ground together and placed into a porcelain crucible which was then heated to 150°C for 24 hours.

4.2.3 Drug Molecules Used for Intercalation Experiments

A set of experiments involving drug molecule intercalation was also performed. These molecules were selected for the appropriate functional groups present on the drugs, or the general size and shape of the molecules. For these tests, three drugs were examined. The first was acetylsalicylic acid (aspirin), a painkiller (Aldrich Chemicals, Figure 4.2.3.1) the second was cephalexin, an anti-bacterial agent (Fluka Chemicals, Figure 4.2.3.2) and the third was indomethacin, an anti-inflammatory (Aldrich Chemicals, Figure 4.2.3.3).

Acetylsalicylic acid – A 0.05M solution of this material was produced from 0.225g of solid acetylsalicylic acid crystals mixed with 25 cm^3 of ethanol. This material was insoluble in water and thus ethanol was required to produce a test solution. To a small portion of this solution was added 0.075g of either MCPM or butylamine intercalated MCPM.

These solutions were then left for 7 days and then the products were analysed by X-ray diffraction to determine any changes to the materials. The same procedure was adopted using MCPM and a butylamine intercalated MCPM with both the indomethacin and cephalexin solutions.
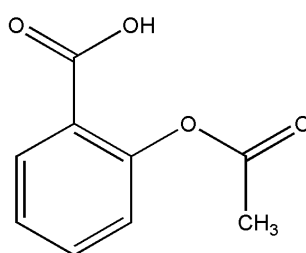
Figure 4.2.3.1: Chemical Structure of Acetylsalicylic Acid

Cephalexin – A 0.05M solution was produced from 0.433g of solid cephalexin hydrate crystals and mixed with ~25 cm^3 of ammonium hydroxide solution. This material was insoluble in water, ethanol and most organic solvents but was soluble in ammonium hydroxide.
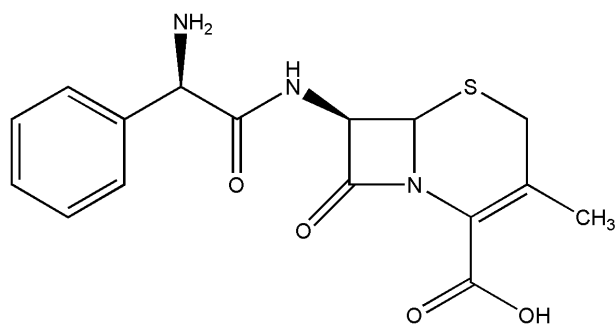
Figure 4.2.3.2: Chemical Structure of Cephalexin

Indomethacin - A 0.05M solution of this material was produced from 0.433g of solid cephalexin hydrate crystals and mixed with ~ 25 cm^3 of ethanol. This material was insoluble in water and thus ethanol had to be employed.
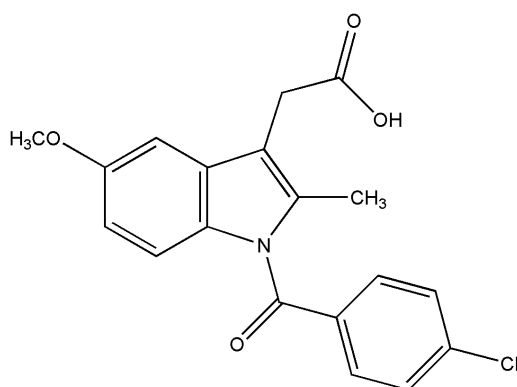
Figure 4.2.3.3: Chemical Structure of Indomethacin

Control experiments were also performed to determine whether any changes in the calcium phosphate samples were due to the solvent used in the reaction or due to the incorporation of the drug species. Samples of MCPM (0.075g) and butylamine intercalated MCPM were added to separate vials containing ammonium hydroxide or ethanol solvents only and left for the same time period.

4.2.4 Effect of Water on the MCPM Samples

0.3g of MCPM was used in each case and this was employed in one of two forms. The first form used excess water to half fill a sample vial containing the solid MCPM sample. The

second used enough water to form a paste when mixed with MCPM. These materials were left overnight initially and then a longer time period of 10 days was employed with daily sampling. The material was then filtered in the excess water case or dried in air at room temperature for the paste form. The samples were then analysed by X-ray diffraction. The same mass (0.3g) of propylamine and butylamine intercalated MCPM was also tested in the form of a paste or with excess water for the same time period. These intercalated samples were used to determine the effect of a much higher pH upon the products formed when the material was left in water.

4.2.5 Organic Solvent Effects on MCPM

0.3g portions of MCPM were added to a small range of solvents to determine the effects of solvent upon the structure of this phase. In this case, ethanol, acetone (Aldrich) and DMF (Fisher Scientific) were attempted. Further experiments were also conducted using 0.3g of propylamine, butylamine and pentylamine intercalated MCPM with acetone, ethanol and DMF to determine the effect of the solvent on the intercalated MCPM host structure. In all cases, the samples were left in solution for 7 days.

4.2.6. Attempted Exfoliation of MCPM

The main aim from these set of experiments was to separate the layers of a layered host material. Therefore it was sensible to expand the interlayer region of the material in preparation for the exfoliation. Thus amine intercalated MCPM samples were used.

In most cases, 0.15g of amine intercalated MCPM was used from propylamine to hexylamine intercalated phases. A later experiment used an octylamine intercalated phase, due to the increase layer separation afforded by the longer chains in the amine, once the structure was formed.

From the general structure of the calcium phosphate host phase, when the amine molecule was added to the host, the amine functional group would point towards the phosphate units due to hydrogen bonding. This would mean the alkyl chain of the amine would point into the interlayer region in MCPM. Therefore non-polar solvents such as hexane or toluene were added to the intercalated sample to determine whether solvation of the alkyl chains on the amine would be sufficient to allow the MCPM layers to slide over each other and thus exfoliate. Ultrasonification was also employed to potentially enhance the layer sliding using vibrational excitation of the material for 10, 20 or 30 minute intervals.

A second exfoliation method was also employed using 0.05M tetrabutylammonium bromide solutions [TBA-Br] (Fluka Chemicals) in ethanol. This species had been used previously with the analogous zirconium phosphate phases to exfoliate these species.[25] This initial concentration of solution was believed to be too weak and therefore a higher concentration (0.25M) was also attempted. In addition to these factors, pH could also have played an active role in the exfoliation and thus a more alkaline version of TBA was employed using the hydroxide form [TBA-OH] (Fluka Chemicals) again in a 0.25M ethanolic solution concentration.

4.2.7 Characterisation of Prepared MCPM Phases

The composition and structure of all these materials was investigated by powder X-ray diffraction using a Siemens D5000 diffractometer (transmission mode with Cu Kα_1 radiation). The samples were dried and ground before the X-ray diffraction was performed.

Thermogravimetric (TG) and differential thermal analysis (DTA) were performed on a Stanton Redcroft STA-780 thermogravimetric analyser at a heating rate of 3°C min^{-1} under air up to a temperature of 350°C until a stable plateau in the sample mass was achieved.

FT-IR was used for further characterisation of the bond types that are present in the material. These measurements were performed on a Perkin-Elmer Paragon 1600 Fourier transform infrared spectrometer in transmission mode, using the KBr solid disc method.

4.3 Results and Discussion

The principal method used in these experiments to determine whether intercalation had occurred was by powder X-ray diffraction. If substantial intercalation had occurred, leading to an increased separation between the layers, then this would be apparent from the shift in the main diffraction peaks to lower 2θ angle. This is a consequence of Bragg's law, (See section 2.3.1.2), whereby an increase in d-spacing of a reflection will be evident from a smaller 2θ diffraction angle.

4.3.1 Amine Intercalation

From X-ray diffraction data it appeared that attempts to intercalate monoamines from propylamine to octylamine were successful up to heptylamine (see Figure 4.3.1.1). This was evidenced by a shift of the principal diffraction peak (labelled 010 on figure 4.3.1.1) from the starting angle in MCPM of $7.4°$ 2θ to a lower angle, indicative of an increase in interlayer separation. There was no intercalation with the addition of octylamine into MCPM as the MCPM pattern remained and no changes in the diffraction pattern were observed. This would therefore suggest that the size of this molecule was too large to be directly incorporated into the interlayer spacing within this structure. This size limitation was further supported by the incomplete intercalation (host peaks still present, marked in green in figure 4.3.1.1) observed for the heptylamine intercalated sample, even after an additional 2 days in solution to allow for further time for the intercalation to occur.
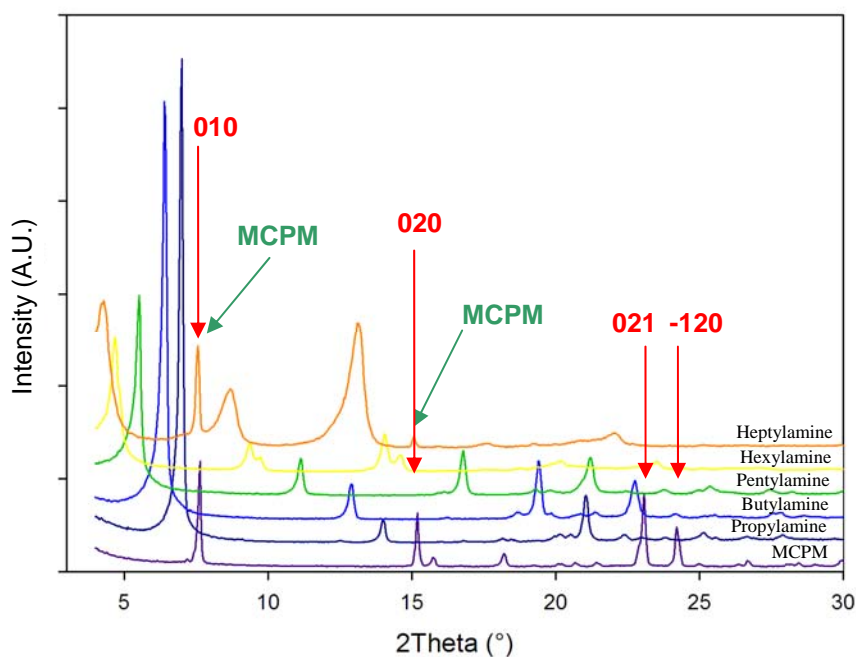
Figure 4.3.1.1: X-ray Diffraction Pattern for Monoamine Intercalated MCPM from Propylamine to Heptylamine (hkl values of MCPM peaks marked in red).

Although the direct intercalation of octylamine into MCPM was unsuccessful, when a butylamine intercalated MCPM sample was used instead of pure MCPM, it was found that octylamine could be intercalated. This octylamine intercalated MCPM phase (see figure 4.3.1.2) possessed a main diffraction peak at such a low 2θ diffraction angle, that some of the left side of the peak was beyond the accessible range of the D5000 diffractometer.
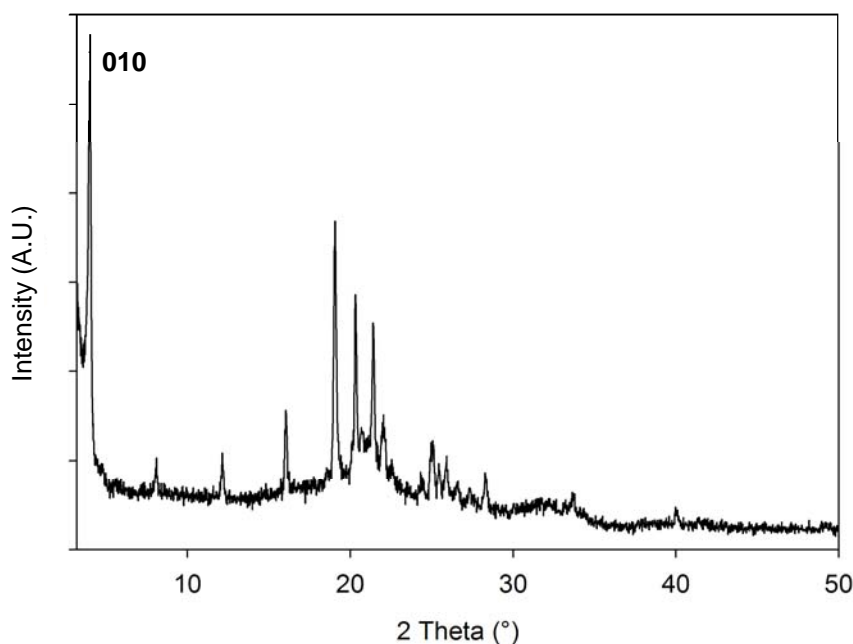
Figure 4.3.1.2: X-ray Diffraction Pattern for Octylamine Intercalated MCPM.

This successful octylamine intercalation using a pre-intercalated sample, suggested that a stepwise opening of the layers was possible. Thus a dodecylamine (12 carbons) sample was then attempted. From the shift in 2θ diffraction angle observed with the other monoamine samples, the intense first diffraction peak would occur at an angle too low for the diffractometer used. There were however further diffraction peaks on the patterns (hkl = 020, 021 labelled on the MCPM pattern in figure 4.3.1.1) produced that would also shift. These peaks are likely to be at an observable 2θ angle and thus should shift, to provide evidence of intercalation.

Dodecylamine is solid at room temperature and had to be heated to ~ 40°C to melt and allow possible reactions to occur. When the dodecylamine sample and MCPM were filtered, it was not possible to remove all the solid amine from the sample, even when washed with copious amounts of ethanol. Although this amine was more soluble in water than ethanol, MCPM was also soluble in water and thus this solvent could not be used. Gentle warming of

the ethanol solvent and the flask aided removal of some of the amine. The use of other solvents such as acetone was found to cause irreversible changes to the MCPM structure (a control reaction confirmed this) and thus could not be attempted. The diffraction pattern produced for this material was overwhelmed by the solid amine's crystal structure and hence it was not possible to determine whether intercalation had occurred.

From analysis of the X-ray powder diffraction patterns of all the successful intercalations, it was possible to obtain a basic understanding of the arrangement of the intercalated molecules from the changes in diffraction angle of the diffraction peaks as the amine chain size was increased. If the intercalated species were arranged in a regular fashion, then each additional carbon added to the amine chain would be related to the increase in d-spacing. From the Bragg equation, a decrease in 2θ diffraction angle for the principal diffraction peak would be observed with an increase in the d-spacing.

An estimation of how the amine molecules were aligning in the planes of the host MCPM structure could be produced from analysis of the principal diffraction peak (hkl=010) in each monoamine diffraction pattern (See table 4.3.1.1). The increase in planar spacing shown from the change in d-spacing was calculated.

Table 4.3.1.1: Relationship of d-Spacing Value of the Main Diffraction Peak (010) against the Carbon Length of the Amine

Carbon Length	d-Spacing Value of Main Peak (Å) (Error $\pm$ 0.12)
0	11.94
3	12.73
4	13.83
5	16.04
6	18.85
7	20.76
8	22.03
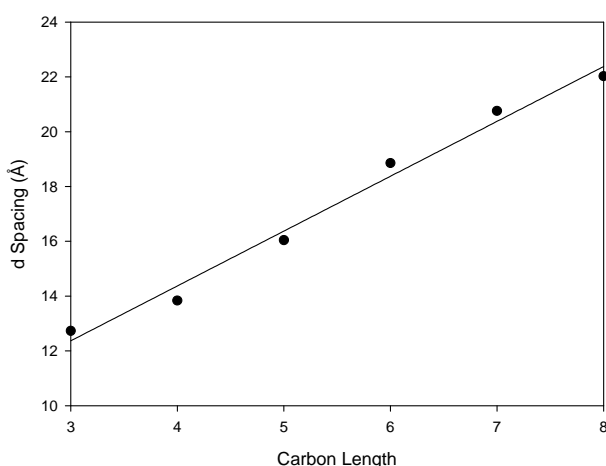
Figure 4.3.1.3: Plot of the Change in d-Spacing upon Increasing the Carbon Length of the Amine Molecule Intercalated in MCPM.

A plot of these values was prepared and from this data, a gradient of 2.002 Å per additional carbon atom was calculated. This plot is shown in figure 4.3.1.3. Using the gradient of the graph, applying trigonometry principles and assuming angled bilayers of the amine chains were formed, it was possible to estimate the tilt angle of the amine chains.

As a gradient of more than 1.26 Å[26] has been calculated, it can be deduced that a bilayer of amine chains had formed in the interlayer region.

This tilt angle of the chains, assuming an angled bilayer, was calculated at 52.5° to the calcium phosphate layer plane (See figures 4.3.1.4 & 5). Following analysis of the MCPM structure, an approximate layer thickness of the material could be estimated using the chain length & tilt angle of the amine, an estimation of the van der waals distance and the d-spacing of the main diffraction peak. This resulted in a layer thickness calculated at ~ 5.6 Å. This value was reasonably consistent with the layer thickness shown in figure 4.3.1.5.
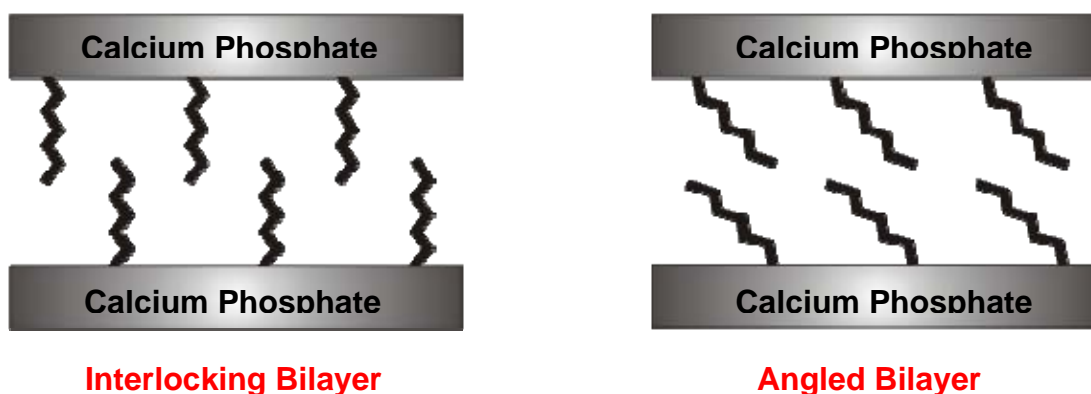
Figure 4.3.1.4: Schematic Representation of the Arrangement of Amine Molecules within the Layers of MCPM.

Similar trends of the increase in d-spacing with increasing carbon chain length have been observed in layered zirconium and titanium phosphate phases. In these examples, layered titanium phosphates have been used to intercalate monoamines into γ-titanium phosphate ($Ti(PO_4)(H_2PO_4) \cdot 2H_2O$)[27]. Linear increases in d-spacing were observed with the formation of a bilayer of intercalating species in the interlayer of this γ-phase with the chains of these species tilted at an angle of 65°.

The zirconium phosphate phases mentioned in Chapter 1 have also been used to intercalate species between their layers with similar results to the MCPM phase. Monoamines have been successfully intercalated into γ-ZrP ($Zr(PO_4)(H_2PO_4) \cdot 2H_2O$)[17] as a bilayer, with a tilt angle of 43°. Aminoalcohol species were also intercalated into α-ZrP ($Zr(HPO_4)_2 \cdot H_2O$).[18] These materials again display a similar trend to the MCPM phase with the formation of a bilayer of aminoalcohol species in the interlayer of the phosphate host, with the chains tilted at an angle of 67° in the fully intercalated phase.

Since a tilted bilayer of intercalating species was observed in these related, layered phosphate materials, it is feasible to suggest that a similar arrangement of the amine species could be possible within the MCPM structure.

The lack of diffraction data of sufficient quality and detail prevented a full structure determination of the intercalated phases. Instead, a rationalisation of the position of the intercalated molecules within the parent MCPM structure must be undertaken.

A view of the structure is shown in figures 4.3.1.5[23] & 4.3.1.6 and it can be seen that large voids exist in the structure. In figure 4.3.1.5, schematic amine molecules have been added and calculations made of the layer thickness based upon structural information obtained.[21] An additional small void that might provide further intercalation possibilities is also evident and is shown by 'B' in both figures.
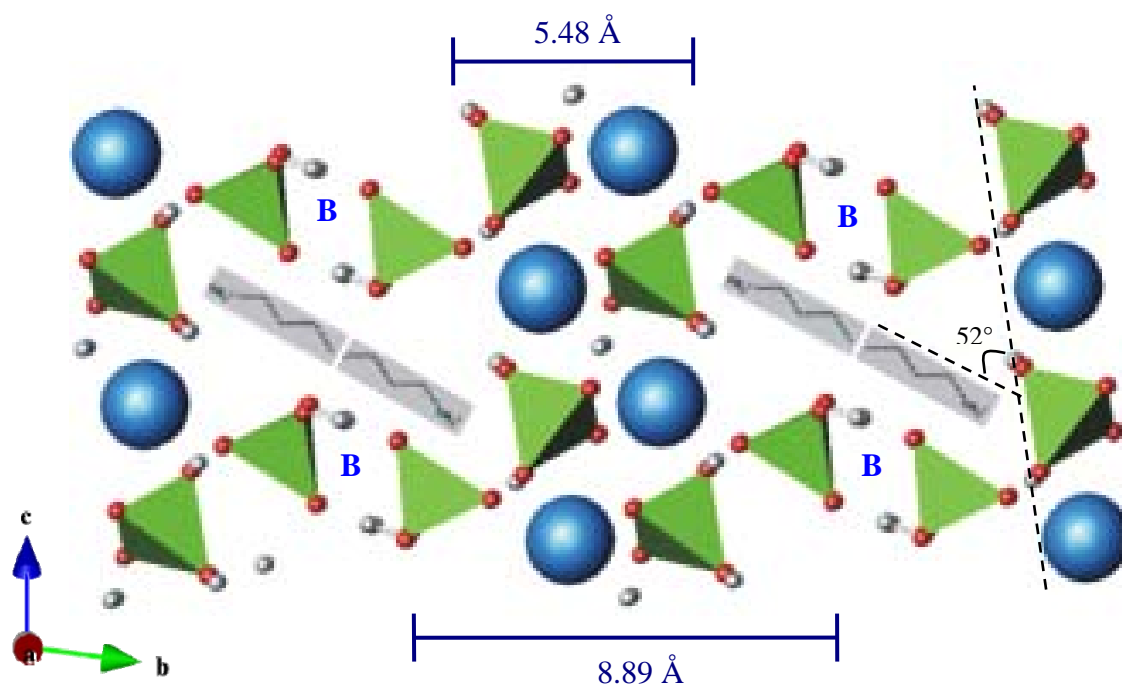
Figure 4.3.1.5: Schematic Representation of One Proposed Arrangement of Amine Molecules within the Layers of MCPM Assuming an Angled Bilayer was formed.

The space filling model also indicates that there are only two potential binding sites shown as 'A' and 'B' in figure 4.3.1.6. Both of these voids have potential for amine intercalation as they present P-OH functionality which is the likely binding site for the NH_2 of the amine. From the intercalation reactions in zirconium phosphate,[16,17] the electrostatic hydrogen bonding interactions of the amine functional group with the acidic phosphate units is responsible for successful
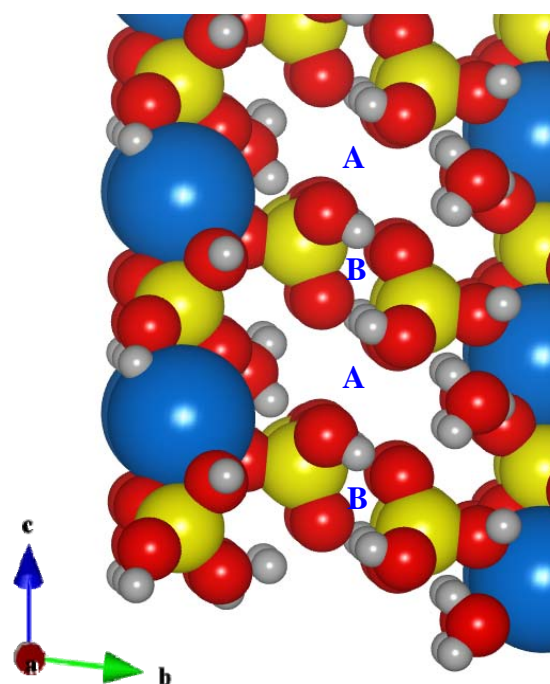
Figure 4.3.1.6: Space Filling Model of MCPM Showing the Voids within the Structure. The Two Voids are Labelled A & B (Atom Colours - Ca=blue; P=yellow; O=red; H=grey)

intercalation in zirconium phosphate. Hydrogen bonding reactions occur due to protonation of the NH_2 amine group to NH_3^+. This interacts with the P-O$^-$ bond formed on the phosphate unit by the proton donation to the formerly NH_2 group of the amine species.

The same proton donation reaction is possible in MCPM when in the presence of amine and therefore this method of interaction is expected to occur. From the increase in layer spacing on the addition of amine, this molecule is suspected to form as a bilayer inside void 'A' in figure 4.3.1.6. If the amine had positioned itself in the void 'B', a larger increase in layer separation might have been suspected due to the size of the void being much smaller compared to the size of the amine (~ 5 Å for chain length of propylamine).

To determine whether mixed molecules, could be simultaneously intercalated, a series of pre-intercalated samples were subsequently treated with different amines. The first example chosen used an excess of propylamine with a pentylamine pre-intercalated sample. From the X-ray diffraction pattern produced for this material, only a propylamine intercalated MCPM phase was observed. This result was further investigated using other amine intercalated species, such as pentylamine added to a propylamine pre-intercalated sample and propylamine added to a butylamine intercalated sample. In these cases, pentylamine and propylamine intercalated phases were seen respectively. These results suggested that whichever amine is in excess would become the intercalating species. This result also indicated that this calcium phosphate material was capable of interchanging species provided the correct conditions were provided.

To further determine the effect of excess amine on the products formed, a dilute solution (0.2M) of amine in ethanol solvent was used with MCPM and left for the same time period. From earlier experiments, ethanol was shown to have no intercalation or degrading effect upon MCPM and thus could be readily used as a solvent. The amine intercalated

MCPM phase was formed as observed when using pure amine. However, it took 16 days to complete this reaction when using the dilute solution. Thus the use of pure amine solution was necessary to produce the intercalated samples overnight and the quicker reaction time also reduced the potential effects of water degradation of the MCPM phase (See section 4.3.7 for more details).

4.3.2 Thermogravimetric Analysis of Amine Intercalated MCPM

Thermogravimetric analysis was performed on the amine intercalated samples to determine the quantity of amine present between the layers of MCPM. The materials were heated at a controlled rate from room temperature to 500°C. Different heating rates were used depending upon the data required. A faster rate (5 – 10°C min^{-1}) showed a more pronounced energy change on the DTA thermal plot, however, a lack of resolution between different mass loss events were occasionally observed. This occurred when a transition temperature was reached before the mass loss from the previous transition had finished. Slow heating rates (~ 3°C) were then used to allow resolved mass losses to be observed. Thus most analyses were performed using both heating rates, initially a fast heating rate was used to determine possible transition temperatures and where mass losses occurred. A second slow run was then used to enable accurate measurements of the observed mass losses with plateaus in the sample mass before further analysis continued.

Preliminary results of this analysis indicated that there were approximately 3 – 5 moles of amine per mole of calcium phosphate present in the fully intercalated material. This value however was suspected to be an overestimate due to the presences of some surface amine. Therefore, samples were washed with ethanol prior to analysis to remove any surface amine. Then, sufficient time was allowed for the samples to dry before analysis. Three phase

transitions were observed for the parent MCPM data sets analysed and these are displayed as a decomposition scheme shown in figure 4.3.2.1.

$$Ca(H_2PO_4) \cdot H_2O \xrightarrow[- H_2O]{100 - 120°C} Ca(H_2PO_4) \xrightarrow[- H_2O]{220 - 240°C} Ca(H_2P_2O_7) \xrightarrow[- H_2O]{300 - 350°C} \gamma\text{-}Ca(PO_3)_2$$
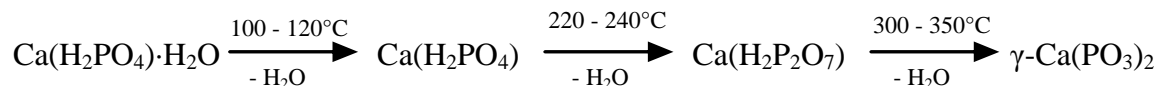
Figure 4.3.2.1: Reaction Scheme for the Decomposition of MCPM in Thermogravimetric Analysis

Analysis of the TGA data for the butylamine intercalated samples showed a further transition at ~ 400°C. This was believed to be due to the combustion of most of the amine from the structure as there were no further transitions and little mass loss on the sample from ~ 400 – 500°C. The analysis of the amine intercalated MCPM sample was difficult due to the consistent loss of amine from the structure. This occurred continuously above 100°C and thus horizontal mass loss plateaus were not observed in all the amine intercalated samples tested with this type of analysis. There was however, a definite reduction in the gradient of the mass losses observed. This partial 'plateau' was determined to be the end point of each transition. It was after this plateau that the temperature was once again allowed to increase toward the next transition.

A value of 1.1 – 1.5 moles of amine was calculated from these amine intercalated MCPM samples. Therefore, when compared to the preliminary analysis, it was apparent that a large excess of amine appeared to stick to the surface of the material unless it was thoroughly washed with ethanol. The use of this solvent had the potential to also wash some of the amine from between the layers of the material. However, it was believed that the hydrogen bonding in the interlayer and van der waals forces between the alkyl chains of the amines should have been sufficient to minimise these losses sufficiently to give a valid analysis.
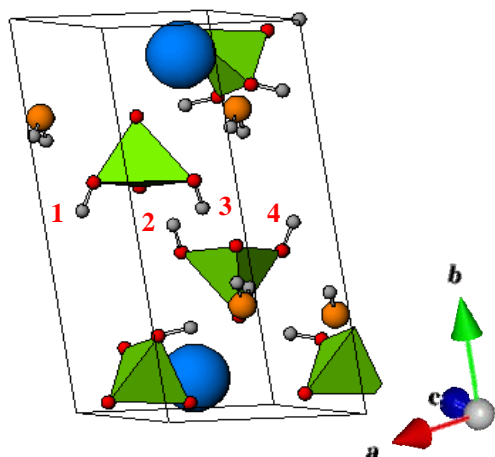
Figure 4.3.2.2: Structural Representation of the Unit Cell of MCPM. (Black Cube Represents Unit Cell with Crystal Axes for Reference). Hydroxyl Groups Numbered.

From the unit cell shown in figure 4.3.2.2, there are four hydroxyl groups present in the structure per calcium ion in MCPM. Thus four moles of amine could potentially bind in the interlayer of this structure. TGA analysis showed therefore that the MCPM structure was not fully loaded with amine molecules after the intercalation reaction. This provided further proof that not all the voids in MCPM have accommodated, or were capable of accommodating, amine molecules. Since it was not entirely clear at which point amine was removed from the structure during the heating process of the TGA analysis, it seemed likely that slightly more than 1.5 moles of amine was present in the MCPM structure. It could be deduced that two of the hydroxyl groups per calcium in the unit cell were responsible for the intercalation process in MCPM. Due to the relative size of the amine molecules, it can be suggested that the amine molecules would arrange themselves within in the larger void space in the MCPM structure (void B, figure 4.3.1.6). The position of this void in the structure would mean that in figure 4.3.2.2, the two hydroxyl groups that are likely involved with the intercalation of amine into MCPM would be hydroxyl groups 1 and 4.

4.3.3 Fourier Transform Infrared Analysis of Amine Intercalated MCPM

Infrared spectra were also obtained for the amine intercalated species. From the analysis of a propylamine intercalated MCPM sample, (Shown in figure 4.3.3.1), vibrational frequencies at 3448, 2970, 1636, 1525, 1474, 1395 1080 and 980 cm^{-1} were observed. Any further values below 1000 cm^{-1} are in the fingerprint region and will not be considered further.
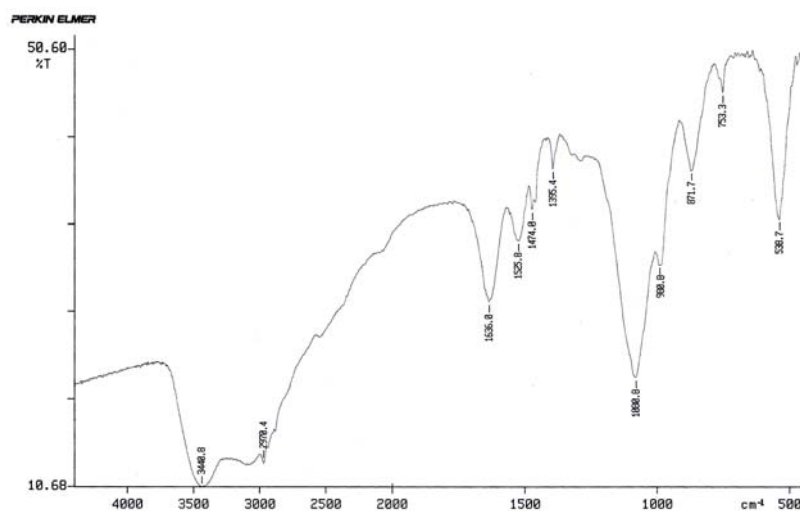
Figure 4.3.3.1: Intra-red Spectrum of Propylamine Intercalated MCPM

Assignments of the appropriate bands suggested one N-H stretching frequency at 3448 cm^{-1} and a bending mode at 1525 cm^{-1} for the amine functional group. Therefore this could be suggestive that all the amine molecules were positioned in a similar environment within the structure. The general broadness of the peak suggested some interference due to the OH stretch that would also be present in this region, but may also have suggested a range of similar sites exist. The 2970 cm^{-1} stretch was assigned to C-H bonds present on the alkyl chains on the amine molecules. In this case, only one stretch was observed which would suggest that all the C-H bonds were equivalent. Similarly, only two bending modes (symmetric and anti-symmetric) of the C-H bonds in the amine chains were located at 1474

and 1395 cm^{-1}. The stretching modes for the alkyl chains were not particularly strong on the spectrum but this could have been due to partial masking of the vibration by water and amine stretches.

The band at 1636 cm^{-1} was likely to be due to O-H present either as water of crystallisation or as hydroxyl groups present in the phosphate $H_2PO_4^-$ unit in the MCPM structure. The latter was less likely due to the likely acid-base reaction of this phosphate unit with the neat amine solution used in the intercalation process. However, it was feasible that full intercalation had not occurred and therefore some water remained in the structure. The final assigned bands at 1080 cm^{-1} and 980 cm^{-1} were due to the vibrational mode of the phosphate unit. These two values corresponded to the stretching modes of P-O bonds on the phosphate units.

4.3.4 Intercalation of Diamines and Molecules Possessing Other Functional Groups

Following the success of the monoamine intercalations in MCPM, other types of amine molecules with 2 or more carbon chains present, as well as molecules containing different functional groups, were also attempted to expand the portfolio of possible intercalating species.

Attempts to intercalate small chained (2-6 carbons) diamines and triamines showed no changes in their X-ray diffraction patterns when compared to MCPM. These results were somewhat surprising as the relative dimensions of these molecules were similar to the monoamines. However, the presence of additional alkyl functionality appeared significant and repulsion between the side alkyl chains compared to the single chained monoamines may have been the reason for the lack of intercalation. This would increase the steric hindrance between amine molecules and this could make them more difficult to pack into the interlayer region therefore preventing reaction.

The same procedure was attempted for some small chained α,ω-diaminoalkanes. Reactions with 1,3-diaminopropane to 1,6-diaminohexane provided no evidence of intercalation as there were no changes observed in their X-ray diffraction patterns. A possible explanation for this could be the distance between the hydroxyl binding sites in the host MCPM were too far apart. This would prevent both terminal amine groups on the diaminoalkane species from hydrogen bonding in the structure. This would suggest that the intercalation was not occurring in void 'B' (see figures 4.3.1.5 & 4.3.1.6), as there appears to be potential for great flexibility in the orientations of bound species at this position. Therefore it might be that intercalation was only possible in the cavity site (indicated in figure 4.3.1.5 by the presence of amine molecules) within the MCPM structure.

The intercalation of small molecules that might not cause an increase in layer spacing such as methanol, ammonia, acetonitrile and dichloromethane (DCM) were also attempted at this point. In this case, X-ray diffraction could not be used to confirm if a successful reaction had occurred and therefore other techniques such as TGA and FTIR were used. TGA was performed against an MCPM control to determine whether additional mass losses or energy changes were observed in the intercalated sample and therefore show that these small molecules were present in the material. FTIR was used to check for additional bond stretches not observed in the parent material such as N-H (for ammonia), C-N (for acetonitrile), C-Cl (for DCM) and C-O (for methanol, as O-H would be present in the host material). No additional stretches were observed in the FTIR spectra of the intercalated species and no additional mass losses or energy changes compared to the host phase were observed in the TGA analysis. This suggested that no reaction had occurred with these small molecules and the MCPM host structure.
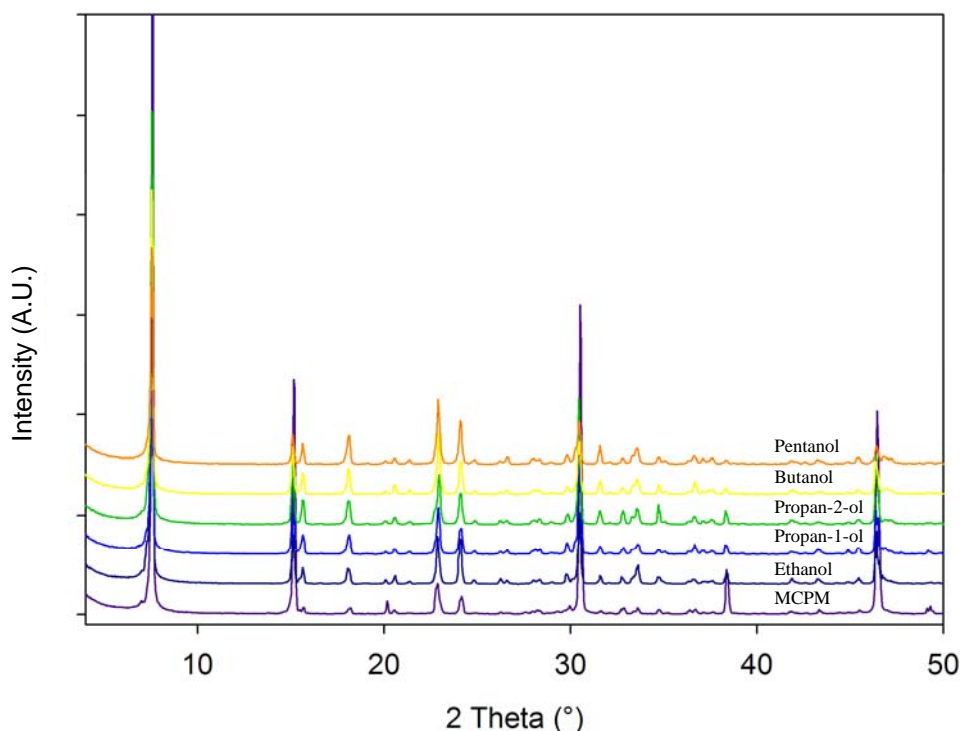
Figure 4.3.4.1: X-ray Diffraction Pattern for Alcohol Intercalated MCPM Samples

After investigating molecules with amine groups, the next class of molecules to be examined was the straight chained alcohols (See figure 4.3.4.1). Ethanol was the first species that was investigated and this molecule did not intercalate, even after a few days in solution. Following this result, a range of alcohols were attempted, as ethanol may have been too small to cause an observable increase in layer spacing within MCPM. The other alcohols tested included propan-1-ol, butan-1-ol and pentan-1-ol and two branched alcohols (propan-2-ol and butan-2-ol), however, none of these molecules caused any observable change in the diffraction patterns produced, after significant reaction times. Two small chained carboxylic acids were also attempted in an effort to determine the effect of a more acidic proton (compared with alcohols) on the hydrogen bonding ability of the intercalating species within the layers of MCPM. Ethanoic acid (glacial) and propionic acid were used for this purpose, however, once again, no intercalation was observed with either species.

A possible explanation for the amine intercalation being successful and the hydroxyl group intercalations being unsuccessful could have related to the stronger interactions due to acid-base reaction between the amines and the P-O-H groups on the phosphates. This would have provided greater stability due to further hydrogen bonding present in the hybrid phase. The hydroxyl groups would not produce this acid-base reaction, being acidic in nature and therefore the intercalation reaction would not occur by this route.

4.3.5 Attempted Intercalation of MCPM with Amino Acids

The success in intercalating amines within MCPM demonstrated that layered calcium phosphates could act as host materials and this led to a study of the bifunctional amino acids. There is much interest in the potential of hybrid materials containing biomolecules or drugs, particularly as a delivery mechanism. The biocompatibility and relative solubility of MCPM as a host is an attractive feature.

Five amino acids were initially chosen to test their intercalation potential with MCPM. The choice of the initial five amino acids was based upon the functional groups present or the general size of the amino acids. The choice of arginine and lysine (see figure 4.3.5.1) was based upon the additional amine functional groups present on the amino acids. Glycine and alanine were chosen due to their small size, with cysteine chosen because of the potential for the additional hydrogen bonding from the S-H bond in this molecule.

The use of amino acids as intercalating species in MCPM did present a problem due to these materials being solid at room temperature and therefore when using typical intercalation reactions there was a need for them to be in liquid form. MCPM is unstable in water and therefore the minimisation of the amount of water or the use of alternative solvents such as ethanol was required. However, the amino acids used namely alanine, arginine, cysteine, glycine and lysine were not sufficiently soluble in any solvent tested other than water.
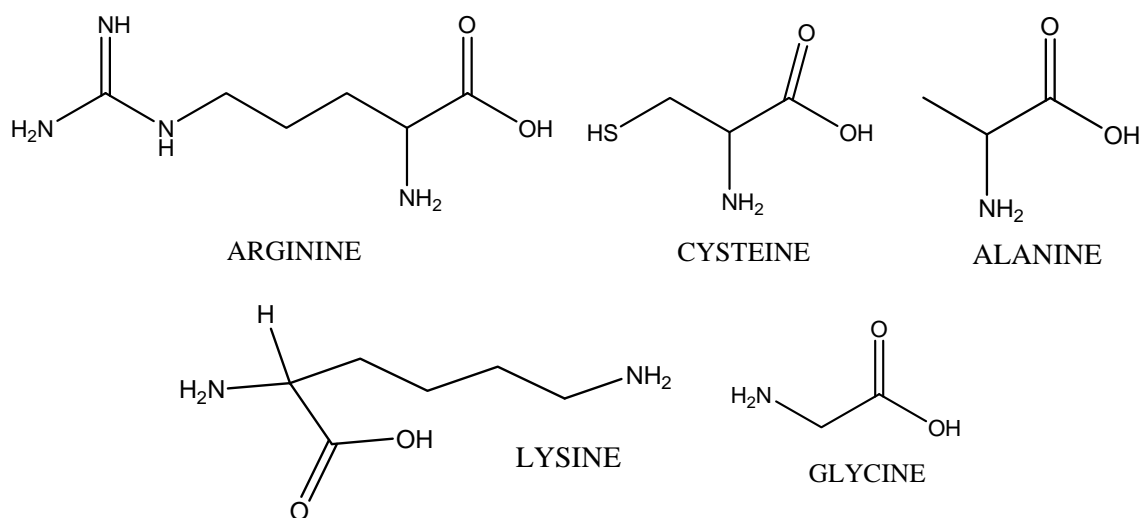
Figure 4.3.5.1: Structure of the Amino Acids Chosen for this Investigation

A number of organic solvents were tested including DMF, THF, ethanol, acetone, acetonitrile, DMSO, DCM and triethylamine, but proved unsuccessful in dissolving the amino acids. A chromatography solvent composed of butanol/ethanoic acid/water in the ratio of 60/15/25% by volume proved successful in dissolving the amino acids. However, when the water was removed, and the solvent composed of butanol/ethanoic acid in the ratio 70/30% the attempt was unsuccessful. It was therefore apparent that the presence of water was necessary for the dissolution of the amino acids.

A number of experiments were then undertaken where water was included as a minimum component of a co-solvent system. In the first set of these experiments, a saturated solution of each of the five chosen amino acids was added to 0.5g MCPM and left initially overnight and then for a extended time period of 7 days. When these 5 samples were analysed by X-ray diffraction, the alanine, glycine and cysteine containing phases had converted from MCPM to brushite overnight. Arginine and lysine containing MCPM samples had converted to hydroxyapatite. This different phase formation was due to the higher pH of the resulting

amino acid solution and therefore caused the formation of hydroxyapatite. More details about this phase formation can be found in section 4.3.7.

A set of experiments was conducted using a small quantity (0.3g) of lysine or arginine dissolved in a minimal amount of water together with 15 cm^3 of ethanol as the excess solvent. To this solution, 0.3g of MCPM was added and left for 1 day. In this case, the MCPM was stable but no intercalation was detected. A longer time period of 4 days was also applied, however, no intercalation or degradation was observed. This was probably due to the lack of an excess of intercalating species.

It would appear that the use of water to dissolve the amino acid was sufficient to destabilise the MCPM phase. Therefore, in an attempt to overcome this problem, methanol was used, as it has a similar polarity to water. Sonification was employed to reduce the amino acid particle size and hopefully aid some dissolution of the reagents. When the five samples were reacted overnight, MCPM was shown to be present, with a small amount of the solid amino acid also detected in some of the powder X-ray diffraction patterns. Sonification did not appear to improve the dissolution of the amino acids in the organic solvent, thus reinforcing the requirement for water to allow the amino acid to dissolve.

From the above results, it was clear that amino acids would not readily intercalate in the pure MCPM phase. However, it might be possible to promote the intercalation reaction by the use of amine intercalated version of MCPM where the host layers are already separated.

Butylamine intercalated MCPM was chosen, as this had been used previously to allow octylamine to be intercalated and therefore showed potential for stepwise opening of the layers. Lysine and arginine were initially chosen as the amino acids to test, due to the additional amine functional groups being favourable for exchange with butylamine and compatible with MCPM. These were added to a minimal amount of water to form a saturated

solution before the butylamine intercalated MCPM was added. These samples were left for 2 days before analysing by powder X-ray diffraction. In both samples, either solid amino acid or hydroxyapatite was observed. It was therefore concluded that the amino acid solutions would not intercalate in the MCPM phase and they were causing decomposition of the phase. The fact that structural rearrangement was observed with both MCPM and the butylamine intercalated MCPM would suggest that a larger interlayer spacing for the amine intercalated phase had no effect upon any potential intercalation, as no change in d-spacing was observed on either powder X-ray diffraction pattern. The same was true for the lack of shift in 2θ for the hydroxyapatite phase formed with these samples compared to a 'control' phase (pure hydroxyapatite from reagent bottle) therefore showing that no reaction with the amino acid had occurred.

In addition to the above amino acid intercalation using solvent methods, solid state reactions were also proposed. Unfortunately, the crystalline amino acids would melt around 220 - 230°C and MCPM was known to change phase above 180°C to form an anhydrous phase ($Ca(H_2PO_4)_2$) and around 220°C, MCPM would convert to the calcium acid pyrophosphate phase ($CaH_2P_2O_7$) of calcium phosphate. Therefore, an intermediate temperature of 150°C was attempted to determine whether the lower temperature would be sufficient to enable some form of intercalation to occur. However, the MCPM phase decomposed at this temperature, in the presence of the solid amino acid, to form monetite ($CaHPO_4$). In addition, the solid amino acids could not easily be removed from the MCPM sample without the use of water which would cause further complications. Therefore this method was not pursued any further.

The selection of the 5 amino acids used with these investigations was chosen for their expected compatibility and intercalation potential with MCPM. Therefore the examination of

the other amino acids was believed to have no advantage since these species contained incompatible functional groups. Hence the amino acid intercalation reactions were not pursued further.

4.3.6 Drug Molecule Intercalation Reactions

Small drug molecules were tested to determine whether these larger molecules would intercalate into the layered structure of MCPM. Three drug molecules were tested with MCPM and a butylamine pre-intercalated MCPM phase. In all the samples tested with the indomethacin, cephalexin and acetylsalicylic acid drug molecules, no intercalation was observed. The only observable effect of these drug solutions upon the calcium phosphate were a change in the structure of MCPM to brushite ($CaHPO_4 \cdot 2H_2O$) which occurred due to the presence of a small quantity of water in the ethanol solvent used in these reactions. When the control samples were analysed, one notable change in structure of the MCPM sample occurred when the ammonium hydroxide was used to dissolve the cephalexin drug. The acidic MCPM phase reacted with the ammonium hydroxide to form ammonium phosphate ($NH_4H_2PO_4$). Thus any changes in the structure of the MCPM when using cephalexin was due to the solvent reaction with the host material rather than any form of intercalation. The diffraction patterns produced for this MCPM phase when cephalexin was present matched perfectly with the control reaction and therefore no intercalation of the drug molecule was observed.

4.3.7 Effect of Water on MCPM

The effect of water upon the structure of MCPM was significant. The addition of water to a sample of MCPM will cause a change in structure from $Ca(H_2PO_4)_2 \cdot H_2O$ to $Ca(HPO_4) \cdot 2H_2O$ (brushite) with an acidification of the resulting solution. This brushite phase

was determined by powder X-ray diffraction analysis of the powder products remaining after leaving the MCPM in excess water for 1-3 days, as shown on figure 4.3.7.1. This reaction must have occurred by a dissolution/re-precipitation method, as some of the material noticeably dissolved when added in water and an acidic solution (pH = 3-4) was formed.
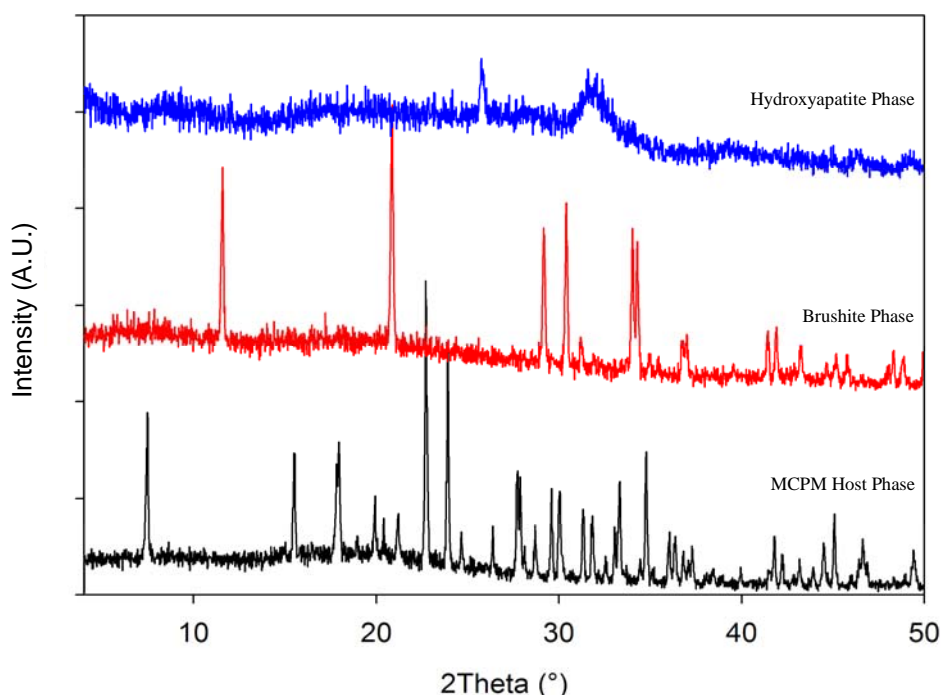
Figure 4.3.7.1: X-ray Diffraction Pattern Showing Phases Formed when MCPM and Butylamine Intercalated MCPM were exposed to Water.

The effect of adding an amine intercalated sample into excess water produced interesting results. In contrast to the pure MCPM results, an alkaline solution was formed with the intercalated phase having a slightly reduced solubility. X-ray diffraction analysis of the powder remaining after the overnight treatment revealed the formation of a poorly crystalline hydroxyapatite phase (See figure 4.3.7.1).

The amount of water present with the MCPM was important in determining the formation of a particular phase. When only a limited amount of water was used to maintain the amine intercalated MCPM samples as a paste, a brushite phase was formed. This

experiment was repeated several times and similar results were obtained each time. This result was unusual due to the expectation that the high pH of the solution would favour the formation of hydroxyapatite preferentially as was seen in the excess water experiments.

A possible explanation for this phase formation could have been due to the limited water quantity with the highly soluble acidic MCPM phase producing localised acidity. When a small quantity of water was present, the acidic calcium phosphate might have produced regions of low pH, which might not have been neutralised by the small amount of alkaline amine that was intercalated in the MCPM layers and therefore favoured brushite formation rather than hydroxyapatite.

4.3.8 Organic Solvent Effects on Amine Intercalation in MCPM

When a dilute solution of amine was used rather than pure amine, a much longer reaction time was observed. The main solvents that were investigated for these solutions were ethanol, acetone and DMF. DMF was chosen due to its small size and high polarity and interestingly although there was no evidence of reaction, there was a greater proportion of fine white powder present when the MCPM sample was filtered, with the vast majority of this material passing through the filter paper. This fine material still possessed the MCPM structure, although the diffraction peaks were broader indicating a smaller size of the particles. This suggested that this solvent caused some degradation of the MCPM sample, but not sufficient to cause the material to convert to hydroxyapatite or brushite but enough to reduce the particle size significantly.

Control experiments were also performed on these samples using only MCPM, without prior monoamine intercalation, and these results showed that DMF caused degradation of the host material and acetone caused a partial dehydration of the MCPM phase, due to the high affinity of this solvent for water thus leaching it from the MCPM structure.

A final set of experiments was conducted using propyl-, butyl- and pentylamine pre-intercalated MCPM with ethanol, acetone or water solvents. When any of the three amine intercalated MCPM samples was added to the ethanol solvent, no change in structure was observed. When water solvent was used, the formation of poorly crystalline hydroxyapatite was observed as detailed in section 4.3.7.

When acetone was used as the solvent, unusual diffraction patterns were formed with a shift of the first peak to higher angle. This was especially apparent with the propylamine sample that shifted beyond the position of pure MCPM as shown in figure 4.3.8.1. This shift could have been due to solvation of the intercalated amine and associated water to leave a partial or fully dehydrated MCPM phase.
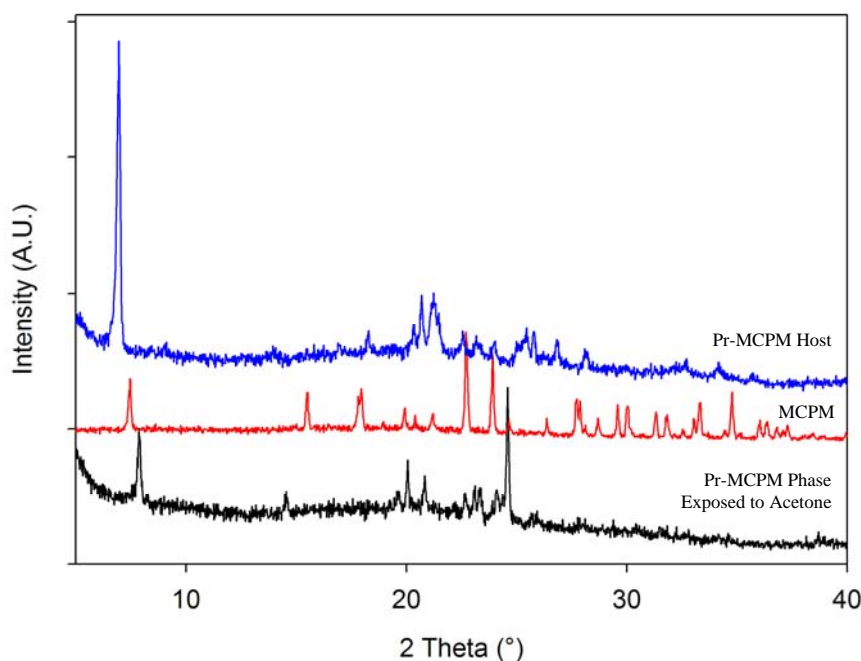
Figure 4.3.8.1: X-ray Diffraction Pattern Showing Phase Formed when Propylamine Intercalated MCPM was Exposed to Acetone.

If the water or amine molecules were removed from between the layers, the layers could move closer together than observed in the host MCPM structure. Thus a smaller interlayer spacing than the host structure could be observed on the powder X-ray diffraction

patterns hence the shift to higher 2θ. A similar shift was also observed with the butylamine and pentylamine intercalated phases.

Even though the exact reason for the formation of the unknown phase was not clear, it could be concluded that both DMF and acetone were not viable solvents for reactions involving MCPM or amine intercalated MCPM as they destabilised the structure. Ethanol, however, had no effect upon the structure and should be considered as the preferred solvent.

4.3.9 Attempted Exfoliation of MCPM

From the nature of the 'clay-like' layered structure of MCPM with weak interlayer bonding, it might be feasible to initiate an exfoliation of the layers. Often exfoliation could be induced with appropriate exfoliating species and examples included those used with clay materials[28] and related phosphate species.[25,26] In this work, a similar approach was attempted, using tetrabutylammonium salts. Another class of exfoliation-initiating species that have also been reported previously and were investigated here were the surfactant molecules, possessing long bulky alkyl 'tails' and positively charged 'head' groups.[25]

From the experimental section of this thesis, a brief overview of exfoliation (Section 2.2.5) was presented. For this process to occur, the presence of a certain moiety in the interlayer region of the layered material was required which is bound sufficiently strongly to the layers but has weak bonding between them. Disruption of the weak forces linking the layers together would lead to the breakdown of the 3-dimensional layered structure, thus leading to exfoliation.

The first set of exfoliation experiments that were attempted used amine intercalated versions of MCPM with the exfoliating species tetrabutylammonium bromide [TBA-Br]. In this case, propylamine, butylamine, pentylamine and hexylamine intercalated forms of MCPM were tested with various concentrations of TBA-Br. Initially, a 0.05M solution of

TBA-Br was attempted and left overnight. When powder X-ray diffraction analysis was performed, no change in the structure was observed. Therefore, a longer time period of 2 days and a more concentrated solution (0.25M) was used to determine whether this would cause exfoliation. The more concentrated solution did not cause exfoliation as the X-ray diffraction peaks still remained. Furthermore, thorough washing of the samples was required and in some cases, centrifugation was necessary to separate the calcium phosphate powder from the solution as the particle size was much smaller after the treatment.

Further exfoliation experiments were also attempted with MCPM using the much greater interlayer spacing provided by the octylamine intercalated MCPM samples. Thus TBA-Br and TBA-OH solutions were attempted with this phase and once again, no observable change in the diffraction pattern was evident with this material. This would further suggest that no exfoliation had occurred as there were clearly defined peaks in the diffraction pattern, due to the intact 3-dimensional layered arrangement. Even with the larger interlayer region, either the interlayer forces were strong enough to hold the layers together or the exfoliating species were too bulky to pass through into the interlayer region and disrupt the interlayer forces within the MCPM structure.

The use of solvent for the exfoliation was necessary due to the inherent water instability of MCPM. The TBA-Br and TBA-OH species were soluble in ethanol and this solvent was observed previously not to intercalate or affect the stability of the MCPM. Non-polar organic solvents might have proved useful for solvating the alkyl chains when an amine intercalated MCPM sample was present but the polar TBA molecules would not dissolve in these solvents and therefore this solvent could not be used with these molecules directly.

In a separate experiment, an amine intercalated version of MCPM was used with neat hexane solvent and sonication to attempt to disrupt the apparent van der waals forces holding

the alkyl chains and therefore the 3-dimensional structure together. Unfortunately this technique did not cause exfoliation and the crystalline host material diffraction peaks were still present. The same experiment was repeated with a 50/50 mixed ethanol/hexane solution using butylamine intercalated MCPM with sonication and when the sample was analysed using X-ray diffraction, the host material peaks were still present. A longer time period in solution, using the same sample, was therefore performed, but even after 4 days the host material peaks were still present, suggesting that this mixed solvent was not causing the phase to exfoliate.

4.4 Conclusions

From the results obtained, monoamines were successfully intercalated into MCPM. The longer chained (> 6 carbons) species had to be pre-intercalated in a step-wise fashion which enabled these larger species to be inserted into the interlayer region. Although there was insufficient X-ray diffraction data to determine the location of the amine within the MCPM structure, this species is likely to be located in the larger void (void B, figure 4.3.1.6) in this material. This is supported by the TGA data which suggested that less than 2 moles of amine per formula unit were present. The structural representation (figure 4.3.2.2) shows 2 hydroxyl groups which point into the large void in the structure. These hydroxyls could enable hydrogen bonding of the amine to the MCPM layers which would allow intercalation of the amine species into the MCPM phase.

The attempted intercalation of other diamine and diamino species was not successful. This was possibly due to the steric interactions between the molecules being too great, particularly if these molecules were present in the interlayer region. In addition, the intercalation of small biomolecules such as amino acids proved too difficult to achieve. The problem with these species was their inherent solubility in water which could not be used with MCPM as it caused this calcium phosphate phase to dissolve. A wide range of solvents were trialled but none could be found that would dissolve the amino acid and not react with the MCPM material.

MCPM was shown to be unstable in aqueous conditions and would readily decompose to either hydroxyapatite or brushite. The choice of decomposition products was also dependent upon whether any intercalants were present. If a high solution pH (pH > 7) was present, then hydroxyapatite ($Ca_6(PO_4)_{10}(OH)_2$) was formed in preference to brushite which formed at low pH.

The intercalation of species that did not contain an amine group, such as alcohols and carboxylic acids, proved to be unsuccessful. This showed that it was essential for the amine group to be present in order for the intercalation reaction to occur.

Many attempts were made to exfoliate either the MCPM host structure or the amine intercalated version of the MCPM structure. However, exfoliation of MCPM was not achieved due to either the choice of exfoliating species or the stability of the layers when the exfoliating species was present. Disruption of the alkyl chains of the monoamines when they were intercalated in MCPM also did not allow successful exfoliation of this phase. This was probably due to the inherent stability of the layered structure.

4.5 References

1. MacIntire, W.; Hardin, L.; Oldham, F., *Ind. Eng. Chem.,* **28**, 711, (1936).
2. Hill, W.; Faust, G.; Reynolds, D., *Am. J. Sci.,* **242**, 457, (1944).
3. Brown, E.; Lehr, J.; Smith, J.; Frazier, W., *J. Agric. Food Chem.,* **11**, 214, (1963).
4. Vallet-Regi, M.; Gonzalez-Calbet, J., *Progr. in Solid State Chem.,* **32**, 1, (2004).
5. Dorozhkin, S., *J. Mater. Sci.,* **42**, 1061, (2007).
6. Cousin, O.; Mentre, O.; Huve, M.; Abraham, F., *J. Solid State. Chem.,* **157**, 123, (2001).
7. Mathew, M.; Takagi, S., *J. Res. Nat. Inst. Stand. Tech.,* **106**, 1035, (2001).
8. Vallet-Regi, M., *J. Chem. Soc., Dalton Trans.,* **(2)**, 97, (2001).
9. Ribeiro, C.; Barrias, C.; Barbosa, M., *Biomaterials,* **25**, 4363, (2004).
10. Barroug, A.; Kuhn, L.; Gerstenfeld, L.; Glimcher, M., *J. Orth. Res.,* **22**, 703, (2004).
11. Barralet, J.; Tremayne, M.; Lilley, K.; Gbureck, U., *Chem. Mater.,* **17**, 1313, (2005).
12. Murugan, R.; Ramakrishna, S., *Composites Sci. and Tech.,* **65**, 2385, (2005).
13. Chu, M.; Liu, G., *Nanotechnology,* **16**, 1208, (2005).
14. Viswanath, B.; Ravishankar, N., *Scripta Materialia,* **55**, 863, (2006).
15. Furuichi, K.; Oaki, Y.; Ichimiya, H.; Komotori, J.; Imai, H., *Sci. Tech. Adv. Materials,* **7**, 219, (2006).
16. Clearfield, A.; Smith, D., *Inorg. Chem.,* **8**, 431, (1969).
17. Alberti, G.; Marmotti, F.; Cavaglio, S.; Severi, D., *Langmuir,* **16**, 4165, (2000).
18. Benes, L.; Melanova, K.; Zima, V.; Patrono, P.; Galli, P., *Eur. J. Inorg. Chem.,* **2003**, 1577, (2003).
19. Benes, L.; Zima, V.; Melanova, K.; Steinhart, M.; Kriechbaum, M.; Amenitsch, H.; Bernstorff, S., *J. Phys. Chem. Solids,* **65**, 615, (2004).
20. Lehr, J.; Smith, D.; Brown, W., *S.E. Regional Meeting, Am. Chem. Soc.,* **October 1952**, 1, (1952).
21. Maclennan, G.; Beevers, C., *Acta Cryst.,* **9**, 187, (1956).
22. Lima, C.; Airoldi, C., *Solid State Sci.,* **6**, 1245, (2004).
23. *ATOMS*, Shape Software: 2005.
24. Webb, L. Synthesis and Characterisation of Calcium Phosphate Biomaterials. PhD Thesis, The University of Birmingham, (2007).
25. Kim, H.; Keller, S.; Mallouk, T., *Chem. Mater.,* **9**, 1414, (1997).
26. Kaschak, D.; Johnson, S.; Hooks, D.; Kim, H.; Ward, M.; Mallouk, T., *J Am. Chem. Soc.,* **120**, 10887, (1998).
27. Menendez, A.; Barcena, M.; Jaimez, E.; Garcia, J.; Rodriguez, J., *Chem. Mater.,* **5**, 1078, (1993).
28. Nam, P.; Fujimori, A.; Masuko, T., *J. App Poly. Sci.,* **93**, 2711, (2004).

Chapter 5:

Calcium Phosphate Bone Cements

5.1 Introduction

Calcium phosphate cements were first discovered by *Brown and Chow* in 1983[1,2] and are generally formed by a combination of one or more calcium phosphate phases, which upon mixing with a liquid phase, usually water, form a paste which is able to precipitate crystals of calcium phosphate and sets by the entanglement of these crystals. These materials have great potential as bone cements and bone substitutes due to their high biocompatibility, largely linked to their similar composition to bone minerals. This contrasts with current commonly used polymer-based cements (e.g. polymethylmethacrylate, [PMMA][3,4] which often possess toxic monomers and elevated setting temperatures. An additional benefit of calcium phosphate cements [CPC] over many polymer based materials is their potential resorption. In some applications it can be beneficial for the implanted cement to be resorbed by the body thus eliminating the need for surgical removal. Some CPC compositions offer appropriate solubility which can be matched to the regrowth of local bone tissue.

Various combinations of calcium phosphate and related calcium salts have been investigated as potential cements leading to two main end products. These end products are *brushite* (Calcium hydrogen phosphate dihydrate ($CaHPO_4 \cdot 2H_2O$)) or *apatite* such as hydroxyapatite ($Ca_{10}(PO_4)_6(OH)_2$) or a calcium-deficient apatite ($Ca_9(HPO_4)(PO_4)_5OH$)[5]. The formation of either brushite or apatite is not just dependent on stoichiometry but upon the pH-dependent solubility of the calcium and phosphate components present. Below a key pH value of 4.2[6] brushite is formed and above it hydroxyapatite is formed.

Brushite cements have much better solubility compared with apatite based cements at physiological pH values and are dissolved more quickly from the site of implantation.[7] Obviously this can be disadvantageous if resorption occurs too rapidly and leads to a deterioration of the mechanical strength of the material as it dissolves. Brushite is only

meta-stable and in some circumstances will convert to apatite under physiological conditions which will reduce the overall resorption rate of the cement.[8,9] These CPCs can be used in many applications but neither CPC phase can be used for load bearing applications, due to their brittleness compared with other polymer systems (e.g. PMMA based systems).[4]

During the hardening process, the small cement crystals will interlock with each other and form a micro/nanoporous structure. The porosity of the cement depends upon the processing conditions of the reagents or the mixing conditions for the cement itself. This allows some control over the properties of the cement which can be adopted depending upon the required conditions.[10] These parameters are discussed in more detail later in this section.

The general setting states of the two types of cements are noticeably different. Apatite based cements will slowly change from a viscous gel to a solid state whereas brushite based cements change from a runny liquid to solid very quickly. The cement setting reaction proceeds via an exothermic process and in some cases this releases more thermal energy than in the methylmethacrylate polymerisation reaction to produce the polymer cement systems. However, unlike the polymer cements, the rate of thermal energy release is slow enough that it can be ignored.[11] This slow exothermic reaction makes the use of these cements very favourable as they cause less thermal damage to the surrounding tissues in the implant area.[12]

The setting reaction for the calcium phosphate cement systems can occur by three reaction routes depending upon the choice of the cement components and pH.

$$Ca(H_2PO_4)_2 \cdot H_2O + \beta\text{-}Ca_3(PO_4)_2 + 7H_2O \rightarrow 4CaHPO_4 \cdot 2H_2O \qquad (1)$$

$$2Ca_4(PO_4)_2O + 2CaHPO_4 \rightarrow Ca_{10}(PO_4)_6(OH_2) \qquad (2)$$

$$3\alpha\text{-}Ca_3(PO_4)_2 + H_2O \rightarrow Ca_9(HPO_4)(PO_4)_5OH \qquad (3)$$
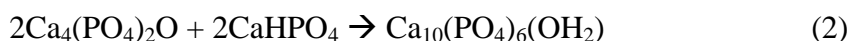
Reaction 1 proceeds via an acid/base neutralisation with $Ca(H_2PO_4)_2 \cdot H_2O$ [MCPM] being the acidic species and $\beta\text{-}Ca_3(PO_4)_2$ [β-TCP] being slightly alkaline, leading to the

neutral brushite species (CaHPO$_4$·2H$_2$O).[13] Reaction 2 occurs in a similar manner to reaction 1 except that Ca$_4$(PO$_4$)$_2$O is alkaline and CaHPO$_4$ is slightly acidic, leading to the formation of an alkaline apatite phase. Reaction 3 occurs via a dissolution/re-precipitation mechanism, to convert the alkaline tricalcium phosphate phase to the calcium deficient hydroxyapatite phase.

CPC setting reactions need to occur reasonably quickly to prevent delays during surgical operations because excessive waiting time for the materials to set is impractical. However, the time needs to be sufficient so that the cement components can be mixed and applied to the appropriate site before hardening to a non-mouldable state. Therefore as brushite cements react quickly, they often contain retardants to slow down the setting reaction sufficiently so that the cement paste remains workable for longer to enable it to be moulded into position before it sets.[14] In ideal cements, good mechanical properties should be reached quickly, in a similar timeframe to the setting reaction so that any initial load will not cause load slipping at the interfaces.

5.1.1 Cement Setting Stages and Modification of Setting Times

The setting of CPC occurs in three distinct stages.[1] The first is the dissolution of reactants into calcium and phosphate ions in the mixing liquid, the second is the formation of crystals and the third involves the growth of the formed crystals.

There are many ways to alter the setting times of the cement to match the requirements of the cement's usage. Reducing reagent particle size will help decrease the time required to reach a set cement. There is however an increase in the potential agglomeration of the particles as their general size is reduced. If one of the reagents were to be changed for a more or less soluble material, the setting time would change accordingly. Therefore the choice of reacting MCPM with either β-TCP or the more soluble α-TCP will increase or decrease the

setting time respectively. However, in either case, the TCP material must be soluble in the solvent used to allow the cement reaction to complete. Therefore pH can be a critical factor in determining how fast the cements will actually set.

Nucleation of the crystals in the cement can also be altered to either speed up the reaction by adding seed nuclei[15] or partially saturating the reagent solution with similar ions or slowed down by using inhibitors such as magnesium ions[9,16,17] (apatite cements), pyrophosphate[7,8,11] or citrate ions (brushite cements).[1] These inhibiting strategies can also be applied to the growth of the crystals once they have nucleated. Pyrophosphate ions are believed to bind with the nuclei of calcium salts in solution and stop the ions from forming crystal lattices. This will reduce the size of the crystals formed by slowing crystal growth and aggregation.[7] An advantage to the use of citrate ions in the cement has been shown to be a reduction in the viscosity[18,19] offering the potential for injectable cement pastes. Citric acid has been found naturally in human bone and has previously been used as a chelating agent[6] in biomaterial trials and has been shown to be nontoxic.[19] The citric acid has also been used to retard the dissolution/re-precipitation reaction in the cement during mixing[3] and therefore allows a more homogenous mixture. However, this longer setting time tends to reduce the strength of the cement during setting but, once set, the cement tends to be stronger due to lower porosity[15] and better binding of the cement crystals.

In addition to altering the physical properties of the solid reagents, the powder to liquid ratio of the cement will also affect the setting time of the cement. As shown by *Grover et al.*,[20] varying the powder to liquid ratio from 1.25g/mL to 2.25g/mL increased the compressive strength of the cement from 4 to 25 MPa. However, when a powder to liquid [P/L] ratio of 2.75g/mL was used, a decrease in strength was observed. The initial increase in

strength of the cements with P/L ratios from 1.25 to 1.75g/mL was due to a decrease in the porosity of the cement sample.

A further modification of the liquid phase was also performed by *Takagi et al.*[21] This involved the addition of sodium hydrogen phosphate (Na_2HPO_4) to water and therefore formed a phosphate containing liquid phase. This liquid phosphate solution was added to the solid reagents $CaHPO_4$ and $Ca(OH)_2$ and allowed to set to form a hydroxyapatite based cement. The addition of the phosphate solution was critical for increasing the phosphate concentration in the liquid phase, so that re-precipitation of the cement phase could occur quickly and the cement could set rapidly.

5.1.2 Improving the Strength of Cements

To improve the strength of cements, some novel ideas have been proposed. One route utilised a composite material containing natural organic polymers such as collagen[22] or chitosan.[23] Collagen has been known to enhance cell adhesion onto calcium phosphate surfaces such as hydroxyapatite and tricalcium phosphate [TCP].[22] Therefore a combined collagen-calcium phosphate bone cement could provide the enhanced cell adhesion[22] properties together with favourable mechanical and resorption properties. However, hydroxyapatite and TCP have limited resorption rates and therefore alternative calcium phosphate phases have to be investigated to improve the rate of resorption. Chitosan has also been used to strengthen the calcium phosphate cements by binding the solid components more effectively, however, it has not been fully investigated as a component of a calcium phosphate cement composite.

Another type of resorbable fibre called polyglactin has also been tested to increase the elasticity and flexing strength of brushite cements, as this property is a current weakness with this type of cement. Short fibres were either randomly or regularly arranged within the cement

paste and then the composite was then left to harden.[24] Once set, it was discovered that the material had improved elasticity without any detrimental effect upon the compressive strength of the material.

There have been a few attempts to improve the strength of calcium phosphate cements by actually varying the cement forming calcium phosphate end product. So far, the orthophosphate based (PO_4^{3-}) bone cements have been discussed, however, pyrophosphate ($P_2O_7^{4-}$) ion based cements have also been produced, since these ions have also be found in the body[8,25] during the bone mineralisation process. These cements are mentioned only briefly here for completeness, as these pyrophosphate based cements represent another large area of research which will not be investigated further in this thesis.

5.1.3 Testing Cements

There are many approaches to test the set cements physical and mechanical properties. One particular method of testing is to prepare cement samples in a specific geometry, the most usual shape being a cylinder of known diameter and length, using controlled environmental conditions where possible, such as humidity and temperature. The initial and final setting times can then be assessed using Gilmore needles to judge the effect of different properties on the setting time of the cylinders. A duplicate sample of these cylinders can then placed into an axial hydraulic press and the ultimate compressive strength of the cylinder can be measured. More details about these techniques can be found in the experimental section (Chapter 2.3.7) of this thesis.

5.1.4 Desirable Properties of Cements

There are a number of essential properties that cements require in order to enable them to be viable for biomaterial applications. These properties include ease of preparation, low curing temperature and a relatively quick setting time (~ 15 minutes) sufficient to allow working time with mechanical strength increasing quickly as it sets.[3] Good biocompatibility, osteoinductivity, appropriate resorption rates and low cost are considered advantageous, if not essential properties for cements to possess.

5.1.5 Calcium Phosphate Cements as Drug Carriers

In order for a material to be used as a drug delivery system, it should have the ability to contain a drug and also retain it at a specific target site. It should then be able to deliver this drug consistently at a constant rate to the surrounding tissues. Ideally, the delivery vehicle should also degrade over time, with injection capabilities to minimise invasive surgery. The interest in layered calcium phosphates as cements and as hosts for intercalation experiments is due to their potential to fulfil these properties.

Under certain conditions, the addition of a drug solution to a layered calcium phosphate can allow intercalation reactions to occur between the calcium phosphate and the drug species thereby incorporating the drug in the layered phosphate phase. If this layered calcium phosphate material is then used as a component in cement formulation it could provide a potential vehicle for a drug delivery system.

The use of layered materials, with accessible interlayer regions, provides large surface areas with which to bind drug molecules. This approach has the potential to store a greater quantity of drugs as '3-dimensional' structures rely on the external surface of each particle adsorbing the drug species.[10] The increased quantity of drugs present in the material could

mean that a longer time period of sustained release could be maintained or a higher dosage could be administered, if preferable.

In orthopaedic procedures, there is an advantage to the use of a cement drug delivery system. This is because this method provides a site specific release. This would allow only local release of the drug when the calcium phosphate is resorbed, thereby reducing some of the side effects observed with drugs administered by inoculation methods where a significant "whole body" concentration is required for the drug to be effective.[26] Unfortunately, the process of adding drugs to either the powder or liquid intermediate mix of the calcium phosphate cements usually has a detrimental effect upon the mechanical or physical properties of the cement.[26]

5.1.6 Aims

The main aim of this section of research was to concentrate on whether we could use a modified MCPM phase as a route to produce new brushite cements. This method could allow intercalated molecules between the layers of MCPM to be introduced into the cement in a controlled manner with homogenous distribution. This property would be useful for the application of drug delivery systems or for optimising the cement setting characteristics (such as the addition of a retardant).

This chapter investigated this proof of concept, by the use of amine intercalated MCPM, with the presence of the amine used to increase the pH of the brushite cement. This provided a retardation of the setting reaction, in order to produce a more workable cement for biomaterial application.

In addition to using modified MCPM, the alkaline component of the cement was also varied to determine whether changing this component from the sparingly soluble tricalcium phosphate to calcium oxide (which is slightly more soluble) would affect the formation of a

viable cement system. Calcium carbonate was also tested as a cement component with the aim being to introduce porosity into the cement by the decomposition of this reagent releasing gaseous CO_2 into the setting cement therefore making it porous.

5.2 Experimental

It is well known that the reaction of MCPM ($Ca(H_2PO_4) \cdot H_2O$) with β-tricalcium phosphate ($Ca_3(PO_4)_2$) [TCP] can lead to a brushite cement,[27] as shown by the reaction scheme below.

$$Ca(H_2PO_4)_2 \cdot H_2O + Ca_3(PO_4)_2 + 7H_2O \rightarrow 4CaHPO_4 \cdot 2H_2O$$
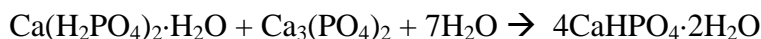
The above reaction is very rapid and has been known to produce a set cement within 10 minutes.[13,27] To our knowledge, this cement reaction has not been examined when the MCPM component has been modified by the intercalation of organic species. The formation of the amine intercalated MCPM phase was presented in detail in Chapter 4.

5.2.1 Cement Formulation with Amine Pre-Intercalated MCPM and β-TCP

To form the amine intercalated MCPM, a small quantity of MCPM was mixed with excess amine in a sample vial and this solution was left overnight to react. Powder X-ray diffraction was performed on the material to determine whether full intercalation had occurred and if not, a further intercalation period was undertaken. Once full intercalation had been achieved the material was washed with ethanol to remove any remaining surface amine before it was used in the cement formation reactions.

Preliminary cement reactions were then attempted using various quantities of MCPM retaining a 1:1 stoichiometric ratio with the TCP reagent and the components were homogenously mixed before adding a small quantity of water to form a firm paste. Since powder X-ray diffraction analysis of the samples was required, a reasonably large cement mass (> 0.3g) was required, with the sample needing to set overnight.

Once the sample size was determined, the first cement experiments were then prepared. From the TGA analysis of the amine intercalated MCPM material in Chapter 4

(section 4.3.2), 1.1 to 1.4 moles of amine was determined to intercalate per mole of calcium phosphate. As some variation on the quantity of amine was observed, a set mass of 0.3g was chosen to be used for the MCPM components with an equivalent mass of TCP. This would mean that in some experiments, a slight excess of TCP would be observed. The control brushite cement used a 1:1 stoichiometric ratio but since the components present were varied in the experiments, different ratios were also explored and are displayed in table 5.2.1.1.

For these experiments, a mass of amine intercalated MCPM or pure MCPM was mixed with β-TCP (see table 5.2.1.1 for masses) and set quantities of water to form two alternatives, either a paste (2 to 3 drops from 1 cm^3 syringe) or a liquid phase (excess water ~ 1 cm^3). A homogenous mixture was formed using a spatula to mix and smooth the cement once the components were added and this material was initially left to set at room temperature in a fumehood overnight. In the fumehood, the fast air flow was found to dry the cements too rapidly to enable a reaction to occur and therefore for the remainder of the experiments (beyond the initial trials), the samples were left to set on the open bench at room temperature.

Table 5.2.1.1: Reaction Conditions Used for the Cement Setting Reactions of Butylamine Intercalated MCPM with β-TCP Samples Including Controls

ID No.	Amine-MCPM Host	Amine-MCPM Mass (g)	β-TCP Mass (g)	Approximate Ratio of Amine-MCPM:TCP	Water Volume	pH Balance
1	Butyl	0.3	0.369	1:1.4	2-3 drops	None
2	Butyl	0.3	0.369	1:1.4	1 cm^3	None
3	Butyl	0.3	0.738	1:2.8	2-3 drops	None
4	Butyl	0.3	0.738	1:2.8	1 cm^3	None
5	Butyl	0.3	1.107	1:4.2	2-3 drops	None
6	Butyl	0.3	1.107	1:4.2	1 cm^3	None
7	Butyl	0.6	0.369	1.5:1	2-3 drops	None
8	Butyl	0.6	0.369	1.5:1	1 cm^3	None
9	Butyl	0.3	0.369	1:1.4	2-3 drops	7
10	Butyl	0.3	0.369	1:1.4	1 cm^3	7
11	Butyl	0.3	0.369	1:1.4	2-3 drops	4
12	Butyl	0.3	0.369	1:1.4	1 cm^3	4
Controls						
13	Butyl	0.3	0	-	2-3 drops	None
14	Butyl	0.3	0	-	1 cm^3	None
15	Butyl	0	0.369	-	2-3 drops	None
16	Butyl	0	0.369	-	1 cm^3	None
17	MCPM	0.3	0	-	2-3 drops	None
18	MCPM	0.3	0	-	1 cm^3	None
19	MCPM	0.3	0.369	1:1	2-3 drops	None
20	MCPM	0.3	0.369	1:1	1 cm^3	None
21	MCPM	0.3	0.369	1:1	2-3 drops	7
22	MCPM	0.3	0.369	1:1	1 cm^3	7
23	MCPM	0.3	0.369	1:1	2-3 drops	4
24	MCPM	0.3	0.369	1:1	1 cm^3	4
25	Butyl	0.3	0	-	2-3 drops	7
26	Butyl	0.3	0	-	1 cm^3	7
27	Butyl	0.3	0	-	2-3 drops	4
28	Butyl	0.3	0	-	1 cm^3	4

A complete set of experiments was then conducted with variations of both the amine intercalated MCPM and TCP masses as well as some pH control within the sample mixtures. When amine intercalated forms of MCPM were tested, both butylamine and propylamine intercalated MCPM were used and a full set of appropriate control experiments was also performed. These experiments are summarised in tables 5.2.1.1 and 5.2.1.2.

Table 5.2.1.2: Reaction Conditions Used for the Cement Setting Reactions of Propylamine Intercalated MCPM with β-TCP Samples Including Controls

ID No.	Amine-MCPM Host	Amine-MCPM Mass (g)	β-TCP Mass (g)	Approximate Ratio of Amine-MCPM:TCP	Water Volume	pH Balance
1	Propyl	0.3	0.369	1:1.3	2-3 drops	None
2	Propyl	0.3	0.369	1:1.3	1 cm^3	None
3	Propyl	0.3	0.738	1:2.6	2-3 drops	None
4	Propyl	0.3	0.738	1:2.6	1 cm^3	None
5	Propyl	0.6	0.738	1:1.3	2-3 drops	None
6	Propyl	0.6	0.738	1:1.3	1 cm^3	None
7	Propyl	0.6	0.369	1.5:1	2-3 drops	None
8	Propyl	0.6	0.369	1.5:1	1 cm^3	None
9	Propyl	0.3	0.369	1:1.3	2-3 drops	7
10	Propyl	0.3	0.369	1:1.3	1 cm^3	7
11	Propyl	0.3	0.369	1:1.3	2-3 drops	4
12	Propyl	0.3	0.369	1:1.3	1 cm^3	4
Controls						
13	Propyl	0.3	0	-	2-3 drops	None
14	Propyl	0.3	0	-	1 cm^3	None

The pH controlled cements used dilute orthophosphoric acid (~1M) to lower the pH value when amine intercalated MCPM samples were used and dilute (~1M) sodium hydroxide solution to raise the pH when MCPM was present in the control samples.

5.2.2 Cement Formulation with Amine-MCPM and Calcium Oxide

Calcium oxide is known to be more soluble in water than TCP which might therefore speed up the reaction rate between the amine intercalated-MCPM and calcium oxide. This experimental set used the same procedure as in section 5.2.1 but with calcium oxide instead of TCP. This calcium oxide reagent has been used previously[17,28-30] to produce cements and therefore was a viable alternative to TCP. The balanced equation for this reaction is shown below and indicates that a molar ratio of 1:1 for the MCPM and calcium oxide will produce brushite. The same problem with the varying amine content in MCPM will also be present as observed in section 5.2.1. Therefore a set mass of amine intercalated MCPM was also used. In this case, 0.2g of MCPM with 0.044g CaO was found to be sufficient to produce enough material for analysis. The same quantity of water was added as used in section 5.2.1 to allow

for component mixing and reaction. The cement forming equation for these experiments is shown below.

$$Ca(H_2PO_4)_2 \cdot H_2O + CaO + 2H_2O \rightarrow 2CaHPO_4 \cdot 2H_2O$$

The same reaction series was used as in section 5.2.1 with the appropriate control experiments also performed. These experimental conditions are shown in tables 5.2.2.1 and 5.2.2.2.

Table 5.2.2.1: Reaction Conditions Used for the Cement Setting Reactions of Butylamine Intercalated MCPM and Calcium Oxide Samples Including Controls

ID No.	Host Phase Present	Amine-MCPM Mass (g)	CaO Mass (g)	Approximate Ratio of Amine-MCPM:CaO	Water Volume	pH Balance
1	Butyl	0.2	0.044	1:1.4	2-3 drops	None
2	Butyl	0.2	0.044	1:1.4	1 cm^3	None
3	Butyl	0.2	0.088	1:2.8	2-3 drops	None
4	Butyl	0.2	0.088	1:2.8	1 cm^3	None
5	Butyl	0.4	0.088	1:1.4	2-3 drops	None
6	Butyl	0.4	0.088	1:1.4	1 cm^3	None
7	Butyl	0.4	0.044	1.5:1	2-3 drops	None
8	Butyl	0.4	0.044	1.5:1	1 cm^3	None
9	Butyl	0.2	0.044	1:1.4	2-3 drops	7
10	Butyl	0.2	0.044	1:1.4	1 cm^3	7
11	Butyl	0.2	0.044	1:1.4	2-3 drops	4
12	Butyl	0.2	0.044	1:1.4	1 cm^3	4
Controls						
13	Butyl	0	0.044	-	2-3 drops	None
14	Butyl	0	0.044	-	1 cm^3	None
15	MCPM	0.2	0.044	1:1	2-3 drops	None
16	MCPM	0.2	0.044	1:1	1 cm^3	None
17	MCPM	0.2	0.044	1:1	2-3 drops	7
18	MCPM	0.2	0.044	1:1	1 cm^3	7
19	MCPM	0.2	0.044	1:1	2-3 drops	4
20	MCPM	0.2	0.044	1:1	1 cm^3	4

As similar results were obtained with both butylamine and propylamine intercalated MCPM in section 5.2.1, only the butylamine-MCPM reagent would be used together with calcium oxide to form the brushite cements in these experiments.

5.2.3 Cement Formulation Replacing Tricalcium Phosphate with Calcium Carbonate

Preliminary experiments were performed using 0.3g of pure MCPM as well as propylamine and butylamine intercalated MCPM. These were mixed with 0.12g of calcium carbonate and either a small quantity of water or excess water (1 cm^3) was added to these samples and the resulting mixed cement was left overnight to harden in the same PTFE mould used in section 5.2.1. The reaction scheme is displayed in the equation below and a ratio of 0.9:1 MCPM:calcium carbonate was used for these preliminary experiments.

$$Ca(H_2PO_4)_2 \cdot H_2O + CaCO_3 + 2H_2O \rightarrow 2CaHPO_4 \cdot 2H_2O + CO_2$$

Further experiments with this reagent were not pursued due to the poor quality of the cement produced in these preliminary experiments.

5.2.4 Cement Formulation with Varying Amounts of Amine-MCPM and MCPM

These experiments used the same procedure as in 5.2.1 above but with varying ratios of MCPM and amine intercalated MCPM reagents with the TCP component. Three different ratios of both types of MCPM were tested with approximately 1:3, 1:1 and 3:1 of MCPM:Amine-MCPM being used with 0.369g of β-TCP. A summary of the experiments that were attempted are listed in table 5.2.4.1 including control experiments. These samples were left overnight on the open bench to set before analysis using powder X-ray diffraction.

Table 5.2.4.1: Reaction Conditions Used for the Cement Setting Reactions with Varying Amounts of Butylamine Intercalated MCPM and MCPM with β-TCP Samples

ID No.	MCPM Mass (g)	Butylamine-MCPM Mass (g)	β-TCP Mass (g)	Approximate Ratio of MCPM:Amine-MCPM	Water Volume	pH Balance
1	0.075	0.225	0.369	1:2.2	2-3 drops	None
2	0.15	0.15	0.369	1:0.7	2-3 drops	None
3	0.225	0.075	0.369	3:0.7	2-3 drops	None
4	0.075	0.225	0.369	1:2.2	1 cm^3	None
5	0.15	0.15	0.369	1:0.7	1 cm^3	None
6	0.225	0.075	0.369	3:0.7	1 cm^3	None
Controls						
7	0.075	0.225	0	1:2.2	2-3 drops	None
8	0.15	0.15	0	1:0.7	2-3 drops	None
9	0.225	0.075	0	3:0.7	2-3 drops	None
10	0.075	0.225	0	1:2.2	1 cm^3	None
11	0.15	0.15	0	1:0.7	1 cm^3	None
12	0.225	0.075	0	3:0.7	1 cm^3	None

5.2.5 Cement Formulation for Compressive Strength Testing and Setting Times

When the compressive strength measurements were performed, the samples were prepared using a PTFE mould which kept the diameter and length of each sample constant at 6mm and 15 mm respectively. Each cylinder prepared was carefully measured in advance of testing and only whole cylinders with no obvious visual defects were tested.

Compressive strength tests were performed on a range of different cements with varying compositions to test the effect of the amine intercalated MCPM component upon the overall strength of the cement cylinders. Compressive strength measurements were performed on brushite cements prepared with 5, 10 and 25% propylamine or butylamine intercalated MCPM and control samples with 100% MCPM. At least 6 samples were tested from the sample batch of 10 cylinders prepared for each percentage of amine intercalated MCPM or control sample. Only whole cylinders with no imperfections and a length, once prepared for the measurement, of more than twice their diameter were tested. This relationship was important to produce a reliable test as the compressive strength values would be incorrect if this parameter was not met.

Setting tests were also performed using a similar process of preparing a cement cylinder with a diameter of 8 mm and length of 15 mm. The larger diameter was chosen to give a greater surface area for the needle tests so that a new position for each test could be chosen to check for indentations. This would prevent compaction of the cement and hence reduce the risk of a quicker setting time than the true value. Setting times were obtained for brushite cements prepared with 5, 10 and 25% propylamine and butylamine intercalated MCPM and control samples with pure MCPM, with repetitions of between 4 and 6 samples to give a more reliable setting time. The quantities of each reagent added to give the correct percentage of each component are shown in table 5.2.5.1 below.

Table 5.2.5.1: Quantity of Reagents to Prepare Cement for Compressive Strength Measurement

Amine-MCPM Content (%)	Amine Intercalated MCPM Mass (g)	MCPM Mass (g)	β-TCP Mass (g)
0	0.000	0.300	0.369
5	0.015	0.285	0.369
10	0.030	0.270	0.369
25	0.075	0.225	0.369

5.2.6 Characterisation of Materials Prepared

The cements formed in sections 5.2.1 – 5.2.4 possessed varying compositions of solid components and therefore powder X-ray diffraction was primarily used to analyse which phases were present. This preliminary investigation did not seek to determine accurate phase compositions, as it was focussed on identifying brushite cement compositions with potential for further investigation, given their setting times and strengths.

The set cements were ground using a pestle and mortar to form a homogenous powder that could then be used for the X-ray diffraction analysis. Strength tests were performed using compressive strength measurements on a set cement cylinder. The full experimental technique can be found in section 2.3.7.1. When the setting time was investigated for certain cements

compositions, the Gilmore needle test was performed. This technique is explained in more detail in section 2.3.7.2.

5.3 Results and Discussion

The main aim for this section of the thesis was to test the effect of using a modified MCPM in the formation of brushite cements. The reaction products were analysed using powder X-ray diffraction and the strength and setting times of some of the brushite cement formulations were assessed. Different cement formulations were attempted, as shown in sections 5.2.1 – 4, and the effects of the various formulations upon the cement strength and setting time were recorded, using the techniques discussed in section 5.2.5. The composition and performance of the cements was stated in sections 5.3.1 – 5.3.4. The setting times and compressive strength tests of the MCPM and TCP brushite cements system are shown in sections 5.3.5 and 5.3.6.

5.3.1 Cement Formulation with Amine Pre-Intercalated MCPM and β-TCP

To test the influence of amine modified MCPM on cement formation, a series of experiments were undertaken. A standard route to form brushite cements was via the reaction of MCPM with β-TCP and water.[13] However, in our modified reaction, butylamine intercalated MCPM was used to completely or partially replace MCPM in the reaction with β-TCP. The results for the mixture of butylamine-MCPM with TCP and water, with and without pH control, can be seen in table 5.3.1.1A & B. In almost every case, the samples dried overnight in the fumehood to form a white powdery material. X-ray diffraction analysis showed that no reaction had actually occurred with the non-pH balanced cement samples and the mixed phase products consisted of the initial reactants butylamine-MCPM and β-TCP. These results were repeated with the samples left overnight on the open bench, therefore increasing the drying time as airflow over the samples was reduced and allowed more time for the water mediated cement reaction to occur before the mixture dried.

Table 5.3.1.1A: Results for the Cement Setting Reactions of Butylamine Intercalated MCPM with β-TCP

ID No.	Amine-MCPM Host	Amine-MCPM Mass (g)	β-TCP Mass (g)	Approximate Ratio of Amine-MCPM:TCP	Water Volume	pH Balance	Reaction Products as Identified by Powder XRD	Successful Cement?
1	Butyl	0.3	0.369	1:1.4	2-3 drops	None	Butylamine Intercalated MCPM [Bu-MCPM] and β-TCP	N
2	Butyl	0.3	0.369	1:1.4	1 cm^3	None	Bu-MCPM and tricalcium phosphate [β-TCP]	N
3	Butyl	0.3	0.738	1:2.8	2-3 drops	None	Bu-MCPM and β-TCP	N
4	Butyl	0.3	0.738	1:2.8	1 cm^3	None	Bu-MCPM and β-TCP	N
5	Butyl	0.3	1.107	1:4.2	2-3 drops	None	Bu-MCPM and β-TCP	N
6	Butyl	0.3	1.107	1:4.2	1 cm^3	None	Bu-MCPM and β-TCP	N
7	Butyl	0.6	0.369	1.5:1	2-3 drops	None	Bu-MCPM and β-TCP	N
8	Butyl	0.6	0.369	1.5:1	1 cm^3	None	Bu-MCPM and β-TCP	N
9	Butyl	0.3	0.369	1:1.4	2-3 drops	7	Bu-MCPM, β-TCP & Some Brushite	Y
10	Butyl	0.3	0.369	1:1.4	1 cm^3	7	Bu-MCPM, β-TCP & Some Brushite	Y
11	Butyl	0.3	0.369	1:1.4	2-3 drops	4	Brushite with some Bu-MCPM and β-TCP	Y
12	Butyl	0.3	0.369	1:1.4	1 cm^3	4	Brushite with some Bu-MCPM and β-TCP and unknown phase	Y

Table 5.3.1.1B: Controls Sample Results for the Cement Setting Reactions of Butylamine Intercalated MCPM with β-TCP
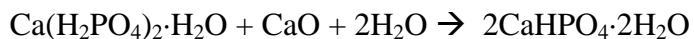
							Controls	
ID No.	Amine-MCPM Host	Amine-MCPM Mass (g)	β-TCP Mass (g)	Approximate Ratio of Amine-MCPM:TCP	Water Volume	pH Balance	Reaction Products as Identified by Powder XRD	Successful Cement?
13	Butyl	0.3	0	-	2-3 drops	None	Bu-MCPM	-
14	Butyl	0.3	0	-	1 cm^3	None	Bu-MCPM	-
15	Butyl	0	0.369	-	2-3 drops	None	β-TCP	-
16	Butyl	0	0.369	-	1 cm^3	None	β-TCP	-
17	MCPM	0.3	0	-	2-3 drops	None	MCPM	-
18	MCPM	0.3	0	-	1 cm^3	None	MCPM	-
19	MCPM	0.3	0.369	1:1	2-3 drops	None	Brushite – sets quickest	Y
20	MCPM	0.3	0.369	1:1	1 cm^3	None	Brushite mainly & MCPM	Y
21	MCPM	0.3	0.369	1:1	2-3 drops	7	Formed brushite with excess TCP	Y
22	MCPM	0.3	0.369	1:1	1 cm^3	7	Mixed brushite and TCP	Y
23	MCPM	0.3	0.369	1:1	2-3 drops	4	Brushite. Tiny amount of MCPM and TCP	Y
24	MCPM	0.3	0.369	1:1	1 cm^3	4	Brushite phase with some excess TCP	Y
25	Butyl	0.3	0	-	2-3 drops	7	Bu-MCPM and unknown phase - first peak 2θ sits between Bu-MCPM and MCPM first peak position.	N
26	Butyl	0.3	0	-	1 cm^3	7	Brushite, Bu-MCPM and same unknown phase.	N - Weak
27	Butyl	0.3	0	-	2-3 drops	4	Same unknown phase	N
28	Butyl	0.3	0	-	1 cm^3	4	Brushite and same unknown phase	Y

The likely reasons for the lack of reaction observed in the non-pH balanced cement samples in table 5.3.1.1A may have been due to the partial dissolution of the intercalated MCPM in water which released the intercalated amine and therefore raised the pH of the surrounding solution. The high pH would have retarded the rate of formation of brushite which occurs preferentially at pH values lower than 4.2.[6] If the reaction rate had been slowed down sufficiently, then it could be feasible that the samples dried out before any reaction had occurred and therefore brushite would not be observed in the samples. A further possibility is the high pH of the resultant solution caused by the release of amine from the intercalated MCPM would have reduced the dissolution rate of the alkaline β-TCP and thus the reaction would have proceeded more slowly.

When pH control was introduced into the samples, brushite was observed in the set samples, with the mixed components hardening quickly, especially the pH 4 balanced samples. X-ray diffraction analysis of the sample confirmed the presence of brushite which can be clearly seen in figure 5.3.1.1. In addition, there was the presence of an unknown phase (unknown B, section 5.3.4) with an intermediate peak position between butylamine intercalated MCPM and the MCPM host phase in the cement sample. Possible explanations for the appearance of this unknown are given in section 5.3.4.

The paste form of the pH 4 controlled phase produced the hardest material of the four pH controlled samples that were tested in this experimental set, as evidenced by the necessity to grind the products prior to powder X-ray diffraction analysis.
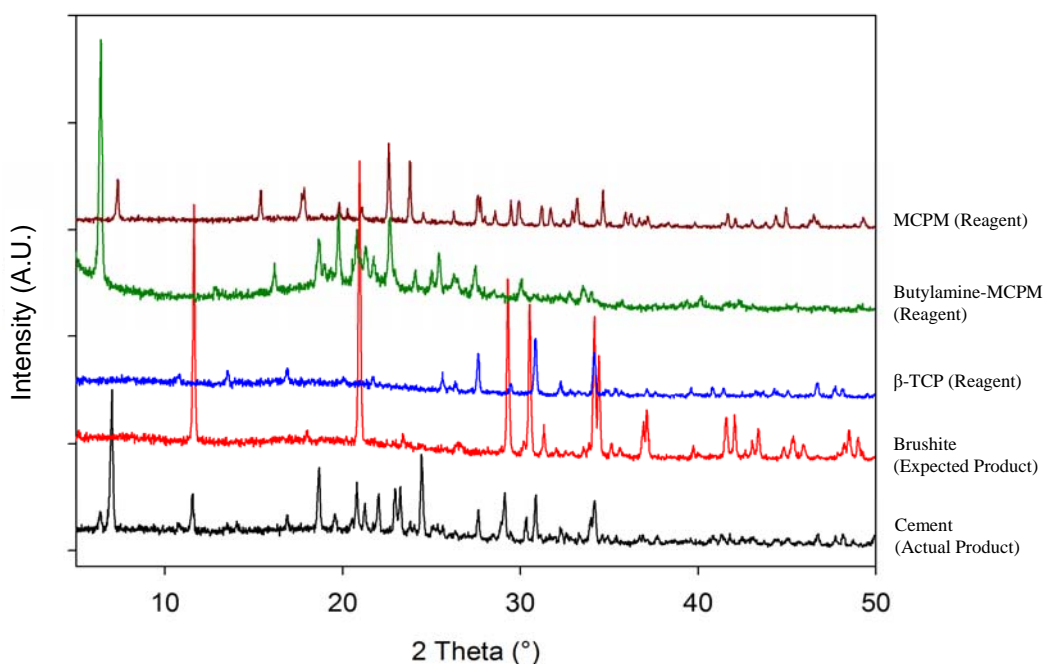
Figure 5.3.1.1: X-ray Diffraction Pattern for pH4 Balanced Brushite Cement Using Butylamine Intercalated MCPM and β-TCP Components.

Control experiments (table 5.3.1.1B) were conducted by mixing β-TCP with water or butylamine-MCPM with water and left to dry overnight. Powder X-ray diffraction analysis of the products showed no change in composition. From the observations described in Chapter 4, in excess water, butylamine-MCPM will normally convert to hydroxyapatite. This was not observed in this case, which suggested that the solution had dried or reacted too quickly to allow time for the phase conversion to hydroxyapatite to occur.

The pure MCPM and β-TCP control reaction in paste form produced one of the hardest materials to grind with respect to all the samples produced in this experimental set and hardened very quickly (this material was almost completely set in 5 minutes). This cement was expected to be hard to grind as it represented the standard cement composition. From literature,[6,31,32] its compressive strength values have been reported to range from 1 – 24 MPa depending upon how long the cement was left to harden and if any retardants were present.

When excess water was used to produce the reference MCPM and TCP cement, the sample produced was easier to grind than the paste version but was still relatively hard. In this excess water form of the control cement, X-ray diffraction analysis indicated that as well as the main brushite phase, there was also evidence of MCPM. This suggested that the MCPM was in a slight excess, which might account for some of the difference in the hardness of the material during the grinding process.

The results for the cements containing propylamine intercalated MCPM with TCP were slightly more complex (See Table 5.3.1.2). The cement samples prepared without any pH balancing showed no signs of forming brushite.

In some of the samples that were not pH balanced, although the powder X-ray diffraction pattern showed that little reaction between the starting reagents had occurred, a variation in the appearance of the propylamine intercalated MCPM phase was observed. This was evident from a shift in the second diffraction peak (on figure 5.3.1.2) to a higher 2θ diffraction angle compared to the non-intercalated MCPM phase (change of $\sim 0.46° = 0.70\text{Å}$ d-spacing). The first diffraction peak on figure 5.3.1.2 relates to the presence of excess propylamine intercalated MCPM. Peaks from this phase can be seen in figure 5.3.1.2 together with some from the propylamine-MCPM starting material. This unknown phase (A) was observed only with the propylamine intercalated MCPM samples and one explanation for this occurrence was believed to be due to the partial dehydration of the intercalated MCPM phase.

Table 5.3.1.2: Results of the Cement Setting Reactions of Propylamine Intercalated MCPM with β-TCP Samples Including Controls

ID No.	Amine-MCPM Host	Amine-MCPM Mass (g)	β-TCP Mass (g)	Approximate Ratio of Amine-MCPM:TCP	Water Volume	pH Balance	Reaction Products as Identified by Powder XRD	Successful Cement?
1	Propyl	0.3	0.369	1:1.3	2-3 drops	None	Pr-MCPM and β-TCP	N
2	Propyl	0.3	0.369	1:1.3	1 cm^3	None	Pr-MCPM and β-TCP	N
3	Propyl	0.3	0.738	1:2.6	2-3 drops	None	β-TCP, Pr-MCPM and unknown phase A	N
4	Propyl	0.3	0.738	1:2.6	1 cm^3	None	Pr-MCPM and β-TCP	N
5	Propyl	0.6	0.738	1:1.3	2-3 drops	None	Pr-MCPM with β-TCP	N
6	Propyl	0.6	0.738	1:1.3	1 cm^3	None	Pr-MCPM with β-TCP	N
7	Propyl	0.6	0.369	1.5:1	2-3 drops	None	Pr-MCPM with β-TCP	N
8	Propyl	0.6	0.369	1.5:1	1 cm^3	None	Pr-MCPM with β-TCP	N
9	Propyl	0.3	0.369	1:1.3	2-3 drops	7	MCPM and TCP with low intensity brushite phase	Y
10	Propyl	0.3	0.369	1:1.3	1 cm^3	7	Brushite, β-TCP and unknown A (same as in sample 3,4)	N
11	Propyl	0.3	0.369	1:1.3	2-3 drops	4	Brushite, β-TCP and some unknown A (same as in sample 3,4)	Y
12	Propyl	0.3	0.369	1:1.3	1 cm^3	4	Brushite and β-TCP	Y
Controls								
13	Propyl	0.3	0	-	2-3 drops	None	Pr-MCPM	-
14	Propyl	0.3	0	-	1 cm^3	None	Pr-MCPM – reduction in the intensity of peaks	-
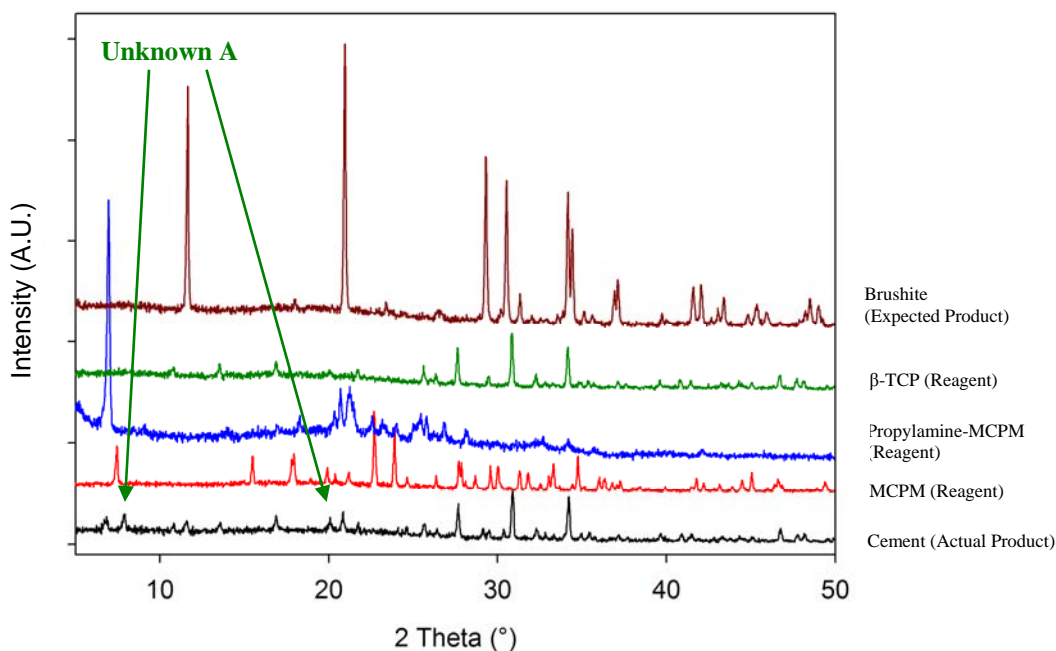
Figure 5.3.1.2: X-ray Diffraction Pattern for Brushite Cement Formation Using Propylamine Intercalated MCPM and β-TCP Components Showing the Unknown Phase.

Another explanation for this observation could have been due to some solubility of propylamine in the water used to form the cement. This could have removed some of the amine from between the layers of MCPM, thus reducing the amount present in the un-reacted, modified MCPM component. With less amine present, the amine species could realign between the layers in the MCPM structure leading to a potentially reduced interlayer spacing.

A similar peak shift was also observed in three of the pH controlled experiments which, if the previous explanation is correct, would suggest that some of the amine had leached out of the MCPM layers, reacted with the acid and thus reduced the quantity of amine present in MCPM. However, the control samples, when only the propylamine intercalated MCPM phase and water were present, showed no change in 2θ diffraction angle, even after repetitions were performed.

When the pH was controlled in the propylamine intercalated MCPM containing samples, brushite was observed in the cements as well as this unknown phase mentioned

above. In the paste form of the cement at pH 7, only a limited reaction seemed to have occurred with mainly MCPM and TCP phases present. Possible reasons for this reduced reactivity could again have been due to the presence of some amine, thus the increased pH (pH 7) could slow the reaction rate, sufficiently so that the sample dried before the cement reaction had run to completion. When more water was present, X-ray diffraction indicated that the sample contained brushite with low intensity starting material peaks which suggested that the reaction had proceeded further but had not completed fully before the cement had dried.

Both of the pH 4 balanced samples produced brushite as the major phase product but low intensity peaks due to excess β-TCP in the samples was also observed. In addition, these pH controlled samples took much longer times to set; in fact an extra day beyond the usual 1 day setting time observed with the butylamine intercalated cement samples was required. This observation was unusual as the pH balanced samples normally set more quickly than the cements without pH balancing. A possible explanation for this effect could relate to the reaction between propylamine and orthophosphoric acid (used to lower pH), which could have produced a retarding effect upon the overall setting of these cements. A set of reactions were completed using pure propylamine and orthophosphoric acid to maintain the same pH 4 and 7 values then MCPM and TCP were added to this solution. It was observed that these cements took longer to set when the acid and amine were present.

From the results in this section, it was apparent that using 100% amine intercalated MCPM was detrimental to the formation of a viable cement. When pH control was used, the cement successfully formed, but with some excess starting reagents still present. It appeared that some retarding effect had occurred due to the presence of amine and led to an incomplete reaction.

5.3.2 Cement Formulation with Amine-MCPM and Calcium Oxide

Some preliminary cement samples were also prepared using calcium oxide instead of β-tricalcium phosphate to determine whether this change of alkaline reagent would have any effect upon the outcome of the cement setting reaction or the rate of setting.

X-ray diffraction patterns were collected on the cements listed in table 5.3.2.1 containing calcium oxide and amine intercalated MCPM. The samples prepared without pH balancing showed only starting materials were present in the set products. Therefore little reaction has occurred between the reagents before the sample had dried overnight. In three of the samples prepared, some hydroxyapatite (HA) was also observed. Previous studies (Chapter 4) have shown that amine intercalated MCPM in excess water converts over time to this hydroxyapatite phase due to the high pH of the solution present. As calcium oxide is more soluble in water than TCP, a higher solution pH was likely to be maintained and therefore the conversion of MCPM to HA was expected if the main brushite forming reaction had not occurred preferentially.

Table 5.3.2.1: Reaction Conditions Used for the Cement Setting Reactions of Butylamine Intercalated MCPM and Calcium Oxide Samples Including Controls.

ID No.	Amine-MCPM Host	Amine-MCPM Mass (g)	CaO Mass (g)	Approximate Ratio of Amine-MCPM:CaO	Water Volume	pH Balance	Reaction Products as Identified by Powder XRD	Successful Cement?
1	Butyl	0.2	0.044	1:1.4	2-3 drops	None	Bu-MCPM and $Ca(OH)_2$	N
2	Butyl	0.2	0.044	1:1.4	1 cm^3	None	Bu-MCPM, $Ca(OH)_2$ and Hydroxyapatite [HA]	N
3	Butyl	0.2	0.088	1:2.8	2-3 drops	None	$Ca(OH)_2$ with Bu-MCPM	N
4	Butyl	0.2	0.088	1:2.8	1 cm^3	None	Hydroxyapatite and $Ca(OH)_2$	N
5	Butyl	0.4	0.088	1:1.4	2-3 drops	None	Bu-MCPM and HA	N
6	Butyl	0.4	0.088	1:1.4	1 cm^3	None	Bu-MCPM only	N
7	Butyl	0.4	0.044	1.5:1	2-3 drops	None	Bu-MCPM and some Hydroxyapatite	N
8	Butyl	0.4	0.044	1.5:1	1 cm^3	None	Bu-MCPM and $Ca(OH)_2$	N
9	Butyl	0.2	0.044	1:1.4	2-3 drops	7	Bu-MCPM and brushite	Y
10	Butyl	0.2	0.044	1:1.4	1 cm^3	7	Bu-MCPM and more intense brushite peaks	Y
11	Butyl	0.2	0.044	1:1.4	2-3 drops	4	Bu-MCPM, unknown B and low intensity brushite phases	Y
12	Butyl	0.2	0.044	1:1.4	1 cm^3	4	Unknown phase B and some Bu-MCPM	N
Controls								
13	None	0	0.044	-	2-3 drops	None	$Ca(OH)_2$ and CaO	-
14	None	0	0.044	-	1 cm^3	None	CaO and $Ca(OH)_2$	-
15	MCPM	0.2	0.044	1:1	2-3 drops	None	Brushite and MCPM	-
16	MCPM	0.2	0.044	1:1	1 cm^3	None	Brushite and MCPM	-
17	MCPM	0.2	0.044	1:1	2-3 drops	7	Brushite	-
18	MCPM	0.2	0.044	1:1	1 cm^3	7	Brushite and excess $Ca(OH)_2$	-
19	MCPM	0.2	0.044	1:1	2-3 drops	4	Brushite and MCPM	-
20	MCPM	0.2	0.044	1:1	1 cm^3	4	Brushite and MCPM	-

The pH balanced experiments using calcium oxide and butylamine intercalated MCPM samples with orthophosphoric acid (for lowering pH) produced brushite in the set cement, although there was the presence of a significant amount of butylamine-MCPM starting reagent (see table 5.3.2.1 and figure 5.3.2.1). This butylamine-MCPM starting material could be present due to an imbalance in the cement components caused by the reaction between the orthophosphoric acid, used to lower pH, and the calcium oxide alkaline cement component. As calcium oxide is relatively soluble in water and in dilute orthophosphoric acid, this component was likely to react and therefore the 1:1 cement component mixture of calcium oxide to MCPM would be altered, potentially leaving excess butylamine-MCPM in the set cement.

The pH 4 balanced cements also produced an unknown phase which had been observed in the mixed intercalated and non-intercalated MCPM experiments in section 5.3.4 below. The presence of this unknown phase was believed to be due to the reaction of orthophosphoric acid (used to alter the pH of the cement sample) with the amine that would have been in solution when the MCPM dissolved. A more detailed discussion is given in section 5.3.4.
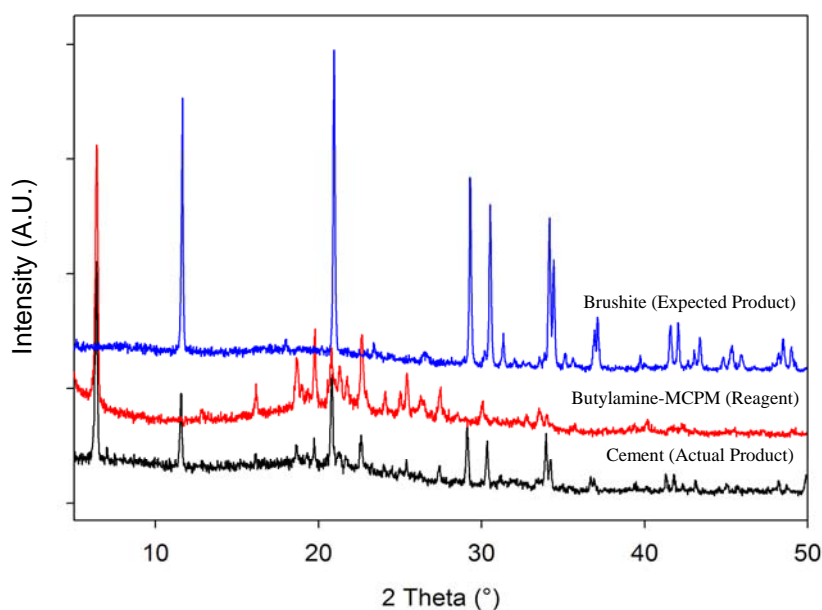
Figure 5.3.2.1: X-ray Diffraction Pattern for pH 7 Balanced Brushite Cement Using Butylamine Intercalated MCPM and Calcium Oxide Components

The control reactions for these experiments produced the expected phases in all cases. The most intense brushite peaks were produced in the control samples that were pH 4 balanced and only low intensity MCPM starting material peaks remained, due to a small amount of this reagent being in excess. In all four pH balanced control reactions, brushite was produced as the main product which is evident by the powder X-ray diffraction pattern shown in figure 5.3.2.2. Brushite was also produced as the major product when MCPM was used without pH balance as a final set of control samples. This suggested that the amine intercalated MCPM was responsible for slowing the reaction rate of the cements.
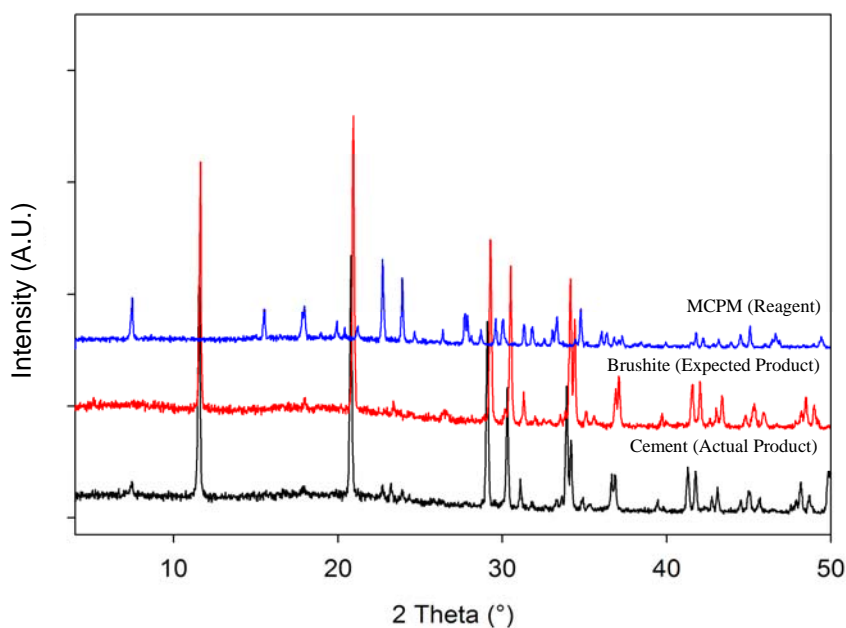
Figure 5.3.2.2: X-ray Diffraction Pattern for pH 4 Balanced Brushite Cement Control Experiment
Using MCPM and Calcium Oxide Components

When no MCPM was present, the calcium oxide reacted with the water in the cement mix to form calcium hydroxide. This phase change however, had little effect upon the main cement reaction as calcium hydroxide would react in a similar fashion to calcium oxide. As excess water was present in the samples, this side reaction should not have influenced the cement formation.

From the results in this section, it was apparent that the replacement of β-TCP with calcium oxide proved to have no beneficial effect upon the production of successful cements. However, when pH control was used, brushite was successfully formed with some excess starting reagents still present, probably due to the retarding effect caused by the presence of amine. Therefore we can conclude that the change of reagent had no significant effect upon cement formation.

5.3.3 Cement Formulation Replacing Tricalcium Phosphate with Calcium Carbonate

The aim of these experiments was to introduce porosity into the cements by the decomposition of calcium carbonate (as opposed to calcium oxide). This would release gaseous CO_2, which may provide some degree of porosity on reaction.

Although a porous cement would not be useful for load bearing applications as it is likely to be too soft and brittle, porosity could be useful if the cement was to be used as a scaffold in non load bearing applications. Calcium carbonate (from coral) has been used in the past as a scaffold for bone ingrowth.[23,33] However, this reagent has not been used to our knowledge, as a component of a cement. Calcium sulfate, however, has been used previously in cements, where this reagent has been added as a foaming agent[34] and then any excess calcium sulfate was washed out to leave a porous structure. Calcium carbonate would be better suited for this purpose as it could also act as the alkaline component when mixed with the acidic MCPM phase to form the brushite cement as well as being the foaming agent.

Unfortunately when the control samples were tested, the release of gas was quite rapid and the cement cylinders were found to be very fragile and generally crumbled when removed from the mould. When a small percentage of amine-MCPM was added, the cements took many days to harden and were very brittle. When the cylinders were removed from the mould they would generally collapse and some possessed large areas of un-reacted starting materials. X-ray diffraction analysis of these cylinders showed that very little brushite was present and mostly MCPM (or amine intercalated MCPM) and calcium oxide was observed, even with the control samples. Therefore this carbonate reagent was not used for further investigation due to the poor quality of the cement produced in these preliminary experiments.

5.3.4 Cement Formulation with Varying Amounts of Amine-MCPM and MCPM

Results from sections 5.3.1 to 5.3.3, indicated that using 100% amine intercalated MCPM as one of the cement components increased the setting time beyond the point of allowing the cement to form before the mixture had dried. X-ray diffraction indicated that the cement reaction was severely inhibited by the modified MCPM. As a compromise, a series of experiments were undertaken using a smaller quantity of butylamine-MCPM as a cement reagent. It was thought that this would still allow the formation of a brushite cement but with the benefits of an increased and therefore useable setting time compared to standard brushite cements. This allowed the feasibility of modified MCPM as a delivery host to be investigated. The results of these experiments are listed in table 5.3.4.1.

When the X-ray diffraction patterns for the three different percentages of MCPM and amine-MCPM (see table 5.3.4.1) for the cement paste were compared, similar results were observed in all three patterns. A reasonable quantity of the starting materials had reacted to form brushite, especially in the samples where the un-modified MCPM was the majority phase compared to the intercalated phase. However, there was also an unknown phase present that could not be identified in the samples that were mixed with a large excess of water. This phase had a low angle peak with a larger 2θ (i.e. smaller interlayer separation) value than butylamine intercalated MCPM (7.05° compared with 6.38°) but smaller 2θ value than the pure MCPM phase (7.46°). This unknown phase and brushite can be seen in the diffraction pattern shown in figure 5.3.4.1 which represents the 50/50 excess water cement (sample no. 5, table 5.3.4.1).

The unknown phase possessed an intermediate layer separation, indicated from the position of the first diffraction peak on the diffraction pattern at 7.05° 2θ between MCPM and butylamine-MCPM (12.52Å compared with 11.83Å and 13.83Å respectively). This peak shift

(1.3Å between butylamine-MCPM peak and unknown peak) possibly occurred due to the loss of some of the amine from between the layers of MCPM or a rearrangement of the amine within the layers of MCPM, due to partial dissolution of some of the MCPM in the presence of water. The fact that a larger spacing than pure MCPM was still observed would suggest that some amine was still present in the MCPM thus keeping an increased layer separation.

Table 5.3.4.1: Results of the Cement Setting Reactions with Varying Amounts of MCPM and Butylamine Intercalated MCPM with β-TCP Samples

ID No.	MCPM Mass (g)	Butylamine Intercalated MCPM Mass (g)	Ratio	β-TCP Mass (g)	Water Volume	Reaction Products as Identified by Powder XRD	Successful Cement?
1	0.075	0.225	1:2.2	0.369	2-3 drops	Brushite, Bu-MCPM, and TCP	Y
2	0.15	0.15	1:0.7	0.369	2-3 drops	Brushite, TCP and MCPM	Y
3	0.225	0.075	3:0.7	0.369	2-3 drops	Brushite, TCP and Butylamine-MCPM	Y
4	0.075	0.225	1:2.2	0.369	1 cm^3	Brushite, Bu-MCPM and unknown B (same phase)	Y
5	0.15	0.15	1:0.7	0.369	1 cm^3	Unknown B (same phase)	N
6	0.225	0.075	3:0.7	0.369	1 cm^3	Brushite, MCPM and unknown B (same phase)	Y
Controls							
7	0.075	0.225	1:2.2	0	2-3 drops	Brushite, Bu-MCPM and unknown B (same phase)	-
8	0.15	0.15	1:0.7	0	2-3 drops	Brushite and unknown B(same phase)	-
9	0.225	0.075	3:0.7	0	2-3 drops	MCPM and unknown B (same phase)	-
10	0.075	0.225	1:2.2	0	1 cm^3	Brushite, Bu-MCPM, and unknown B (same phase)	-
11	0.15	0.15	1:0.7	0	1 cm^3	Unknown phase B (same phase)	-
12	0.225	0.075	3:0.7	0	1 cm^3	Brushite, MCPM and unknown B	-
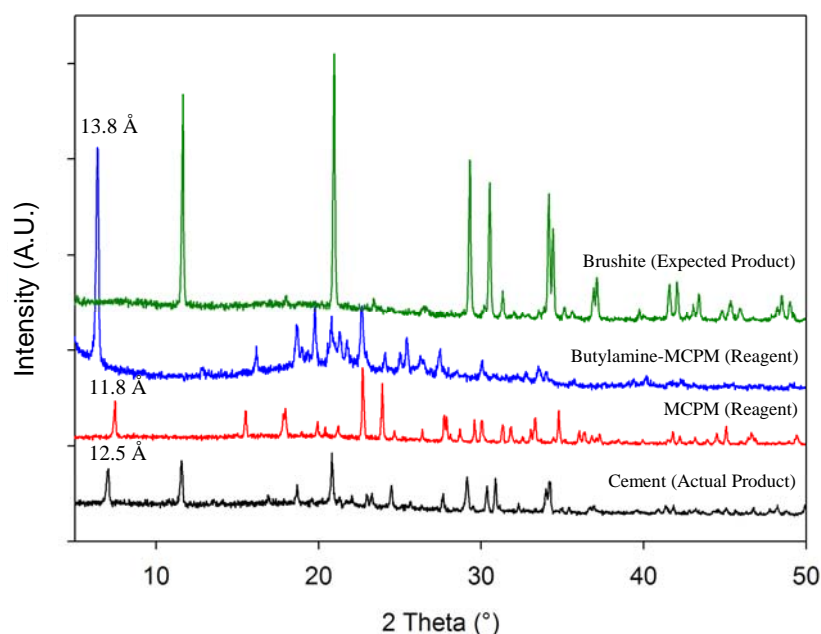
Figure 5.3.4.1: X-ray Diffraction Pattern of Brushite Cement (Excess Water 50/50 Mix) Showing Brushite and also the Presence of Unknown Phase B with Comparison to the MCPM and Butylamine-MCPM Starting Materials

The X-ray diffraction pattern for the 3:0.7 MCPM/butylamine-MCPM phase is shown in figure 5.3.4.2 (sample ID 3 from table 5.3.4.1). This cement phase contained brushite and MCPM as major phases with a small quantity of TCP remaining. This suggested that the sample had dried before the cement formation reaction was complete. The fact that a partial reaction had occurred suggested that the presence of amine MCPM in the mixture was still responsible for reducing the rate of reaction, but as a smaller quantity of this material was used, this still allowed the formation of brushite in the cement. This result was promising, as it implied that a lower percentage of amine MCPM would slow brushite precipitation without stopping its formation and therefore further experiments with even lower percentage of amine-MCPM were attempted. These are discussed briefly later in this section and in detail in sections 5.3.5 & 5.3.6.
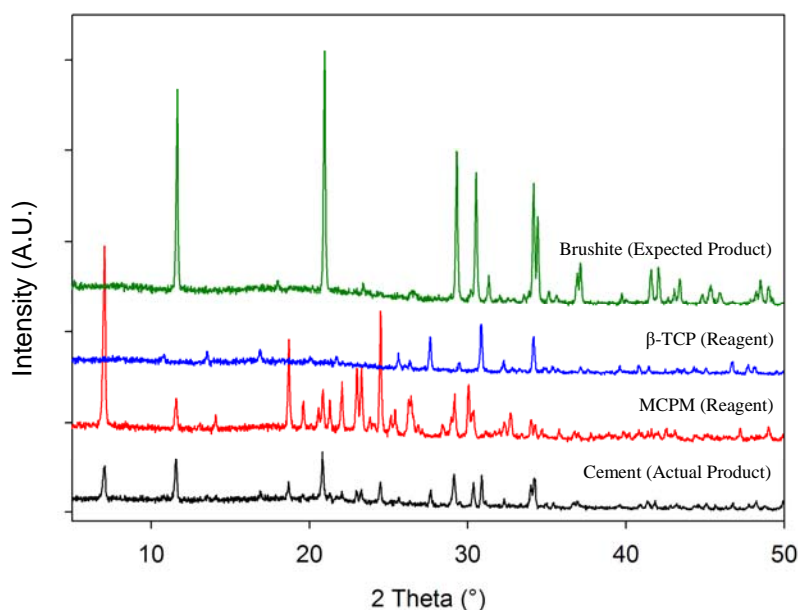
Figure 5.3.4.2: X-ray Diffraction Pattern of a 3:0.7 Mixed MCPM/Butylamine Intercalated MCPM Brushite Cement Compared to the Starting Materials.

The control experiments performed for these experiments showed the presence of brushite in some of the samples, even though TCP was not present. The formation of brushite in these samples could be explained due to the slow decomposition reaction of MCPM to brushite when MCPM was left in water for a considerable time period. The control samples produced were very weak and could be easily crushed, which suggested that although brushite was present, a cement had not actually been formed.

The same 'unknown' phase (B) was also seen in the control samples, either with excess water or when in a paste form. The presence of this unknown phase could suggest that either an intermediate quantity of amine was present in the entire MCPM material or that a rearrangement of the amine within the amine intercalated MCPM layers had occurred. Both of these processes could have occurred due to the presence of water used to solvate the reagents during the mixing process.

This amine species would also raise the pH of the water solution which could have been responsible for retarding the reaction rate as each cement sample also showed the presence of starting materials in the set product.

From the results obtained from the 1:2.2, 1:0.7 and 3:0.7 MCPM:amine intercalated MCPM ratio samples, the latter ratio produced the most intense brushite diffraction peaks as it was closest in composition to the reference brushite cement. Following this, a further set of experiments were conducted with even lower percentages of amine-MCPM (5% and 10% samples) to investigate the rate of reaction of brushite formation and determine when starting materials were no longer present in the set cement.

The X-ray diffraction pattern for the 10% amine-MCPM cements (shown on figure 5.3.6.2) showed intense brushite peaks, with a very small peak set due to the same unknown phase (B) also present. The X-ray diffraction patterns of the 5% amine-MCPM component showed an effectively pure brushite cement was present with insignificant amounts of other phases. The presence of this unknown phase directly related to the amount of modified MCPM used as a reagent.

Due to the greater potential of brushite cements with the lower amine intercalated MCPM content, 0, 5, 10 and 25% samples were examined in more detail in sections 5.3.5 and 5.3.6 where the setting time and compressive strength of these cements were investigated.

5.3.5 Setting Times on Prepared Brushite Cements

These setting tests were performed on the MCPM and β-TCP brushite cement systems only, since no other viable cement compositions were identified in these experiments.

The setting times of the cements were determined using the Gilmore needles technique, briefly explained in section 5.2.5. The average setting times for cement compositions with 25, 10, and 5% propyl- and butylamine intercalated MCPM (all from the same amine-MCPM batch) and also a pure MCPM control are shown in figure 5.3.5.1.
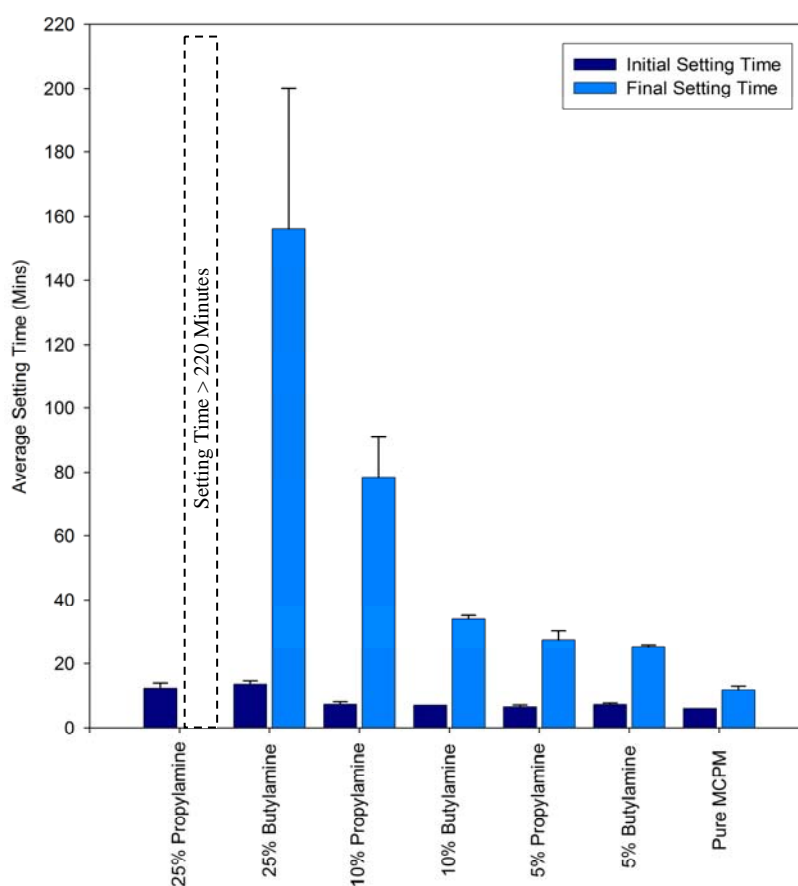
Figure 5.3.5.1: Bar Chart Displaying the Average Initial and Final Setting Times of a Series of Brushite Cements with Errors Included.

From this data, a general trend in the setting times was clearly evident which indicated that the higher the amine content, the longer the setting time. Also, the final setting times of

propylamine intercalated samples were longer than their butylamine intercalated counterparts. This was most evident with the 10% butylamine setting time which was considerably shorter than the equivalent propylamine sample. To check the validity of these results, five further samples of this cement were prepared and all samples set in a similar time period. This suggested that this was a consistent result. The trend for the higher amine content was still apparent as the 25% propylamine sample did not set and both of the 25% amine examples were unusable as cements.

In summary, the greater pKa value of pure propylamine (pKa=10.84)[35] compared with butylamine (pKa=10.61)[35] might have accounted for the quicker setting time of the butylamine-MCPM brushite cement, since a lower solution pH was responsible for producing quicker setting brushite cements. The lower the percentage of amine intercalated MCPM, the quicker the cement would set. The effect was most evident in the cements with 10% amine-MCPM content. At 25%, the cement reaction was too compromised to be viable and at 5%, the amine was too dilute to have a significant effect on the setting time.

5.3.6 Compressive Strength Testing on Prepared Brushite Cements

The compressive strength of the cements was determined using a hydraulic press. This was used to test cement compositions containing MCPM with 25, 10, and 5% propyl- and butylamine intercalated MCPM present, with tricalcium phosphate providing the alkaline component for this system, and also pure MCPM samples were also prepared as controls. Three separate batches of each cement type (i.e. 25, 10, 5, 0% amine-MCPM content) were prepared with at least 8 cement cylinders tested from each batch. The results are shown in figure 5.3.6.1.

From the data shown in figure 5.3.6.1 it was apparent that 25% amine-MCPM content reduced the strength of the cement considerably, with butylamine-MCPM giving the lowest

compressive strength of the entire series. It was likely that this resulted from the larger quantity of amine intercalated MCPM increasing the pH of the cement reaction and therefore reducing the rate of formation of brushite. This was supported by the X-ray diffraction analysis presented in section 5.3.1, as it shows evidence of starting materials present in the set cement confirming an incomplete reaction had occurred. The MCPM component was known to have low compressive strength and therefore any remaining in the set cement would have had a detrimental effect on the overall strength of the cement.
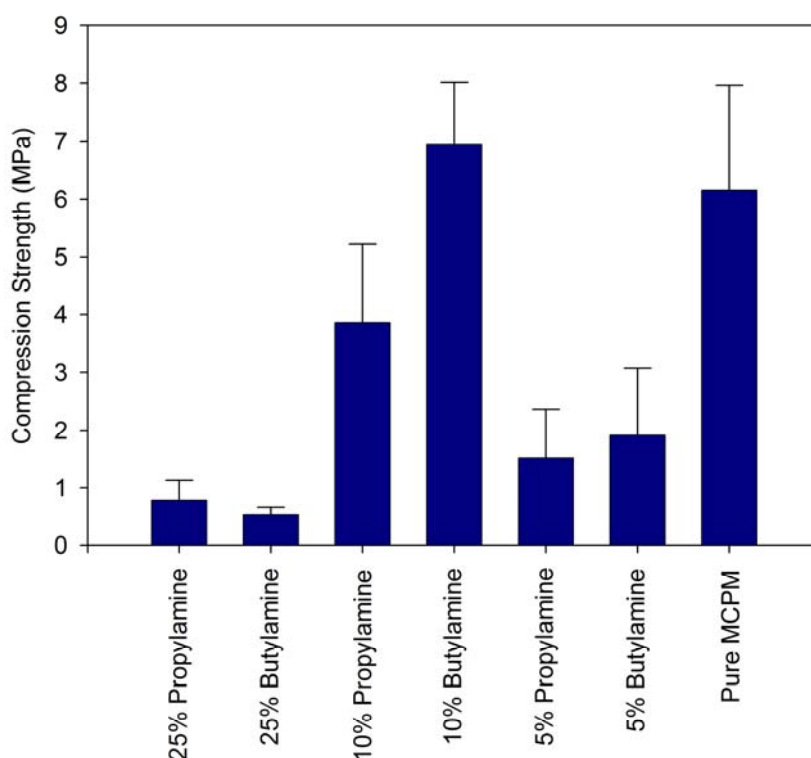
Figure 5.3.6.1: Bar Chart Displaying Compressive Strength of a Series of Brushite Cements with Errors Included.

It was clear that the 10% amine-MCPM containing cements produced considerably harder cements compared with the 25% cements. In fact, the 10% butylamine-MCPM containing cement strength was even stronger, although not significantly different to that of the pure MCPM control cylinders. This cement also displayed a quicker overall setting

reaction than its 10% propylamine counterpart. If the brushite crystals could form a better overlap, the cement cylinder could spread the compressive load more effectively and therefore a stronger cement cylinder would be formed.

However, when only 5% amine content was used, the compressive strength was markedly reduced when compared to the 10% samples. From this data and the setting time data in figure 5.3.5.1, it was clear that the lower amine content had less of an effect upon the reaction rate of the cement components (less of a pH increase) therefore the reaction occurred more quickly and smaller crystals could have been formed with less overlap and thus, potentially, a weaker cement was prepared.
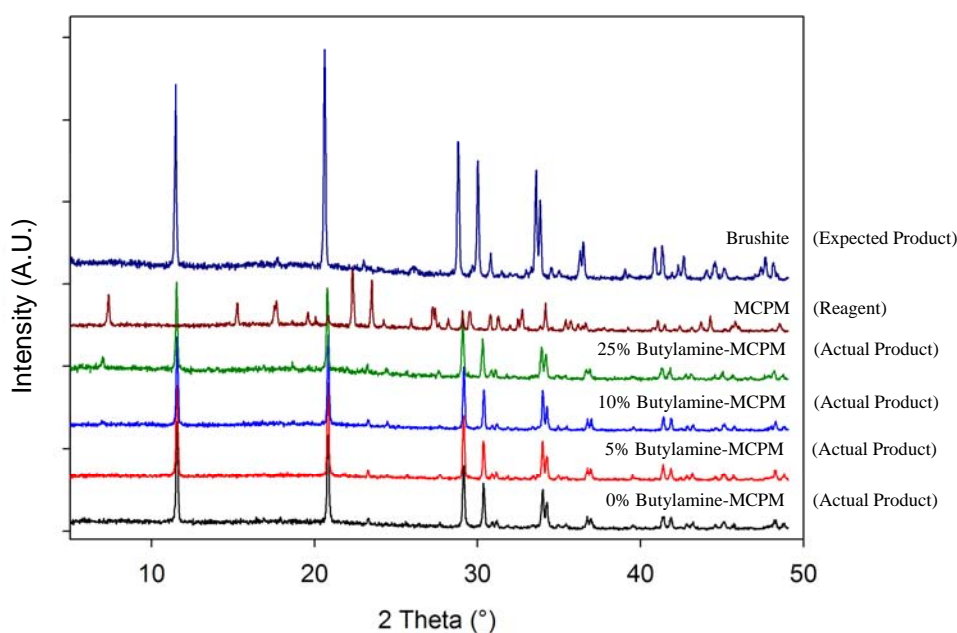
Figure 5.3.6.2: X-ray Diffraction Pattern Comparing the Cement Samples Prepared Using 0, 5 and 10% Butylamine-Intercalated MCPM with MCPM in Brushite Cement Formation.

Due to the large difference in strength values between the 10%, 5% and 0% amine-MCPM samples, powder X-ray diffraction analysis of the samples was performed and the comparison is shown in figure 5.3.6.2. From these results, there was no discernable difference in the phases present or the intensity of the diffraction patterns of the cement

compositions and therefore the samples appeared identical. Therefore the strength difference of the cements was not due to the phases present in the samples but could have been due either to the crystal size and packing or to unforeseen defects in the cement cylinders causing premature fracture and thus lower strength values than expected.

5.4 Conclusions

When pure MCPM and β-TCP were used as a reference reaction, the cement produced when mixed as a paste, set very rapidly. It hardened sometimes before the sample was even placed fully into the mould for the setting reaction tests. This reaction would be too rapid to be used in clinical applications without the addition of retardants. The results obtained when amine intercalated MCPM was used in the cements produced a retarding effect upon the setting reaction of the brushite cement.

However, when MCPM was completely replaced with the amine intercalated MCPM, the reaction was effectively stopped and the mixed components would dry before any reaction had occurred. When different ratios of MCPM and amine intercalated MCPM were used increased setting times, compared to the control experiments, were observed with the formation of some brushite in the cement. Further proof of brushite formation was evident from an increase in the compressive strength of the 10% butylamine cement samples. This was measured as having a similar strength to the control samples. These 10% amine cement samples produced promising results; however, no experiments were conducted upon the biocompatibility of such a system.

When TCP was replaced by calcium oxide as the alkaline component of the cement, no brushite cements were produced. As no brushite was formed, setting time and compressive strength tests were not performed on these samples. Therefore all setting time reactions and compressive strength tests were conducted on the MCPM – TCP brushite cement system only. The control samples (pure MCPM and β-TCP) showed reasonable compressive strengths, within the range given in the literature.[6,31,32] However, these values were on the lower side of the strength scale, which suggested that the cements had either not fully reacted or had not completely dried before they were tested. Therefore further tests with different cement

reaction times would need to be conducted to establish the 'true' compressive strength values of the series of cement samples that were analysed in this chapter.

The 10% amine-MCPM containing cement samples produced promising results with a significant retardation in the setting time with a relatively strong cement compared with the control (MCPM only) samples. Therefore this modified MCPM reagent could offer a potentially suitable retardant for brushite cements. However, no experiments were conducted upon the biocompatibility of such a system. This would need to be performed to test whether the presence of this amine reagent was actually beneficial for its use as a biomaterial.

5.5 References

1. Bohner, M., *J. Mater. Chem.,* **17**, 3980, (2007).
2. Brown, W.; Chow, L., *J. Dent. Res.,* **62**, 672, (1983).
3. Lewis, G., *J. Biomed. Mater. Res.,* **76B**, 456, (2005).
4. Kenny, S.; Buggy, M., *J. Mater. Sci: Mater in Med,* **14**, 923, (2003).
5. Dorozhkin, S., *J. Mater. Sci.,* **42**, 1061, (2007).
6. Barralet, J.; Grover, L.; Gbureck, U., *Biomaterials,* **25**, 2197, (2004).
7. Grover, L.; Gbureck, U.; Young, A.; Wright, A.; Barralet, J., *J. Mater. Chem.,* **15**, 4955, (2005).
8. Alkhraisat, M.; Marino, F.; Rodriguez, C.; Jerez, L.; Cabarcos, E., *Acta. Biomater.,* **4**, 664, (2008).
9. Alkhraisat, M.; Marino, F.; Retama, J.; Jerez, L.; Cabarcos, E., *J. Biomed. Mater. Res.,* **84A**, 710, (2008).
10. Ginebra, M.; Traykova, T.; Planell, J., *J. Controlled Release,* **113**, 102, (2006).
11. Bohner, M.; Gbureck, U., *J. Biomed. Mater. Res.,* **84B**, 375, (2008).
12. Schnieders, J.; Gbureck, U.; Thull, R.; Kissel, T., *Biomaterials,* **27**, 4239, (2006).
13. Mirchi, A.; Lemaitre, J.; Terao, N., *Biomaterials,* **10**, 475, (1989).
14. Gbureck, U.; Dembski, S.; Thull, R.; Barralet, J., *Biomaterials,* **26**, 3691, (2005).
15. Bohner, M.; Gbureck, U.; Barralet, J., *Biomaterials,* **26**, 6423, (2005).
16. Lilley, K.; Gbureck, U.; Knowles, J.; Farrar, D.; Barralet, J., *J. Mater. Sci.,* **16**, 455, (2005).
17. Dorozhkin, S., *J. Mater. Sci.,* **43**, 3028, (2008).
18. Gbureck, U.; Barralet, J.; Spatz, K.; Grover, L.; Thull, R., *Biomaterials,* **25**, 2187, (2004).
19. Barralet, J.; Tremayne, M.; Lilley, K.; Gbureck, U., *Chem. Mater.,* **17**, 1313, (2005).
20. Grover, L.; Gbureck, U.; Wright, A.; Tremayne, M.; Barralet, J., *Biomaterials,* **27**, 2178, (2006).
21. Takagi, S.; Chow, L.; Ishikawa, K., *Biomaterials,* **19**, 1593, (1998).
22. Tamimi, F.; Kumarasami, B.; Doillon, C.; Gbureck, U.; Nihouannen, D.; Cabarcos, E.; Barralet, J., *Acta. Biomater.,* **4**, 1315, (2008).
23. Xu, H.; Burguera, E.; Carey, L., *Biomaterials,* **28**, 3786, (2007).
24. Gorst, N.; Perrie, Y.; Gbureck, U.; Hutton, A.; Hofmann, M.; Grover, L.; Barralet, J., *Acta. Biomater.,* **2**, 95, (2006).
25. Gbureck, U.; Holzel, T.; Biermann, I.; Barralet, J.; Grover, L., *J. Mater. Sci.,* **19**, 1559, (2008).
26. Paul, W.; Sharma, C., *J. Biomat Appl,* **17**, 253, (2003).
27. Hamanishi, C.; Kitamoto, K.; Ohura, K.; Tanaka, S.; Do, Y., *J. Biomed. Mater. Res.,* **32**, 383, (1996).
28. Boudeville, P.; Serraj, S.; Leloup, J.; Margerit, J.; Pauvert, B.; Terol, A., *J. Mater. Sci: Mater in Med,* **10**, 99, (1999).
29. Gbureck, U.; Grolms, O.; Barralet, J.; Grover, L.; Thull, R., *Biomaterials,* **24**, 4123, (2003).
30. Serraj, S.; Boudeville, P.; Terol, A., *J. Mater. Sci: Mater in Med,* **12**, 45, (2001).
31. Pittet, C.; Lemaitre, J., *J. Biomed. Mater. Res.,* **53B**, 769, (2000).
32. Temenoff, J.; Mikos, A., *Biomaterials,* **21**, 2405, (2000).
33. Barralet, J.; Grover, L.; Gaunt, T.; Wright, A.; Gibson, I., *Biomaterials,* **23**, 3063, (2002).

34. Fernandez, E.; Vlad, M.; Gel, M.; Lopez, J.; Torres, R.; Cauich, J., *Biomaterials,* **26**, 3395, (2005).
35. Stark, J.; Wallace, H., *Chemistry Data Book*. Second ed.; John Murray Ltd.: London, 1999.

Chapter 6:

Preparation and Modification of Calcium Based Pyrophosphates

6.1 Introduction

6.1.1 Background

Condensed phosphates are formed from the condensation of two or more phosphate (PO_4^{3-}) units, leading to the formation of P-O-P linkages, with a phosphorus to oxygen ratio range of $5/2 < O/P < 4$[1]. This can provide a range of structural motifs including chains, layers and 3-dimensional frameworks. The most frequently found are the linear chains, with stoichiometry $[P_nO_{(3n+1)}]^{(n+2)-}$. The simplest and most common of these are the pyrophosphates $(P_2O_7^{4-})$ possessing one P-O-P bond in each unit.[2] Condensed phosphates have received considerably less attention than simple phosphates. However, a number of potentially interesting layered pyrophosphate phases containing calcium have been identified. Studies on these and related phases are described in this chapter.

Pyrophosphates are formed from partially condensed orthophosphate tetrahedra (PO_4^{3-}) and are produced by corner sharing one of the oxygen atoms between two phosphorus atoms to form the $P_2O_7^{4-}$ anion.

One of the simplest ways to form condensed phosphates is by the elimination of water from two hydrogen orthophosphates to produce the pyrophosphate species as shown in figure 6.1.1.1.
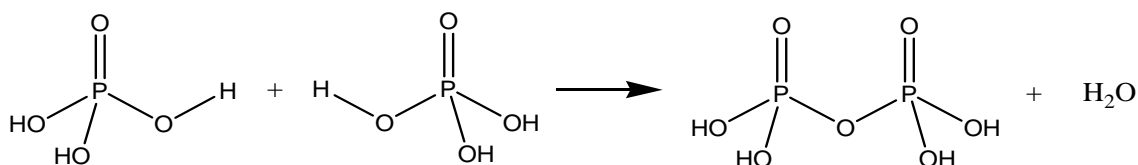
Figure 6.1.1.1: Condensation Reaction of Two Hydrogen Orthophosphates.

The pyrophosphate anion has another useful feature which is its ability to form a range of acid anions such as $H_3P_2O_7^-$, $H_2P_2O_7^{2-}$ and $HP_2O_7^{3-}$. This acidic property is similar to those

observed with the orthophosphate species (due to the protons present to charge balance the PO_4^{3-} units) but is generally less common with condensed phosphates and polyphosphates (PO_3^-) not showing this feature. With these acidic pyrophosphates, the addition of sufficient heat will cause further condensation by elimination of water to form polyphosphates. Therefore these acidic pyrophosphate phases can be considered as intermediate phases and careful consideration of temperature and heating times need to be undertaken if single phase examples are to be isolated.

The exact form of the condensed product is also partly dependent upon the cation that is present. The presence of monovalent cations $(M_2^I H_2 P_2 O_7)$ will tend to lead to the formation of long chained linear polyphosphates $(M^I PO_3)_n$ when heated, whereas most divalent cation acid pyrophosphates $(M^{II} H_2 P_2 O_7)$ will display condensation products apparently related to their size. The larger species (e.g. Sr, Ba and Pb)[2] form long straight chained species whereas smaller divalent ions (e.g. Mg, Mn, Fe, Co, Ni and Cu)[2] commonly form cyclotetraphosphates $(M_2^{II} P_4 O_{12})$.

6.1.2 Synthesis Methods

There are many different routes to the synthesis of the pyrophosphate phases. One example involves the neutralisation of pyrophosphoric acid with an appropriate stoichiometric amount of alkali carbonate. This method is relatively simple but the amounts of reagent and sample temperature (to avoid decomposition of the acid) are critical for the formation of the appropriate phase.

Classical thermal formation methods are also appropriate to produce pyrophosphate materials. Divalent cation pyrophosphates can be produced by the reaction of the carbonate form of the metal ion with ammonium hydrogen orthophosphate (Equation 1). The temperature and time are dependent upon the choice of ion.

$$2M^{II}CO_3 + 2(NH_4)_2HPO_4 \rightarrow M_2^{II}P_2O_7 + 4NH_3 + 2CO_2 + 3H_2O^{[2]} \quad \text{(Equation 1)}$$
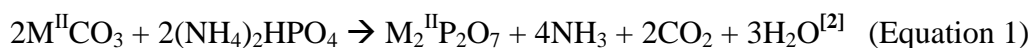
Another alternative route to condensed phosphates is via flux methods. These employ an excess of one particular reagent which, at an appropriate reaction temperature, will form a liquid phase that enhances the mixing and diffusion of the reagents and therefore allows the reaction to proceed more readily. One of the most useful fluxes in condensed phosphate synthesis is orthophosphoric acid (H_3PO_4). It is believed that at reaction temperatures (~ 100°C)[2] pyrophosphoric acid ($H_4P_2O_7$) is formed. This reagent however can further condense (to form polyphosphoric acid) and thus the temperature, reaction time and the other reagents present are important considerations. Also, sodium polyphosphate ($Na(PO_3)$) has been used as a flux agent but a much higher temperature (~ 600°C) is required to melt this reagent and therefore form the flux.

Ion exchange methods have also been used for the formation of some of these metal pyrophosphates. The formation of several pyrophosphates has been achieved by the exchange of the metal chloride or nitrate with the silver pyrophosphate phase ($Ag_4P_2O_7$). However, silver is a relatively expensive reagent and therefore this technique is generally less popular.

Pyrophosphates can also be formed by the condensation of their orthophosphate analogues. However, the orthophosphate species concerned must possess a source of hydrogen, either as the dihydrogenorthophosphate ($H_2PO_4^-$) or monohydrogenorthophosphate (HPO_4^{2-}) forms, to allow for the elimination of water and condensation to occur. Therefore at the appropriate temperature for the chosen ion, two moles of the orthophosphate can condense releasing water as a by-product. This method has been used to prepare sodium and calcium pyrophosphates (Equations 2 & 3).

$$2Na_2HPO_4 \rightarrow Na_4P_2O_7 + H_2O \quad \text{(Equation 2)}$$

$$2CaHPO_4 \rightarrow Ca_2P_2O_7 + H_2O \quad \text{(Equation 3)}$$
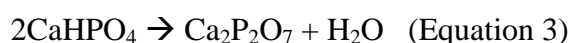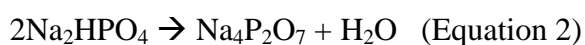
The formation of acid pyrophosphate is possible with the use of the dihydrogen phosphate reagent ($H_2PO_4^-$). This will condense upon heating to produce the acid pyrophosphate species in the presence of divalent cations such as calcium or strontium (Equation 4).[2]

$$Sr(H_2PO_4)_2 \rightarrow SrH_2P_2O_7 + H_2O \quad \text{(Equation 4)}$$
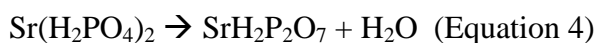
However, this method can be quite sensitive, with a slight increase in temperature or longer reaction times causing further condensation to the polyphosphate form ($M(PO_3)_2$). Despite this difficulty, this method will produce good phase purity when the appropriate conditions are established.

6.1.3 General Aims

As stated previously in this thesis, calcium phosphate materials are of interest due to their inherent biocompatibility. The use of such species for biomaterial applications is therefore clearly advantageous as they are found naturally in the body. Of particular interest is the isolation of novel calcium phosphates. Calcium pyrophosphate systems having potential to provide new materials have been identified. These materials are particularly interesting as calcium pyrophosphate dihydrate is found to be linked to certain forms of arthritis and crystal deposition diseases.[3,4] The formation of this crystalline phase in certain positions, particularly in the joints, is therefore detrimental. However, this phase and similar phases, are present in the body as essential stores of phosphate, with enzymes, such as alkaline phosphatase known to hydrolyse phospho-ester bonds[5] (P-O-P) to release orthophosphate units (PO_4^{3-}) for use in the body. Therefore it is conceivable that biomaterials based on pyrophosphate phases can utilise these phosphatase enzymes[6-8] thus allowing them to elicit an advantageous biological response to enhance resorption and release phosphate or calcium to the surrounding tissues.

There are a number of different known phases of calcium pyrophosphate and many analogues of these phases can be synthesised. The presence of some of these as crystals in the body gives some indication of the increased stability compared to the orthophosphate phases which usually are reabsorbed relatively quickly *in vivo.*

These pyrophosphate materials have an enigmatic nature because, as mentioned earlier, some pyrophosphate species (e.g. calcium pyrophosphate dihydrate) are known to be insoluble in certain environments (such as in the joints[7]) whereas they are soluble in other parts of the body (where enzymes can act, such as alkaline phosphatase[6,8]). In addition, these pyrophosphate ions have also been identified to cause an inhibitory effect upon the crystal growth of hydroxyapatite or brushite phases in bone cements, where the pyrophosphate ion would need to be soluble to cause this effect[9,10] (see Chapter 5). Therefore the complex nature of the properties of these materials requires further investigation.

A survey of the structurally characterised calcium pyrophosphates indicates that a number of these phases have layered structures with potential for further modification. Therefore the aim of this section of research was to prepare and characterise further examples of biocompatible layered metal pyrophosphates. The intention was to use ion exchange, intercalation and exfoliation experiments on these and similar layered pyrophosphates to achieve this purpose.

The main phases that have been investigated in this section of the thesis were calcium pyrophosphate tetrahydrate ($Ca_2P_2O_7 \cdot 4H_2O$), and calcium disodium pyrophosphate ($CaNa_2P_2O_7 \cdot 4H_2O$), which both possess layered structures. The calcium pyrophosphate tetrahydrate phase was of interest as it possesses water molecules in its interlayer region. Two of these four water molecules appear to be only weakly bound and therefore may have potential to be easily exchanged with other species. Calcium disodium pyrophosphate was

investigated due the apparent accessibility of the sodium ions within the structure, suggesting potential for exchange by other cations.

Calcium acid ($CaH_2P_2O_7$) pyrophosphate was also used as a comparison because this phase is not layered but does contain a pyrophosphate unit. The same experiments were therefore performed on the calcium acid pyrophosphate phase in order to compare the results with the layered pyrophosphate phases.

6.2 Experimental

6.2.1 The Synthesis of Calcium Pyrophosphate Tetrahydrate

This method was adapted from a procedure by *Christoffersen et al.*[7] using the same reagents. A mass of 5.985g of sodium pyrophosphate decahydrate was added to 750 ml of deionised water, with stirring to aid dissolution. This colourless solution was heated to approximately 45°C whilst the solution was being stirred and a saturated aqueous solution containing 4.95g of anhydrous calcium chloride was added. The cloudy white suspension was continuously stirred at this temperature for 5 days to allow full precipitation of the desired product. The material was then filtered under vacuum and washed with copious amounts of de-ionised water. The solid white crystalline material was then left in air at room temperature overnight to dry before X-ray diffraction was performed.

6.2.2 High Temperature Powder X-ray Diffraction of Calcium Pyrophosphate Tetrahydrate

A full temperature sweep of this material was performed from 25°C to 750°C at 25°C intervals in the D5005 X-ray diffractometer with *in situ* furnace. A series of scans were also performed after this heating regime, at room temperature, to determine whether this material would re-absorb water from the air after the heat treatment.

In addition to the above *in situ* heating method, separate samples of calcium pyrophosphate tetrahydrate were also heated in a tube furnace from 200 to 550°C in 50°C intervals. Two further temperatures at 700°C and 800°C were also included. Between 200 and 400°C, the furnace was pre-heated before the sample was added. This was to stop the effects of any temperature overshoot by the furnace. These samples were allowed to cool to room temperature and then the material was analysed on the D5000 powder X-ray diffractometer.

6.2.3 Attempted Intercalation of Calcium Pyrophosphate Tetrahydrate

0.3g of calcium pyrophosphate tetrahydrate was added to 5 cm^3 of pure and 0.1M solutions (diluted with water) of amines and alcohols and other polar and non-polar molecules listed in table 6.2.3.1. The molecules were chosen for their relative size, shape and pKa. The material was left in these solutions for up to 25 days with periodic sampling and analysis performed using powder X-ray diffraction, to determine if any structural changes had occurred.

Further experiments were also conducted using the same intercalating species on a portion of the calcium pyrophosphate tetrahydrate host that had been heated to 110°C (~0.2g). This heating step was used to remove the hydrogen bonded water molecules from the interlayer region of this material. From TGA analysis (See section 6.3.2 for more details) this phase was show to be the calcium pyrophosphate monohydrate analogue.

A final species that was investigated was a neutral molecule 4,4-bipyridyl (figure 6.2.3.1) that has been used in previous intercalations[11-14] in layered materials where the two nitrogen atoms positioned at each end of the molecule offer potential for hydrogen bonding. This compound (0.25g) was mixed with 10 cm^3 of either ethanol or 2M ammonia/ethanol to form a relatively weak solution (0.1M).
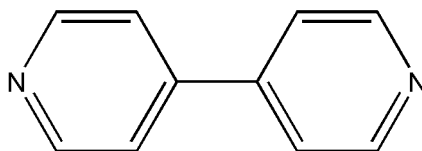
Figure 6.2.3.1: Structure of 4,4-Bipyridyl

Table 6.2.3.1: List of Intercalating Species with Concentrations for Intercalation Reactions in Calcium Pyrophosphate Tetrahydrate and Monohydrate Analogues

Intercalating Species	Concentration	Days in Solution
Butylamine	Pure and 0.1M	25
Heptylamine	Pure and 0.1M	25
Diethylamine	Pure and 0.1M	25
Dipropylamine	Pure and 0.1M	25
Triethylamine	Pure and 0.1M	25
Tributylamine	Pure and 0.1M	25
Tetrabutylammonium hydroxide	0.1M	25
Tetrabutylammonium bromide	0.1M	25
Dry methanol	0.1M	16
Ethanol	0.1M	16
Butanol	0.1M	16
Pentanol	0.1M	16
Ethan-1,2-diol	0.1M	16
Butan-1,4-diol	0.1M	16
Acetonitrile	Pure	16
Ammonia/water	35% Solution	16
Ammonia/ethanol	2M	16
Deionised water	Pure	16

Reflux Intercalation Methods with Calcium Pyrophosphate Tetrahydrate

Calcium pyrophosphate tetrahydrate (0.2g) was added to 25 cm^3 of dry methanol and heated under reflux in a 100 cm^3 round bottomed flask with condenser for 24 hours. This experiment was also repeated using ethanol and a methanol/water (1:1) mix to determine the effects of different solvents, again with the same volume of solvent and length of reaction time.

Solvothermal Intercalation Experiments in Calcium Pyrophosphate

Calcium pyrophosphate tetrahydrate and monohydrate were added separately to 10 cm^3 of solution (~ half filled reaction vessel) containing either pure solvent or an intercalating species in solvent and sealed in an Anton Parr hydrothermal vessel. This was

heated over a range of temperatures from 100°C to 200°C. Tables 6.2.3.2 & 6.2.3.3 list the solvents, intercalating species, concentration and temperature ranges that were attempted.

Table 6.2.3.2: Initial Solvent and Temperatures Trials Used for Solvothermal Intercalation in Calcium Pyrophosphate Tetrahydrate

Mass Used (g)	Solvent and Filling Level	Temperature (°C)
0.3	Methanol (half fill)	100
0.3	Methanol (half fill)	150
0.3	Methanol (half fill)	200
0.3	Ethanol (half fill)	100
0.3	Ethanol (half fill)	150
0.3	Ethanol (half fill)	200
0.3	Propylamine (half fill)	100
0.3	Butylamine (half fill)	100
0.3	Dipropylamine (half fill)	100
0.3	Acetonitrile (half fill)	100
0.3	35% Ammonia solution in water (half fill)	100
0.3	2M Ammonia/ethanol (half fill)	100
0.3	Ethanoic acid (half fill)	100
0.3	Propanoic acid (half fill)	100
0.3	Oxalic acid ($C_2O_4H_2$) 0.5M in water (half fill)	100
0.3	Citric acid ($C_4O_7H_4$) 0.5M in water (half fill)	100

Table 6.2.3.3: Solvothermal Intercalation in Calcium Pyrophosphate Tetrahydrate and Monohydrate Using a Range of Solvents and Temperatures

Intercalating Species	Solvent	Concentration	Temperature (°C)	Approx. Filling Level (%)
Ethylamine	Water	70%	100	50
Propylamine	Ethanol	0.5M	100	50
Butylamine	Ethanol	0.5M	100	50
Butylamine	Ethanol	0.5M	150	50
Propylamine	Water	0.5M	100	50
Butylamine	Water	0.5M	150	50
Butylamine	Pure	99%	150	50
Butylamine	Water	0.2M	175	50
Butylamine	Water	0.2M	200	50
Ammonia	Ethanol	2M	150	50
Ammonium hydroxide	Pure	97%	150	50
Water	Pure	-	150	50

Melt Occlusion Experiments with Calcium Pyrophosphate Tetrahydrate

0.2 g of calcium pyrophosphate tetrahydrate was added to 1g of the compounds listed in table 6.2.3.4 and intimately ground together using a pestle and mortar and heated to 150°C for 24 hours.

Table 6.2.3.4: Compounds Used for Occlusion in Calcium Pyrophosphate Tetrahydrate

Chemical	Mass (g)
Tetrabutylammonium bromide	1g
Tetrabutylammonium hydroxide	1g
Magnesium nitrate	1g
Lithium nitrate	1g
Sodium nitrate	1g
Silver nitrate	1g
Silver chloride	1g
Lithium chloride	1g
Ammonium chloride	1g
Aspirin	1g
Indomethacin	1g

6.2.4 Exfoliation Attempts with Calcium Pyrophosphate Tetrahydrate

One of the aims of this research was to test the exfoliation properties of layered calcium phosphates. Therefore calcium pyrophosphate tetrahydrate was also tested. When exfoliation experiments were conducted with MCPM samples in Chapter 4, tetrabutylammonium (TBA) bromide and hydroxide exfoliating solutions were chosen. These same species will therefore be attempted here. This calcium pyrophosphate phase does not suffer from water instabilities and therefore water was used due to the better solubility of TBA in this medium. 0.1M solution of both TBA bromide and hydroxide were prepared and 0.2g of calcium pyrophosphate tetrahydrate was added to these and left in solution up to 6 days with daily sampling. Samples were washed and dried at room temperature and analysed using powder X-ray diffraction.

An observation about this particular calcium phosphate phase was the ability for this material to swell considerably when left in water for a few hours. Attempts to perform X-ray diffraction analysis on the expanded layer form of this phase have proved unsuccessful as a solid material was required. Even when a wet paste form was analysed, an identical pattern to the tetrahydrate phase was observed.

An adaptation of the above experimental procedure was performed whereby the pyrophosphate was allowed to stand in water for four hours before the TBA exfoliating species was added. The resulting solution was left for a further 6 days before analysing.

A separate experiment was also completed where this expanded material was sonicated in water for 30 minutes to determine whether the extra swelling might allow the layers to separate under gentle agitation.

A final experiment was conducted using 1,6-diaminohexane as an alternative exfoliating species which had previously been used to separate layered aluminium triphosphate species.[15]

6.2.5 The Synthesis of Calcium Disodium Pyrophosphate Tetrahydrate

This calcium disodium pyrophosphate tetrahydrate phase was formed by the addition of a dilute solution of calcium chloride to sodium pyrophosphate. The concentration of calcium to sodium was varied to determine the best yield of the desired product. From the initial method adapted from *Cheng et al.*[16] who mixed a 1mM $CaCl_2$ solution in deionised water (25 cm^3) with a 0.1M $Na_4P_2O_7 \cdot 10H_2O$ in 25 cm^3 of water which was first neutralised with 1M HCl solution. These two solutions were poured together in approximately equal volumes whilst stirring, to form a white precipitate. For this purpose, the neutralisation of the sodium pyrophosphate was not necessary and a 0.05M calcium chloride solution gave the best yield of the desired phase.

To synthesise a large batch of this material, 11.15g of sodium pyrophosphate decahydrate was added to 250 cm^3 of water with stirring and gentle warming (to aid dissolution) to form a 0.1M solution. A 0.05M calcium chloride solution was prepared by adding 1.375g of anhydrous powder to 250 cm^3 of deionised water again with stirring. These solutions were then poured together in equal measures to yield a white cloudy precipitate that was left to stand overnight which produced a white crystalline solid.

6.2.6 Ion/Proton Exchange, Amine Intercalation and Attempted Exfoliation of Calcium Disodium Pyrophosphate

Initially ion exchange was investigated using a potassium salt in an attempt to expand the layers in this material enabling further exchange with other ions. Room temperature ion exchange was attempted using either a 10:1 or 25:1 ratio of potassium chloride to calcium disodium pyrophosphate (0.25g) in ~ 100 cm^3 of water. This was stirred overnight for a total of 16 hours. A separate exchange was also attempted using potassium nitrate 25:1 instead of chloride to determine whether this would have an effect. A room temperature exchange was also attempted using 10 cm^3 of a saturated solution of potassium nitrate (due to availability).

A more forceful approach was also attempted using a reflux reaction in a saturated solution (10 cm^3) of potassium nitrate to determine whether this would produce the required phase. The reflux time was varied from 2 - 24 hours to determine the minimum time required to minimise decomposition of the material but still enable full exchange.

Proton Exchange

Proton exchange experiments were also performed on the host calcium disodium pyrophosphate phase by the addition of different strength mineral and organic acids, in an attempt to form a layered polymorph of the calcium acid pyrophosphate phase ($CaH_2P_2O_7$) with potential for intercalation.

A range of concentrations of hydrochloric acid were used to determine at which point proton exchange could occur without being too strong to dissolve the sample. Ethanoic acid was also attempted as it is a much weaker acid and might have less effect upon the stability of the pyrophosphate layers. Table 6.2.6.1 lists the acids and concentrations that were used.

Table 6.2.6.1: Concentration of Acid Used to Modify the Calcium Disodium Pyrophosphate

Acid Used	Concentration (mol dm^{-3})
Hydrochloric	1
Hydrochloric	0.5
Hydrochloric	0.25
Hydrochloric	0.1
Hydrochloric	0.05
Hydrochloric	0.025
Hydrochloric	0.01
Hydrochloric	0.005
Hydrochloric	0.0025
Ethanoic	1
Ethanoic	0.5
Ethanoic	0.25
Ethanoic	0.1
Propanoic	1
Propanoic	0.5

The calcium disodium pyrophosphate was left for 2 hours in each solution and the sample was periodically swirled to create a cloudy suspension. After this time period, the sample was filtered and dried in air. A longer reaction time period of 6 hours was used with the weak 0.005M and 0.0025M HCl solutions as these very dilute solutions might have required more time for the reaction to run to completion.

Intercalation

Intercalation experiments were performed on the calcium disodium pyrophosphate phase and the (1M ethanoic) acid modified analogue of this material using monoamines as the intercalating species. A calcium disodium pyrophosphate mass of 0.3g was added to 10 cm^3

of pure propylamine, butylamine or hexylamine and this phase was left in solution for 2 days before analysing by powder X-ray diffraction.

Exfoliation Attempts

Calcium disodium pyrophosphate tetrahydrate host material and the organic acid modified analogue of this phase were added to 0.2M aqueous solutions of TBA-Br, TBA-OH and the surfactant tetradecyltrimethylammonium bromide. These samples were left for 1 day before being filtered under suction and washed with deionised water.

6.2.7 The Synthesis of Calcium Acid Pyrophosphate

This material was formed using two different procedures. The first method involved the direct heating of MCPM to 225°C to produce the required phase. The second method used an orthophosphoric acid flux method to produce the calcium acid pyrophosphate phase. The direct heating method produced an impure phase with additional unidentifiable calcium phosphate phases. The acid flux method, however, produced a pure single phase acid pyrophosphate phase. This method used orthophosphoric acid (85% by weight in water) and calcium hydroxide mixed homogenously in a 3:1 ratio and then heated at 150°C for 12 - 24 hours. A sample size of 6g orthophosphoric acid with 1.2988g of calcium hydroxide was sufficient to give a reasonable yield of product, without the mixing step producing excessive steam, causing loss of the fine calcium hydroxide powder during the mixing process.

6.2.8 Attempted Intercalation in Calcium Acid Pyrophosphate

Intercalation experiments were performed on the calcium acid pyrophosphate phase prepared using acid flux and direct heating methods. These were performed using monoamines as the intercalating species. A calcium acid pyrophosphate mass of 0.2g was added to pure propylamine, butylamine, hexylamine or octylamine to half fill a medium size

sample vial (volume ~ 10 cm^3) and this phase was left in solution for 7 days. After the reaction time, the amine was removed by filtration and the calcium phosphate was washed with ethanol to remove any surface amine before analysing by powder X-ray diffraction.

In addition, two diamines (diethylamine and dipropylamine), two carboxylic acids (ethanoic and propanoic (1M diluted)) and five amino acids (alanine, arginine, cysteine, glycine and lysine) were also tested, to broaden the spectrum of potential intercalation compounds.

The diamine and carboxylic acid species were prepared following the same methods used with the monoamine species. In the amino acid experiments, 3g of the solid amino acid was added to 5-10 cm^3 of water to form a saturated or semi-saturated solution before 0.2g of the calcium acid pyrophosphate (acid flux method) was added to these solutions. The samples were left for 7 days with periodic sampling and analysis by powder X-ray diffraction.

A control experiment was also performed with this calcium acid pyrophosphate phase using 0.3g of this material added to pure deionised water and left for 24 hours. The sample was then dried in air at room temperature and analysed by powder X-ray diffraction.

6.2.9 Characterisation of Prepared Phases

The composition and structure of all the calcium based pyrophosphate materials were investigated by powder X-ray diffraction using a Siemens D5000 diffractometer (transmission mode with Cu Kα_1 radiation). High temperature X-ray diffraction data were collected using a Siemens D5005 diffractometer which has an in situ Anton Parr heating stage. This instrument collects data in reflection mode in a θ-θ arrangement through 5 - 60° using a static alumina sample holder inside the heating stage.

Thermogravimetric (TG) and differential thermal analysis (DTA) were performed on a Stanton Redcroft STA-780 thermogravimetric analyser at a heating rate of 3°C min^{-1} under air

when carbon was present in the samples. Where no carbon components were present, a Rheometric Scientific STA 1500 instrument was used due to the increased sensitivity and resolution from this device. All experiments were conducted in air at a heating rate of 3°C min^{-1} unless otherwise stated.

Fourier transform infrared analysis was used to determine the effects of organic modification in the calcium pyrophosphate species. From the vibrational excitation of the chemical bonds present, characteristic absorption frequency bands in the infrared spectrum would be observed. Analysis of these absorption bands showed which functional groups were present in the material. These measurements were performed on a Perkin-Elmer Paragon 1600 FT-IR spectrometer in transmission mode using the KBr solid disc method.

Once the phases were prepared, if a known reference phase could be identified, indexing of the phases was performed. This involved using the indexing program *CELL*[17] to refine the unit cell parameters of the experimental data with the reference values and a closeness of agreement between these values was produced (R Factor). The full data set are shown in the appendix with a summary table of the values given in the appropriate results sections for each phase.

6.3 Results and Discussion

6.3.1 The Synthesis of Calcium Pyrophosphate Tetrahydrate

The preparation of this phase was adapted from the method given by *Christoffersen et al.*[18] In their method, an excess of sodium chloride and a raised temperature was used to aid the formation of the appropriate phase. The excess sodium chloride was found to be unnecessary for the method used, as this excess was believed to decrease the overall quantity of calcium ions present in the solution for larger crystal growth. The drying temperature was important however, as shown from the TGA analysis in section 6.3.2, the first water molecule was lost at 40°C. Therefore, if the sample was dried above room temperature, a smaller d-spacing for the principal diffraction peak was observed due to a contraction of the interlayer separation.

The reaction time also appeared to be important, with five days giving the most crystalline, single phase sample. The diffraction pattern and structural representation for this phase using a five day preparation time can be seen in figures 6.3.1.1 and 6.3.1.2.
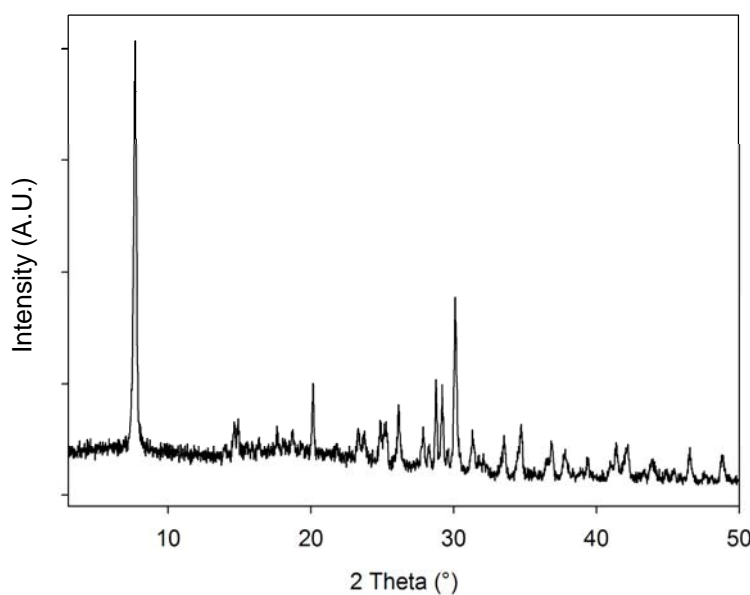
Figure 6.3.1.1: X-ray Diffraction Pattern of Calcium Pyrophosphate Tetrahydrate
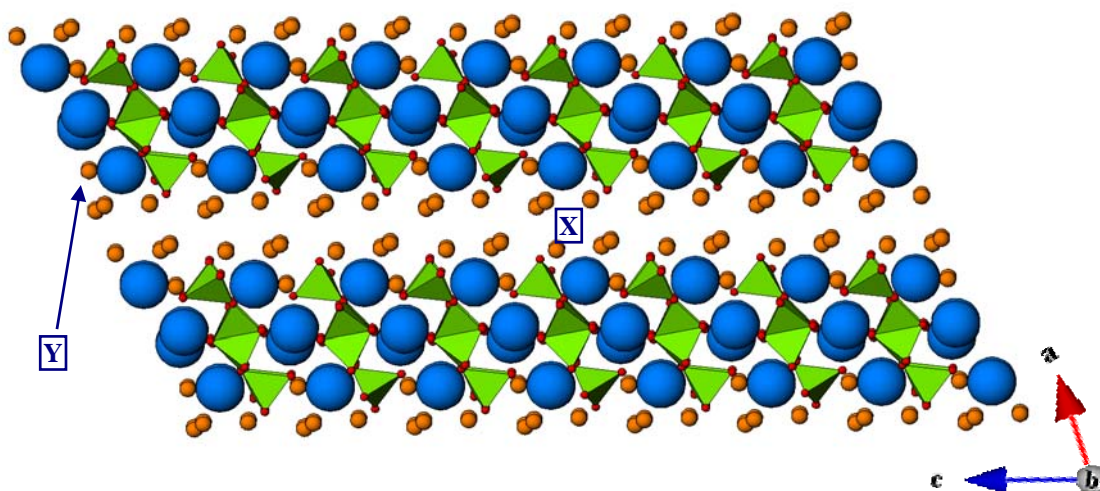
Figure 6.3.1.2: Structural Representation of Calcium Pyrophosphate Tetrahydrate. (Blue Spheres = Calcium, Green Tetrahedra = Pyrophosphate units, Orange Spheres = Water Molecules) (Label X = Water Molecules Lost Below ~ 100°C, Label Y = Water Molecule Lost ~ 300°C)

From the structural representation[19] of calcium pyrophosphate tetrahydrate shown in figure 6.3.1.2, the layered nature of this material is evident, with most of the water molecules in the interlayer region. The structure of this material was confirmed by indexing the experimental X-ray diffraction data (figure 6.3.1.1) from the samples using *CELL*[17] with a known reference sample[18] from the ICSD[20,21] crystal structure database. The unit cell data was refined and listed in table 6.3.1.1 with the full data presented in Appendix 3. The close agreement of these values, together with a low R factor, confirms that the experimental structure is consistent with the reference phase.

Table 6.3.1.1: Indexed Unit Cell Parameters for Calcium Pyrophosphate Tetrahydrate (Space group = $P2_1/c$)

Unit Cell Parameters	Values	Reference Values[18]
a (Å)	12.26(2)	12.287
b (Å)	7.49(1)	7.511
c (Å)	10.69(2)	10.775
α (°)	90	90
β (°)	112.54(7)	112.540
γ (°)	90	90
R Factor = 0.00000074		

6.3.2 Thermogravimetric Analysis of Calcium Pyrophosphate Tetrahydrate

From figure 6.3.2.1, it was possible to determine that the calcium phosphate material possessed 4 water molecules per mole of calcium pyrophosphate. These water molecules were lost in 3 distinct stages. The first water molecule was lost at ~ 40°C (Labelled A, figure 6.3.2.1), the next 2 water molecules were lost at ~ 80°C (Labelled B, figure 6.3.2.1) and the final water molecule was lost at ~ 300°C (Labelled C, figure 6.3.2.1). Although three distinct mass losses were observed on the TGA analysis, a comparison to the structural representation in figure 6.3.1.2 showed two types of water environments, which could account for the vast difference in temperatures where the water molecules were lost. These are labelled as X and Y on figure 6.3.1.2.
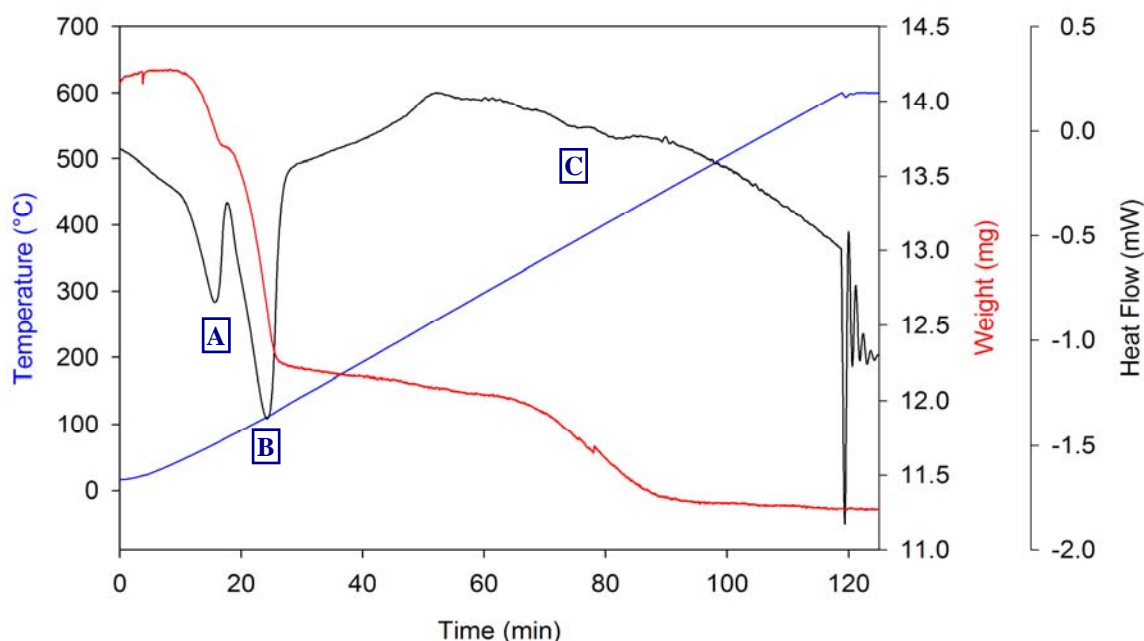
Figure 6.3.2.1: Thermogravimetric Analysis (Rheometric STA 1500) of Calcium Pyrophosphate Tetrahydrate. (Label A = Energy Change due to Loss of a Water Molecule at 40°C, Label B = Energy Change due to Loss of Two Water Molecules at 80°C, Energy Change due to Loss of a Water Molecule at 300°C)

The TGA analysis shows that the first two water losses, labelled A and B on the TGA plot, were lost at relatively low temperatures (below 100°C). This would suggest that the

molecules were only weakly bound in the structure. Comparison to the structural representation in figure 6.3.1.2 shows that the environment labelled X on this figure would be the most likely site for the loss of these water molecules. The mass loss on the TGA plot at ~ 300°C (Labelled C, figure 6.3.2.1) could be due to loss of the water which is bound to the calcium ions in the structure. From analysis of the representation in figure 6.3.1.2, the loss of the water molecules labelled Y could be responsible for the mass loss at this temperature.

As mentioned in section 6.3.4, when a sample of the calcium pyrophosphate tetrahydrate was heated to 110°C, a partly dehydrated phase was formed. From the TGA analysis, this part dehydrated phase was likely to contain only one mole of water (i.e. calcium pyrophosphate monohydrate) bound to the calcium ions in the structure (Labelled Y on figure 6.3.1.2).

6.3.3 High Temperature Powder X-ray Diffraction of Calcium Pyrophosphate Tetrahydrate

The initial phase changes for the calcium pyrophosphate phase were determined using thermogravimetric analysis (TGA) as seen in section 6.3.2. However, the actual phases produced can not be determined by this method, thus *in situ* high temperature X-ray diffraction (HTXRD) was performed. This analysis was achieved by heating the sample from room temperature to 750°C in 25°C increments. The temperature range from 400°C to 700°C was not studied in detail in the main scan, as no phase changes were observed in both the TG and preliminary HTXRD analyses.

There was one potential problem with the use of the fully hydrated calcium pyrophosphate sample. When this material was heated from 50 to 100°C, the flat sample surface required for this analysis appeared to expand and buckle within the holder and thus a good quality X-ray diffraction data set was not obtained above this temperature. To overcome

this problem, two separate data sets were recorded, using the same sample batch - one below 100°C using the fully hydrated sample and one set from 100°C onwards using a previously heated sample. The two good data sets were then combined to produce the full data series. The diffraction data are presented in figure 6.3.3.1.

From this data, it was evident that 4 phases were present during the heating cycle. The initial phase was calcium pyrophosphate tetrahydrate present from 25°C to 75°C. At 100°C a partially dehydrated phase (monohydrate) was formed. This monohydrate phase (from TGA analysis) remains stable to 275°C. At 300°C, an amorphous phase was produced that remained in this form until 700°C when the anhydrous calcium pyrophosphate phase was formed. The crystallinity of this phase increased as the temperature increased to 750°C and this phase remained, once cooled to room temperature.

Table 6.3.3.1: Indexed Unit Cell Parameters for Anhydrous Calcium Pyrophosphate (Space group=$P4_1$)

Unit Cell Parameters	Values	Reference Values[22]
a (Å)	6.71(4)	6.686
b (Å)	6.71(4)	6.686
c (Å)	24.24(9)	24.147
α (°)	90	90
β (°)	90	90
γ (°)	90	90
R Factor = 0.00000014		

Indexing was attempted on the three crystalline phases using *CELL*.[17] The results for the tetrahydrate phase have already been covered in section 6.3.1. The monohydrate phase was not indexed as no reliable cell was obtained from *CRYSFIRE[23]* analysis. The anhydrous calcium pyrophosphate phase however was indexed using a known reference sample[22] from the ICSD[20,21] crystal structure database. The results are listed in table 6.3.3.1, with the full

data presented in Appendix 4. The close agreement of these values together with a low R

factor confirmed that the experimental structure was consistent with the reference phase.
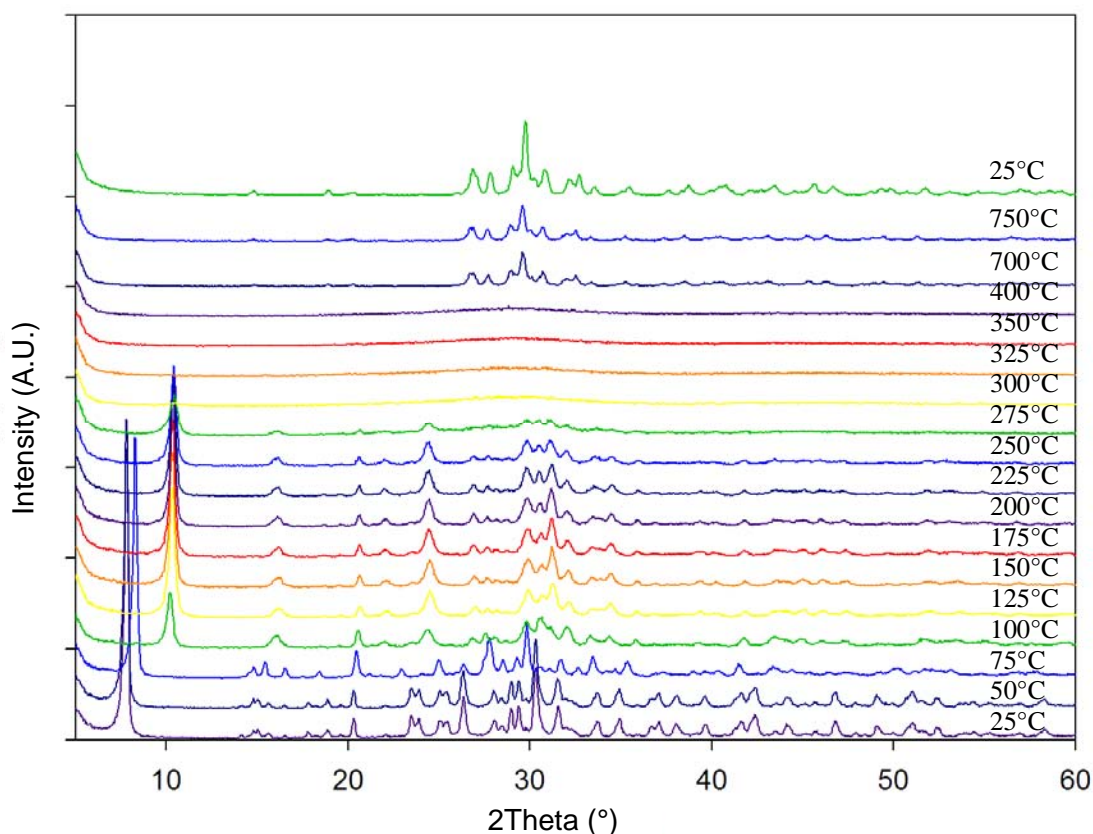
Figure 6.3.3.1: High Temperature Powder X-ray Diffraction (D5005) Patterns of Calcium Pyrophosphate Heated from Room Temperature to 750°C.

External Heating Procedure on Calcium Pyrophosphate Tetrahydrate

In these experiments, separate samples of calcium pyrophosphate tetrahydrate were

heated to various temperatures in a furnace and then cooled to room temperature, before

powder X-ray diffraction analysis was performed. These experiments were performed to test

the stability of the phases that were formed in the *in situ* HTXRD procedure above. The

external heating method would heat a sample of calcium pyrophosphate tetrahydrate above

the transition temperature of each phase and then cool the sample to room temperature. If the

phase was stable, it would still be present when the sample was at ambient temperature.

The data obtained from these experiments shows that the same three phases were present when the sample was cooled to room temperature. These can be observed in figure 6.3.3.2. The first phase formed was the monohydrate phase where the first diffraction peak has shifted from 7.7° 2θ to ~ 10.3° 2θ with the loss of water. This monohydrate phase would normally form above 100°C and was stable up to 300°C. Above this temperature, the crystallinity of the sample was reduced and the first diffraction peak had disappeared at 350°C. This material went through an amorphous phase transition from 350 to 400°C.
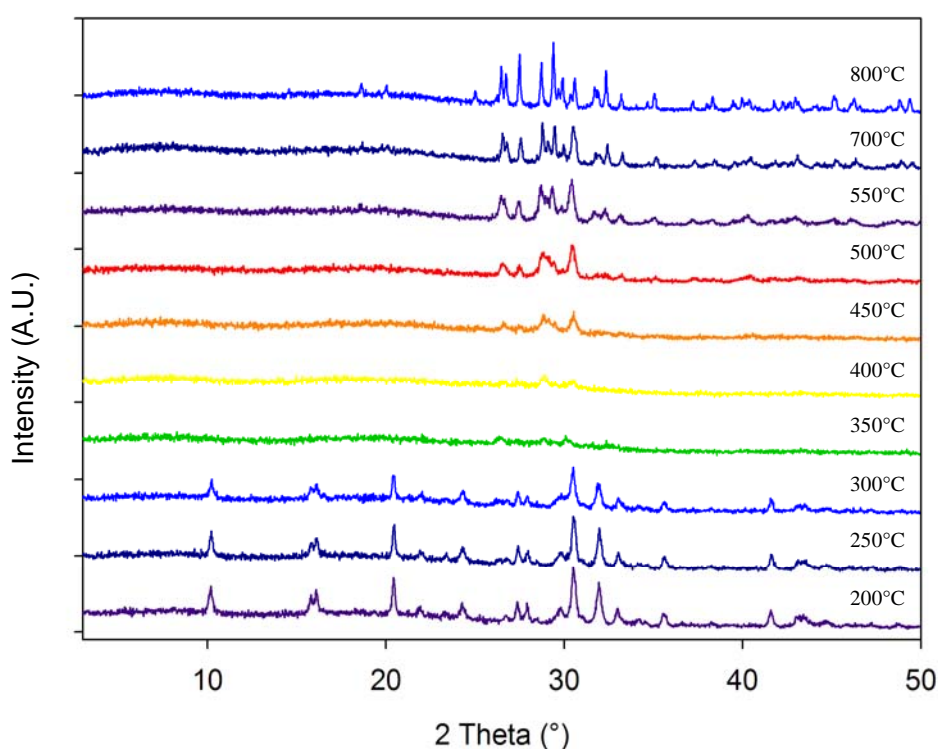
Figure 6.3.3.2: X-ray Diffraction Pattern of a Series of High Temperature Calcium Pyrophosphate Samples

From 400°C and above, the appearance of the final phase occurred, which was the anhydrous calcium pyrophosphate phase. As the temperature increased, the crystallinity of the sample increased which was evident in the intensity and sharpness of the diffraction peaks produced on the X-ray diffraction patterns at 800°C. Indexing was performed on this sample

and similar values were obtained for the unit cell parameters, as shown in table 6.3.3.1, for the high temperature X-ray diffraction analysis of the calcium pyrophosphate tetrahydrate phase.

6.3.4 Attempted Intercalation of Calcium Pyrophosphate Tetrahydrate

The first reactions that were attempted with this phase were the intercalation of monoamines into the structure. These were attempted following the successful intercalation of these species in MCPM (Chapter 4). From the intercalation behaviour of monoamines in MCPM and zirconium phosphate,[24-26] it was likely that the amine functional group would react by accepting protons either from the host phase or from the solution. Therefore the intercalation of amines might require acidic protons to be present in the calcium phosphate layer. Analysis of the calcium pyrophosphate tetrahydrate structure showed that it did not possess any acidic protons to allow this process to occur. Thus intercalation of amines in this structure was more difficult and would have to occur through hydrogen bonding routes or by the exchange of water molecules from the interlayer region. Analysis of the powder X-ray diffraction patterns produced for each sample after the allotted reaction time showed no obvious change in the diffraction pattern when compared to the host phase and therefore intercalation of these amine species had not occurred.

The next set of intercalation species that were attempted were the short chained (1–10 carbon atoms) alcohols. The X-ray diffraction patterns produced following these reactions showed only starting material diffraction peaks. As these molecules would not be charged species and methanol is a similar size to water, a direct exchange with water was expected to occur. However, there was no C-O stretch observed in the FTIR spectrum for this sample, which would have been present had methanol been intercalated in the structure.

When acetonitrile and ammonia solutions were tested, no changes were observed in either the powder X-ray diffraction pattern or the FTIR spectrum of the sample indicative of a successful intercalation reaction with these species.

Attempted Intercalation of the Calcium Pyrophosphate Monohydrate Analogue

An extension to the experiments was conducted by replacing the calcium pyrophosphate tetrahydrate host with the monohydrate analogue of this material (prepared by heating the host phase to 110°C for a few hours to remove some of the weakly bound water present in the interlayer region). The same intercalating species were then added to this phase which, due to the extra voids in the structure left by the loss of water, might be more susceptible to react with the intercalating species.

The addition of excess water to this monohydrate phase showed a change in structure back to the tetrahydrate phase. This was evident in the X-ray diffraction pattern shown in figure 6.3.4.1 where the first diffraction peak shifted from 10.1° to 7.7° 2θ diffraction angle. The quantity of water present in the material was again assessed using TGA analysis and four moles of water were present in the re-hydrated phase.

This observation suggested that the monohydrate structure has potential to intercalate species as it would accept water back into the structure. The intercalating species used however, would have to be neutral and polar to mimic water molecules and therefore intercalation would have to occur using hydrogen bonding as an additional stabilising factor.

To this end, alcohols, ammonia solutions, acetonitrile (for contrast) and 4,4-bipyridyl molecule were tested as intercalating species. These molecules were chosen due to their different polarities, size and hydrogen-bonding abilities to test the intercalation potential of this pyrophosphate phase.
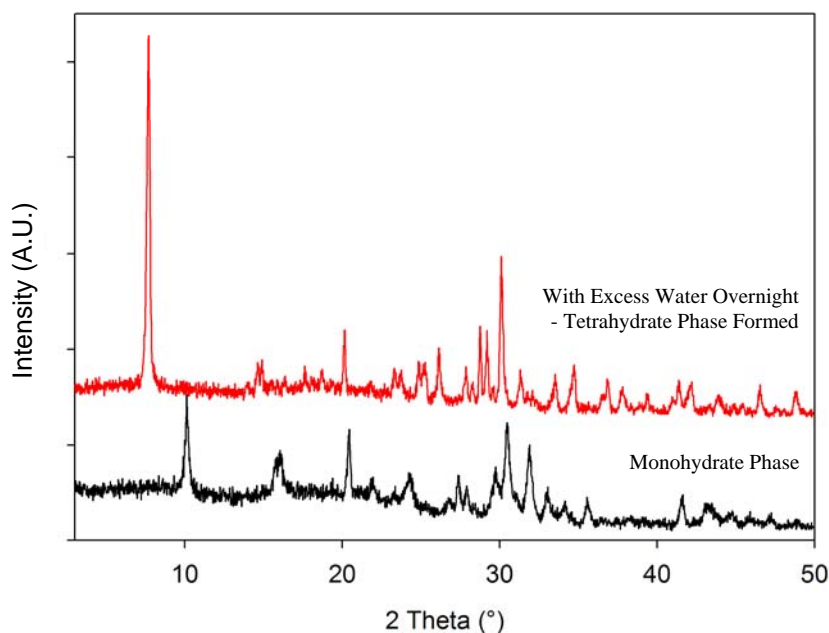
Figure 6.3.4.1: X-ray Diffraction Pattern of Calcium Pyrophosphate Monohydrate after Soaking in Water Overnight.

From the X-ray diffraction analyses of the alcohol, ammonia, acetonitrile and 4,4-bipyridyl (structure in section 6.2.3.1) intercalation experiments, no observed change in the diffraction pattern was seen, even after 10 days in solution, therefore suggesting that intercalation was not successful.

Reflux Intercalation Methods with Calcium Pyrophosphate Tetrahydrate

This set of experiments was performed to test whether more forceful conditions were required to enable intercalation to be successful as all the room temperature experiments showed no change in structure. Unfortunately, no positive changes in the diffraction patterns of all samples tested were observed. When dry methanol was used, the solvent dehydrated the tetrahydrate sample to form the monohydrate analogue. Therefore this procedure was abandoned in favour of a closed solvothermal system to potentially reduce the possibility of the materials dehydrating during the reaction.

Solvothermal Intercalation Experiments in Calcium Pyrophosphate Tetrahydrate

This procedure was used to determine if, under increased temperature and pressure, intercalation of species could be accomplished. In the initial trials with this material, methanol and ethanol were added to the calcium pyrophosphate tetrahydrate phase and heated between 100 and 200°C. In addition to the alcohol species, further samples using amines, ammonia, carboxylic acids and acetonitrile were investigated at 100°C. These experiments were further extended using various intercalating species at different temperatures and concentrations with the results of these experiments listed in tables 6.3.4.1, 6.3.4.2 and 6.3.4.3.

From the results observed in table 6.3.4.1, with the experiments conducted at 100°C, the calcium pyrophosphate tetrahydrate host phase was still present in most of the samples tested except when acetonitrile or branched carboxylic acids were present. At 150 and 200°C, the calcium pyrophosphate tetrahydrate in the presence of ethanol or methanol, dehydrated to form calcium pyrophosphate monohydrate.

Since straight chained carboxylic acids are a similar size to water, an increase in layer spacing of the calcium pyrophosphate phase might not be observed on the X-ray diffraction patterns and therefore a false negative could be recorded. Therefore FTIR spectra were obtained to confirm whether C=O or C-O stretches were observed, which were characteristic of the presence of carboxylic acids in the sample. These were not seen and therefore intercalation of this species had not occurred.

The branched chain acids were tested because of the extra steric effects caused by their shape which should promote an increase in layer spacing if successful intercalation occurred. However, when citric acid was used, (figure 6.3.4.2) the concentrated 0.5M

Figure 6.3.4.2: Chemical Structure of Citric and Oxalic Acids.

solution caused the sample to dissolve. Oxalic acid was attempted next and although this species did not dissolve the calcium phosphate, a side reaction occurred to produce calcium oxalate (CaC_2O_4). This suggested that the high acidity of the oxalic acid must have dissolved the pyrophosphate and precipitated the oxalate form. Therefore these two branched acids were retried at much lower concentrations (0.1M), but once again, the same effects were observed. No further experiments were attempted with these branched chain acid species.

Acetonitrile was tested as it had a high polarity and therefore might exchange with water, however, it lacks hydrogen bonding ability and therefore might not stabilise the structure sufficiently. The powder X-ray diffraction data showed no change had occurred and therefore FTIR analysis was attempted. Unfortunately, no $C\equiv N$ stretch was observed consistent with the intercalation of this species into the structure.

Table 6.3.4.1: Results of Initial Solvent and Temperature Trials for Solvothermal Intercalation in Calcium Pyrophosphate Tetrahydrate.

Mass Used (g)	Solvent and Filling Level	Temperature (°C)	Phase(s) Observed
0.3	Methanol (half fill)	100	Calcium pyrophosphate tetrahydrate
0.3	Methanol (half fill)	150	Calcium pyrophosphate monohydrate
0.3	Methanol (half fill)	200	Calcium pyrophosphate monohydrate
0.3	Ethanol (half fill)	100	Calcium pyrophosphate tetrahydrate
0.3	Ethanol (half fill)	150	Calcium pyrophosphate monohydrate
0.3	Ethanol (half fill)	200	Calcium pyrophosphate monohydrate
0.3	Propylamine (half fill)	100	Calcium pyrophosphate tetrahydrate
0.3	Butylamine (half fill)	100	Calcium pyrophosphate tetrahydrate
0.3	Dipropylamine (half fill)	100	Calcium pyrophosphate tetrahydrate
0.3	Acetonitrile (half fill)	100	Both calcium pyrophosphate tetrahydrate and monohydrate
0.3	35% Ammonia solution in water (half fill)	100	Calcium pyrophosphate tetrahydrate
0.3	2M Ammonia/ethanol (half fill)	100	Calcium pyrophosphate tetrahydrate
0.3	Ethanoic acid (half fill)	100	Calcium pyrophosphate tetrahydrate
0.3	Propanoic acid (half fill)	100	Calcium pyrophosphate tetrahydrate
0.3	Oxalic acid ($C_2O_4H_2$) 0.5M in water (half fill)	100	Calcium oxalate
0.3	Citric acid ($C_4O_7H_4$) 0.5M in water (half fill)	100	Sample dissolved

Based upon some of the observations from the experiments shown in table 6.3.4.1, an extended range of sample concentrations and reaction temperatures were tested to determine whether these would affect the outcome of the calcium pyrophosphate phase produced. The results for these additional experiments are shown in table 6.3.4.2.

When pure or diluted monoamines solutions were used at 100°C - 150°C, the only change observed in the samples was a partial dehydration of the host phase to give a mixed tetrahydrate and monohydrate product. At higher temperatures than 150°C, the use of diluted or pure amine was sufficient to cause the host phase to decompose to hydroxyapatite.

This decomposition was also observed when water was used to half fill the hydrothermal bomb and heated to 150°C. A poorly crystalline apatite phase was formed due to the slow decomposition of the calcium pyrophosphate phase to hydroxyapatite, $Ca_{10}(PO_4)_6(OH)_2$.

Table 6.3.4.2: Results of Solvothermal Intercalation Reactions in Calcium Pyrophosphate **Tetrahydrate** Using a Range of Solvents, Concentrations and Temperatures

Intercalating Species	Solvent	Concentration	Temperature (°C)	Approx. Filling Level (%)	Calcium Pyrophosphate Phase Observed
Ethylamine	Water	70%	100	50	Tetrahydrate
Propylamine	Ethanol	0.5M	100	50	Mixed tetrahydrate and monohydrate
Butylamine	Ethanol	0.5M	100	50	Tetrahydrate
Butylamine	Ethanol	0.5M	150	50	Mixed tetrahydrate and monohydrate
Propylamine	Water	0.5M	100	50	Mixed tetrahydrate and monohydrate
Butylamine	Water	0.5M	100	50	Mixed tetrahydrate and monohydrate
Butylamine	Pure	99%	150	50	Monohydrate
Butylamine	Water	0.2M	175	50	Decomposed to hydroxyapatite
Butylamine	Water	0.2M	200	50	Decomposed to hydroxyapatite
Butylamine	Pure	99%	150	50	Monohydrate
Ammonia	Ethanol	2M	150	50	Calcium pyrophosphate monohydrate
Ammonium hydroxide	Pure	97%	150	50	Calcium pyrophosphate monohydrate
Water	Pure	-	100	50	Decomposed to hydroxyapatite

Finally, ammonia solutions were attempted using either water or ethanol as the main solvent with heating stages at 100 and 150°C. When 100°C was used, the host tetrahydrate phase remained intact with no form of intercalation or noticeable degradation. However, when

the temperature was increased to 150°C, the monohydrate phase was again observed with no intercalation.

Above 150°C, a decomposition of the calcium pyrophosphate material was observed, which under alkaline or neutral pH conditions would form a poorly crystalline hydroxyapatite phase. As this observation was based on a limited number of samples, more results were assessed to determine whether temperature was the sole cause of the decomposition.

Solvothermal Intercalation Experiments in Calcium Pyrophosphate Monohydrate

Based upon the results obtained from the tetrahydrate form, shown in table 6.3.4.2, it was decided to replace this tetrahydrate phase with the monohydrate analogue and use the same intercalating species. These experiments were carried out to confirm whether the solvent or the temperature was responsible for the determination of the calcium pyrophosphate phase produced. The results for these experiments are shown in table 6.3.4.3.

From these results, it was clear that the temperature of the solvothermal reaction was responsible for the outcome of the sample phase produced. When 100 - 150°C temperatures were used, the calcium pyrophosphate monohydrate starting phase was still observed. The one exception to this rule occurred when water was the solvent. In this case, a poorly crystalline hydroxyapatite phase was formed, as observed in the experiments using calcium pyrophosphate tetrahydrate. The results are shown in table 6.3.4.2.

When the calcium pyrophosphate monohydrate phase was heated to 200°C in methanol or ethanol, degradation of the material occurred to form monetite ($CaHPO_4$). The X-ray diffraction pattern for this phase can be seen in figure 6.3.4.3. The solvents are known to be slightly acidic and therefore an altered decomposition product was formed due to the different pH. When the alkaline butylamine species was present at this temperature, poorly crystalline hydroxyapatite was formed.

Table 6.3.4.3: Results of Solvothermal Intercalation Reactions in Calcium Pyrophosphate **Monohydrate** Using a Range of Solvents, Concentrations and Temperatures

Intercalating Species	Solvent	Conc.	Temperature (°C)	Approx. Filling Level (%)	Calcium Pyrophosphate Phase Observed
Methanol	Pure (dry)	98%	100	50	Monohydrate
Ethanol	Pure (dry)	99%	100	50	Monohydrate
Methanol	Pure (dry)	98%	150	50	Monohydrate
Ethanol	Pure (dry)	99%	150	50	Monohydrate
Methanol	Pure (dry)	98%	200	50	Decomposed
Ethanol	Pure (dry)	99%	200	50	Decomposed
Ethylamine	Water	70%	100	50	Monohydrate
Butylamine	Ethanol	0.5M	100	50	Monohydrate
Ammonia	Ethanol	2M	150	50	Monohydrate
Ammonium Hydroxide	Pure	97%	150	50	Monohydrate
Water	Pure	-	150	50	Decomposed
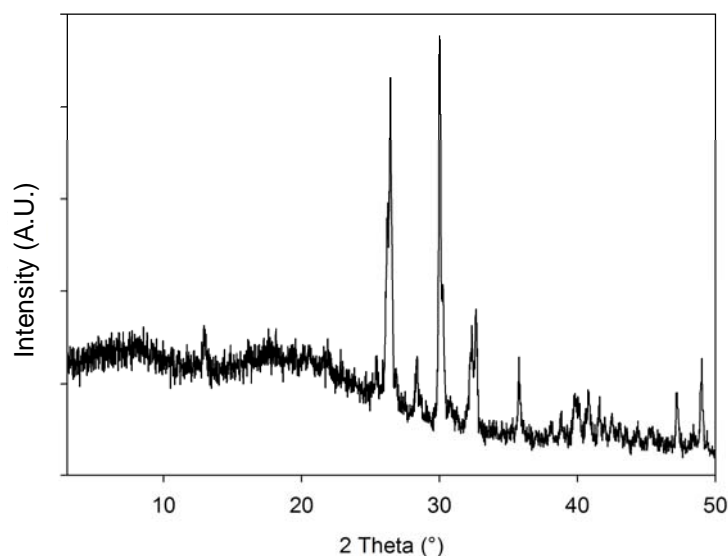
Figure 6.3.4.3: X-ray Diffraction Pattern of Calcium Pyrophosphate Tetrahydrate Dehydrated at 110°C then Solvothermally Heated in Ethanol at 200°C to Form Monetite.

Since all reactions conducted with this calcium pyrophosphate monohydrate phase had either decomposed or shown no positive reaction to the intercalating species present, these experiments were not pursued any further.

Melt Occlusion Experiments with Calcium Pyrophosphate Tetrahydrate

It is possible that only neutral compounds can be inserted between the layers of the calcium pyrophosphate tetrahydrate structure. Research conducted on zeolite framework structures,[27,28] have shown that salt occlusion is possible (where cations and anions are introduced simultaneously) thus maintaining charge balance.

Reactions were undertaken where calcium pyrophosphate tetrahydrate was heated with a large excess of a salt (such as lithium, sodium or magnesium nitrate, see table 6.2.3.4). Following this, samples were analysed by powder X-ray diffraction. Samples were washed prior to analysis as the presence of the added salt would otherwise dominate the pattern and mask any changes to the calcium pyrophosphate tetrahydrate structure. However, the problem with this washing procedure was the possibility that the water might also remove some of the occluded material from between the layers of the pyrophosphate. In all the washed samples, no change in the diffraction patterns was observed. Therefore this suggested that the pyrophosphate phase had not occluded any material, as some of these occluded ions should still have been present in the interlayer, even after the washing procedure.

6.3.5 Exfoliation Attempts with Calcium Pyrophosphate Tetrahydrate

From an examination of the structure of the calcium pyrophosphate tetrahydrate, it was believed that a separation the layers could be achieved by disrupting the hydrogen bonding of the water molecules in between each calcium pyrophosphate layer. If the apparent weak bonding between the calcium pyrophosphate layers could be disrupted then individual calcium pyrophosphate layers could be separated. Therefore, a bulky tetrabutylammonium salt [TBA] was used which was water soluble and from its size, it should fit in the interlayer region. This should cause sufficient expansion of the layers so that the forces holding these together are too weak to stabilise the 3-dimensional layered structure.

The exfoliating solutions were prepared using TBA bromide or TBA hydroxide, with either ethanol or deionised water as the solvent for each TBA species. The calcium pyrophosphate was added to a small quantity of solvent and left for two hours before the TBA solutions were added. These were then left for up to 6 days with periodic sampling and were analysed by powder X-ray diffraction. No observable changes to the structure were noted in all samples and therefore exfoliation using this TBA species was not successful.

Interestingly, the pyrophosphate material displayed a noticeable expansion in its bulk when water was initially added. This was encouraging as it is a property of clay-like materials which readily exfoliate. Therefore the material was placed in an ultrasonic waterbath for 30 minute to agitate the layers further and potentially exfoliate the material. Following this procedure, the material was dried in air at room temperature and powder X-ray diffraction indicated that only the original calcium pyrophosphate tetrahydrate host phase was present.

Attempts to intercalate 1,6-diaminohexane and then use non-polar solvents to exfoliate this layered material were not successful as the initial intercalation step could not be achieved.

In summary, it appears that the calcium pyrophosphate tetrahydrate phase is very stable as a 3-dimensional layered material and exfoliation has not been achieved. This is somewhat surprising given its structure but it is likely that the presence of water molecules directly coordinated to the calcium ions in some way prevent separation of the layer prior to complete disruption of the layers.

6.3.6 The Synthesis of Calcium Disodium Pyrophosphate

The calcium disodium pyrophosphate tetrahydrate phase represents another example of a layered pyrophosphate. This material contains water molecules and sodium ions in apparently easily accessible positions. These features of the pyrophosphate material were of interest for this research with the potential for layer expansion by the replacement of either some of the sodium ions or water molecules and therefore this material was investigated.

A range of different concentrations of calcium chloride solutions were tested to determine the optimum conditions for the synthesis of calcium disodium pyrophosphate tetrahydrate. Table 6.3.6.1 shows the results of the different concentrations and whether the desired phase was formed.

Table 6.3.6.1: Effect of Differing Concentrations of Calcium Chloride on the Product Formed

Concentration Calcium chloride ($moldm^{-3}$)	Mass of calcium chloride required for 25 cm^3 soln. (g)	Solid Product Formed
<0.025	<0.0687	None – colourless solution
0.04	0.110	Unknown white precipitate
0.05 - 0.075	0.1375 - 0.2063	Calcium disodium pyrophosphate formed
>0.1	>0.2750	Amorphous phase

From the results shown in table 6.3.6.1, the optimum solution concentrations were a 0.05M calcium chloride with 0.1M sodium pyrophosphate, as expected for the stoichiometry $CaNa_2P_2O_7 \cdot 4H_2O$. The 0.1M sodium pyrophosphate solution concentration was chosen due to the balance between dissolution time and solution volumes. The crystalline sodium pyrophosphate could take ~ 15 minutes to dissolve and a large sample yield could be achieved with a 250 cm^3 solution volume.

When a 0.1M $CaCl_2$ solution was used with the 0.1M sodium pyrophosphate, an amorphous white solid was produced. Observations using light microscopes revealed a more

rounded particle for this amorphous phase compared with shiny plate-like crystallites of the calcium disodium pyrophosphate phase. This morphology is typical of amorphous phases.

From the structural representation[19] of calcium disodium pyrophosphate tetrahydrate shown in figure 6.3.6.1, the layered nature of the material is evident, with the sodium ions in apparently easily accessible positions. The structure of this material was confirmed by indexing the experimental X-ray diffraction data (figure 6.3.6.2) from the samples using *CELL*[17] with a known reference sample[16] from the ICSD[20,21] crystal structure database. The unit cell data was refined and listed in table 6.3.6.2 with the full data presented in Appendix 5. The close agreement of these values together with a low R factor proved that the experimental structure was consistent with the reference phase.
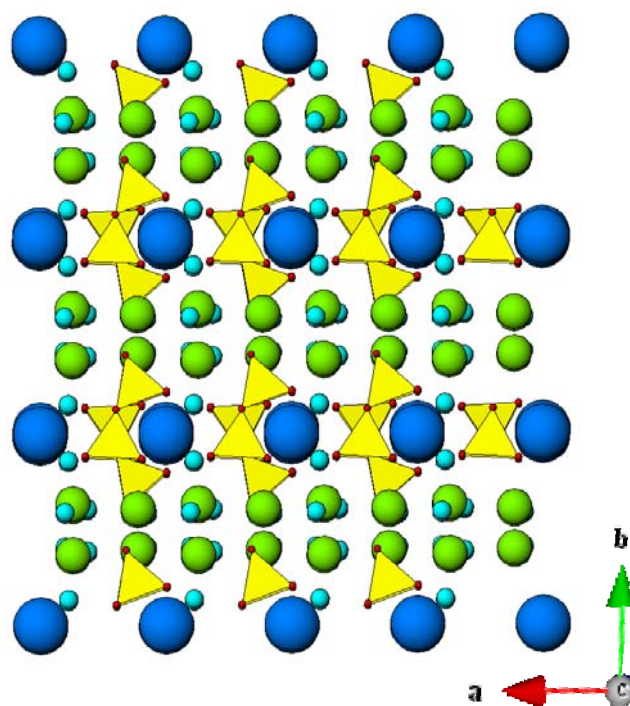
Figure 6.3.6.1: Structural Representation of Calcium Disodium Pyrophosphate. (Dark blue = calcium ions; green = sodium; yellow polyhedra = phosphate; light blue = water)

The position of the sodium ions in this structure, situated almost in the interlayer region of this layered material (green ions in figure 6.3.6.1), suggested that they might be

more accessible for exchange. Replacement of some of the sodium ions in the structure by larger monovalent cations would enable expansion of the layers of this material. This potential exchange ability was the main reason for the experimentation with this phase. Further details on the ion exchange can be found in section 6.3.8. The expansion of the layers could aid the potential exfoliation of the material, if an exfoliating species was used at a later stage.

Table 6.3.6.2: Indexed Unit Cell Parameters for Calcium Disodium Pyrophosphate Tetrahydrate
(Space group=Pc)

Unit Cell Parameters	Values	Reference Values[16]
a (Å)	5.69(1)	5.673
b (Å)	8.45(1)	8.480
c (Å)	10.56(2)	10.529
α (°)	90	90
β (°)	106.10(7)	106.100
γ (°)	90	90
R Factor = 0.00000070		
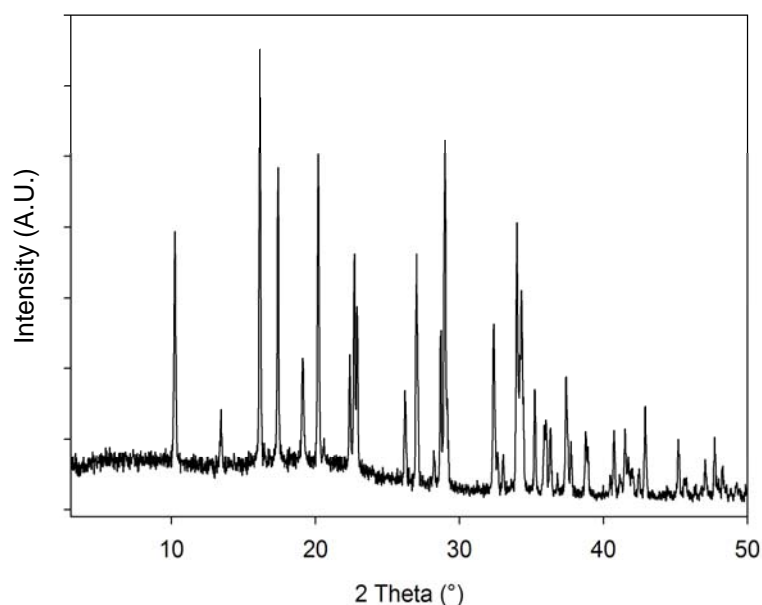
Figure 6.3.6.2: X-ray Diffraction Pattern of Calcium Disodium Pyrophosphate.

6.3.7 Thermogravimetric Analysis of Calcium Disodium Pyrophosphate Tetrahydrate

Thermogravimetric analysis confirmed the stoichiometry of this phase as $CaNa_2P_2O_7 \cdot 4H_2O$. The water molecules were lost from the sample in two distinct steps. The first at ~ 40°C and the second at ~ 100°C, as seen in figure 6.3.7.1. The two 'bumps' that were observed on the graph between 20 and 40 minutes were artefacts of the instrument and did not relate to any mass or energy changes from the sample itself. The sample mass of the material was confirmed to stabilise around 450°C thus indicating the removal of all the water. From the mass losses observed, the water content was calculated at ~ 3.5 moles, therefore close to the expected value for the tetrahydrate form.
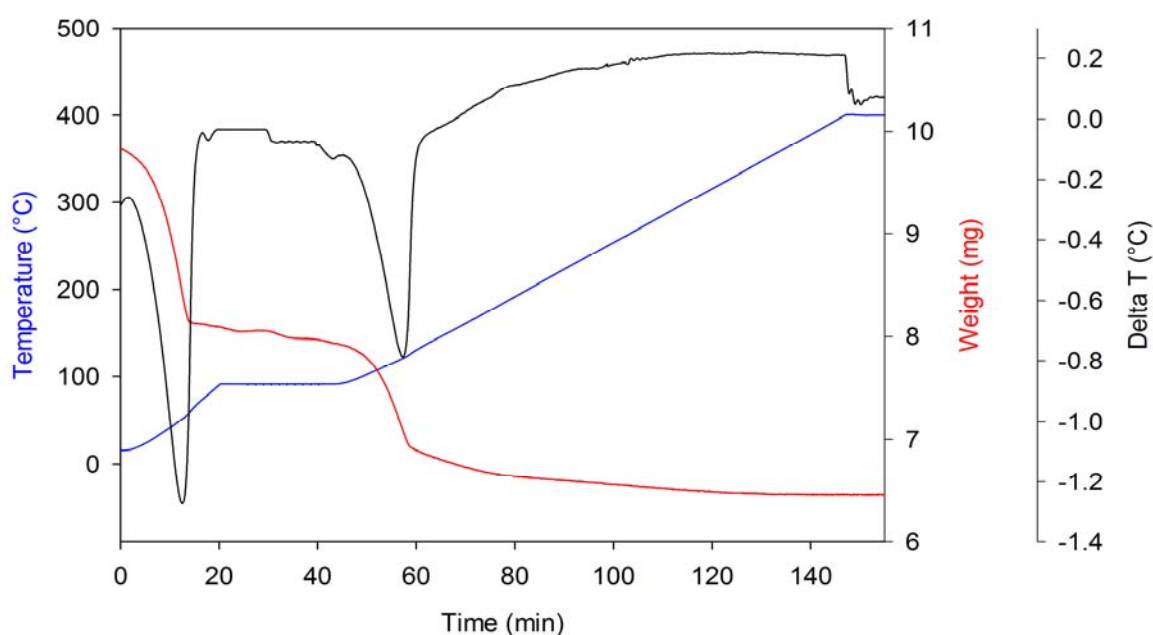
Figure 6.3.7.1: Thermogravimetric Analysis of Calcium Disodium Pyrophosphate Tetrahydrate.

6.3.8 Ion/Proton Exchange, Amine Intercalation and Attempted Exfoliation of Calcium Disodium Pyrophosphate

The room temperature ion exchange reactions proved unsuccessful in exchanging any of the sodium ions from the structure. This observation suggested that the sodium ions were

held more strongly in the structure than anticipated. Therefore more forceful conditions were trialled to determine whether ion exchange would be possible in this material.

Reflux reactions with potassium nitrate solution proved to be very successful in exchanging the sodium ions with potassium to form a calcium dipotassium pyrophosphate phase ($CaK_2P_2O_7$). It was determined from a series of different reflux times that 2 hours was required to enable full exchange to the calcium dipotassium pyrophosphate phase. A longer time period also proved successful in exchanging sodium for potassium ions but it also increased the risk of hydrolysis of the pyrophosphate and degradation of the material.

From the structural representation shown in figure 6.3.8.1 for the calcium dipotassium pyrophosphate phase, it can be observed that a complete structural rearrangement had occurred from the layered phase $CaNa_2P_2O_7 \cdot 4H_2O$ (where each pyrophosphate unit links to 3 calcium ions, (figure 6.3.6.1)) to a 3-dimensional $CaK_2P_2O_7$ phase (where each pyrophosphate unit links to 6 calcium ions (figure 6.3.8.1)).

The X-ray diffraction pattern for this material was compared to the ICSD[20,21] crystal structure database. Indexing of the unit cells using *CELL*[17] of both the experimental and reference data[29] from the ICSD database gave similar values with a low R factor (error approximation). This confirmed the structural representation[19] shown in figure 6.3.8.1 to be a close approximation to the actual structure. The unit cell data was refined and listed in table 6.3.8.1 with the full data presented in Appendix 6.

The preparation of this phase using the reported method[29] involves a high temperature (> 1300°C) melt using potassium carbonate and calcium polyphosphate. Therefore the method described in this thesis represents a much lower temperature alternative to synthesise this material.

Table 6.3.8.1: Indexed Unit Cell Parameters for Calcium Dipotassium Pyrophosphate (Space group = P2$_1$/n)

Unit Cell Parameters	Values	Reference Values[29]
a (Å)	9.84(2)	9.818
b (Å)	5.69(1)	5.676
c (Å)	13.03(2)	13.006
α (°)	90	90
β (°)	104.21(5)	104.220
γ (°)	90	90
R Factor = 0.00000067		
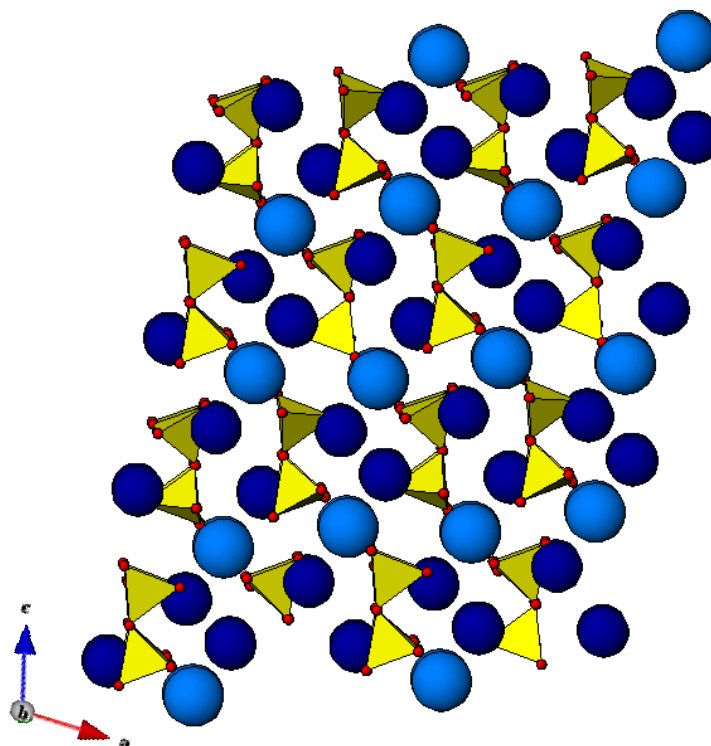
Figure 6.3.8.1: Structural Representation of Calcium Dipotassium Pyrophosphate. (Light blue = calcium ions; dark blue = potassium; yellow polyhedra = phosphate)

As this research has focussed upon layered materials and as the structure of this dipotassium phase is clearly 3-dimensional, no further reactions were carried out on this phase.

Proton Exchange in Calcium Disodium Pyrophosphate

Previous success with intercalation experiments with MCPM, which contained accessible protons, prompted a series of experiments to modify calcium disodium pyrophosphate by replacing the sodium ions with protons. If successful, this would potentially provide a layered polymorph of the calcium acid pyrophosphate phase ($CaH_2P_2O_7$) which contrasts with most of the polymorphs of this structure being 3-dimensional. The earlier results in this section indicated that the sodium ions in the structure were shown to have been exchangeable with potassium and therefore the exchange with protons should have been feasible. A proton exchange method previously successful with layered alkali metal titanates (such as $Na_2Ti_3O_7$)[13] was attempted. Table 6.3.8.2 summarises the results of using various acids at different concentrations and whether proton exchange was possible in the calcium disodium pyrophosphate structure.

Table 6.3.8.2: Results Summary of Calcium Disodium Pyrophosphate Acid Modification

Acid Used	Concentration (mol dm^{-3})	Effect on $CaNa_2P_2O_7 \cdot 4H_2O$
Hydrochloric acid	1	Dissolved
Hydrochloric acid	0.5	Dissolved
Hydrochloric acid	0.25	Mostly dissolved
Hydrochloric acid	0.1	Decomposed to unknown phase
Hydrochloric acid	0.05	Decomposed to unknown phase
Hydrochloric acid	0.025	Decomposed to unknown phase
Hydrochloric acid	0.01	Unknown and host phases
Hydrochloric acid	0.005	Unknown and host phases
Hydrochloric acid	0.0025	Unknown and host phases
Ethanoic acid	1	Modified
Ethanoic acid	0.5	Modified
Ethanoic acid	0.25	Modified
Ethanoic acid	0.1	Modified
Propanoic acid	1	Modified
Propanoic acid	0.5	Modified

The 1M to 0.25M hydrochloric acid concentrations caused the calcium sodium pyrophosphate phase to dissolve, even at room temperature. Thus layered titanates demonstrate more resistant to the hydrolysis effects of strong acids compared to the pyrophosphate layers.

A less concentrated acid solution was attempted using 0.1M hydrochloric acid and the sample was still present after the 2 hours reaction time. Analysis of the X-ray diffraction pattern for this material (figure 6.3.8.2, red pattern) showed that the host material was still present without any peak shifting, thus it was unlikely that proton exchange had occurred. In addition to the host pattern, the appearance of another unknown phase was observed with a larger d-spacing of 11.6 Å. The same unknown phase was also observed in the samples prepared with the 0.05, 0.025 and 0.01M hydrochloric acid solutions.

Two very dilute hydrochloric acid solutions (0.005M and 0.0025M) were attempted to protonate the pyrophosphate samples potentially without forming this unknown phase. Thus a longer reaction time of 8 hours was used (due to the weak solution concentration). However, the same phase change to the unknown material was still observed.

A separate experiment was performed using hydrochloric acid that had been buffered to pH 4 using sodium hydroxide solution. No observable change in structure was seen for this phase when the X-ray diffraction patterns were analysed after 2, 4 and 6 hours in solution. This was further proof that the phase was reasonably stable but would not easily proton exchange, even though there were many protons in solution. Attempts to use reflux methods to proton exchange caused the calcium disodium pyrophosphate phase to dissolve. This suggested that the sodium ions were not readily exchangeable in the structure.
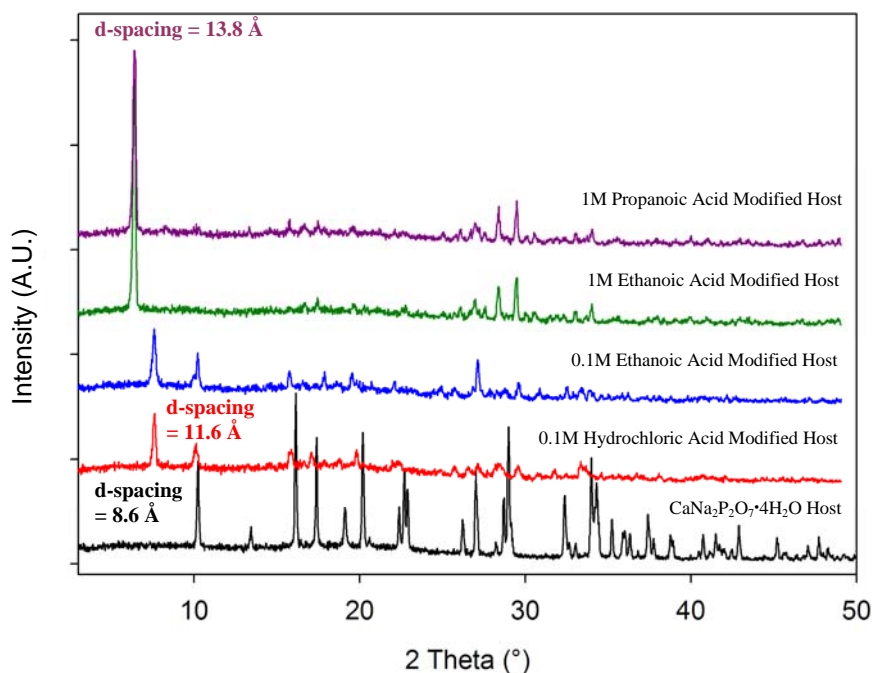
Figure 6.3.8.2: X-ray Diffraction Pattern Showing the Phases Formed When Different Concentrations of Mineral and Organic Acids were Added to Calcium Disodium Pyrophosphate.

An extension to this line of research was conducted using organic acids such as ethanoic and propanoic acid solutions instead of mineral acids. This procedure was used to confirm whether the use of weaker organic acids (pKa = 4.7 to 4.8 c.f. HCl pKa = -8.0) at similar or stronger concentrations would allow proton exchange in this pyrophosphate phase. The resulting diffraction data from these experiments are also shown in figure 6.3.8.2 (green and purple lines). From this figure, it was apparent that a further change in structure had occurred with the addition of ethanoic or propanoic acid with no host peaks remaining. This new phase could not be identified on the JCPDS[30] X-ray database and possessed a greatly increased d-spacing (13.8 Å) compared to the host phase (8.6 Å). Thus more analyses were performed on this phase in order to attempt to identify this unknown phase. A further experiment using a weaker 0.1M ethanoic acid solution on the host phase caused only a

partial phase change with some host material remaining as can be observed in figure 6.3.8.2 (blue line).

The structure of the propanoic acid phase was found to be identical to the ethanoic acid phase. Intercalation of the acid into the layered structure was unlikely to have occurred; otherwise a larger interlayer spacing for the propanoic phase (smaller diffraction angle) would have been expected, due to the longer carbon chain length. This phase was therefore checked against the JCPDS powder X-ray diffraction database[30] and no known pyrophosphate or orthophosphate phases could be matched to this particular phase.

Due to the unusual results obtained with the organic acids, further experiments were conducted which took the acid modified calcium disodium pyrophosphate and exposed these samples to either a base, namely butylamine or water. This treatment caused a further structural change to the sample, producing yet another unknown phase. With both the butylamine and water exposed samples, a first peak shift to higher 2θ diffraction angle compared to the acid modified phase was observed. The majority of the diffraction peaks were still due to the acid modified phase being present as can be seen on figure 6.3.8.3. The sample exposed to water still contained some of the original acid modified phase as well as this new phase. This suggested that a partial reaction had occurred. The change in structure for the acid modified phase with butylamine could not be rationalised from powder X-ray diffraction alone and therefore further analysis using TGA, microscopy and FTIR was performed.
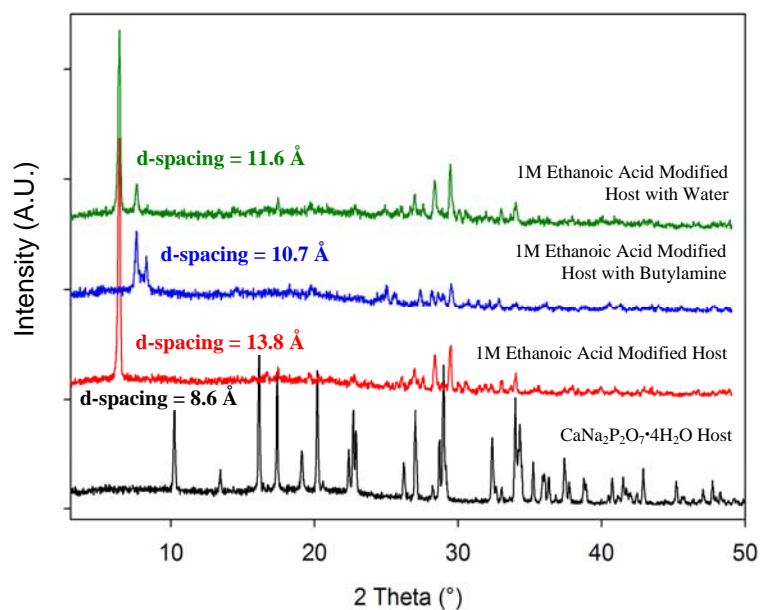
Figure 6.3.8.3: X-ray Diffraction Pattern Comparison of Experiments with Ethanoic Acid Modified Calcium Disodium Pyrophosphate.

Thermogravimetric analysis showed a minor difference when the host phase was compared to the acid modified phase and the acid modified samples treated with butylamine or water. The DTA trace of the TGA analysis for all four samples was identical to the host phase (figure 6.3.7.1), as only two endothermic troughs at 40°C and 100°C were observed. Since no further energy changes were observed at temperatures above 100°C, it could be assumed from this analysis that only water was being lost from these four samples.

From this analysis, the acid modified phase possessed a higher water content of 3.8 moles (c.f. 3.5 in the host phase) with the further modified phases using butylamine or water possessing 2.8 moles of water. This difference in water content was not sufficient to explain the increase in the d-spacing of ~5.2 Å, evident from the X-ray diffraction patterns in figure 6.3.8.3. Therefore further analysis needs to be performed.

The four samples shown on figure 6.3.8.3 were examined under an optical microscope. The host material contained many spherical particles with very few shiny

crystallites present. The addition of acid to the host phase showed a remarkable change in the appearance of the sample. The particles were less spherical in appearance with many needle-like crystallites present and a more crystalline lustre to the sample. When either butylamine or water was added to the acid modified sample, there was a further increase in the number of needles present and the entire sample seemed to be composed of small needle crystals. This observation suggested that there was an alteration to the pyrophosphate phase when acid was added, and then another modification when butylamine or water was used on this acid modified phase. From the microscopy examination, it was not clear whether there were one or two phases present in the samples produced after the reaction with water or butylamine as the sample contained a mass of tiny crystals. Single crystal X-ray diffraction was sought for these materials; however, the crystals were too small to enable this analysis to be performed.

FTIR analysis of the acid modified phase, the acid modified material with butylamine or water and the host calcium disodium pyrophosphate phase was performed to clarify if there was any difference between the modified and host materials (see figure 6.3.8.4). The FTIR analysis of the acid modified host with butylamine or water was identical and therefore only one of these two analyses are shown on figure 6.3.8.4.

There were some minor differences in the stretching frequency in the phosphate region of the IR spectra (1200 – 1000 cm^{-1}). The stretches occurred at a slightly higher frequency with the modified phases compared to the host. There was the presence of a very broad O-H stretch around 3200 cm^{-1} in all three samples which was likely to be from the presence of water in the structure. This stretch would also have been seen if ethanoic acid was present in the sample due to the acidic carboxylate group. However, no carbonyl stretch was observed in the sample between 1850 and 1750 cm^{-1} which indicated that ethanoic acid or its carboxylate

derivative was not present in the material. As no acid was present on the surface or in the structure of the material it was concluded that the O-H stretch must have been due to water in the structure. A comparison of the butylamine treated acid modified pyrophosphate phase with the acid modified host phase possessed identical stretching frequencies. This suggested that no modifications or extra functional groups were present in the sample after butylamine was added.

In summary, the FTIR analysis of all three phases showed no additional functional groups were present in the calcium disodium pyrophosphate phase when either organic acids, amines or water were used on the host structure or its acid modified analogue. Therefore any changes evident from the powder X-ray diffraction patterns after the treatments must have been due to either a structural rearrangement or changes in the water content of the host phase.
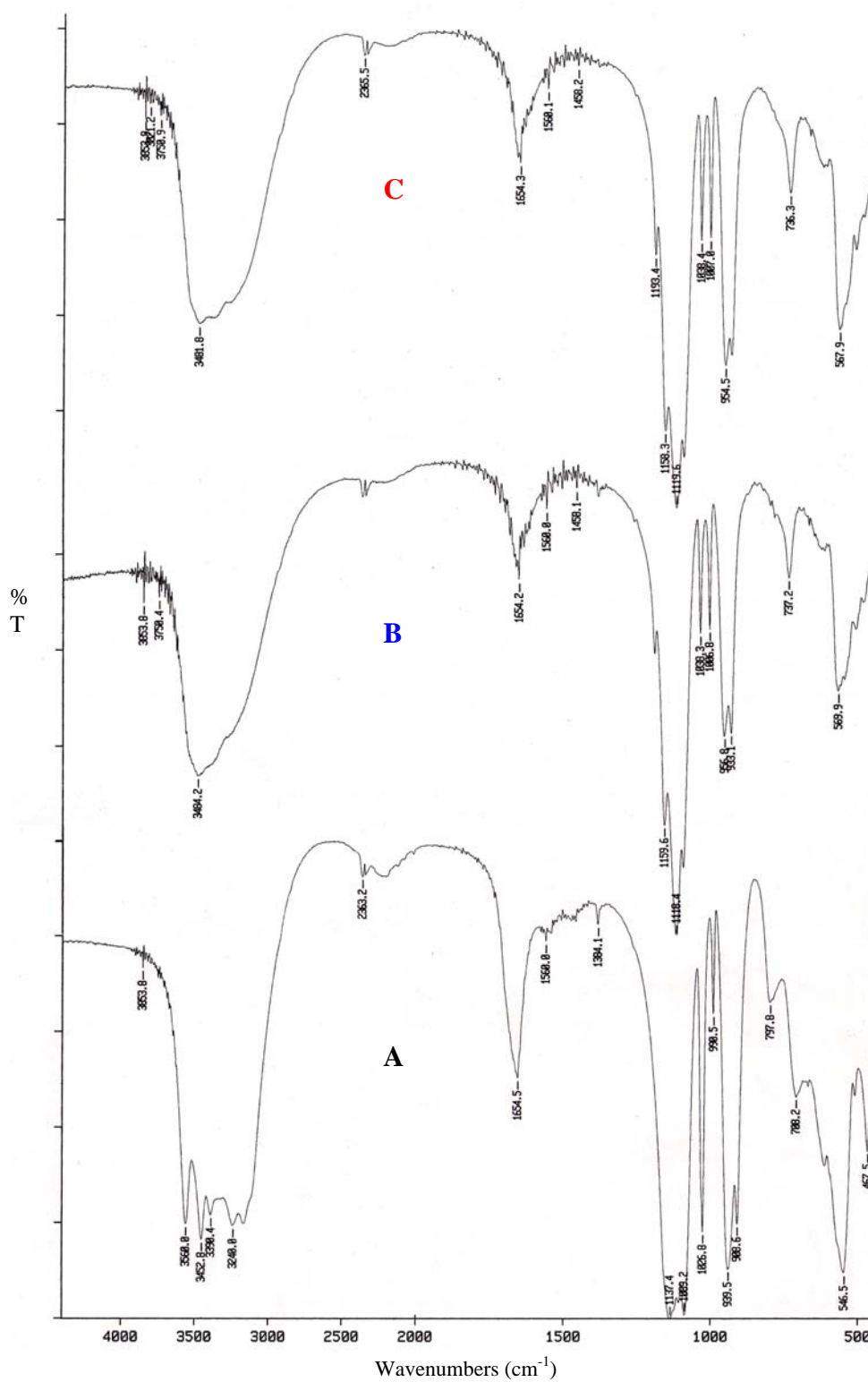
Figure 6.3.8.4: FTIR Analysis of Calcium Disodium Pyrophosphate Host Material and Acid Modified Phases (C= Ethanoic Acid Modified Phase with Butylamine; B = Ethanoic Acid Modified Phase; A= Host Phase).

Amine Intercalation in Calcium Disodium Pyrophosphate (Pure and Acid Modified Phases)

The pure monoamines propylamine, butylamine and hexylamine were initially added to the calcium disodium pyrophosphate host phase and the resulting samples were left for 2 days, with occasional stirring. When the samples were analysed using powder X-ray diffraction, no reaction had occurred.

When the acid modified version of calcium disodium pyrophosphate was used, the intercalation was attempted with the same three amines. Two days were initially allotted as a sufficient reaction time. Analysis revealed that no reaction had occurred, therefore a longer time period of 4 days was also attempted. The powder X-ray diffraction patterns for the longer reaction time samples showed that a change to the structure had occurred.

FTIR analysis showed that no organic acid was present in this acid modified phase but from the XRD analysis, the addition of excess amine to this phase did have some effect upon the structure. Only the first peak in the three X-ray diffraction patterns had shifted to higher 2θ diffraction angle, with the remainder of the pattern matching the acid modified phase. FTIR showed that no N-H amine stretches were observed and therefore no amine was actually present in the structure. This was suggestive of a partial dehydration of the phase rather than intercalation since only the first peak in the diffraction patterns had shifted.

Exfoliation Attempts in Calcium Disodium Pyrophosphate

Attempts to exfoliate the host and acid modified pyrophosphate phases using the standard exfoliating species TBA-Br and TBA-OH have proved unsuccessful. In addition, the use of a surfactant based exfoliant such as tetradecyltrimethyl ammonium bromide also had little effect on the acid modified calcium disodium pyrophosphate structure. The only observable difference after the reaction was a shift in the first diffraction peak to a higher 2θ.

This effect was also observed with the addition of amine to this acid modified phase and therefore further confirmed the earlier suggestion that a partial dehydration of the phase could have occurred.

6.3.9 The Synthesis of Calcium Acid Pyrophosphate

The acid flux method used to produce the calcium acid pyrophosphate phase formed a single phase product and the X-ray diffraction pattern for this phase can be seen in figure 6.3.10.1.

Larger batches could be produced by this method using more than 6g of reagents; however, the crucible used to mix the components may need to be cooled. This was due to the large exothermic reaction causing some of the fine calcium hydroxide powder to be expelled as the sample steamed. Slow addition could avoid this problem but might cause other issues with the stoichiometry during the mixing process. It would be difficult to add both the calcium hydroxide powder and orthophosphoric acid reagents together in the correct ratios at the same time.

An alternative method was trialled to produce the calcium acid pyrophosphate which involved the direct heating of MCPM to 225°C. However, an impure phase was produced containing the desired phase together with an additional unidentifiable calcium phosphate phase.

6.3.10 Attempted Intercalation in Calcium Acid Pyrophosphate

The intercalation reaction of this particular phase with butylamine and hexylamine produced a low angle diffraction peak when the samples were analysed by powder X-ray diffraction. This peak moved to lower angle when the alkyl chain length of the amine was increased. However, no host peak shifts occurred which would have been expected had the

amine penetrated through the crystal structure. This suggested that the amine was reacting with the surface of the host material to form a new phase.

A complete set of amine intercalations were therefore performed, with a much greater reaction time, to determine whether this would have an effect upon the extent of the reaction of the amine with the host structure. The X-ray diffraction patterns produced for the acid pyrophosphate samples after exposure to the amine solutions possessed low angle peaks (Figure 6.3.10.1) which shifted to lower 2θ as the amine chain length was increased. However, the X-ray diffraction peaks consistent with the acid pyrophosphate host phase remained in exactly the same position without any shift. This would not have been expected had intercalation occurred. Therefore it was concluded that either a surface reaction or a dissolution/re-precipitation mechanism had occurred when the amine solution was present. This enabled the formation of a new phase with some of the host calcium acid pyrophosphate still present.

First Peak d-Spacings
Host Phase = 5.0 Å
Propylamine = 14.2 Å
Butylamine = 16.5 Å
Hexylamine = 20.7 Å
Octylamine = 25.1 Å
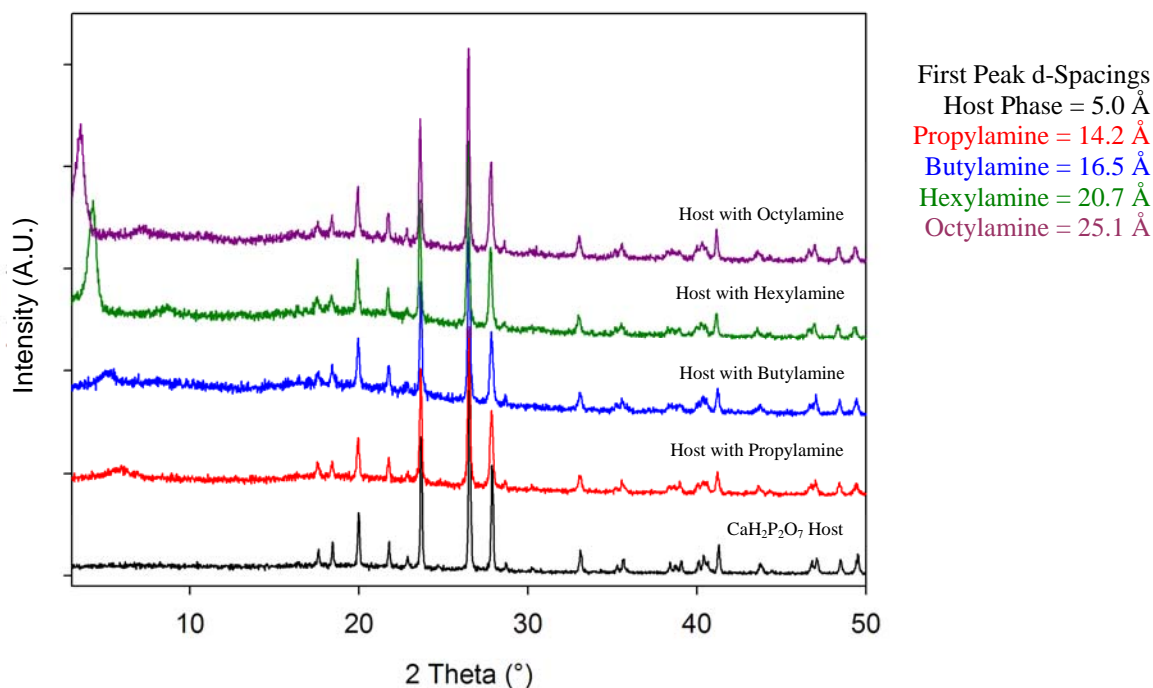
Figure 6.3.10.1: X-ray Diffraction Patterns of Calcium Acid Pyrophosphate with Monoamines.

The size of the low angle peak, especially with the larger chained amine species, could suggest that a significant proportion of the sample had converted to this new phase. A known amount of a reference material (such as zirconium or silicon oxide) should be added to the sample to compare peak heights and therefore estimate the conversion to this new phase.

The X-ray diffraction analysis does not give a clear indication of what is happening when amine was added to this phase and the crystals are too small for single crystal X-ray diffraction analysis. Therefore, further analytical techniques such as FTIR, TGA and SEM therefore need be sought to give more information on this material.

Amino Acid Intercalation and the Effect of Water

The main aim of this section of experiments was to test whether amino acids, initially used in Chapter 4, would react with this calcium acid pyrophosphate phase. As mentioned in Chapter 4, the amino acids would only dissolve in water. Therefore the calcium acid pyrophosphate was tested in water to confirm that this phase was stable in this medium. A change in structure was observed when this phase was added to water, as seen from the powder X-ray diffraction pattern shown in figure 6.3.10.2. This new phase could not be identified to any known calcium phosphate phase.

This water control experiment was used therefore as a comparison in all the amino acid reactions conducted in this section. In all these reactions, a change in structure of the calcium acid pyrophosphate phase was observed after 1 day in solution. However, this change in structure was identical to the water control reaction and therefore the host structure was only reacting with the water in the amino acid solutions. Although the amino acid solutions possessed different pH values, the same phase was formed in all cases whether the solution was mildly acidic or alkaline.
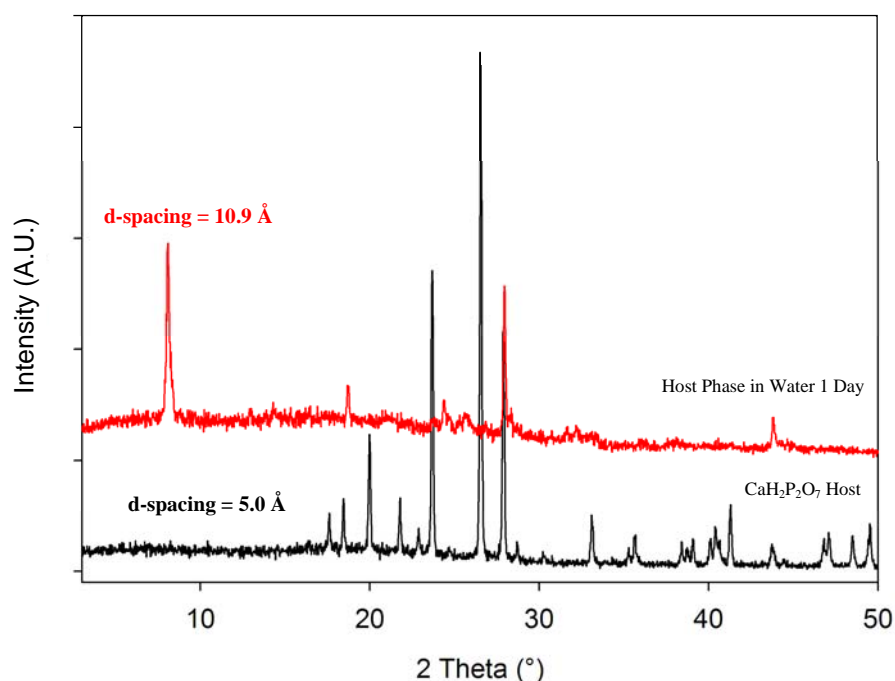
Figure 6.3.10.2: X-ray Diffraction Patterns of Calcium Acid Pyrophosphate in Water.

This phase change in water was not expected and the new phase that was formed had a much larger d-spacing (10.9 Å) compared to the host phase (5.0 Å). This peak combined with the additional peaks at 18° and 24° 2θ and their relative intensities was consistent with the sample possessing a layered structure (intensity ratio ~ 3:1.5:1).[31,32] Therefore the calcium acid pyrophosphate sample was left in these amino acid solutions for a total of 7 days, in order to determine whether intercalation might have been possible given a longer time period. Unfortunately, no further structural changes from the water control phase were observed in these samples when the X-ray diffraction patterns were examined. Further investigation needs to be performed with this material, which, due to time constraints, was not possible.

6.4 Conclusions

The three calcium based pyrophosphate phases calcium pyrophosphate tetrahydrate, calcium disodium pyrophosphate and calcium acid pyrophosphate were successfully synthesised. Modification of the materials was then attempted and a summary of these findings is given below.

Calcium Pyrophosphate Tetrahydrate

From the analysis of the structure of calcium pyrophosphate tetrahydrate it was found to possess a layered structure. This layering had the potential for intercalation reactions whereby molecules could be held in the interlayer region of the material. However, all experiments that were performed as this material showed no signs of intercalation, even when using relatively forceful conditions such as refluxing in boiling solvent or in a sealed solvothermal vessel. Potential explanation for this lack of successful intercalation could have been a result of the neutral charge in the interlayer region and the absence of protons in this region. Since a successful route to intercalation involved an acid-base reaction with the intercalating species and the host, the lack of protons in this phase prevented this mechanism from occurring. A neutral interlayer charge (due to charge balancing between the pyrophosphate units and metal ions) would also have prevented electrostatic attraction of a particular charged intercalating species with an opposite charge in the interlayer of the host phase.

This calcium pyrophosphate tetrahydrate material was found to possess the ability to vary its water content. This became evident on the larger scale production of the host phase. It was observed that when this material was in excess water, a visible expansion in the material occurred when it was left to settle in a sample vial. However, attempts to characterise this

phase proved unsuccessful. This was due to the fact that as the material was removed from water for analysis, the material would revert to the tetrahydrate phase.

Calcium Disodium Pyrophosphate

From the structural analysis of the calcium disodium pyrophosphate phase, the sodium ions within the structure were determined to be accessible and therefore potentially exchangeable. The ion exchange reactions with potassium were proved successful only when the aqueous potassium source was refluxed with the host phase. However, attempts to proton exchange the calcium disodium phase to form a layered calcium acid pyrophosphate caused the sample to dissolve or form an unknown phase. Similar observations were also noted when intercalation reactions were attempted with this phase.

Calcium Acid Pyrophosphate

When pure amines were added to this calcium acid pyrophosphate phase, analysis by X-ray diffraction showed an additional low angle peak was observed. This was indicative of a reaction with the amine, as the peak position was dependent upon the chain length of the amine. However, the host structure X-ray pattern was also found to be present without any shift in its peak positions. This was inconsistent with successful intercalation reactions. Therefore either a surface reaction or a partial dissolution/re-precipitation of the material had occurred. This produced another unknown phase that possessed a low angle X-ray diffraction peak.

A change in structure was also observed when a control reaction using water was performed. This produced an unidentifiable phase with a low angle peak at 8° 2θ diffraction angle. This phase was formed in all the amino acid intercalation reactions due to the aqueous solutions used. Long time exposure of this calcium acid pyrophosphate phase in the amino

acid solutions showed no further reaction between the pyrophosphate and the amino acid solutions. Further experiments were required with this phase in order to determine whether this material possessed a layered structure, with the potential for successful intercalation reactions.

6.5 References

1. Durif, A., *Crystal Chemistry of Condensed Phosphates*. Plenum Press: New York, 1995; p 408.
2. Averbuch-Pouchot, M.; Durif, A., *Topics in Phosphate Chemistry*. World Scientific Publishing: 1996.
3. Beutler, A.; Rothfuss, S.; Clayburne, G.; Sieck, M.; Schumacher, H., *Arthritis and Rheumatism,* **36**, 704, (1993).
4. Ishikawa, K.; Masuda, I.; Ohira, T.; Yokoyama, M., *J. Bone Joint Surg.,* **71A**, 875, (1989).
5. Grover, L.; Gbureck, U.; Wright, A.; Tremayne, M.; Barralet, J., *Biomaterials,* **27**, 2178, (2006).
6. Yoza, N.; Onoue, S.; Kuwahara, Y., *Chemistry Letters*, 491, (1997).
7. Shinozaki, T.; Xu, Y.; Cruz, T.; Pritzker, K., *J. Rheum.,* **22**, 117, (1995).
8. Xu, Y.; Cruz, T.; Pritzker, K., *J. Rheum.,* **18**, 1606, (1991).
9. Alkhraisat, M.; Marino, F.; Rodriguez, C.; Jerez, L.; Cabarcos, E., *Acta. Biomater.,* **4**, 664, (2008).
10. Barralet, J.; Grover, L.; Gbureck, U., *Biomaterials,* **25**, 2197, (2004).
11. Gago, S.; Pillinger, M.; Ferreira, R.; Carlos, L.; Santos, T.; Goncalves, I., *Chem. Mater.,* **17**, 5803, (1995).
12. Ferragina, C.; Rocco, R.; Giannoccaro, P.; Patrono, P.; Petrelli, L., *J. Incl. Phen. Mol. Recog. in Chem.,* **63**, 1, (2009).
13. Ferragina, C.; Ginestra, A.; Massucci, M.; Patrono, P.; Tomlinson, A., *J. Phys. Chem.,* **89**, 4762, (1985).
14. Ferragina, C.; Ginestra, A.; Massucci, M.; Mattogno, G.; Patrono, P.; Giannoccaro, P.; Cafarelli, P.; Arfelli, M., *J. Mater. Chem.,* **5**, 461, (1995).
15. Checker, N. The Synthesis and Properties of Novel Condensed Phosphate. PhD Thesis, The University of Birmingham, (2006).
16. Cheng, P.; Pritzker, K., *Acta Cryst.,* **36B**, 921, (1980).
17. *CELL*, Pye, M., Inorganic Chemistry Laboratory, Oxford.
18. Christoffersen, M.; Balic-Zunic, T.; Pehrson, S.; Christoffersen, J., *J Cryst. Growth,* **212**, 500, (2000).
19. *ATOMS*, Shape Software: 2005.
20. Fletcher, D.; McMeeking, R.; Parkin, D., *J. Chem. Inf. Comput. Sci.,* **36**, 746, (1996).
21. Allen, F., *Acta Cryst.,* **58B**, 380, (2002).
22. Boudin, S.; Grandin, A.; Borel, M.; Leclaire, A.; Raveau, B., *Acta Cryst.,* **49C**, 2062, (1993).
23. *CRYSFIRE*, Shirley, R., Guildford, Surrey: 2002.
24. Alberti, G.; Marmotti, F.; Cavaglio, S.; Severi, D., *Langmuir,* **16**, 4165, (2000).
25. Benes, L.; Melanova, K.; Zima, V.; Patrono, P.; Galli, P., *Eur. J. Inorg. Chem.,* **2003**, 1577, (2003).
26. Benes, L.; Zima, V.; Melanova, K.; Steinhart, M.; Kriechbaum, M.; Amenitsch, H.; Bernstorff, S., *J. Phys. Chem. Solids,* **65**, 615, (2004).
27. Viertelhaus, M.; Taylor, A.; Kloo, L.; Gameson, I.; Anderson, P., *RSC: Dalton Trans.,* **2006**, 2368, (2006).
28. Worboys, L.; Edwards, P.; Anderson, P., *Chem. Comm.,* **2002**, 2894, (2002).
29. Sandstroem, M.; Fischer, A.; Bostroem, D., *Acta Cryst.,* **59E**, 139, (2003).
30. *Joint Committee on Powder Diffraction Standards (JCPDS)*, 1999.

31. Tanaka, H.; Oomori, K.; Hino, R., *J.Colloid Interf. Sci,* **273**, 685, (2004).
32. Tanaka, H.; Watanabe, T.; Chikazawa, M.; Kandori, K.; Ishikawa, T., *Colloids and Surfaces,* **139A**, 341, (1998).

Chapter 7:

Final Conclusions and Further Work

From the research conducted in this thesis, some overall conclusions can be drawn, along with some suggestions of where further work might usefully be directed.

In the work on metal alkyl phosphates, it was found that materials could be prepared using calcium, strontium and magnesium metal ions with straight and branched chain alkyl components. Initial attempts to add functionality to the alkyl chain during the intermediate phase preparation proved unsuccessful, probably as a result of side reactions. However, from the experiments with these alkyl phosphates, the structure of strontium pentyl and phenyl phosphates were determined using single crystal X-ray diffraction. These represent a rare family of hybrid materials whose structures have been characterised with certainty and provides a rare insight into the orientation of organic side chains in such structures.

There is much scope for further work with these materials relating to the possible modification of the alkyl chains in order to improve their potential properties, either before the formation of the alkyl phosphate or by post-synthesis modification. This might involve finding alternative preparative methods to avoid potential side-reactions during the phosphate ester intermediate preparation step. This could also explore the use of organic protecting groups stable to the formation reactions. Further experiments could also be conducted in order to attempt to exfoliate this layered material. Current methods have either had no effect or caused complete collapse of the structure.

Experiments with MCPM proved that it is possible to intercalate small straight chained amines into this layered material. However, more complicated molecules, such as drug molecules, could not be accommodated via the methods used. Therefore further work needs to be completed to test whether a many stage pre-intercalation of this material would allow sufficient space for the insertion of drug molecules. Further modification of the

structure might be necessary in order to allow better binding of the drug to the interlayer region.

The calcium phosphate bone cement investigations indicated that a low percentage of amine intercalated MCPM, when mixed with pure MCPM during the cement preparation, increased the setting time of the cement to a more useable timescale for surgical application. This proved the concept that modified MCPM may offer an alternative route to tailoring the properties of bone cements. However, more extensive reactions using the MCPM and TCP system need to be completed in order to confirm whether using this modified cement can lead to a stronger cement than the unmodified brushite cement. Additionally, in this initial study the potential effect of the release of the amine species was not considered and this needs to be assessed to determine whether the cements produced retain biocompatibility.

The calcium pyrophosphate materials, namely, calcium pyrophosphate tetrahydrate and calcium disodium pyrophosphate phases were prepared successfully and are shown to have a greater stability in water compared to MCPM. However, the calcium acid pyrophosphate phase, when in contact with water overnight, produced an unknown phase. The X-ray diffraction pattern showed a low angle diffraction peak and the intensities of the peaks suggested an expanded layered structure had been formed. Unfortunately, time permitted only some preliminary investigations on the intercalation properties of this material. Therefore, further experiments and analyses are needed to determine whether this material has potential as a host material for intercalation species.

The modification of the chosen pyrophosphate materials using intercalation or exfoliation methods, proved difficult to achieve. These reactions with calcium pyrophosphate tetrahydrate or calcium disodium pyrophosphate either had no effect upon the structures or caused rearrangements to produce unknown phases.

Further investigation of the calcium based pyrophosphates could be conducted on the ion/proton exchange of calcium disodium pyrophosphate. Potassium ions were successfully exchanged for sodium in this phase with a complete change of structure from a layered material to a 3-dimensional structure. Proton exchange methods were attempted which produced some unknown phases but did not replace the sodium ions with protons. Therefore an alternative method which could be attempted would be the ion exchange of sodium for ammonium ions with a subsequent calcination step to remove ammonia and leave protons in the material. Such acidic solids have previously been shown to provide improved intercalation behaviour.

This investigation into pyrophosphate materials uncovered some unknown phases, suggesting there is still much scope for new and interesting phases to be isolated. Of the phases that have been isolated, one obvious route to obtain structural detail would be via single crystal X-ray diffraction but the synthetic methods would need to be optimised to enable this.

Bibliography

1. *Joint Committee on Powder Diffraction Standards (JCPDS)*, 1999.
2. *ATOMS*, Shape Software: 2005.
3. Ajayan, P.; Schadler, L.; Braun, P., *Nanocomposite Science and Technology*. Wiley VCH: 2003.
4. Alberti, G.; Casciola, M.; Costantino, U., *J. Colloid Interf. Sci.,* **107**, 256, (1985).
5. Alberti, G.; Cavalaglio, S.; Dionigi, C.; Marmotti, F., *Langmuir,* **16**, 7663, (2000).
6. Alberti, G.; Costantino, U., *J. Molec. Catal.,* **27**, 235, (1984).
7. Alberti, G.; Giontella, E.; MurciaMascaros, S., *Inorg. Chem.,* **36**, 2844, (1997).
8. Alberti, G.; Marmotti, F.; Cavaglio, S.; Severi, D., *Langmuir,* **16**, 4165, (2000).
9. Ali, A.; Mustarelli, P.; Quartarone, E.; Magistris, A., *J. Mater. Res.,* **14**, 327, (1999).
10. Alkhraisat, M.; Marino, F.; Retama, J.; Jerez, L.; Cabarcos, E., *J. Biomed. Mater. Res.,* **84A**, 710, (2008).
11. Alkhraisat, M.; Marino, F.; Rodriguez, C.; Jerez, L.; Cabarcos, E., *Acta. Biomater.,* **4**, 664, (2008).
12. Allen, F., *The Cambridge Struct. Database, Acta Cryst.,* **58B**, 380, (2002).
13. Andersen, B.; Hirschfeld, P.; Slezak, J., *Phys. Rev.,* **76B**, Article:020507, (2007).
14. Averbuch-Pouchot, M.; Durif, A., *Topics in Phosphate Chemistry*. World Scientific Publishing: 1996.
15. Backov, R.; Bonnet, B.; Jones, D.; Roziere, J., *Chem. Mater.,* **9**, 1812, (1997).
16. Barralet, J.; Grover, L.; Gaunt, T.; Wright, A.; Gibson, I., *Biomaterials,* **23**, 3063, (2002).
17. Barralet, J.; Grover, L.; Gbureck, U., *Biomaterials,* **25**, 2197, (2004).
18. Barralet, J.; Tremayne, M.; Lilley, K.; Gbureck, U., *Chem. Mater.,* **17**, 1313, (2005).
19. Barroug, A.; Kuhn, L.; Gerstenfeld, L.; Glimcher, M., *J. Orth. Res.,* **22**, 703, (2004).
20. Benes, L.; Melanova, K.; Zima, V.; Patrono, P.; Galli, P., *Eur. J. Inorg. Chem.,* **2003**, 1577, (2003).
21. Benes, L.; Zima, V.; Melanova, K.; Steinhart, M.; Kriechbaum, M.; Amenitsch, H.; Bernstorff, S., *J. Phys. Chem. Solids,* **65**, 615, (2004).
22. Benmore, R.; Coleman, M.; McArthur, J., *Nature,* **302**, 516, (1983).
23. Beutler, A.; Rothfuss, S.; Clayburne, G.; Sieck, M.; Schumacher, H., *Arthritis and Rheumatism,* **36**, 704, (1993).
24. Bhambhani, A.; Kumar, C., *Chem. Mater.,* **18**, 740, (2006).
25. Bohner, M., *J. Mater. Chem.,* **17**, 3980, (2007).
26. Bohner, M.; Gbureck, U., *J. Biomed. Mater. Res.,* **84B**, 375, (2008).
27. Bohner, M.; Gbureck, U.; Barralet, J., *Biomaterials,* **26**, 6423, (2005).
28. Boudeville, P.; Serraj, S.; Leloup, J.; Margerit, J.; Pauvert, B.; Terol, A., *J. Mater. Sci: Mater in Med,* **10**, 99, (1999).
29. Boudin, S.; Grandin, A.; Borel, M.; Leclaire, A.; Raveau, B., *Acta Cryst.,* **49C**, 2062, (1993).
30. Brown, E.; Lehr, J.; Smith, J.; Frazier, W., *J. Agric. Food Chem.,* **11**, 214, (1963).
31. Brown, W.; Chow, L., *J. Dent. Res.,* **62**, 672, (1983).
32. *EVA X-ray Evaluation*, Bruker-AXS.
33. Casciola, M.; Alberti, G.; Donnadio, A.; Pica, M.; Marmotti, F.; Bottino, A.; Piaggio, P., *J. Mater. Chem.,* **15**, 4262, (2005).
34. Casciola, M.; Chieli, S.; Costantino, U., *Solid State Ionics,* **46**, 53, (1991).
35. Casciola, M.; Costantino, U.; Calvei, A., *Solid State Ionics,* **61**, 245, (1993).
36. Cave, M.; Farrar, D.; Wright, A., *Key Engineering Materials,* **361-363**, 383, (2008).
37. Checker, N. PhD Thesis. University of Birmingham, (2006).

38. Chen, W.; Feng, L.; Qu, B., *Chem. Mater.,* **16**, 368, (2004).

39. Cheng, P.; Pritzker, K., *Acta Cryst.,* **36B**, 921, (1980).

40. Christoffersen, M.; Balic-Zunic, T.; Pehrson, S.; Christoffersen, J., *J Cryst. Growth,* **212**, 500, (2000).

41. Chu, M.; Liu, G., *Nanotechnology,* **16**, 1208, (2005).

42. Clearfield, A.; Smith, D., *Inorg. Chem.,* **8**, 431, (1969).

43. Cousin, O.; Mentre, O.; Huve, M.; Abraham, F., *J. Solid State. Chem.,* **157**, 123, (2001).

44. Currey, J., *Handbook of Composites.* Elsevier Science Publishers B. V. 1983: 1983; p 501.

45. Danjo, M.; Baba, Y.; Tsuhako, M.; Yamaguchi, S.; Hayama, M.; Nariai, H.; Motooka, I., *Bull. Chem. Soc. Japan,* **68**, 1607, (1995).

46. Dickens, B.; Bowen, J., *Acta. Cryst.,* **27B**, 2247, (1971).

47. Dines, M.; Digiacomo, P.; Callahan, K.; Griffith, P.; Lane, R.; Cooksey, R., *ACS Symp. Ser. No. 192.* Washington D.C., 1982.

48. Ding, Y.; Jones, D.; Maireles-Torres, P.; Roziere, J., *Chem. Mater.,* **7**, 562, (1995).

49. Dorozhkin, S., *J. Mater. Sci.,* **42**, 1061, (2007).

50. Dorozhkin, S., *J. Mater. Sci.,* **43**, 3028, (2008).

51. Durif, A., *Crystal Chemistry of Condensed Phosphates.* Plenum Press: New York, 1995; p 408.

52. Dyer, A.; Leigh, D., *J. Inorg. Nucl. Chem.,* **34**, 369, (1972).

53. Espina, A.; Jaimez, E.; Khainakov, S.; Trobajo, C.; Garcia, J.; Rodriguez, J., *J. Mater. Res.,* **13**, 3304, (1998).

54. Espina, A.; Menendez, F.; Jaimez, E.; Khainakov, S.; Trobajo, C.; Garcia, J.; Rodriguez, J., *Mater. Res. Bull.,* **33**, 763, (1998).

55. Fernandez, E.; Vlad, M.; Gel, M.; Lopez, J.; Torres, R.; Cauich, J., *Biomaterials,* **26**, 3395, (2005).

56. Ferragina, C.; Ginestra, A.; Massucci, M.; Mattogno, G.; Patrono, P.; Giannoccaro, P.; Cafarelli, P.; Arfelli, M., *J. Mater. Chem.,* **5**, 461, (1995).

57. Ferragina, C.; Ginestra, A.; Massucci, M.; Patrono, P.; Tomlinson, A., *J. Phys. Chem.,* **89**, 4762, (1985).

58. Ferragina, C.; Rocco, R.; Giannoccaro, P.; Patrono, P.; Petrelli, L., *J. Incl. Phen. Mol. Recog. in Chem.,* **63**, 1, (2009).

59. Fletcher, D.; McMeeking, R.; Parkin, D., *J. Chem. Inf. Comput. Sci.,* **36**, 746, (1996).

60. Fosslien, E., *Ann. Clin. Lab. Sci.,* **31**, 25, (2001).

61. Furuichi, K.; Oaki, Y.; Ichimiya, H.; Komotori, J.; Imai, H., *Sci. Tech. Adv. Materials,* **7**, 219, (2006).

62. Gago, S.; Pillinger, M.; Ferreira, R.; Carlos, L.; Santos, T.; Goncalves, I., *Chem. Mater.,* **17**, 5803, (1995).

63. Gao, W.; Liu, Q.; Yang, L.; Yu, Y.; Li, F.; Jin, C., *Phys. Rev.,* **80B**, Article:094523, (2009).

64. Gbureck, U.; Barralet, J.; Spatz, K.; Grover, L.; Thull, R., *Biomaterials,* **25**, 2187, (2004).

65. Gbureck, U.; Dembski, S.; Thull, R.; Barralet, J., *Biomaterials,* **26**, 3691, (2005).

66. Gbureck, U.; Grolms, O.; Barralet, J.; Grover, L.; Thull, R., *Biomaterials,* **24**, 4123, (2003).

67. Gbureck, U.; Holzel, T.; Biermann, I.; Barralet, J.; Grover, L., *J. Mater. Sci.,* **19**, 1559, (2008).

68. Geesink, R.; de Groot, K.; Klein, C., *J. Bone Joint Surg.,* **70B**, 17, (1988).

69. Ginebra, M.; Traykova, T.; Planell, J., *J. Controlled Release,* **113**, 102, (2006).

70. Gorst, N.; Perrie, Y.; Gbureck, U.; Hutton, A.; Hofmann, M.; Grover, L.; Barralet, J.,

Acta. Biomater., **2**, 95, (2006).

71. *DSPACE*, Greaves, C., University of Birmingham: 1982.

72. Greenwell, C.; Harvey, M.; Boulet, P.; Bowden, A.; Coveney, P.; Whiting, A., *Macromolecules,* **38**, 6189, (2005).

73. Grover, L.; Gbureck, U.; Wright, A.; Tremayne, M.; Barralet, J., *Biomaterials,* **27**, 2178, (2006).

74. Grover, L.; Gbureck, U.; Young, A.; Wright, A.; Barralet, J., *J. Mater. Chem.,* **15**, 4955, (2005).

75. Hamanishi, C.; Kitamoto, K.; Ohura, K.; Tanaka, S.; Do, Y., *J. Biomed. Mater. Res.,* **32**, 383, (1996).

76. Harwood, L.; Claridge, T., *Introduction to Organic Spectroscopy*. Oxford University Press.

77. Hill, W.; Faust, G.; Reynolds, D., *Am. J. Sci.,* **242**, 457, (1944).

78. http://encarta.msn.com/, Cross Section of a Bone. (2007).

79. http://encarta.msn.com/, Cross Section of a Tooth. (2007).

80. Huang, Q.; Wang, W.; Yue, Y.; Hua, W.; Gao, Z., *Micro. Meso. Mater.,* **67**, 189, (2004).

81. Ishikawa, K.; Masuda, I.; Ohira, T.; Yokoyama, M., *J. Bone Joint Surg.,* **71A**, 875, (1989).

82. Ishikawa, T.; Tanaka, H.; Yasukawa, A.; Kandori, K., *J. Mater. Chem.,* **5**, 1963, (1995).

83. Jackson, L.; Kariuki, B.; Smith, M.; Barralet, J.; Wright, A., *Chem. Mater.,* **17**, 4642, (2005).

84. Kaschak, D.; Johnson, S.; Hooks, D.; Kim, H.; Ward, M.; Mallouk, T., *J Am. Chem. Soc.,* **120**, 10887, (1998).

85. Kenny, S.; Buggy, M., *J. Mater. Sci: Mater in Med,* **14**, 923, (2003).

86. Kijima, T.; Ueno, S.; Goto, M., *J. Chem. Soc: Dalton Trans.,* **1982**, 2499, (1982).

87. Kim, H.; Keller, S.; Mallouk, T., *Chem. Mater.,* **9**, 1414, (1997).

88. Kim, S.; Kim, S., *J. Applied Poly. Sci.,* **103**, 1262, (2007).

89. Kumar, C.; Bhambhani, A.; Hnatiuk, N., *Handbook of Layered Materials*. Marcel Dekker: New York, 2004.

90. Leclaire, A.; Caignaert, V.; Raveau, B., *Solid State Sci.,* **7**, 109, (2005).

91. Lee, B.; Samuels, W.; Wang, L.; Exarhos, G., *J. Mater. Res.,* **11**, 134, (1996).

92. Lee, J.; Fujita, K.; McElroy, K.; Slezak, J.; Wang, M.; Ajura, Y.; Bando, H.; Ishikado, M.; Masui, T.; Zhu, J.; Balatsky, A.; Eisaki, H.; Uchida, S.; Davis, J., *Nature,* **442**, 546, (2006).

93. Lee, Y.; Hahm, Y.; Matsuya, S.; Nakagawa, M.; Ishikawa, K., *J. Mater. Sci.,* **42**, 7843, (2007).

94. Lehr, J.; Smith, D.; Brown, W., *S.E. Regional Meeting, Am. Chem. Soc.,* **October 1952**, (1952).

95. Lewis, G., *J. Biomed. Mater. Res.,* **76B**, 456, (2005).

96. Lilley, K.; Gbureck, U.; Knowles, J.; Farrar, D.; Barralet, J., *J. Mater. Sci.,* **16**, 455, (2005).

97. Lima, C.; Airoldi, C., *Solid State Sci.,* **6**, 1245, (2004).

98. Liou, S.; Chen, S.; Liu, D., *J. Biomed. Mater. Res.,* **73B**, 117, (2005).

99. Livage, J.; Barboux, P.; Vandenborre, M.; Schmutz, C.; Taulelle, F., *J. Non-Cryst Solids,* **147-8**, 18, (1992).

100. Lopez-Heredia, M.; Sohier, J.; Gaillard, C.; Quillard, S.; Dorget, M.; Layrolle, P., *Biomaterials,* **29**, 2608, (2008).

101. Ma, J.; Xu, J.; Ren, J.; Yu, Z.; Mai, Y., *Polymer,* **44**, 4619, (2003).

102. MacIntire, W.; Hardin, L.; Oldham, F., *Ind. Eng. Chem.,* **28**, 711, (1936).

103. Maclennan, G.; Beevers, C., *Acta Cryst.,* **9**, 187, (1956).

104. Mathew, M.; Takagi, S., *J. Res. Nat. Inst. Stand. Tech.,* **106**, 1035, (2001).

105. Menendez, A.; Barcena, M.; Jaimez, E.; Garcia, J.; Rodriguez, J., *Chem. Mater.,* **5**, 1078, (1993).

106. Mirchi, A.; Lemaitre, J.; Terao, N., *Biomaterials,* **10**, 475, (1989).

107. Mott, C., *Catalysis Today,* **2**, 199, (1988).

108. Murugan, R.; Ramakrishna, S., *Composites Sci. and Tech.,* **65**, 2385, (2005).

109. Mutin, H.; Guerrero, G.; Vioux, A., *Comp. Rend. Chemie,* **6**, 1153, (2003).

110. Nakato, T.; Furumi, Y.; Terao, N.; Okuhara, T., *J. Mater. Chem.,* **10**, 737, (2000).

111. Nam, P.; Fujimori, A.; Masuko, T., *J. App Poly. Sci.,* **93**, 2711, (2004).

112. Nelson, A.; Toy, A., *Inorg. Chem.,* **2**, 775, (1963).

113. NIST; What is a Fourier Transform Spectrometer. "http://physics.nist.gov/Divisions/Div842/Gp1/fts_intro.html ", (2002).

114. Okuda, T.; Ioku, K.; Yonezawa, I.; Minagi, H.; Kawachi, G.; Gonda, Y.; Murayama, H.; Shibata, Y.; Minami, S.; Kamihira, S.; Kurosawa, H.; Ikeda, T., *Biomaterials,* **28**, 2612, (2007).

115. OliveraPastor, P.; MairelesTorres, P.; RodriguezCastellon, E.; JimenezLopez, A.; Cassagneau, T.; Joner, D.; Roziere, J., *Chem. Mater.,* **8**, 1758, (1996).

116. Paul, W.; Sharma, C., *J. Biomat Appl,* **17**, 253, (2003).

117. Peng, L.; Yu, J.; Li, J.; Li, Y.; Xu, R., *Chem. Mater.,* **17**, 2101, (2005).

118. Pittet, C.; Lemaitre, J., *J. Biomed. Mater. Res.,* **53B**, 769, (2000).

119. Pospisil, M.; Capkova, P.; Merinska, D.; Malac, Z.; Simonik, J., *J. Colloid Interf. Sci.,* **236**, 127, (2001).

120. *CELL*, Pye, M., Inorganic Chemistry Laboratory, Oxford.

121. Ribeiro, C.; Barrias, C.; Barbosa, M., *Biomaterials,* **25**, 4363, (2004).

122. Roveri, N.; Falini, G.; Tampieri, A.; Landi, E.; Sandri, M.; Sidoti, M., *Mater. Sci. Eng.,* **23C**, 441, (2003).

123. Sagiv, J., *J. Am. Chem. Soc.,* **102**, 92, (1980).

124. Sandstroem, M.; Fischer, A.; Bostroem, D., *Acta Cryst.,* **59E**, 139, (2003).

125. Schnieders, J.; Gbureck, U.; Thull, R.; Kissel, T., *Biomaterials,* **27**, 4239, (2006).

126. Seo, K.; Kim, D., *Polymer Eng. Sci.,* **46**, 1318, (2006).

127. Serraj, S.; Boudeville, P.; Terol, A., *J. Mater. Sci: Mater in Med,* **12**, 45, (2001).

128. *SHELXL*, Sheldrick, G., University of Gottingen.

129. Sheng, Y.; Zhou, B.; Zhao, J.; Tao, N.; Yu, K.; Tian, Y.; Wang, Z., *J. Colloid Interf. Sci.,* **272**, 326, (2004).

130. Shinozaki, T.; Xu, Y.; Cruz, T.; Pritzker, K., *J. Rheum.,* **22**, 117, (1995).

131. *CRYSFIRE*, Shirley, R., Guildford, Surrey: 2002.

132. Smart, L.; Moore, E., *Solid State Chemistry*. CRC Press: 2005.

133. Spori, D.; Venkataraman, N.; Tosatti, S.; Durmaz, F.; Spencer, N.; Zurcher, S., *Langmuir,* **23**, 8053, (2007).

134. Stark, J.; Wallace, H., *Chemistry Data Book*. Second ed.; John Murray Ltd.: London, 1999.

135. Suchanek, W.; Yoshimura, M., *J. Mater. Res.,* **13**, 94, (1998).

136. Sue, J.; Gam, K., *Chem. Mater.,* **16**, 242, (2004).

137. Sun, L.; Boo, W.; Browning, R.; Sue, H.; Clearfield, A., *Chem. Mater.,* **17**, 5606, (2005).

138. Takagi, S.; Chow, L.; Ishikawa, K., *Biomaterials,* **19**, 1593, (1998).

139. Tamimi, F.; Kumarasami, B.; Doillon, C.; Gbureck, U.; Nihouannen, D.; Cabarcos, E.; Barralet, J., *Acta. Biomater.,* **4**, 1315, (2008).

140. Tampieri, A.; Celotti, G.; Landi, E.; Sandri, M.; Falini, G.; Roveri, N., *J. Biomed. Mater. Res.,* **67A**, 618, (2003).
141. Tanaka, H.; Chikazawa, M., *J. Mater. Chem.,* **9**, 2923, (1999).
142. Tanaka, H.; Chikazawa, M., *Mater. Res. Bull.,* **35**, 75, (2000).
143. Tanaka, H.; Masuda, K.; Hino, R., *J. Colloid Interf. Sci.,* **254**, 331, (2002).
144. Tanaka, H.; Oomori, K.; Hino, R., *J. Colloid Interf. Sci.,* **273**, 685, (2004).
145. Tanaka, H.; Watanabe, T.; Chikazawa, M.; Kandori, K.; Ishikawa, T., *Colloids and Surfaces,* **139A**, 341, (1998).
146. Tanaka, H.; Yasukawa, A.; Kandori, K.; Ishikawa, T., *Colloids and Surfaces,* **125A**, 53, (1997).
147. Tanaka, H.; Yasukawa, A.; Kandori, K.; Ishikawa, T., *Langmuir,* **13**, 821, (1997).
148. Tanaka, T.; Fukuda, K.; Ebina, Y.; Takada, K.; Sasaki, T., *Advanced Materials,* **16**, 872, (2004).
149. Temenoff, J.; Mikos, A., *Biomaterials,* **21**, 2405, (2000).
150. Tenhuisen, K.; Martin, R.; Klimkiewicz, M.; Brown, P., *J. Biomed. Mater. Res.,* **29**, 803, (1995).
151. Tisdel, C.; Goldberg, V.; Parr, J.; Bensusan, J.; Staikoff, L.; Stevenson, S., *J. Bone Joint Surg.,* **76**, 159, (1994).
152. Vallet-Regi, M., *RSC: Dalton Trans.,* **2001**, 97, (2001).
153. Vallet-Regi, M.; Gonzalez-Calbet, J., *Prog. Solid State Chem.,* **32**, 1, (2004).
154. Viertelhaus, M.; Taylor, A.; Kloo, L.; Gameson, I.; Anderson, P., *RSC: Dalton Trans.,* **2006**, 2368, (2006).
155. Viswanath, B.; Ravishankar, N., *Scripta Materialia,* **55**, 863, (2006).
156. Wan, Y.; Hong, L.; Jia, S.; Huang, Y.; Zhu, Y.; Wang, Y.; Jiang, H., *Composites Sci. and Tech.,* **66**, 1825, (2006).
157. Webb, L. Synthesis and Characterisation of Calcium Phosphate Biomaterials. University of Birmingham, (2007).
158. Weller, M., *Inorganic Materials Chemistry*. Oxford University Press: 1994.
159. Worboys, L.; Edwards, P.; Anderson, P., *Chem. Comm.,* **2002**, 2894, (2002).
160. Xu, H.; Burguera, E.; Carey, L., *Biomaterials,* **28**, 3786, (2007).
161. Xu, Y.; Cruz, T.; Pritzker, K., *J. Rheum.,* **18**, 1606, (1991).
162. Yamamoto, N.; Hiyoshi, N.; Okuhara, T., *Chem. Mater.,* **14**, 3882, (2002).
163. Yamanka, S., *Inorg. Chem.,* **15**, 2811, (1976).
164. Yoon, K.; Sung, H.; Hwang, Y.; Noh, S.; Lee, D., *Applied Clay Science,* **38**, 1, (2007).
165. Yoza, N.; Onoue, S.; Kuwahara, Y., *Chemistry Letters*, 491, (1997).
166. Zheng, J.; Wang, J.; Gao, S.; Yao, K., *J. Mater. Sci.,* **40**, 4687, (2005).

Appendices

Appendix 1: Average Setting Times of a Series of Brushite Cements

Amine-MCPM Content in Cement	Average Initial Setting Time (Min)	Error (St. Dev.)	Average Final Setting Time (Min)	Error (St. Dev.)
25% Propylamine	12.5	1.6	Not Set (>165)	-
25% Butylamine	13.8	1.0	156.0	44.1
10% Propylamine	7.3	0.8	78.5	12.4
10% Butylamine	7.0	0	34.0	1.2
5% Propylamine	6.5	0.6	27.5	2.9
5% Butylamine	7.3	0.5	25.3	0.5
Pure MCPM	6.0	0	12.0	1.2

Appendix 2: Average Compression Strength of Different Cement Compositions

Amine-MCPM Content in Cement	Compression Strength (MPa)	Standard Deviation (MPa)
25% Propylamine	0.78	0.35
25% Butylamine	0.52	0.13
10% Propylamine	3.86	1.36
10% Butylamine	6.95	1.06
5% Propylamine	1.51	0.86
5% Butylamine	1.92	1.15
Pure MCPM (control)	6.16	1.80

Appendix 3: *CELL* Refinement Data for Calcium Pyrophosphate Tetrahydrate

	a	b	c	α	β	γ	Abs.	Zero	
Initial	12.256620	7.493671	10.688666	89.999997	112.536390	89.999997	0.000000	-0.267318	
Final	12.256543	7.493671	10.688599	89.999997	112.535520	89.999997	0.000000	-0.267315	
ESD	0.020019	0.009991	0.015999	0.000000	0.071388	0.000000	0.000000	0.036033	
2θ (Obs)	2θ (Calc)	*h*	*k*	*l*	d (Obs)	d (Calc)	Dif.	Weight	Sin^2 (Obs-Calc)
7.686	7.536	1	0	0	11.493	11.722	0.228	1.000	0.00017
14.631	14.562	0	1	1	6.049	6.078	0.028	1.000	0.00015
14.897	14.811	1	1	-1	5.942	5.976	0.034	1.000	0.00019
16.359	16.334	1	0	-2	5.414	5.422	0.008	1.000	0.00006
17.644	17.688	0	0	2	5.023	5.010	-0.012	1.000	-0.00012
20.129	20.149	1	1	-2	4.408	4.403	-0.004	1.000	-0.00006
23.285	23.271	3	0	-2	3.817	3.819	0.002	1.000	0.00005
23.502	23.460	0	2	0	3.782	3.789	0.007	1.000	0.00014
23.719	23.757	2	1	1	3.748	3.742	-0.006	1.000	-0.00013
25.141	25.138	0	2	1	3.539	3.540	0.000	1.000	0.00001
25.286	25.288	1	2	-1	3.519	3.519	0.000	1.000	0.00001
26.117	26.140	3	1	-2	3.409	3.406	-0.003	1.000	0.00009
27.431	27.371	1	2	1	3.249	3.256	0.007	1.000	0.00024
27.871	27.784	2	2	-1	3.199	3.208	0.010	1.000	0.00036
28.226	28.279	2	2	0	3.159	3.153	-0.006	1.000	-0.00022
28.771	28.831	1	2	-2	3.100	3.094	-0.006	1.000	-0.00025
29.552	29.477	4	0	-2	3.020	3.028	0.008	1.000	0.00032
30.077	30.159	2	2	-2	2.969	2.961	-0.008	1.000	-0.00036
31.296	31.320	4	0	0	2.856	2.854	-0.002	1.000	-0.00011
34.735	34.736	3	0	2	2.581	2.581	0.000	1.000	0.00000
36.777	36.757	3	1	-4	2.442	2.443	0.001	1.000	0.00011
41.363	41.370	5	1	0	2.181	2.181	0.000	1.000	-0.00004
48.803	48.781	2	2	-5	1.865	1.865	0.001	1.000	0.00014
50.761	50.762	3	3	2	1.797	1.797	0.000	1.000	0.00000
Wavelength for the Above Lines is 1.54060 Å									
R Factor = 0.00000074									

Appendix 4: *CELL* Refinement Data for Anhydrous Calcium Pyrophosphate

	a	b	c	α	β	γ	Abs.	Zero	
Initial	6.714364	6.714364	24.235208	89.999997	89.999997	89.999997	0.000000	0.000000	
Final	6.714365	6.714365	24.235212	89.999997	89.999997	89.999997	0.000000	-0.066692	
ESD	0.003767	0.003767	0.008865	0.000000	0.000000	0.000000	0.000000	0.016263	
2θ (Obs)	2θ (Calc)	*h*	*k*	*l*	d (Obs)	d (Calc)	Dif.	Weight	Sin^2 (Obs-Calc)
14.573	14.542	0	0	4	6.073	6.086	0.013	1.000	0.00007
18.621	18.608	1	1	0	4.761	4.765	0.003	1.000	0.00004
19.612	19.654	0	1	4	4.523	4.513	-0.010	1.000	-0.00012
20.030	20.004	1	1	2	4.429	4.435	0.006	1.000	0.00008
26.185	26.187	1	1	5	3.401	3.400	0.000	1.000	-0.00001
26.463	26.462	0	2	0	3.365	3.365	0.000	1.000	0.00000
26.719	26.721	0	2	1	3.334	3.334	0.000	1.000	-0.00001
27.497	27.481	0	2	2	3.241	3.243	0.002	1.000	0.00006
28.713	28.708	0	2	3	3.107	3.107	0.001	1.000	0.00002
29.386	29.395	0	0	8	3.037	3.036	-0.001	1.000	-0.00004
29.666	29.662	1	2	0	3.009	3.009	0.000	1.000	0.00002
29.903	29.895	1	2	1	2.986	2.986	0.001	1.000	0.00004
30.340	30.349	0	2	4	2.944	2.943	-0.001	1.000	-0.00004
30.570	30.583	1	2	2	2.922	2.921	-0.001	1.000	-0.00006
31.703	31.700	1	2	3	2.820	2.820	0.000	1.000	0.00001
31.878	31.901	1	1	7	2.805	2.803	-0.002	1.000	-0.00010
32.340	32.329	0	1	8	2.766	2.767	0.001	1.000	0.00005
33.195	33.207	1	2	4	2.697	2.696	-0.001	1.000	-0.00006
34.659	34.651	0	2	6	2.586	2.587	0.001	1.000	0.00004
35.051	35.044	1	1	8	2.558	2.559	0.000	1.000	0.00003
37.214	37.212	0	2	7	2.414	2.414	0.000	1.000	0.00001
38.311	38.333	1	1	9	2.348	2.346	-0.001	1.000	-0.00012
39.458	39.433	0	1	10	2.282	2.283	0.001	1.000	0.00014
39.965	39.991	0	2	8	2.254	2.253	-0.001	1.000	-0.00015
41.751	41.748	1	1	10	2.162	2.162	0.000	1.000	0.00002
42.960	42.959	0	2	9	2.104	2.104	0.000	1.000	0.00001
45.148	45.126	1	2	9	2.007	2.008	0.001	1.000	0.00014
49.367	49.375	0	2	11	1.845	1.844	0.000	1.000	-0.00005
Wavelength for the Above Lines is 1.54060 Å									
R Factor = 0.00000014									

Appendix 5: *CELL* Refinement Data for Calcium Disodium Pyrophosphate Tetrahydrate

	a	b	c	α	β	γ	Abs.	Zero	
Initial	5.686248	8.453327	10.557506	89.999997	106.099880	89.999997	0.000000	-0.085974	
Final	5.686246	8.453327	10.557503	89.999997	106.099840	89.999997	0.000000	-0.085978	
ESD	0.010813	0.008307	0.020247	0.000000	0.076164	0.000000	0.000000	0.048486	
2θ (Obs)	2θ (Calc)	*h*	*k*	*l*	d (Obs)	d (Calc)	Dif.	Weight	$\sin^2$ (Obs-Calc)
10.250	10.371	0	1	0	8.623	8.523	-0.100	1.000	-0.00019
13.451	13.539	0	1	1	6.577	6.535	-0.042	1.000	-0.00018
16.152	16.125	1	0	0	5.483	5.492	0.009	1.000	0.00007
17.427	17.386	0	0	2	5.085	5.097	0.012	1.000	0.00011
19.132	19.184	1	1	-1	4.635	4.623	-0.012	1.000	-0.00015
20.216	20.219	1	0	-2	4.389	4.388	-0.001	1.000	-0.00001
22.797	22.688	0	2	1	3.898	3.916	0.018	1.000	0.00037
27.081	26.997	1	0	2	3.290	3.300	0.010	1.000	0.00033
28.743	28.815	1	1	-3	3.103	3.096	-0.008	1.000	-0.00030
29.023	29.018	1	1	2	3.074	3.075	0.001	1.000	0.00002
33.098	33.134	2	1	-1	2.704	2.702	-0.003	1.000	-0.00017
35.276	35.282	0	0	4	2.542	2.542	0.000	1.000	-0.00003
36.342	36.362	0	3	2	2.47	2.469	-0.001	1.000	-0.00010
36.905	36.894	0	1	4	2.434	2.434	0.001	1.000	0.00006
40.768	40.733	1	2	-4	2.212	2.213	0.002	1.000	0.00020
41.573	41.606	0	3	3	2.171	2.169	-0.002	1.000	-0.00019
41.96	41.961	1	3	-3	2.151	2.151	0.000	1.000	0.00000
42.937	42.968	2	1	2	2.105	2.103	-0.001	1.000	-0.00019
45.240	45.188	2	3	-1	2.003	2.005	0.002	1.000	0.00032
54.116	54.124	0	5	0	1.693	1.693	0.000	1.000	-0.00005
Wavelength for the Above Lines is 1.54060 Å									
R Factor = 0.00000070									

Appendix 6: *CELL* Refinement Data for Calcium Dipotassium Pyrophosphate

	a	b	c	α	β	γ	Abs.	Zero	
Initial	9.841128	5.691359	13.036997	89.999997	104.218280	89.999997	0.000000	0.002677	
Final	9.841110	5.691358	13.036973	89.999997	104.217860	89.999997	0.000000	0.002676	
ESD	0.017903	0.005949	0.019485	0.000000	0.052444	0.000000	0.000000	0.045764	
2θ (Obs)	2θ (Calc)	*h*	*k*	*l*	d (Obs)	d (Calc)	Dif.	Weight	$\sin^2$ (Obs-Calc)
18.603	18.639	1	0	2	4.766	4.757	-0.009	1.000	-0.00010
20.270	20.275	1	1	1	4.377	4.376	-0.001	1.000	-0.00001
20.982	20.993	0	1	2	4.231	4.228	-0.002	1.000	-0.00003
24.333	24.331	2	1	0	3.655	3.655	0.000	1.000	0.00001
26.060	26.005	2	0	2	3.417	3.424	0.007	1.000	0.00021
28.222	28.226	0	0	4	3.160	3.159	0.000	1.000	-0.00002
29.667	29.667	1	1	3	3.009	3.009	0.000	1.000	0.00000
31.411	31.413	0	2	0	2.846	2.845	0.000	1.000	-0.00001
32.369	32.299	3	1	-2	2.764	2.769	0.006	1.000	0.00032
35.684	35.702	1	1	4	2.514	2.513	-0.001	1.000	-0.00009
36.512	36.534	2	2	-1	2.459	2.458	-0.001	1.000	-0.00011
37.674	37.69	4	0	0	2.386	2.385	-0.001	1.000	-0.00009
38.283	38.269	3	1	-4	2.349	2.35	0.001	1.000	0.00007
38.380	38.357	2	2	1	2.343	2.345	0.001	1.000	0.00013
38.948	38.961	0	1	5	2.311	2.310	-0.001	1.000	-0.00007
41.201	41.219	2	2	2	2.189	2.188	-0.001	1.000	-0.00010
41.394	41.427	4	0	-4	2.180	2.178	-0.002	1.000	-0.00019
42.918	42.884	3	1	-5	2.106	2.107	0.002	1.000	0.00020
43.801	43.858	2	2	-4	2.065	2.063	-0.003	1.000	-0.00035
45.452	45.401	3	0	-6	1.994	1.996	0.002	1.000	0.00032
47.212	47.251	1	2	-5	1.924	1.922	-0.001	1.000	-0.00025
48.147	48.114	0	2	-5	1.888	1.89	0.001	1.000	0.00022
49.141	49.111	1	3	-1	1.853	1.854	0.001	1.000	0.00020
Wavelength for the Above Lines is 1.54060 Å									
R Factor = 0.00000067									